FAULT ACTIVITY AND PALAEOSEISMICITY
DURING QUATERNARY TIME
IN SCOTLAND

Volume 1 : Text (and Colour Plates)

This thesis is submitted
for the degree of
Doctor of Philosophy

by
Philip S. Ringrose
B.Sc. (Edinburgh)

May 1987

Department of Applied Geology
University of Strathclyde
Glasgow

COVER PLATE

FAULT ACTIVITY ...

Thin-section of (post-2400 years BP) fault gouge at Kinloch Hourn. Note:

1. The sheared boundary between the light-coloured phase (top) and the darker phase (bottom).
2. The sharp, straight dislocation line in the darker phase (centre).
3. Rounded quartz clasts (white). (Scale bar - 2mm).

PALAEOSEISMICITY ...

Thin-section of late-glacial outwash sands at Meikleour which underwent (earthquake-induced) liquefaction soon after deposition. Note the poorly compacted nature of the grains. The pore space has been subsequently infilled by calcite (allowing this thin-section to be made). Grain-size and porosity details are given in Appendix 6. (Scale bar - 2mm).
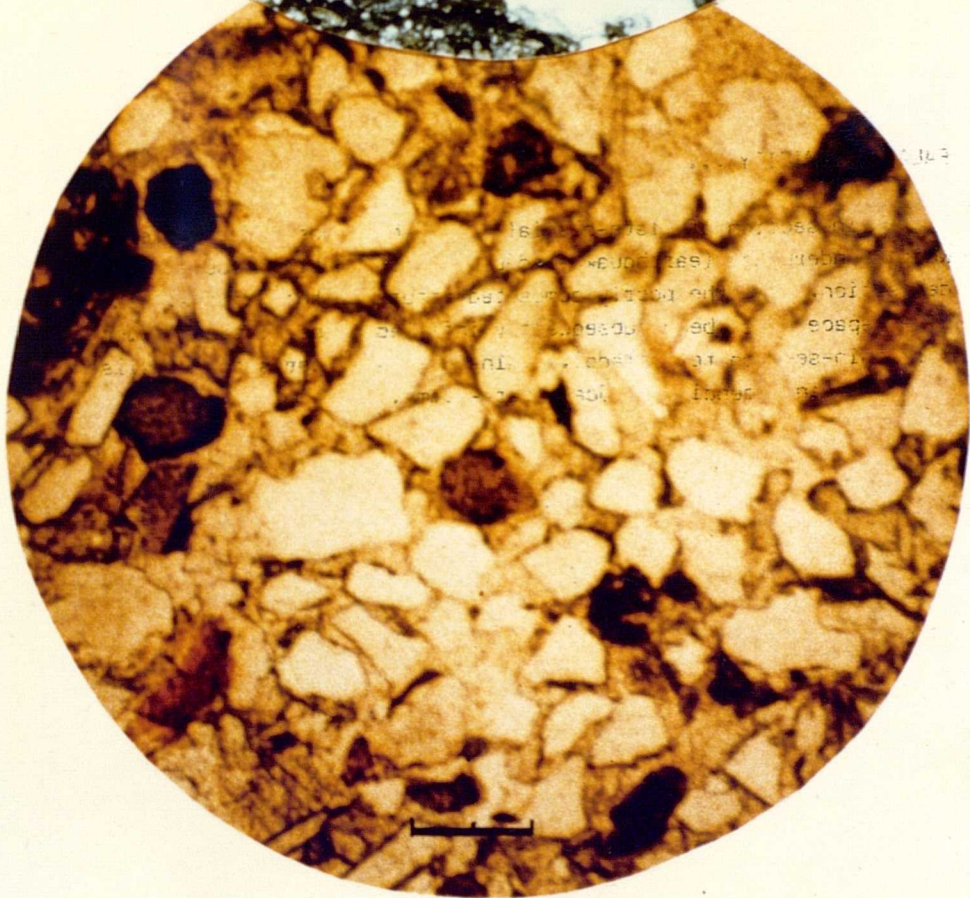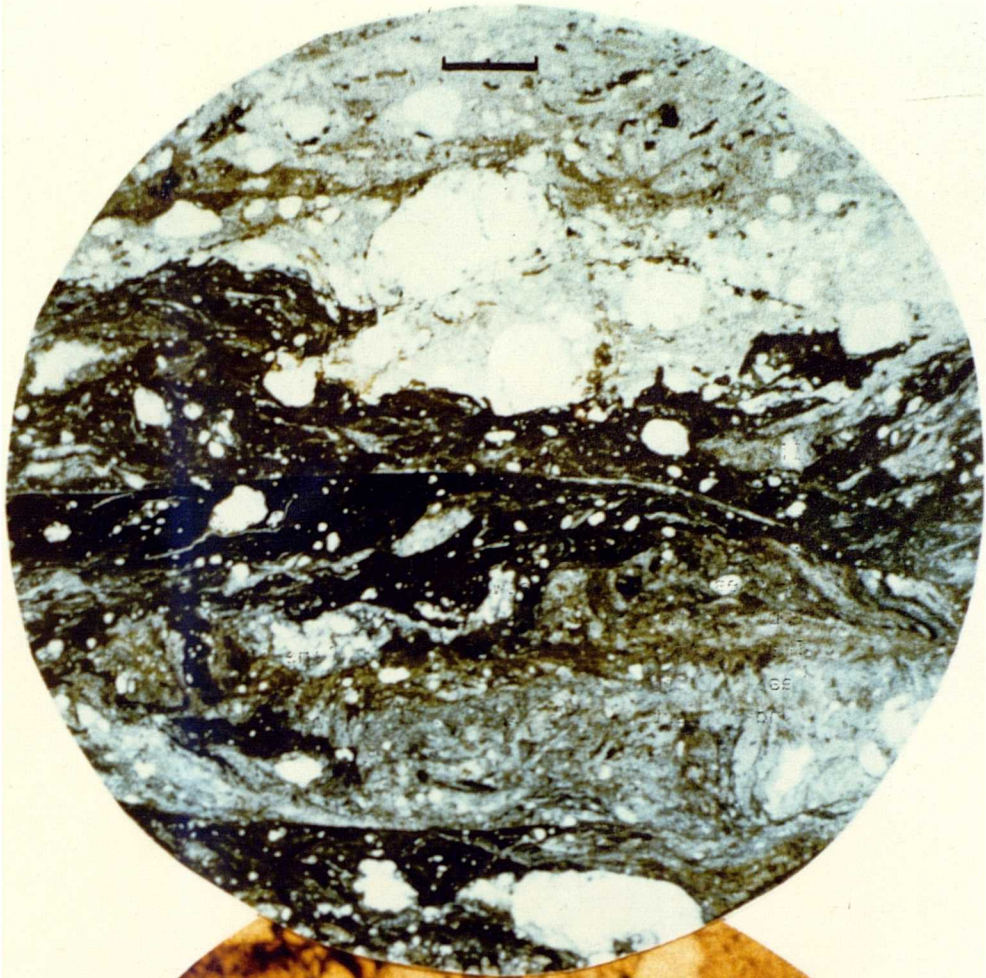
ABSTRACT

Field study at seven Scottish sites has resulted in the following evidence for late- and post-glacial earthquakes and fault movements.

a)   Glen Roy, western Highlands: Earthquake-induced deformation structures are observed in 10,000 year-old lake deposits, and can be related to a surface fault rupture and several landslides. The deformation structures have been mapped over an area of 100 sq. km and display most intense deformation in a central area, with decreasing degrees of deformation in peripheral zones. This zonation is interpreted in terms of varying intensities of ground-shaking during a major earthquake. The field data indicate a magnitude 6.25 event.

b)   Kinloch Hourn, western Highlands: A prominent, 14-km long fault displays evidence for recurrent movement. A magnitude 5.5-6.0 event occurred between 3500 and 2400 years ago, and unquantified movement has occurred since then.

c   Firth of Lorn (west coast): Levelling survey, at two sites, indicates several vertical displacements of up to 3m, of a 10,000 year old raised shoreline.

d)   Lismore (west coast): Lateral fault displacements of c. 0.5m have disrupted present rock and soil morphology and indicate movement in the last few thousand years.

e   Tayside, eastern Scotland: Two sites display soft-sediment deformation structures in late-glacial sands and silts. The structures are interpreted as the result of (unquantified) earthquake ground-shaking.

This field evidence is collectively evaluated in terms of crustal stress, earthquake recurrence and present-day earthquake hazard. Earthquakes as large as magnitude 7 are thought to have occurred but were probably triggered by glacial rebound stesses. Earthquakes upto magnitude 6 have certainly occurred, some as recently as 3000 years ago, and are likely to recur. Present-day surface fault displacements of up to 0.1m are considered likely on fractures favourably orientated with respect to the present-day stress field.

SUMMARY OF CONTENTS

EXPANDED CONTENTS

Palaeoseismicity (continued)

PART III - SCIENCE

PART III A) - FAULT ACTIVITY

PART I

PHILOSOPHY

1. Philosophy of Science
2. Seismotectonic Philosophy
3. Reading this Thesis

1

****
CHAPTER ONE
Philosophy of Science
****

"The mind lingers with pleasure upon the facts that fall happily into the embrace of the theory, and feels a natural coldness towards those that assume a refractory attitude. Instinctively there is a special searching-out of phenomena that support it, for the mind is led by its desires."
wrote T.C. Chamberlin (1879).

All philognosists will know what he means. A scientists loves his ideas, and I love the ideas I have submitted in this thesis. Searching for evidence of earthquakes in the recent geological past in an area where earthquakes are assumed trivial is not only appealing but very close to the bones of inductive science. For it is an issue both within the realm of geology, the long-time queen of inductive science (the earth being our closest sphere of recording past and present to induce the other) and also one close to our perception and concern (Could recent earthquakes have been catastrophic in effect and could they recur?).

So I see this thesis as being deep in the heart of geology and therefore in the thick of the invasion led by Karl Popper who has rejected geology's long-cherished) induction in favour of 'rejection'. Realizing the fallibility of human knowledge, Popper has propagated the theory that men are capable of no more than 'trial and the elimination of error' and that scientific knowledge is conjectural and not logically induced (Popper 1963), such that science comprises the rejection of hypothesis and good science comprises rejectable hypotheses replaced by improved but also eventually rejectable hypotheses. This is the pervading environment within which I have developed my science. It is an excellent framework for the mental sifting of observations, and an approach I have tried to submit to in my study - testing my ideas in the light of field-evidence.

2

However, much as we (scientists) might aim to perform this logic, our practice is more often akin to the romance described by Chamberlin. In my research I set out to find evidence for pre-historic earthquakes; and I found evidence; and I formed hypotheses (which are Popper-ly fallible). Had I set out to find evidence for seismic calm in Scottish pre-history I might well have developed equally fallible hypotheses for the absence of earthquakes. We tend to discover in the direction in which we go. Our science becomes inherently directional as soon as we start thinking since we must start from some position of limited knowledge in order to discover something we did not know before. We are by nature prejudiced. This is somewhat the observation of Kuhn (1962) in 'The Structure of Scientific Revolutions' who saw 'normal science' as the building on a prejudice (or paradigm) and normal scientists as those who consider observation in the context of their 'received view'. A scientific revolution occurs when the basal prejudice is challenged and changed. Good science should then, I suppose, consist not only of testing conjectures (Popper) but also of evaluating prejudice (Kuhn .

In my pursuit of knowledge I carry a prejudice that few of my contemporary scientists hold and one that many consider to be a paradigm of a bygone age (Cavanaugh 1985) - that knowledge of God is revealed to men in the person of Jesus Christ (born 1987 ± 6 years before present) and that he is the source of all things visible and invisible, and that therefore the 'visible-conjectured' comprises only one segment of knowledge. This prejudice gives me a direction in science which is necessarily different from those of, for instance, humanistic prejudice. The pursuit of scientific knowledge is, for me, a limited activity and a transient interest. As a result I do not enjoy the full immersion in it, which humanistic scientists can. My thinking is not completely conjectural. I hope the reader will appreciate my prejudice, determine to evaluate his or her own and decide to accept at least some of my science. Strangely, people readily accept new science and allow it to change their own, but rarely allow new prejudice to influence their own. Perhaps because prejudice is difficult to falsify or prove. As a case in point,

3

Popper's prejudice has been around for quite some time:

> "... like those new teachers of the Greeks, who
> say there is no truth and that the only wise men are
> those who spend their lives in discovering and exposing
> the lies that have been believed in the world."
> (H. Van Dyke 1923).

****

Chapter Two

Seismotectonic Philosophy

****

This is a thesis on geological aspects of the seismotectonics of Scotland. **Seismotectonics** is the study of crustal deformation and the associated release of seismic energy where these have relevance to deformation and seismicity occurring today. It is a discipline driven by the desire to predict and by man's concern about the **vulnerability** of engineered structures and human occupation. What is sought is knowledge of the **risk** of environmental disturbance by earth movement during the lifetimes of structures and civil orders. This risk has been conceptually expressed as

RISK = (environmental) HAZARD x (structural) VULNERABILITY

x (human) VALUE

(Ambraseys 1983).

This study concerns itself with geological aspects of the hazard and specifically the study of the recent geological past to determine the level of present seismotectonic hazard. ['Palaeoseismicity' refers to geological information on seismicity and 'fault activity' refers to geological information on crustal dislocation.] Seismotectonics is an interesting subject since the fundamental geological tenet 'the present in the key to the past' (Hutton 1788) is reversed and predictions about the present and foreseeable future are based on observation of the geological past.

The role of geology in seismotectonic hazard analysis is twofold:

a) Geological processes are crucial to understanding the nature of seismotectonic processes.

b) Geological time provides the necessary sample on which to base the prediction of rare seismotectonic events.

In **Fig.2-1** the upper half of an inverse-logarithmic geological column has been constructed in order to illustrate the

5

relative contribution of geological information in seismotectonic hazard analysis. The whole gamut of geological processes are of general interest (in this study I have occasionally delved right down to the Caledonian! - c.400 million years ago). Most geological processes of relevance to present-day tectonics are covered by the field of **neotectonics**, defined broadly as 'late Cenozoic crustal deformation' (Vita-Finzi 1986). However the time span of interest in the evaluation of seismotectonic hazard is concentrated in the last 10,000 years. Thus a seismotectonic perception is biased towards the present.

The particular role of geology in the prediction of rare seismic events is illustrated in **Fig.2-2**. Instrumental recording of earth noise covers a period of 10^2 years, historical reports provide evidence of earthquakes during the last 10^3 years, and geological and geophysical evidence provides all the remaining information. The historical record provides good information on large events but is increasingly impotent in recording smaller earthquakes (earthquakes less than magnitude 3 are usually not felt by people). This bias becomes even stronger in geological study (where the effects of earthquakes less than magnitude 5 are rarely discernable), so that when considering large, rare earthquakes geological studies become crucial.

This is particularly so in an area like Scotland, where earthquakes are uncommon and the instrumental and historical records contain even less information on rare events. Furthermore, Scotland is not only an area of low seismicity, but it is also a tectonically mysterious area since the effect which the recent ice age has had on crustal deformation is poorly understood. - How fast is the crust rising at present? Will it continue to rise for a long time? Are the earthquakes which have been recorded purely the result of this glacial rebound? Are Scotland's ancient and prominent faults still moving? - Altogether, interesting subject matter!

Small earthquakes occur quite frequently in Scotland. **Fig.2-3** shows instrumental recording of the most recent earthquake to find public attention. This magnitude 3.5 event, of the

29th September, 1986, had an epicentre near Oban and close to the Great Glen fault, and was felt up to 70km away. During the 20-year instrumental record of Scottish earthquakes over 30 events of comparable size (M>3) have occurred. Is this as much as we should expect in Scotland, or could much larger events occur on rare occasions?

****

CHAPTER THREE

Reading this thesis

****

Before conducting any field study, I constructed a simplified flow diagram of the questions of relevance to this study, as then perceived (November 1983). This is shown in **Fig.3-1**. [Production of this diagram was provoked by my attendance at a 'Research Design Course for Geomorphology Students' (sponsored by NERC)]. The study progressed broadly along these lines, and the reader should find answers to most of the questions posed in the flow chart. The final question can be seen as the underlying thread followed during the wanderings of this study - 'What new light does this shed on the potential for earth movements in Scotland?'.

In writing the thesis I have employed the following devices of presentation in order to facilitate and strengthen my argument:

a   I have separated 'review' of previous work (Part II) from new 'science' gathered during the study (Part III), and both of these from derived 'hypotheses' (Part IV). Since the 'science' gathered in this study largely comprises a geologist's interpretation of field-data a large number of hypotheses are nevertheless involved. Consistent with my views on 'Philosophy of Science' (Chapter 1), I consider Part III to comprise as close an approximation to 'pure data' as an observer 'led by his desires' can achieve, and Part IV to be a group of hypotheses based on that data.

b)   I have separated the 'science' into the study of fault-activity (Part IIIA) and of palaeoseismicity (Part IIIB). The difficulty with this is that some field-study sites are discussed in different chapters (e.g. Glen Roy) so that some to-and-froing may be required of the reader. The advantage of this system is that unreasoned association of palaeoseismic evidence and fault movement is avoided and that independent discussion of each theme can be followed unhindered.

8

c) I have written the parts (II & III) on review and science in the
third person (impersonal) and the parts (I & IV) on philosophy
and hypothesis in the first person (personal). This technique
has the advantage of emphasizing the separation of observation
from ideas, and differentiating the portions of the thesis
likely to be of more durable nature from ideas which, with new
observation and prejudice, are bound to change.

d) I have presented the figures and appendices in a separate volume
so that text is easily read alongside illustration. The key
references to each figure are shown in bold type in the text so
that, if required, relevant text may be located when perusing
the illustrations.

It should be possible to begin reading at any chapter in the
thesis, since where previous text is assumed it is cross-referenced.
A 'key word' index is listed in order to locate major terms defined
in the text and used frequently in the thesis. The main localities
referred to in the thesis are illustrated in **Figs. 3-2, 3-3 & 3-4.**

During the course of the study preliminary findings were
published (Davenport & Ringrose 1985, Ringrose & Davenport 1986,
Davenport & Ringrose 1987). The material presented in this thesis
encompasses all that which was included in those publications,
excepting minor alterations. This thesis supersedes those
publications and they are not appended to this volume.

PART II

REVIEW

```
***********************************************************
```
CHAPTER FOUR

The Tectonic Inheritance: Scotland and adjacent areas.
```
***********************************************************
```

4.1 CONTEXT

Because earthquakes are discrete, irregular events, the tectonics of their occurrence is best understood in a neotectonic context, and because their compounded contribution to neotectonic movements may also be irregular, neotectonic processes are only properly understood in terms of long-term tectonics. In this way earthquake events can be more safely judged as being either anomalous or characteristic and as rare or frequent (i.e. the seismotectonic evaluation).

Thus this chapter considers long-term tectonics and structural composition where they have a bearing on the neotectonics of Scotland, and the following two chapters peruse significant earthquake data within the neotectonic timescale itself.

4.2 THE LITHOSPHERIC CONTINUUM

The locations of geophysical profiles mentioned in this section are shown in **Fig.4-1.**

4.2.1 The depth of the Moho

Fig.4-2 shows line drawings of unmigrated WINCH seismic profile data produced by the British Institutions Reflection Profiling Syndicate (BIRPS) (Brewer et al. 1983). On this profile the Moho can be seen as a strong and continuous reflector under the Caledonian Foreland at a depth of 26-30km. However, under the Caledonian orogen the Moho is discontinuous though still apparent at around 30km. Going east into the North Sea the Moho can be observed on SALT profiles to shallow to about 20km depth under the Central Graben (Barton et al. 1984).

4.2.2 <u>The base of the lithosphere</u>

The thickness of the lithosphere in Britain and offshore areas is not well defined, but studies of shear wave velocities (Stuart 1978, Clark & Stuart 1981) give the following estimates:

a) The Caledonian orogen: a lithosphere 110-190km thick with a well developed low velocity layer beneath, and a velocity profile similar to typical continental aseismic platforms.

b) The Precambrian basement terrain of SE England: a lithosphere at least 140km thick with a much less pronounced, or absent, low velocity layer, and a shield-like velocity profile indistinguishable from profiles for the Baltic shield and Hercynian France.

c) The North Sea: a lithosphere thickness of between 80 and 90km with a low velocity layer between 50 and 150km thick beneath, and a velocity profile within the aseismic continental platform category of Knopoff (1972).

Thus onshore Britain has a thicker lithosphere than the offshore North Sea, but in terms of velocity profiles NW Britain and the North Sea are similar (with a well-developed low velocity layer) and markedly different from the Precambrain terrain of SE England (with a poorly developed low velocity layer).

4.2.3 <u>Rheology</u>

The two most fruitful methods of determining lithospheric rheology are the study of the characteristics of transmitted elastic waves and the modelling of observed response to applied deformations. The second of these is considered in chapter eight and the first forms the basis to this initial inquiry.

The WINCH reflection profile brought to attention the following clues concerning the behaviour of the lithosphere:

a) The upper crust over much of the line is seismically transparent, unlike the lower crust which contains abundant reflectors. Very few surface geological discontinuities appear to be significant in the upper crust, in terms of impedance

12

contrast (the exceptions are discussed in §4.3.2, below). This feature will in part be a function of the resolution of the profiling frequency used, nevertheless the profile does tend to suggest a uniformity in rheological behaviour in the upper crust throughout the Caledonian Orogen.

b) The lower crust, having more abundant reflectors, shows a marked change in reflectivity beneath the Southern Uplands at the Iapetus suture. North of the Suture and south of the Highland Boundary Fault the seismically transparent nature of the upper crust extends down to the Moho. This portion of the crust may well have a correspondingly different rheology.

c) Strong and continuous reflectors in the upper mantle, NW of the Highland Boundary Fault, are most reasonably interpreted as planes of localized strain (McGeary & Warner 1985) and seem to imply brittle behaviour deep down in the lithosphere (the inclined Flannin thrust reflector is observed to a depth of 80km). The possibility that these are palaeo-rheological boundaries which indicate little about present rheology, cannot be discounted. However, the fact that the Outer Isles Thrust both controls Palaeozoic and Mesozoic sedimentation and displaces the Moho (extending into the mantle) suggests that at least the uppermost mantle is presently capable of supporting localized zones of deformation (Peddy 1984).

These clues suggest that the Caledonian orogenic belt has a relatively uniform upper crustal rheology, but is seperable into Southern Uplands and Highlands portions in lower crustal and upper mantle rheology. The Highland portion (NW of the Highland Boundary Fault) would appear to behave elastically to much greater depths than the Southern Uplands portion (between the Highland Boundary Fault and the Iapetus suture).

This division into two rheological provinces seems to be supported by the following indirect data:

a) The LISPB refraction experiment also shows a marked difference in velocity profile between the Southern Uplands and the

13

Highlands, though the location of the change is less clear (Bamford 1979).

b) Regional gravity data show a marked difference in character either side of the Highland Boundary Fault according with the two provinces (Hipkin & Hussain 1983).

c) Regional magnetic anomalies, although revealing other major discontinuities such as the Great Glen Fault and the Southern Uplands Fault, also suggest a major province change at the Highland Boundary Fault "marked by an abrupt transition from a chain of positive anomalies to a chain of negative anomalies" (Hall & Dagley 1970).

d) The division accords with the metamorphic province and the basin-and-accretionary-wedge province of surface geology (c.f. Anderton et al. 1979).

4.2.4 Concluding statement

Scotland appears to have the velocity profile of a typical continental aseismic platform. To the east and north the lithosphere thins considerably towards the North Sea grabens. To the south, under Hercynian England, the velocity profile develops shield-like characteristics. The low velocity layer (asthenosphere) is well developed under Scotland and the North Sea, but poorly developed under SE England.

The Scottish area appears to be rheologically divisible into two crustal provinces:

a The metamorphic province (NW of the Highland Boundary Fault) behaving elastically to great depths, even into the mantle.

b) The basin-and-accretionary-wedge province (SE of the Highland Boundary Fault) revealing few seismic reflectors and suggesting a more plastic behaviour.

4.3 LITHOSPHERIC DISCONTINUITIES

A review of considered origins for the many fault and fracture sets of Scottish geology is not regarded as appropriate here. It suffices to document what is observed alongside a general association

14

with the main tectonic episodes. Some consideration of age will be made when discussing fault displacements in section 4.4 below.

Major faults discussed below are shown in **Fig.4-3**. The following abbreviations will be used in this section: GGF-Great Glen Fault, HBF-Highland Boundary Fault, and SUF-Southern Uplands Fault.

4.3.1 Surface discontinuities

The vast majority of fractures originate in three main episodes of tectonism: Caledonian orogenesis, Permo-Carboniferous rifting, and Tertiary volcanism. The resulting dominant fault and fracture trends evident across onshore Scotland are:

a) NE-NNE trending Caledonian strike-slip faults, best developed in the Central Highlands and the eastern Northern Highlands. This set of faults is the most prominent, having the most extensive fractures and including the major province boundaries of the GGF, HBF and SUF (Fig.4-3).

b) WNW-NW trending faults, best developed in the Northern Highlands (Fig.4-4). These may be of Caledonian origin, although association with similar trends in the southern North Sea suggests they are of Permo-Carboniferous age (Threlfall 1981). Some have also been active during the Tertiary (Johnson and Frost 1977).

c) E and ENE trending Permo-Carboniferous rift and wrench faults of the Midland Valley (Fig.4-3), possibly also developed in the SW Highlands.

d) NE trending fractures of the Tertiary volcanic rift developed in the Inner Hebrides and south-west Scotland (Fig.4-4).

Other less prominent fracture trends are:

e) East-west faults of uncertain origin in the south-west Highlands. These are apparent as topographic features between the Caledonian shear zones (Fig.4-4). They may represent axial traces of folds associated with late Caledonian sinistral shear (Threlfall 1981) and are known to cut Devonian rocks (Johnson and Frost 1977).

15

f) Radial and concentric fractures associated with centres of Tertiary volcanism. Auden (1954) noted a radial pattern of fractures appearing to converge on a centre near Eigg in the Inner Hebridies, and some regional arcuate features in the NW Highlands which appear to circle the same centre - **Fig.4-4.**

g) A few fractures appearing to radiate from the Cairngorm mountains (Fig.4-4) (Auden 1954).

These less prominent trends may result from selective emphasis of previously existing discontinuities by volcanic and glacial-loading tectonics. The Tertiary volcanism certainly introduced the new local set of NW-trending fractures, but more distant effects (such as Auden's suggested concentric arcs) were probably re-activation. The discussion of glacial re-activation of faults will emerge in several sections of this thesis, however several suggestions relating fault distribution patterns to glacial loading are of preliminary interest:

a) Auden's radiating fractures from the Cairngorm centre (Fig.4-4).

b) The suggestion of Bostrom (1984, pers. comm.) that fracture patterns associated with the ice margin may be evident in the fractures of the Western Isles.

c) The general prominence of fractures in the western Highlands, largely due to exposure by glacial erosion, but possibly also emphasized by re-activation.

4.3.2 Deep discontinuities

The British Geological Survey 'Tectonic Map of Great Britain' describes only two features as being 'deep seated faults, bounding blocks and controlling sedimentation' - the HBF and the SUF (Fig.4-3). This may have been the case in the Upper Palaeozoic, however the more recent data of the WINCH profile has brought to attention many basins of Mesozoic and Cenozoic age whose sedimentation is controlled by other deep-seated faults. These are the half grabens of the Minch basin against the Minch Fault, the North Lewis basin against the Outer Isles Thrust, and the Colonsay

basin against the GGF; and the synclinal basins of the Stanton trough and the Solway basin (Fig.4-2). What is surprising is that neither the HBF nor the SUF is associated with pronounced Mesozoic basin formation, and that neither appears as a reflector in the profile. One may argue that these faults are too steep or lack the impedance contrast to be imaged properly, but their contrast to the steep, southerly dipping and well-imaged GGF reflector, seen right through the crust, suggests a corresponding contrast in geological significance.

The WINCH profile clearly indicates a profound role for a number of Caledonian thrusts and steep faults in the currently developing tectonics of the lithosphere. The most prominent among these are the Outer Isles Thrust, the Minch Fault, the GGF, the Islay splay of the GGF, the Iapetus Suture, and to a lesser extent the HBF. Several of these faults appear to extend into the upper mantle, where also the Flannan Thrust appears as a strong reflector.

4.3.3 Offshore discontinuities

The prevalent onshore trends are clearly evident on the continental shelf immediately offshore (Fig.4-3). West of Scotland, the shelf geology is dominated by major NE trending Caledonian faults (the GGF, the Camasunary Fault and the Minch Fault), but NW faults which are thought to have accompanied Tertiary igneous activity, are seen and show small dextral offsets of the Caledonian features (McQuillin & Binns 1973). West of Shetland the shelf is dominated by NNE Caledonian faults which were reactivated during the development of deep Mesozoic to Tertiary sedimentary basins (Watts 1971). The Moray Firth shelf shows two dominant fault trends, a NE and a NW system, both corresponding to the onshore trends of the Northern Highlands, but also a subsidiary ENE trend which can be related to the Midland Valley fault trend (Threlfall 1981). However, further offshore in the Viking graben area the northerly graben faults appear superimposed on less prominent NE and NW trends (Threlfall 1981).

Smoothed gravity anomaly data (Donato & Tully 1985) provide a simpler perception of fault orientation, and suggests a gross

division of the shelf into two basic areas:

a) The West of Scotland, Shetland and Moray Firth areas showing NE-ENE and NW fault trends (basement dominated).

b) The Viking to Central Graben areas showing N-NW fault trends (post-Palaeozoic basin dominated).

4.3.4 Concluding statement

Across onshore and offshore Scotland major north-easterly Caledonian faults form the first order grain to the lithosphere, commonly extending from surface to mantle, and controlling offshore basin development. A complex net of other discontinuities indicates a multi-directional second-order grain which has been variously and locally developed by the later tectonism of Permo-Carboniferous rifting, Tertiary volcanism and Quaternary glaciation.

A different grain has developed in the basins of the North Sea where northerly and north-westerly grabens have developed during the Mesozoic and Cenozoic.

4.4 STRAIN HISTORY

4.4.1 The tectonic environment

Since attaching itself to Europe during the Caledonian suturing, Scotland has never been quite sure of its tectonic affinity, whether part of the 'continental' Europe or 'oceanic' North-Atlantic regimes. Various events have been associated with processes of Altantic rifting:

a) the late Carboniferous proto-Atlantic rifting, resulting in the Permo-Carboniferous dyke swarm of Central Scotland (Russell & Smythe 1983, Hazseldine 1984),

b) the Mesozoic opening of the North Atlantic resulting in half-graben basins off western Scotland (McQuillin & Binns 1973), and

c) the Cenozoic opening of the Norwegian/Greenland sea manifested in the Tertiary volcanic activity and associated tectonics (Emeleus 1983).

Other events seem to result from continental tectonism:

18

a) the intracontinental block movements of the Middle Jurassic (Anderton et al. 1979),

b) late Cretaceous basin inversions induced by compressional and strike-slip movements related to Alpine deformation (Zeigler 1982), and

c) the distal effects of Alpine orogenesis, whose stress direction is perhaps reflected in Tertiary dyke orientation (Holgate 1969) and in the orientation of Pleistocene faulting in England (Shotton 1965), and which may have caused the eastward tilting of the British Isles (Anderton et al. 1979).

This duality, which arises from Scotland's location at the edge of a continent undergoing severe compession to the south and active spreading to the west, has resulted in a rapidly changing tectonic history and a presently evasive tectonic regime. Furthermore these long-term tectonic regimes have been interupted by the 'anomalous' tectonics associated with Tertiary volcanic loading and Quaternary ice loading.

4.4.2 Mesozoic epeirogenesis

It was during the Mesozoic that Britain's present tectonic duality was born with the opening of the North Atlantic in the lower Cretaceous. During this time N.W. Europe saw several episodes of uplift and subsidence in a complex succession of differential block-movement, mostly bounded by ancient faults (Anderton et al. 1979). Block movement was particularly marked in the middle Jurassic and early Cretaceous, however, by the late Cretaceous fault-block topography was eliminated and overlain by a blanket of pelagic chalk, during a period of relative stability. The phase of uplift following this continued into the Tertiary. Most of Scotland remained above sea level throughout the Mesozoic; peripheral transgressions are evident in small outliers found onshore in the west and north-east.

4.4.3 Tertiary epeirogenesis

The begining of the Tertiary saw the commencement of a major period of uplift, deformation and widespread erosion, throughout the British Isles. Offshore basins continued to subside, receiving up to

4km of sediment.

Remnants of dissected platforms are seen throughout the Highlands testifying the uplift of former base-levels during the Tertiary. The most prominant levels are of Neogene age, as they 'bevel igneous masses and mid-Tertiary folds and faults' (George 1966). This Neogene surface is inclined gently eastwards from about 1000m in the Hebrides (George 1966) to about 100m in the Buchan region (Hall 1985). Its presence is confirmed in reconstructions of Tertiary drainage, which flowed west to east (Holgate 1969) - Fig.4-5. Greater uplift in the west is also evident in the degree of Tertiary dyke exposure. A major change in the level of exposure across the Great Glen Fault suggests downthrow to the south-east of approximately 0.5km (Speight & Mitchell 1979), and may indicate uplift in terms of block movement as well as regional tilt.

This Neogene surface is evident throughout Britain (for example at 450m in the Peak district of Derbyshire (King 1977)) and descends to a coastal plateau at 200m, or lower, which is dated as Pliocene in southern England (George 1974). Onshore uplift and offshore subsidence of Pliocene strata in southern England indicate c.800m of late Tertiary crustal warping (King 1977). This would appear to correlate with Holgate's (1969) claims for gentle folding, along east-west axes, of the Neogene surface in the Central Highlands.

Thus uplift in Britain has continued throughout the Tertiary, onland uplift being concomitant with offshore subsidence.

4.4.4 Quaternary epeirogenesis

Tertiary uplift is likely to have continued on into the Quaternary; however the onset of glacial isostatic movements makes this difficult to verify. Knowledge of pre-glacial shorelines is needed, but lacking. There are several candidates which have been nominated as such, none of which is categorically outwith the influences of glacial isostasy:-

   a) Rock platforms at heights of c.35m in the Inner Hebrides (Bailey 1924, Sissons 1982). Some of these may be pre-glacial, but Sissons argues that most are glacial and formed under similar

20

conditions to the Main Lateglacial Shoreline (§7.5.2). Their
geographical distribution along the ice margin and their
bevelled morphology strongly support this hypothesis.

b) Marine shell beds, beneath till, at heights of upto 140m located
in the east and south of Scotland. These are certainly
pre-glacial and contain temperate and arctic shell species.
Sutherland (1981) argues that these were deposited in the early
stages of ice-cap growth, when the crust was initially depressed
(i.e. that their elevation results from glacial isostacy).

c) Submerged platforms at depths of 30 to 90m around the west and
north coasts, and inclined northwards (Flinn 1973, Hall & Rashid
1977). These are taken by Flinn to indicate northward tectonic
tilting, but could well be isostatically tilted.

d) Shore levels similar to the present day's. Notches, thought to
be interglacial shorelines, occur at approximately present
sea-level ($\pm$10m) (Sissons 1983), could also contain
preglacial levels.

The most reasonable synthesis is that the first three of these
represent glacio-isostatic and -eustatic shorelines, that tectonic
epeirogenesis is not resolvable, and that the pre-glacial level was
close to that at present. This seems reasonable if a comparison of
uplift rates is made. Constant uplift since the Neogene would occur
at a rate of 0.05m per millennia in the west of Scotland (assuming a
1000m Neogene baselevel), whereas present isostatic uplift is around
2m per millennia. (c.f. uplift in the Himalayas of around 0.3m per
millennia. (Walcott 1973)). An analysis of earth movements and
sea-level change in the last 9000 years, by regression analysis of
all known U.K. data, suggests that components of tectonic sinking in
southern Britain and possibly uplift in the north are present, and of
the order of 1m per millennia (Flemming 1982).

Thus there is no conclusive evidence of tectonic uplift in
Scotland during the Quaternary. However, since glacio-isostatic
movements were imposed on a portion of crust that had been rising
throughout the Tertiary, it is likely that this tectonic uplift is
continuing. With this proviso, Mitchell's (1977) demarcation of three

main tectonic provinces shown in **Fig.4-6** provides an acceptable summary of Quaternary epeirogenesis.

4.4.5 Mesozoic fault movements

The offshore basins of the Moray Firth, Irish Sea, Hebrides, and the north-west continental shelf had developed as faulted grabens through most of the Mesozoic. Most of these faults were NNE trending, with downthrow to the SE. In the inner shelf area basin thicknesses of over 2km were achieved (Chester et al. 1983) Onshore, the Helmsdale and Great Glen Faults were active during this time, having downthrows of the order of a kilometre, together with several kilometres of dextral offset (Chester & Lawson 1983). Most of this activity had ceased by the late Cretaceous.

4.4.6 Tertiary fault movements

Tertiary fault activity was concentrated in around the Hebridean volcanic province - **Fig.4-7**. These Tertiary faults comprise three groups:

a) NNE trending faults bounding half grabens on their SE sides, namely the Minch fault, the Camasunary fault, the Great Glen fault and its southern splays (i.e. continuing activity on some of the Mesozoic graben faults). Displacements on these faults are only evident in the Palaeocene lavas (with downthrows of several hundred metres), except for the Great Glen fault, north of Colonsay, where faulting is evident well into the post-lava sediments (Binns et al. 1975).

b) NW trending faults, offsetting the NNE faults. These are thought to result from the onset of NE-SW extension associated with dyke intrusion (Binns et al. 1975).

c) Faults close to the major volcanic centres and associated with the collapse of lava plateaux. These are not extensive but have substantial throws; 760m on Rassay and 300m across the Inninmore fault, Morvern (Bailey 1924, Binns et al. 1975).

Except for the Great Glen, these fault movements are restricted to the lowest Tertiary (Palaeocene to Eocene), after which only minor basin subsidence occurred in the Inner Hebrides, and was flexural

rather than fault-bounded in form (Evans et al. 1982).

4.4.7 Quaternary fault movements

The following comprises a complete list of reported, onland, Quaternary fault movements:

a) A 50m downthrow to the north, across the Southern Uplands Fault, of a buried channel of the river Nith, occurring some time between the Upper Cretaceous and the onset of glaciation (Lumsden & Davies 1965).

b) Variations in height of the 'high raised coastal platform' of the Inner Hebrides (c. 15,000 years old), suggesting tectonic warping and possibly faulting, especially on the Isle of Rhum (Peacock 1969, 1983).

c) Tilting, and up to 2m vertical offset, of the Main Rock Platform on Mull, (c.10,500 years old) (Gray 1974).

d) 2m vertical offset of the 'parallel roads' of Glen Roy (glacial lake shorelines), (c.10,500 years old) (Sissons & Cornish 1982).

e) Vertical offsets of between 1 and 2m of buried shorelines in the Forth Valley, occurring between 9,600 and 6,500 years BP – Fig.4-8 (Sissons 1972).

The first of these is probably Tertiary in age, and the rest occurred during or soon after glacial conditions. These have not been placed in any tectonic context. The prevailing opinion is that these displacements occurred under anomalous glacial conditions, and that surface faulting of Quaternary age is otherwise unlikely to occur (e.g. Ambraseys & Jackson 1985, p.58).

Offshore, no surface faults have been reported. Quaternary subsidence in the Central graben has been proceeding at ten times the mean Tertiary rates, but appears to be aseismic (Muir Wood 1985).

4.4.8 <u>The Great Glen Fault saga</u>

There is no doubt that this discontinuity has been a major locus of movement during the Phanerozoic. The history of its movement has been a subject of intense debate. The evidence and arguments are conflicting, but those worthy of consideration are listed below.

a) Kennedy (1946) was the first to suggest large strike-slip movement. He postulated a sinistral shift of 105km during the Devonian, based largely on matching the Foyers and Strontian granites. The validity of this match is questionable, particularly in view of geochemical studies showing major differences in the two granites (Harris 1983).

b) Holgate (1969) accepted Kennedy's Devonian shift, but revealed evidence for 30km dextral shift during the Tertiary. His evidence included matching Old Red Sandstone outcrops, Mesozoic outcrop and morphology, Tertiary dyke distribution, and ancient (pre-Tertiary) and Tertiary drainage patterns. He also postulated downthrow to the southeast during the Devonian sinistral movement and to the northwest during the Tertiary dextral movement.

c) Winchester (1973) argued for a 160km sinistral shift of regional metamorphic features. However, an alternative match by Garson and Plant (1972) would result from a 120km dextral offset.

d) Speight and Mitchell (1979) refuted most of Holgate's Tertiary Dextral movement (only allowing vertical movement of c. 0.5km, downthrow to the SE) and postulated a 7-8km dextral shift of Permo-Carboniferrous dykes, before the Tertiary.

e) Seismic profiles in the Moray Firth indicate a 'scissor' pattern of faulting in Mesozoic strata, with variable downthrow, mostly to the south-east, and consistant with moderate dextral displacements during the Mesozoic (Chester & Lawson 1983).

f) Seismic profiles across the fault, west of Colonsay, indicate downthrow to the south-east of post-lava Tertiary sediment, amounting to several hundred metres (date of last movement unknown) (McQuillan & Binns 1975).

g) The main trends in regional magnetic anomalies 'appear to be displaced for the most part sinistrally' (Hall and Dagley

24

1970).

In synthesis, the following is admitted:

1) Major sinistral displacement (c. 100km) probably occurred during the lower Palaeozoic.

2) Post-Palaeozoic dextral displacement is likely, probably occurring during the Mesozoic and amounting to offset of c.7km.

3) Vertical movements of Tertiary age are apparent in the south, and of the order of hundreds of metres.

Some new light on the history of Great Glen faulting will be emitted in chapters 9 and 10.

4.4.9 Concluding statement

Since the Mesozoic rifting and Tertiary volcanism Scotland has developed an increasingly stable tectonism. This relative quiescence was interrupted by the Quaternary glacial-loading tectonism. However, throughout the Cenozoic response to distant Alpine compression and North Atlantic tension has been evident, mainly in epeirogenesis and warping, but also by movement on major discontinuities. This gentle strain-response is likely to be continuing, despite being presently masked by glacio-isostasy.

4.5 PRESENTLY IMPOSED STRESS

This section considers the present regional stress field in NW Europe. Analysis at this scale (NW Europe) essentially provides a 'low pass filter' to resolve purely tectonic stresses. Stresses associated with glacial loading and re-bound, and stress information derived from geological study in Scotland will be considered in chapter 17.

4.5.1 Stress measurements in NW Europe

It is now well established that the stress parameter of most use to regional study is the direction of maximum principal compression (Scheidegger 1982). **Fig.4-9** shows most of the available stress direction measurements in NW Europe. The greatest concentration of measurements occurs in the Alpine Foreland area of central Europe,

where a clear NW-SE trend of maximum compressive stress directions is evident, measurements having a mean of 142+20° (Ahorner 1975). Measurements based on fault-plane-solution averages have very similar compression-axis directions to insitu measurements (Scheidegger 1982). The magnitudes of insitu stress measurements show a clear decrease in excess stress (ie. non-lithostatic) from the Central Alps (upto 36 MPa) northwestwards into the foreland (less than 8 MPa) (Illies et al. 1981).

In Fennoscandia a NNE compression (similar to central Europe) is evident in the north and east, but in the western, coastal zone there is a clear E-W direction of maximum compressive stress. This coastal zone is the only area of NW Europe showing a peculiar stress direction on a regional scale. A seismically active belt immediately off this coast may well be associated with this stress field.

Apart from this NW Europe shows a remarkably consistent north-westerly direction of maximum principal compression.

4.5.2 Clues from NW Europe tectonics

There are a number of indicators of present regional stress in natural strain gauges of Cenozoic tectonics. They are best listed, and followed by a coalescing paragraph.

a   **The Alpine foreland:** Alpine folding terminated during the late Miocene; foreland folding continued up to the mid-Pliocene, since which time only (tectonic) isostatic rebound has occurred (Baumann 1981).

b)   **The Upper Rhine graben:** The response of the Rhinegraben system to Alpine tectonics has involved extensional rift formation during mid-Eocene to lower Miocene times, followed by a period of inactivity. Rifting, under sinistral shear, recommenced during the Pliocene and has continued to the present. This present tectonism is resulting in high local vertical movements (upto 1.0mm p.a.), movements during the last 20,000 years being 10 times average rates during the Pleistocene (Illies et al. 1981).

c)   **The Lower Rhine graben:** 200m of extension since the early

Quaternary has been accomplished on a suite of NW-SE trending, mostly dip-slip faults which are still active (Ahorner 1975).

d) **SE England and northern France:** A NW trending system of fractures of Neogene age indicates a regime of NE-SW tension between early Miocene and early Pleistocene times, apparently cogenetic with the normal faulting of the Lower Rhine embayment. No fractures are observed to cut the onshore Pleistocene (Red Crag) deposits. (Bevan & Hancock 1986).

e) **Cornwall:** A prominent NNW joint set is the main source of thermal brines in mine workings (Klein and Brown 1983) and is similarly orientated to the Sticklepath fault displaying major Tertiary movement (Anderton et al. 1983).

f) **North Sea basins:** Quaternary subsidence rates in a series of three en-echelon NW-SE basins in the North Sea are up to ten times faster than the Tertiary rates (Muir Wood 1985).

Each of these cases of Cenozoic strain capitulates to the present NW-SE direction of compression evident in insitu measurement. There are indications of acceleration of strain rates from the Tertiary into the Quaternary, but also evidence for cessation of tensional fracturing in the early Quaternary (in SE England). The correlation of measured stress with late Cenozoic tectonism makes it clear that the regional stress field primarily results from active intra-plate tectonics. In central Europe this is envisaged as a stress flux from the Alps to their foreland, and is thought to be largely post-orogenic and topographic in origin (Illies et al. 1981). However further away from the foreland, towards the Atlantic, this topographic effect is likely to diminish and be superceded by other components such as 'ridge-push' compression from the North Atlantic spreading ridge (Muir Wood 1985).

4.5.3 The state of stress in Britain

There are only six insitu stress measurements in Britain which have data on both magnitude and direction (Klein & Brown 1983). They are shown in **Fig.4-9** and detailed in Table 4-1. Three fault-plane solutions have been derived and are also shown in Fig.4-9.

Table 4-1 <u>Six British in-situ stress measurements</u>
(From Klein & Brown 1983)

Locality	Depth (m)	Rock type	Magnitude (MPa), Orientation (Dip/dip direction)		
			σ_1	σ_2	σ_3
1) South Crofty mine, Camborne.	790	Granite	45.6(01/129)	19.8(89/012)	12.9(01/220)
2) Channel Tunnel, Dover.	48	Chalk	1.3(horz/024)	0.8(vert)	0.3(horz/114)
3) Dinorwic pumped storage scheme, N. Wales.	320	Slate	17.6(26/300)	8.0(26/198)	6.4(52/074)
4) Meadowbank salt mine, Cheshire.	144	Halite	3.01(52/285)	2.35(19/169)	1.55(31/066)
5) Ireland.	200	-	(horz/164), average horizontal stress = 17.2		
6) Camlough pumped storage scheme, N. Ireland.	195	Dolerite	27.0(13/027)	22.9(08/295)	11.6(74/165)

[All measurements by overcoring methods]

The six insitu stress measurements show little consistency in direction and do not appear to form a clear continuation of the Alpine stress field. However the two NE trending stress measurements (Channel Tunnel and Camlough pumped storage scheme) are both shallow and affected by local factors. The channel tunnel measurements were made at a depth of 48m and were only 75m from an 80m high cliff. The Camlough pumped storage scheme, at a depth of 195m, is situated beneath the slope of a 580m mountain and is within a complex geology of an intrusive ring structure (Klein & Brown 1983). Local topographic and excavation stresses have probably given rise to measurements deviating from the regional field in both cases.

The remaining four measurements have maximum horizontal compressive stress directions orientated between 309° and 349° (i.e. NNW). They each have magnitudes approximating to expected lithostatic stress (Klein & Brown 1983).

In Scotland, the only in situ measurement, at Cruachan pumped storage scheme, provided only magnitude data, and had a vertical stress equivalent to three times the overburden load and a north-south, horizontal component of about four times the overburden load. This was interpreted as implying major, local stress

28

concentration (Knill 1972).

The three fault-plane solutions shown in Fig.4-9 are for events at Kintail, NW Scotland, 1974 (Assumpcao 1981); Carlisle, 1979 (Marrow and Roberts 1984); and North Wales, 1984 (Turbitt et al. 1985). It is not advisable to use single solutions as regional stress measurements, however all three have compression axes consistent with roughly NNW maximum horizontal compressive stress. In North Wales the solution has particularly good correlation with the Dinorwic stress measurement. The Carlisle and Kintail solutions tend to suggest a more northerly compression in this part of the U.K.. All three have a strike-slip form (the Carlisle data could support a thrust component, but strike slip on a steeply inclined fault is favoured).

4.5.4 Concluding statement

British stress measurements clearly show less uniformity than the rest of NW Europe (partly because of the sparsity of measurement). However, a general continuation of the northwesterly Alpine compression is evident, but trending towards NNW rather than NW, especially in northern Britain.

****
CHAPTER FIVE
Fault Activity
****

This chapter considering fault activity also encompasses the field of palaeoseismic study. The following chapter considers only the subset of palaeoseismicity involving surface deformation resulting from earthquake-derived ground shaking.

5.1 DEFINITIONS OF FAULT ACTIVITY

Fault activity essentially refers to displacement (at or near the surface). A present-day **active fault** has been defined as one which has moved within the Holocene Epoch (10,000 years) and which therefore may move in the near future (Bonilla 1970). Strictly speaking fault activity may be aseismic as well as seismic, but an association with macroseismicity is usually advocated in defining what is implicitly **seismically active faulting**. In engineering studies the concept of the **capable fault** is more precisely defined. A fault is considered capable if it shows:

a) evidence of single movement within the past 35,000 years or multiple movements within the past 500,000 years,

b) macroseismic activity associated with it, or

c) structural relationships to known capable faults such that movement of the one may cause movement of the other.

(USNRC, 1973)

The association of fault activity with earthquake events enters the realm of **earthquake stratigraphy,** which involves the correlation of geological manifestations of earthquakes to seismic events. Earthquake stratigraphy encompasses three areas of study.

a) **Instrumental seismicity:** the instrumental recording and analysis of the energy released from modern earthquakes (essentially post 1904).

b) **Historical seismicity:** the historial record of civil and human damage resulting from earthquakes (usually back to around

30

2500 years BP).

c) **Palaeoseismicity:** the recording of pre-instrumental
earthquakes by bedrock structures (faults and fractures),
morphological features (shorelines, streams etc.),
sedimentological criteria (slumps, seismite layers, faults) and
geophysical and geochemical properties in sediments and rocks
(e.g. palaeomagnetic intensity) (Mörner 1985).

The combination of these three areas gives good earthquake
stratigraphy. Ignorance of any one area gives rise to incomplete
stratigraphy. For example, empirical relationships established by
instrumental and historical studies can be used to quantify
palaeoseismic events, and, palaeoseismic events can provide
elucidation of the recurrence levels of modern seismicity.

5.2 INTRAPLATE SEISMICITY AND FAULTING

Although about 90% of the world's earthquakes occur along plate
boundaries, there is something of a mystery surrounding the remaining
10%, the intraplate earthquakes. Because of the clear dominance of
plate-boundary seismicity, intraplate activity has tended to be
regarded as 'anomalous'. For example, several large earthquakes in
the eastern United States (the New Madrid events of 1811-12, up to
M=8.5, and the Charleston 1886, M=7 event) having unusually large
damage areas have been attributed to a separate class of
'superearthquakes' (Seeber 1986). The mystery arises from the
mounting evidence that although intraplate areas are subordinate in
terms of bulk seismicity, they may still be the locus of very large,
and also very rare, earthquakes.

Being rare events these large intraplate earthquakes are
particularly conducive to palaeoseismic study. In the Charleston
area, palaeoseismic studies (Obermeier et al. 1985) indicate at least
two prehistoric earthquakes of comparable size to the 1886 event, and
on the Meers fault, Oklahoma, similar studies (Kerr 1985) indicate at
least three displacements of over a metre in the last 10,000 years on
a fault showing no instrumental seismicity.

The tectonics of intraplate seismicity is poorly understood. Sbar and Sykes (1973) have pointed out that the eastern U.S. earthquakes seem to occur where there is an association of high stress and unhealed faults; activity being seen primarily as re-activation of late-Palaeozoic and younger faults. Gross epicentral lineations evident in the seismicity of the eastern U.S. and northern China lend support to this association and are the basis of supositions for major block movements along sub-plate boundaries (Seeber 1986). In NW Europe the Rhine graben belt of seismicity has been termed one such 'sub-plate boundary' (Muir Wood 1983, 1985), and the major graben-faults in seismically active, axial zones of the North Sea may also be a manifestation of a sub-plate boundary (Davenport 1983). Finally, there is much to suggest that intraplate seismicity is highly variable in time; much more so than plate-boundary seismicity. The Meers fault showing pre-historic but not historic activity has already been mentioned, and studies in the south-eastern U.S. show major changes in seismicity levels over the historic period (Seeber 1986). This is in contrast to plate-boundary areas where, for example, the palaeoseismic studies of Sieh (1978) on the San Andreas Fault, California indicate a very regular occurrence of large earthquakes. Non-stationarity of seismicity has also been described in the diffuse plate-boundary of the Middle East (Ambraseys & Melville 1982).

5.3 GLACIAL FAULTING AND SEISMICITY

There are now many examples of major fault movements occurring soon after major glaciations. The most complete record has been compiled for Fennoscandia by Mörner (1978, 1985). In Sweden there are at least 26 recorded examples of faults with throws exceeding one metre; most of these can be connected with the time of deglaciation, but at least one occurred as recently as early historic (Viking) times. The most spectacular example is the Pärve Fault in northern Sweden which is 150km long and vertically offset by up to 25m (Lagerbäck 1979). These fault movements have been associated with large earthquake events (postulated upto M=8) whose ground shaking is arguably recorded in 'seismic varves' (varve horizons showing

faulting, fracturing, turbidity currents and erosion on a regional
scale) and areas of landsliding and boulder moraines (associated with
fault lines occurring in roughly ellipse-shaped areas).

Similar, but less complete examples are found in Norway (Mörner
1978), Finland (Kujansuu 1964) and Russia (Lundqvist & Lagerbäck
1976). Evidence from other glaciated areas includes deformed
glacial-lake-sediment correlated to an earthquake in Quebec, Canada
(Adams 1982), faulting inferred from shoreline data around Lake
Agassiz, U.S.A. (Walcott 1970) and post-glacial 'pop-up' faults in
New York state, U.S.A. (Sbar & Sykes 1973). (Examples from Scotland
have been documented in §4.4.7.)

The association of large fault movements with the period of
ice-decay is thought to be the consequence of the high rates of
glacio-isostatic uplift during this time - **Fig. 5-1**. This
association is clear from the Swedish evidence. Its theoretical
validity is considered in section 8.3.2. What is less clear is the
relation of seismicity rates to glacial loading and rebound. The
following points are of relevance:-

a) Areas supporting present-day ice caps (Antarctica and Greenland)
   show low levels of seismicity (Sykes 1978).

b) Present Fennoscandian seismicity shows no obvious correlation
   with post-glacial uplift rates, but rather displays a tectonic
   origin by virtue of localized seismic belts (suggesting block
   movement) and energy-release rates which correlate with
   world-wide (tectonic) data (Båth 1978).

c) Recorded seismicity in northern Canada appears to correlate with
   the peripheries of gravity lows, thought to correspond to areas
   of maximum flexure associated with post-glacial uplift (Basham
   et al. 1977, Lambert & Vanicek 1979).

d) Many palaeoseismic studies suggest high levels of ground shaking
   co-incident with fault activity soon after deglaciation (Adams
   1982, Morner 1985, Davenport & Ringrose 1987).

In synthesis, the relationship between present seismicity and
post-glacial rebound is unclear; something of a relationship exists

in Canada, but little in Fennoscandia. With regard to Fennoscandia, Mörner (1980b) has argued that glacial uplift is now complete and that remaining uplift is of tectonic origin (Fig.5-1). Palaeoseismic evidence indicates significant, but unknown, levels of ground shaking during the early stages of deglaciation, but the evidence is too fragmentary to establish long-term relationships throughout the post-glacial time.

5.4 SEISMICITY IN AND AROUND SCOTLAND

The British Isles is an area of low seismicity. NW Europe as a whole has moderate to low seismicity, more than half of it being effectively aseismic (Muir Wood 1985). Two main seismic areas occur, namely

   a) The Rhine graben belt: instrumental seismicity up to M=6.0, historical seismicity up to M=6.5 (Ahorner 1975), and

   b) The western Scandinavia area: instrumental seismicity up to M=6.0, historical seismicity up to M=6.0 (Husebye et al. 1978).

The Rhine graben belt of seismicity continues vaguely north-westwards into the southern North Sea. Faults associated with this belt may well be the loci of some fairly large historical events in the coastal areas of SE England - East Kent 1382, Dover 1580, Colchester 1884 and Dogger Bank 1931 - (Fig.5-2). The rest of the British Isles seems to be seismically distinct from the Rhine graben belt, although Muir Wood (1983, 1985) does suggest that seismicity and faulting in northern England are manifestations of a major NW belt of strike-slip faulting extending from Holland to the Southern Uplands of Scotland. However no established framework exists for explaining British seismicity and it is better to limit discussion here to observation.

Fig.5-2 shows the occurrence of major British earthquakes during the last seven centuries as compiled by Ambraseys and Jackson (1985), and Figs.5-3 to 5-8 show instrumental data from 1967 to 1984 recorded by the British Geological Survey Seismograph Network (Burton & Neilson 1980, Turbitt 1984, 1985). The following points should be noted:-

a) The historical record is poor in the northern half of Britain
   which strongly biases the historical seismicity distribution
   (Fig. 5-2).

b) Recorded seismicity is concentrated in a broad belt running from
   Skye in Scotland, south-eastwards through northern England and
   then veering south-westwards into south Wales. This belt
   co-incides with the main upland areas of Britain (Figs. 5-3, 5-4
   & 5-5).

c) Larger instrumentally-recorded events are especially clustered
   in this belt and locally clustered at three sites: Kintail,
   Carlisle and North Wales (also the locations of the three
   available fault-plane solutions, cf. Fig.4-9) (Fig. 5-6).

d) Scottish seismicity quite clearly delineates a NW-SE lineation
   from the Kintail area to the Stirling area. Some events display
   a weaker lineation along the lines of the Great Glen and
   Highland Boundary Faults. (Fig. 5-7).

e) Very little activity occurs offshore of Scotland until the
   active zone between the Viking Graben and Western Norway is
   encountered (Fig. 5-8).

Most instrumentally recorded U.K. earthquakes occur at depths of
3 to 12km (Marrow pers. comm.). Where events are well located
concentrations around 6km are common (e.g. the Carlisle 1979 event
aftershocks, Marrow & Roberts 1984). However, the recent North Wales
earthquake (1984) occurred at a depth of c.22km. This is unusually
deep and may result from a thicker brittle zone in this area (Turbitt
et al. 1985). Sibson (1983) notes that larger intraplate earthquakes
do tend to come from the base of the seismogenic zone, and a
comparison of historical isoseismal information (Musson et al. 1985,
1986) does suggest that several larger British events have come from
similar depths.

Instrumental coverage of Scotland is good, following the
emplacement of the LOWNET seismograph array in the Midland Valley in
1969. It has since improved with the addition of networks at Kyle (in
1979), Shetland (in 1980), Moray (in 1981) and a sea-bottom
instrument in the North Sea (in 1981) - Fig. 5-9. Prior to this

historical records form the primary source of seismicity data. Two important catalogues are Dollar's (1950) "Catalogue of Scottish Earthquakes 1916-1949" and Davison's (1924) "A History of British Earthquakes". Davison's first record of a Scottish event is for 1597 AD, and the record is extremely sketchy until the 1700's. Whereas in England he documents a substantial record of events throughout the last millenium. Research into Scottish historical seismicity is clearly needed. Furthermore, in view of this short-fall in historical data, palaeoseismic evidence has additional pertinence to the long-term Scottish record.

5.5 SEISMOLOGICAL CONSIDERATIONS

The apparently 'anomalous' nature of intraplate earthquakes is partly resolved by recent developments in seismological theory. Formerly, frequency-magnitude relations were understood in terms of the log-linear Gutenberg-Richter relation which failed to account for the observed distribution at high-magnitude and low frequency - Fig. 5-10A. The deviation of observation from this relationship is in part due to instrumental saturation of the magnitude (M_s) scale (Chinnery & North 1975); however there is now substantial evidence (Main & Burton 1984) that seismicity distribution is better understood in terms of Caputo's (1977) model which takes into account the effects of stress-drop and source dimensions and appears as curvature on the log-linear frequency-magnitude plot Fig. 5-10B. The linearity observed in global seismicity distributions (Fig. 5-10a) can be interpreted as superposition of many such curved distributions from different areas; some distributions show clear bimodality interpreted as resulting from two distinct seismogenic source types or orders of faulting (Main & Burton 1984).

It is interesting that Main and Burton found the clearest bimodal distribution in the intraplate area of New Madrid (Fig. 5-10b). This suggests a possible explanation for the 'anomalous' intraplate 'superearthquakes' (including the New Madrid events of 1811-12) as being associated with a high-magnitude mode of seismicity. Although no clear explanation in terms of fault rupture exists (one might envisage regimes of fault creep, rupture of

multi-discontinuous fractures and major single-continuous fault rupture) the observed bimodality calls for caution in assessing large-earthquake recurrence and emphasizes the need for historic and palaeoseismic data. It is, for example, possible that the high levels of seismicity and faulting during deglaciation result from the permission of a higher order fault-rupture-mode during an anomalous stress distribution.

In their study, Main and Burton (1984) included an analysis of U.K. seismicity. The data base is limited, but they were able to propose:

  a) a maximum fault area of c. 350 km^2,

  b) typical stress drops of 76 bars, and

  c) typical fault movements of 0.2 mm yr^{-1}.

They argue that movement probably occurs on multiples of small faults (with areas of the order of 10 km^2) at rates of 0.1mm yr^{-1} rather than on single fault planes, noting that although higher order fault planes might occur they have not yet been observed. They also suggest that 90% of the observed vertical movement in the U.K. (taken as 1.5mm yr^{-1}) occurs aseismically.

Field data presented in this thesis should help clarify such estimates, but since much of it relates to movements during deglaciation it is likely to reflect different seismologial conditions.

5.6 CONCLUSIONS

Fault activity in Scotland - the 'unknowns' prior to this work:-

  a) No capable faults have been reported.

  b) The historical record of seismicity is poor.

  c) Palaeoseismic evidence, to date, consists of a few vertical displacements (of order 1m) of glacial shorelines, not linked to causative faults.

  d) The tectonics of faulting during deglaciation is poorly understood.

  e) Empirical data are needed to establish the modes of seismic energy release and fault movement in the U.K..

****
CHAPTER SIX
Palaeoseismic Deposits
****

Palaeoseismic deposits are sediments which show signs of earthquake activity, and are essentially the geological record of earthquake intensity. They include re-sedimented earthquake-triggered deposits (such as landslips) as well as previously deposited sediments which show signs of deformation in response to earthquake activity. In this chapter the bulk of the treatment will concern liquefied deposits, since these are the most promising and widely reported paleoseismites.

6.1 EARTHQUAKE-INDUCED LIQUEFACTION - FIELD EVIDENCE

6.1.1 Surface phenomena

Rapid settlements, low-angle landslips, sand boils and collapse craters are among the many phenomena that have occurred during earthquakes and which are attributed to earthquake-induced liquefaction. Many historical accounts of 'the ground opening up and swallowing towns and people' during earthquakes were probably liquefaction phenomena. The entire population and edifice of Helice in Central Greece was 'removed' in the year 373/2 BC by what was almost certainly a coastal landslip resulting from earthquake-induced liquefaction (Seed 1968).

The most complete accounts of liquefaction phenomena come from Japan, where at least 44 earthquakes have caused liquefaction of subsoil in the last century (Kuribayashi & Tatsuoka 1975) - Fig.6-1. The majority of liquefied sites have been soft alluvial deposits, especially in sediment of flood-plains and abandoned river courses. The most commonly observed phenomenon is the spouting of water and sand from cracks in the ground (sand boils). During the Nobi, 1891, M=8.4 earthquake (Fig.6-1) tens of thousands of sand boils were observed, and at one site, water and sand was ejected to heights of over two metres, covering roofs of nearby houses.

Using their data base Kuribayashi & Tatsuoka (1975) demonstrated an approximate relationship between maximum epicentral distance to liquefied site and magnitude. Youd (1977) and Davis & Berrill (1983) found that additional (non-Japanese) data were in agreement with this relationship - **Fig.6-2.** The data indicate a cut-off of about magnitude 5 below which liquefaction does not occur and the occurrence of liquefaction up to 500km from the epicentre of a magnitude-8 event. Although occurrence of liquefaction is highly variable and strongly influenced by site characteristics this gross relationship is clear and is important to palaeoseismic studies.

The remainder of this section (§6.1) will consider correlation of liquefied deposits to earthquake events, focusing on the stratigraphy of such deposits rather than their surface manifestations and resulting soil failures.

6.1.2 Flat-lying deposits

An unequivocal correlation was established when Sims (1975) matched deformation structures in sediments of the lower Van Norman reservoir, San Fernando, California, to historical earthquakes. Sims was able to inspect the lake sediments after the draining of the reservoir following the 1971, San Fernando, earthquake. The sediments (spanning 56 years of deposition) revealed deformation structures at three stratigraphic horizons. These horizons were identified and correlated throughout the extent of the sediments (2 km^2) and had ages (by the counting of lamina) agreeing closely with three major earthquakes in the area, each having local intensities of MM VI or greater. The deformation structures were interpreted as resulting from liquefaction close to the sediment-water interface at the time of the earthquakes. Deformed zones were typically 5-10cm thick, and intercalated with with undeformed sediment. The strength of this correlation led Sims and others to search for similar structures in other young lakes and lake sediments in earthquake-prone areas.

Fig.6-3C shows such structures in Holocene sediments of the ancient Lake Cahuilla, California, where five horizons of structures were found in the uppermost 10m of sediment (Sims 1975). Varved

glacio-lacustrine deposits of the Puget Sound area of Washington
State revealed 21 deformed zones, fourteen of which were interpreted
as earthquake-induced (Sims 1975). This latter stratigraphy revealed
a changing rate of earthquake occurrence; a period of 400 years of
more frequent activity followed by about 1000 years of less frequent
activity, the record covering a period between c.45,000 and 43,000
radiocarbon years BP. Similar structures have been found in the East
Anatolian fault zone, Turkey (Hempton & Dewey 1983), where three
metres of young lacustrine sediment, exposed in channel-cuts on the
shores of Lake Hazar, reveal five distinct horizons of soft-sediment
deformation. The horizons are 5-50cm thick, flat-lying, laterally
continuous for hundreds of metres, separated by undeformed sediment
and possessing planar top and bottom contacts - **Fig.6-3A&B.** Such
deposits have also been reported in Alaska (Sims 1982), Canada (Adams
1982), Jordan (Seilacher 1984) and Iran (Davenport pers. comm.). All
these deposits consist of silt and fine sand in lacustrine sediment
and thus testify to the particular vulnerability of this type of
sediment to earthquake-induced liquefaction.

In considering the genesis of the observed sediment-deformation
structures Sims noted the similarity of structures produced
experimentally by Kuenen (1958). Kuenen had tested the hypothesis
that earthquake vibration could induce load-casting of sand into clay
by sedimenting a layer of sand, with a uneven surface, on top of clay
in an aquarium tank and subjecting the supporting table to blows from
a rubber hammer or short bursts of vibration from an electric motor
with an eccentric weight! By means of this primitive experiment he
produced kidney-shaped load casts, shown in **Fig.6-4,** termed
'ball-and-pillow' structures, and having a strong resemblance to
structures in the geological record - **Fig.6-3D.** The clear
similarity of these structures to the field occurrences documented
above forms the basis to the establishment of a 'diagnostic'
palaeoseismic indicator. It should be noted that other mechanisms can
produce the same structures (section 6.3 below) and need to be
discounted in any such diagnosis.

Sims (1975) proposed the following seven criteria in attempting

to diagnose the occurrence of earthquakes in geologically young sediments:

a) The study area is in a presently seismically active region, with earthquake intensities of MM VI or greater.

b) Potentially liquefiable sediments of lacustrine origin are present.

c) The structures are similar to those observed in the Van Norman Lake or those formed by Kuenen (1958).

d) The structures contain internal features that suggest liquefaction of at least part of the zone.

e) The structure zones are confined to single stratigraphic horizons.

f) Structures are correlative over large areas within the sedimentary basin.

g) The detectable influence of slopes or slope failures is lacking.

These criteria essentially refine a strong case for the occurrence of an earthquake by eliminating slope-generated or locally-derived deformation structures and selecting deposits favouring a genesis involving widespread, catastophic deformations at temporally discrete intervals in an area prone to earthquakes.

6.1.3 Deposits on slopes

The last of Sims' criteria is important in eliminating the possibility of slope-induced liquefaction and deformation from the diagnosis, however it is beyond doubt that earthquakes do induce slope failures, so that seismites on slopes must be considered, even if difficult to decipher.

A more complex form of soft-sediment deformation, attributed to ground shaking from earthquakes has been described by Seilacher (1969, 1984) and termed 'fault-grading'. Seilacher observed a 'fault-grading' stratigraphy in the Miocene, Monterey Shales, California, where he noted a four-fold sequence, shown in **Fig.6-5** consisting of (from top to bottom):

a) **Soupy zone:** a kind of liquefaction has wiped out all previous depositional structures. Indistinct lamination near the top indicates that the uppermost mud layer has gone into suspension.

b) **Rubble zone:** where compaction was somewhat more advanced, larger fragments of the original sediment survived the shock but swim with varying orientation in the soupy matrix.

c) **Segmented zone:** still more coherent older layers only broke along antithetic step-faults of miniature scale. Their offset decreases with depth before they die out, leaving fewer and fewer faults at larger, but still fairly regular intervals. Thus the seismite has no defined base and no basal slip surface.

d) **Undisturbed sediment:** lamination is left undeformed, while major faults may cross the beds at distances of a few metres.

Seilacher argues that this stratigraphy is genetically similar to liquefied deformation in horizontal sediment (as described by Sims) but incorporating the influence of slope. The palaeoslope generates the faulted zone while the sediment is softened under cyclic loading, liquefaction occurring only in the uppermost layer. Stronger shocks or greater slopes would result in complete failure, slumping and turbidity currents. Fault-grading is thus seen as the 'seismite' of gently sloping, fine-grained sediment, analagous to the flat-lying, ball-and-pillow seismite.

Where earthquake-induced liquefaction results in slope failure we might envisage a third species of seismite. Diagnosis here, however is difficult because of the many parameters involved progressive slope failure; site-specific studies are necessary. However it can be said that earthquake-induced failures tend to affect large areas simultaneously and can occur on very gentle slopes (for example, sub-sea failures occurred offshore of California along a 20km stretch of a delta slope inclined at only 0.25° following a M=7 event in 1980 (Field et al. 1982). These features along with associations with fault rupture and other (flat-lying) seismites can allow the assignment of an earthquake origin. Mutti et al. (1984) have described turbidites of exceptionally large volume and areal

42

extent as 'seismoturbidites'. They do not propose clear criteria for identifying these, but suggest a volume and horizontal extent above which a seismic origin is strongly implicated.

6.1.4 Occurrences in the geological record

Pseudo-nodules and ball-and-pillow structures are common throughout the Phanerozoic. They are not evenly distributed but concentrated in certain formations. They have often been confused with and classified alongside load casts and convolute bedding. They are however separate phenomena and have a distinct environmental distribution. They are commonest in shallow-marine, deltaic, lacustrine and fluvial deposits (Allen 1982), and also have a gross tendency to occur in actively-faulting basins (Anderton pers. comm.).

In the documentation of Allen (1982), the term 'pseudo-nodule' is used to describe a single, laterally extensive row of uniformly-sized sand masses of nodular, concretion-like shape occurring in mud or silt (Fig.6-3d), and the term 'ball-and-pillow structure' used to describe a sheet of sand masses of various sizes, packed vertically and horizontally in a mud matrix; pseudo-nodules representing a simple, two-layer case (sand on mud/silt) and ball-and-pillow representing a similar phenomenon affecting multilayers. Anketell et al. (1970) show, experimentally, that these structures are part of a family of deformation structures resulting from gravitational instability in materials which flow easily (which in sediments implies a liquefied or plastic state in at least one member of the sequence). In cross-section nodules, balls or pillows tend to be around 0.5m in lateral dimensions and approximately equidimentional, although markedly elongate forms do occur. They are usually flattened slightly, although again they may be very flattened to give lateral dimensions as much as eight times the vertical (Allen 1982).

In the British Isles alone, well described layers containing these structures have been reported in the:

* Torridonian (Pre-Cambrian) sandstone of Rassay, Western Scotland (Selley et al. 1963).

* Dalradian quartzites of S.W.Scotland (Anderton 1985).

* Devonian sandstones of the Tayside area, Scotland (Paterson pers. comm.).

* Carboniferous sandstones of Ireland (Gill & Kuenen 1957), northern England (Leeder 1986) and South Wales (Kuenen 1948, Weaver 1976).

In several cases the authors suggest a palaeoseismic affiliation to the deposits. Anderton (1985, pers. comm.) has found a clear correlation of the horizons in the Dalradian to periods of rapid basin subsidence and Leeder and Weaver both provide evidence of increased abundance and thickness of the horizons in the vicinity of faults, presumed active at the time. Other means have been postulated for their formation, including wave action (Chadwick 1931, Pederson 1985), downslope movement (Hubert et al. 1976) and differential loading purely due to reversed density gradients (Sorauf 1965). Allen (1982) argues that downslope movement as a primary cause is unlikely, but that (as shown by Anketell et al. 1970) such structures record the condition of instability during liquidization of silt and sand layers. On the basis of field evidence alone this instability is generated by earthquake shaking in a large number of cases. Further treatment of the various mechanisms capable of producing these deposits will be given in section 6.4.

6.1.5 Concluding statement

There is a strong case for a diagnostic seismite in the deformed structures resulting from earthquake-induced liquefaction. Such seismites are most easily discerned in flat-lying deposits, but genetically similar deposits can be detected on slopes. The case rests on a large number of examples relating ball-and-pillow type structures to earthquakes; however there is not a direct correlation since liquefied deposits can be produced by a number of means, ball-and-pillow being essentially a record of gravitational instability under conditions of liquidization. Nevertheless, under favourable conditions, confident diagnosis of an earthquake-induced genesis can, and has been, made.

Table 6-1. LIQUEFACTION TERMINOLOGY

Overall phenomenon - LIQUIDIZATION - formation of liquidized sediment.
(i.e. loss of shear strength in a two phase material: cohesionless particulate solid and fluid.)

Mechanisms of liquidization

LIQUEFACTION: Change in state of the solid phase   FLUIDIZATION: Change in mobility of fluid phase such
leading to suspension of particles in fluid phase   that the solid phase is supported by fluid drag.
(when effective stress reaches zero).

Means of achieving Liquefaction

STATIC: Solely by an increase in pore fluid   DYNAMIC: - Monotonic: change in solid phase
pressure - solid phase de-stabilizing as effective   structure by sufficiently large single impulse load.
stress reaches zero.   - Cyclic: change in solid phase by
                                                  increasing cyclic strain under vibratory loads.

Participating processes (in Liquefaction)

Pore-water pressure changes, structural changes (produced by gravitational instability), cyclic mobility,
various regimes of fluidization, dewatering.

45

6.2 LIQUEFACTION BY CYCLIC LOADING - THEORY

Research into the phenomenon of liquefaction by the civil engineering community is substantial. They use the term 'liquefaction' to describe a variety of situations where soil looses its shear strength and performs mass flow. The purpose of this review is to steer a path through engineering research which leads to a theoretical understanding of the deformation phenomena produced in a cohesionless, saturated sediment during surface shaking resulting from an earthquake (i.e. earthquake-induced liquefaction). Our objective is the interpretation of palaeoseismic deposits produced by this mechanism.

6.2.1 Terminology

The main definitions adopted in this study are shown in Table 6-1. They are based on sedimentological criteria (Lowe 1975, Allen 1982).

Definitions employed in engineering research differ somewhat from these, due to the difference in approach and objective. An appreciation of the engineering perception of liquefaction is however important in order to benifit from their science. The following definitions have been voiced by prominent workers in liquefaction research. [Note that, the engineering usuage of the term 'soil' is adopted in this section (§6.2) and refers to any cohesionless, unconsolidated sediment mass.]

a) Seed and Idriss (1971): **Liquefaction** describes a phenomenon in which cohesionless soil loses its strength during an earthquake and aquires a degree of mobility sufficient to permit movements ranging from several feet to several thousand feet.

b) Dikmen and Ghaboussi (1984): **Complete liquefaction** is defined as a state of zero, or a residual, effective stress.

c) Casagrande (1970): **Cyclic Mobility** is the progressive softening of a portion of the specimen which is observed on small laboratory specimens that are subjected to cyclic loading, but which are sufficiently dense to remain safe against liquefaction failure.

d) <u>Castro (1975):</u> **Cyclic mobility** consists of gradually
increasing cyclic strains, and can occur in loose or dense sands, but
does not entail a loss in shear strength. **Liquefaction** consists
of a loss in shear strength and can only occur in sands that are
looser than the critical state.

e) <u>Morris (1983):</u> **Earthquake-induced liquefaction** is the
destabilization of soil bodies by the generation of pore pressure as
a result of cyclic shearing.

The definition (a) of Seed and Idriss reflects the general
engineering understanding of the phenomenon of liquefaction. This
form of definition is rejected in favour of describing the phenomenon
as **liquidization** and restricting the term **liquefaction** a
mechanism involved (described in Table 6-1). Dikmen and Ghaboussi (b)
define the state at which the mechanism of liquefaction is completed
- i.e. the production of a liquefied material. Casagrande (c)
introduced the term **cyclic mobility** to describe an important
pre-liquefaction process. Cyclic mobility may progress to the extent
that liquefaction is achieved, but is nevertheless a separate
concept. Castro's definition (d) makes clear this distinction between
cyclic mobility and liquefaction, however his adoption of the
critical state (referring to the critical void ratio) as the
essential criterion for achieving liquefaction is really only
appropriate to the monotonic shear failure of soil. It is
nevertheless an important concept in liquefaction by cyclic loading.
Morris (e) provides an acceptable definition of **earthquake-induced**
liquefaction testifying to the key role of pore-pressure in the
process. ·

6.2.2 Basic liquefaction theory

The discourse below is not a systematic theoretical argument,
but a theoretical illustration of the basic parameters involved in
the liquefaction of saturated cohesionless sediment. It is drawn from
the more rigorous treatment of Zienkiewicz & Bettes (1982).

Consider a two phase material with an interstitial fluid
displacing relative to a solid, particulate matrix.

Let the   total stress tensor $= \sigma$ (composed of normal and

shear stress components),

pore pressure $= p$,

averaged displacements of the solid matrix $= u$,

averaged relative displacements of the fluid $= w$.

The actual pore fluid displacement is $\underline{\dfrac{w}{n}}$, where $n =$ the porosity of the solid phase.

Let the   density of the two phase material $= \rho$,

density of the fluid $= \rho_f$.

Equilibrating stress under static conditions

$$\sigma = \sigma' + p \qquad\qquad \dots\dots\dots 1$$

where σ' is the effective stress.

This basic soil mechanics equation defines the condition for static liquefaction which occurs when $\sigma' = 0$, and the pore pressure is sufficient to support the weight of the two phase material.

However, under dynamic conditions account must be made of the body forces and the inertial forces as well as the imposed stress. These result from the strain, $\mathcal{E}$, which the solid-phase skeleton undergoes.

Equilibrating forces acting on the solid skeleton,

$$\sigma \quad + \quad \rho g \quad = \quad \rho\ddot{u} \quad + \quad \rho_f \frac{\ddot{w}}{n} \qquad \dots\dots\dots 2$$

total stress	gravitational force	inertial force of matrix	inertial force of fluid

Furthermore fluid flow through a porous medium will be subject to resistive forces due to fluid viscosity. This resistive force must balance the pore-pressure gradient, such that, assuming slow, laminar flow (Darcy's law),

$$p = \frac{\dot{w}}{k} \qquad\qquad \dots\dots\dots 3$$

where $k =$ the permeability coefficient.

Taking into account the inertial forces of equation 2, and the fluid
drag (equation 3) an equilibrium equation can be obtained. Equilibrating
the forces acting on the fluid,

$$p \quad + \quad \rho_f g \quad = \quad \frac{\dot{w}}{k} \quad + \quad \rho \ddot{u} \quad + \quad \rho_f \frac{\ddot{w}}{n} \quad \ldots .4$$

pressure gradient	hydrostatic gradient	fluid drag	inertial force (grains)	inertial force (fluid)

Thus under dynamic conditions liquefaction will occur when the total
stress on the grains (equation 2) is equal to the pressure of the fluid
(equation 4) to give the $\sigma'=0$ condition (equation 1), this condition
resulting from the complex interaction of gravitational, inertial and
fluid drag forces.

However, under general dynamic conditions laminar flow and
incompressibility are not valid assumptions. In order to account for
these, a volumetric relationship is helpful. Equilibrating the mass
balance of flow, noting that fluid velocity must be equal to the rate
of decrease in pore space and the fluid expansion rate:

$$\dot{w} \quad = \quad \dot{\epsilon} \quad - \left[\frac{(1-n)p}{K_s} + \frac{\dot{\sigma}'}{3K_s} \right] \quad + \quad \frac{\dot{p}n}{K_f} \quad \ldots \ldots .5$$

fluid velocity	rate of pore volume decrease due to skeleton strain			rate of fluid expansion due to pore pressure changes

Pore volume increase ⎫   ⎧hydrostatic change in
associated with the ⎬ by ⎨ pressure   effective
compression of grains⎭   ⎩ increase   stress

where K_s = average bulk modulus of solid

K_f = average bulk modulus of fluid.

The fluid velocity, so derived, adds further complexity to the
terms of equation 4 involving 'w', such that the $\sigma'=0$ condition is
very difficult to conceptualize. Equations 4 and 5 are however
helpful in identifying the many processes operative during dynamic,
cyclic loading of a soil. Some of these are illustrated in

Fig.6-6.

Because of this multiplicity in participating processes, dynamic instability and the onset of liquefaction is highly dependant on inhomogeneities in the soil, such that in a real soil profile "the phenomenon is fundamentally intractable analytically" (Morris 1983). Thus, although theoretical work is vital in appreciating the processes involved in the real system, the predictive science of liquefaction must proceed on the basis of direct experimentation of as real as possible, preferably full-scale, models. What better model than real geological examples? - which is the premise of this thesis.

Before moving onto the real, geological laboratory, valuable concepts and contributing factors should be gleaned from the scaled-down experimental work of engineering studies.

6.2.3 Experimental work

Although attention has been drawn to the short-comings of scaled-down experimental work, with triaxial cells and simple shear tests (especially at the Berkeley school of Seed and co-workers) this kind of work has nevertheless quantified the contribution of the major factors involved (despite doubts concerning the validity of the quantification). It has also highlighted the importance of other factors removed from experimental models or assumed negligible.

Seed and Idriss (1971) have outlined five main factors affecting the liquefaction potential of a soil:

a) **Soil type:** Fine sand tends to liquefy more easily than coarse sand, gravel, silt and clay. Well-graded (ie. poorly sorted) sands are less susceptible than uniformly graded sands.

b) **Relative density or void ratio:** The work of Casagrande (1970) has established the importance of this quantity. Liquefaction is not generally observed in soils exceeding a certain relative density (c.70%).

c) **Confining pressure:** The cyclic load required to initiate liquefaction increases with the initial confining pressure.

d) **Ground shaking:** In general there is a cut-off in the ground acceleration capable of producing liquefaction. Liquefaction around Niigata, Japan (in loose sands) has only been observed where estimated ground accelerations were in excess of 0.13g.

e) **Duration of ground shaking:** Laboratory studies have shown that for any given stress or strain level the onset of liquefaction depends on the duration of shaking.

In addition to these basic factors affecting experimental studies the following factors have been shown to be of major importance when a real soil profile is considered.

f) **Strain history:** Partial liquefaction (involving small strains) is known to increase resistance to reliquefaction. Moderate strains, however, can decrease the resistance to liquefaction. The precise relationship is not known. (Finn et al. 1970.)

g) **Fabric:** Experimentation on the effects of sample preparation for triaxial testing has shown that differences in orientation and packing of grains (of the same composition) can cause of the order of 100% change in the cyclic stress required for liquefaction (Mulilis et al. 1977).

h) **Presence of fines:** Where grain to grain contact is maintained the presence of finer particles increases resistance to liquefaction. Where the quantity of fines is sufficient to support the sand grains response to liquefaction is controlled by the properties of the fines (e.g. compaction and cohesion) (Shen et al. 1977).

i) **Stratification:** Under cyclic loading, pore-pressure build-up will first occur at the layer most prone to the characteristics of the imposed stress. This layer will soften and act as a locus of dynamic instability and will dominate subsequent strains and pore-pressure developments in adjacent layers (Morris 1983).

j) **Spectral content of cyclic load:** Different base motions (from real earthquakes, scaled to the same peak acceleration) cause dramatically different responses in the same soil profile (Ghaboussi & Dikmen 1984). Important factors are:

- **frequency:** moderate frequencies (c. 1 Hz) have a weightier influence on the generation of shear stress and high pore pressures.

- **duration:** smaller cyclic loads imposed for a longer time can cause liquefaction where larger cyclic loads do not.

Having outlined these main factors involved in determining the progress of the liquefaction process, conceptual models can be presented of the likely senario occurring in a soil profile undergoing cyclic loading.

The conditions for dynamic liquefaction are illustrated in **Fig.6–7**. Under monotonic loading, failure occurs at a critical stress ratio and liquefaction occurs soon after as o' reaches zero (Fig.6-7A). Under cyclic loading initial liquefaction occurs as the stress ratio approaches the failure line, but complete liquefaction occurs only after continued loading has driven the stress ratio well into the failure envelope (Fig.6-7B).

Fig.6–8 further illustrates the difference between monotonic-load and cyclic-load liquefaction. Under static or monotonic load conditions the critical void ratio has been shown to be of special importance in determining the onset of liquefaction (i.e. the point at which σ' reaches zero (§6.2.2-equation 1). For any given void ratio the critical void ratio decreases with increasing imposed stress under undrained conditions. This is illustrated in Fig.6-8a where an increased load causes the critical void ratio to move from position 1 to 2, resulting in a critical condition for liquefaction at the central sand layer. Experimental work (Casagrande 1970, Castro 1975) has shown loose, clean sands to be most susceptible to this mechanism of liquefaction.

By contrast, under cyclic loading liquefaction occurs where the pore-pressure generation, due to small inter-grain shears and volume reduction, initiates the 'quick' condition. Seed and Idriss (1971) have shown this condition to occur in a 'zone of liquefaction' (Fig.6-8B). Liquefaction by cyclic loading can occur in very dense

sediment and is favoured in the coarse silt and fine sand grain size range. Fig.6-8A&B thus illustrates how liquefaction occurs in different layers (initially) according to the two different processes. It should be noted that cyclically derived liquefaction could cause liquefaction in another layer under essentially 'static' conditions by virtue of pore water migration. Therefore we are primarily refering to mechanisms of initiating liquefaction.

Thus liquefaction under static conditions occurs in loose sands, in relatively undrained conditions, subjected to a pore pressure increase. Dynamic liquefaction occurs under similar conditions where loading results in shear failure of the soil skeleton such that liquefaction ensues. Earthquake-induced liquefaction occurs (initially) by progressive shear failure under cyclic shear loads and tends to occur in silts and very fine sands (provided they are cohesionless).

The models described above are simplistic but conceptually helpful. We now proceed to elaborate on the factors involved in earthquake-induced liquefaction to produce a more realistic model.

Dikmen and Ghaboussi (1984) have performed a number of more realistic experiments on hypothetical soil profiles subjected to real earthquake time histories - Fig.6-9. Their work has emphasized the importance of the generation of excess pore pressure and the conditions under which it is generated. Their results also confirm the presence of a 'zone of liquefaction' occurring at some depth within the soil profile.

Graphs 'B' and 'C' (Fig.6-9) were produced by subjecting the hypothetical (computer modelling) soil profile 'A' to a single component of the El Centro earthquake of May 1940 (peak acceleration of 0.1g). The soil profile (A) consisted of a uniform sand, 50ft thick (15m), comprised of 10 layer-elements having shear moduli as shown, a relative density of 45%, a coefficient of permeability of 0.003 ft/sec, and resting on a rigid base. The results indicate highest shear stresses and highest ground-surface acceleration occurring in the dry soil profile. However, the profile having a low

coefficient of permeability (thus allowing the development of excess pore pressure) shows a dramatic peak in acceleration at a depth of 25ft (8m). This is thought to be the result of softening due to cyclic mobility and partial liquefaction. The influence of depth of water table (graph E) and permeability (F) were studied by subjecting a slightly different soil profile (D), with a relative density of 60%, to a single component of the Taft earthquake, July 1952, with a peak acceleration of 0.15g. The excess pore pressure ratio was seen to decrease with depth of watertable and with increasing permeability. The depth to maximum ratio increases accordingly.

Some consideration should be given to the depth of the zone of liquefaction. Both Seed & idriss (1971) and Dikmen & Ghaboussi (1984) have modelled thick soil profiles (50ft (15m) or greater) to derive zones of liquefaction between 5ft (1.5m) and 30ft (9m). They do not consider thinner profiles. We could infer that the peak in maximum acceleration and excess pore pressure ratio occurs halfway down any soil profile, as it does in the Dikmen & Ghaboussi model (Fig.6-9 C,E & F), but there is no experimental work to support this. Analysis and modelling of the soil profile at a site near Niigata, Japan (Ishihara & Towhata 1982), where liquefaction occurred after the 1964 earthquake, has shown that liquefaction in a soil 35m thick would be expected in the top 5m. Initial liquefaction was still subsurface (1-4m) but ultimately it was the whole top layer that liquefied (in the model). The site had coarse sand capped by a thin clay layer, and it was the loosest sand, beneath the clay, that liquefied. Thus, we should infer that although modelling indicates a zone of liquefaction at depth, the depth of this zone may be strongly modified by the characteristics of the profile of interest.

6.2.4 Concluding statement

The model for earthquake-induced liquefaction derived from the discussion above incorporates the following main features:

a) The generation of excess pore-water pressure is the critical factor and is determined by the response of the two-phase system to the cyclic shear load.

b) Liquefaction is favoured in fine sands of low relative density

under low confining pressures.

c) Liquefaction can still occur in dense silts under high confining pressures if intensity and duration of ground shaking are sufficient.

d) Liquefaction will initiate at depth within a zone of liquefation.

e) Liquefaction will initiate in a susceptible layer where dynamic instabilities first occur.

6.3 COMPARISON OF THE MODEL WITH THE FIELD EVIDENCE

Of the elements of the model summarized in section 6.2.4 the following are consistent with an earthquake-induced liquefaction hypothesis for the field examples of section 6.1:

a) silts and fine-grained sands are the grain-size range prone to liquefaction.

b) loose, cohesionless sediment under saturated conditions liquefies.

c) the structures produced are of the ball-and-pillow family.

However the following discrepancy is evident. Under the model conditions, liquefaction initiates at depth, pore-pressure generation and confinement being critical in the locus of this depth, whereas, in many of the field examples it is the upper 10-50cm of sediment that liquefies. There are several possible resolutions to this discrepancy:

a) The model is wrong, and the relevance of the mechanism of cyclic loading is questionable.

b) Some assumptions in the model are wrong, and it needs refining.

c) The model is valid, but applicable to only certain field conditions.

The first possibility is discountable in the light of clear correlations of field examples to earthquakes. No obvious shortcomings in the assumptions are apparent, but for the following reasons the third possibility is favoured. The model assumed no cohesion throughout a thick sediment column (valid in many sediment

profiles), but did not encompass profiles with a thin cohesionless
upper layer. Sims (1975) and Hempton and Dewey (1983) both describe
structures in fine-grained lake sediment where clays are likely to
hasten the onset of cohesion in the accumulating profile. There are,
in contrast, field examples which reveal behaviour very similar to
the model. Anderton (1985, pers. comm.) describes a layer in the
Ardrishaig Phyllites of the Scottish Dalradian where liquefaction
occurred at a depth of 30-50 metres below surface, with diapirs of
liquefied sand rising through less mobile upper layers. Furthermore
there may well be a difference in liquefied deposits formed beneath
standing water and those with a subsurface water-table. Japanese sand
boils clearly indicate liquefaction at depth in subaerial deposits,
whereas it is lake sediments which reveal liquefaction of the
(subaquatic) surface layer.

Thus, cohesion and water level are suspected of giving
additional constraints to the mode of response of a soil profile
subjected to earthquake-induced liquefaction. Resolution of this
issue will come in part from additional field evidence (this thesis)
and in part from more appropriate modelling of soil profiles.

6.4 DIFFERENT MEANS OF ACHIEVING LIQUEFACTION

Many different means of generating a liquefied condition in a
saturated, cohesionless sediment have already been alluded to in the
preceeding discourse on earthquake-induced liquefaction. A more
complete list is given below (for main definitions refer to table
6-1):

* static liquefaction: resulting from:-

          a) unloading of sediment

          b) porewater migration

          c) freeze-thaw pressure.

* Dynamic monotonic liquefaction: resulting from:-

          d) normal gravitational loads

          e) slope failure

          f) heavy load impact.

* Dynamic cyclic liquefaction: derived from:-

g) earthquakes

h) Storm-wave loading

i) tsunamis

j) turbidity flows

k) man-made vibration.

Each one of these is a conceivable means of achieving liquefaction, and each will be considered for its likelihood, mode and environment of occurrence in real sedimentological systems, and for relevance to the interpretation of palaeoseismic deposits.

6.4.1 Static liquefaction:

a) Unloading of the sediment column

If the lithostatic or hydrostatic load on a column of sediment is rapidly removed a "$\sigma'=0$" condition may be achieved as a result of the reduction of σ (§6.2.2 eqn.1), provided the rate of pore water dissipation is slow enough. This situation is most easily constructed in lake sediments where the water level is rapidly reduced by a large amount. The critical factor in this scenario is the rate of pore pressure dissipation; sediment of low permeability would be most susceptible.

Vesajoki (1982) proposes this kind of genesis for liquefaction structures in Finnish glacial and post-glacial deposits. In 1859 the water level of Lake Hoytiainen was artificially dropped by 10m, which resulted in the exposure of previously submerged sediments. These sediments contained liquefaction horizons - Fig.6-10a, having structures similar to Kuenen's (Fig.6-4) and were interpreted, by Vesajoki, as resulting from the drop in water level. He suggested that reversed density gradients were produced by compaction of the upper wet sandy sediment and that excess pore pressure was generated in the lower silty sediment causing liquefaction in the silt and load-casting of the sand. He also described a number of glacial deposits with similar structures Fig.6-10b&c and interpreted these as forming under similar conditions of emergence after the draining of glacial lakes. Liquefaction by this method would generate deformation deposits over large areas of lake sediment at a single

57

stratigraphic horizon (c.f. Sims criteria 'b-f', §6.1.2 above).

b) **Pore-water migration**

Local conditions may be such that pore-water migration alone causes the "σ'=0" condition in a sediment column. Landslips following periods of heavy rain are common some of which may result from this kind of liquefaction. Liquefaction by pore-water migration is likely to be a 'side-effect' of many kinds of liquefaction since liquefaction inevitably results in flow of sediment and pore water. Vesajoki (1982) calls upon this method in the interpretation of some of the structures exposed in Lake Höytiäinen, where the drop in lake level seems to be an inadequate explanation.

c) **Freeze-thaw pressure**

The freezing and thawing of water in sediment pores creates large internal pressures and strains on the solid matrix (pressures in excess of 4kg cm^{-2} (4×10^5Pa) have been recorded (French 1976)). The freezing of water is accompanied by a volume increase of approximately 9%, which in a typical soil represents an overall volume increase of 2-5%, depending on the void ratio (Craig 1983).

A large number of glacial, soft-sediment deformation structures have been interpreted as resulting from ice-water phase transition pressures. The field of science here is huge - but it is useful here to identify the basic features of freeze-thaw deformations, in order to differentiate genetic processes. Involution and cryoturbation structures include a variety of density driven soft-sediment deformation structures and they frequently resemble other loading and injection structures. Cryoturbation structures are chaotic deformations resulting from freeze-thaw forces - **Fig.6-11** - but may include density driven deformations. Involutions - **Fig.6-12** - are density driven deformations, in which density differences may be enhanced, or created by, pore-volume changes (due to freeze-thaw) and where plastic flow may be facilitated by related pore-pressure increases (French 1976). Ball-and-pillow structures are often observed in glacial sands and silts, sometimes these have been interpreted as cryoturbation structures - **Fig.6-13a**, but in other

cases load-casting through liquefied sediment is clearly implicated –
Fig.6–13b.

Vandenberghe & Van Den Broek (1982) interpret many glacial
involution horizons, having clear ball-and-pillow structures, as
load-casting of reversed-density-gradient sequences under conditions
of liquefaction. They argue that liquefaction in these cases is
generated by the final (not periodic) melting of the permafrost
layer, which creates excess pore pressures in the unfrozen sediment
above; pore-water confinement being provided by low permeability clay
layers. Under this scenario, conditions for widespread liquefaction
of sandy sediments at the time of permafrost melting are implicated.

Finn et al. (1978) have modelled the liquefaction of thawed
layers in frozen soils and show that coarse-grained sediments (sands
and gravels) are particularly prone to liquefaction under these
conditions, where they would not be expected to liquefy in temperate
conditions. This is partly because of the large amounts of water
available in the system but also because ice can provide a very
effective seal to pore-water migration. The melting of permafrost can
result in trapped layers of thawed soil, having high pore pressures
and thus being prone to liquefaction. For example, such a layer can
form in the river sediment beneath a frozen river. These trapped
layers will be localized, even if occurring over wide tracts of
melting permafrost.

Thus, liquefaction under freeze-thaw conditions tends to favour
coarser sediment, can occur over wide areas, but is expected to be
localized at favourable sites.

6.4.2 Dynamic monotonic liquefaction:

The following three means of achieving liquefaction are all
highly local and site-specific in occurrence. They are, in general,
easily resolved from palaeoseismic liquefaction deposits.

d) **Normal gravitational loads**

Inter-granular strains due to imposed loads result in compaction by re-arrangement of the structure. The accompanied decrease in pore volume raises the pore pressure, in undrained conditions, and may produce the "$\sigma'=0$" condition. Since all sediment has mass, and since its mass is not evenly distributed, gravity-driven redistributions will be ubiquitous in all cases of liquefaction. In most cases this will be in terms of response to the reduction in shear strength by other means (e.g. vibration), but in some cases loading of the sediment will initiate and drive the deformations. In Kuenen's experiment (§6.1.2, Fig.6-4) load-casting beneath a thicker portion of the upper sand layer occurred in response to shock-induced liquefaction, whereas many examples of convolute lamination testify primarily to gravity-driven loading (Allen 1982). Lowe (1975) suggests rapid deposition of sands and gravels is the major cause of liquefaction in sediment sequences, especially in deltaic environments.

e) **Slope failure**

Where the shear strength of a sediment column is not sufficient to support the downslope component of the sediment weight, intergrain shear-strain will occur. Usually shear-strain will initially cause an increase in pore volume (Fig.6-6), but with increasing strains large pore-volume reductions will occur, which under saturated conditions can again herald the "$\sigma'=0$" condition. As with normal gravitational loading of sediment this process may occur as response to shear strength reductions of different origins, or may drive the failure unilaterally.

f) **Heavy load impact**

The impulse of a large load sufficient to produce major strain of the sediment can cause liquefaction. This is a major concern in engineering construction. In natural conditions ice-falls or drop-stones are potential sources of this kind of failure.

6.4.3 Dynamic cyclic liquefaction:

The section of the theory of cyclic loading (§6.2) has relevance to all types of cyclic load. Different cyclic loads do however have different response characteristics in the sediment column, such that most of the conclusions of section 6.2 are specific to earthquake-induced liquefaction.

g) **Earthquakes**

That is liquefaction induced directly by earthquake ground-shaking, and not as a secondary product of tsunamis or turbidity currents produced by earthquakes. Earthquake-induced liquefaction has been considered in sections 6.1, 6.2 & 6.3.

h) **Storm loading**

Wind-driven currents in lake and ocean basins can generate large cyclic loads at the sediment-water interface. Oscillating bottom currents (in water depths of 15-20m) with velocities up to 50 cm/s and mean periods of around 9 seconds have been recorded during intense storm conditions in Norton Sound, Alaska (Cacchione & Drake 1982). Analysis of wave-induced liquefaction in a semi-infinite half-space model of this Sound (Olsen et al. 1982) indicates that liquefaction, near the sediment surface, can occur after ten minutes of loading from a 6-metre storm wave, but does not penetrate to depths greater than 3-4m however long the duration of loading; wave heights of less than 3 metres were incapable of producing liquefaction. In another model, Seed & Idriss (1982) show pore pressure ratios generated under design storm loading of a hypothetical sediment profile - **Fig.6-14a.** This curve has a markedly different form to that for earthquake loading (Fig.6-9). As would be expected, liquefaction under wave loading is a surface phenomenon, initiating near the sediment-water interface and migrating down as loading progresses, whereas earthquake-induced liquefaction is expected to initiate at depth.

Pederson (1985) shows an example of liquefaction structures in lower Jurassic siltstone which occur in a sequence of other

storm-generated structures. The structures are very similar to
Kuenen's (Fig.6-4) but on a much smaller scale (the liquefied horizon
is only 5cm thick).

Another characteristic of wave-induced liquefaction contrasting
it with earthquake-induced liquefaction is the difference in the
probability density function of extreme loading conditions.
Qualitatively, extreme wave loading is generally more frequent than
extreme earthquake loading, magnitudes dependent on local conditions.
This is quantatively illustrated for the North Sea in **Fig.6-14b.**

Liquefaction due to storm-generated, sea-bottom cyclic-loading
is likely to be widely distributed on a similar scale (100's km^2)
to that for moderate earthquakes. However, both the nature of
response of the sediment column and the frequency of occurrence in
stratigraphy show appreciable differences such that the two ought to
be resolvable.

i) Tsunamis

Kastens & Cita (1981) suggest that an unusual stratigraphic unit
in the abyssal Mediterranean Sea, called an 'homogenite', has been
formed by widespread liquefaction resulting from a tsunami produced
by the caldera collapse of the Santorini volcano, 3500 years BP. They
envisage tsunami-derived cyclic stresses liquefying sediment and
stirring it into suspension; the sediment then flows as turbitity
currents to be resedimented in abyssal lows. The case is an
interesting one and a credible example of tsunami-derived
liquefaction. The processes involved would be similar to
storm-wave-induced liquefaction although tsunamis have potential for
extremely large cyclic loading and correspondingly catastrophic
sediment failures.

j) Turbidity flows

A turbidity flow is a liquidized flow. They can result from all
forms of sub-aqueous sediment failure. The liquefaction of a deposit
can evolve directly into a turbidity flow (Lowe 1976). The deposits
formed from such flows are the resedimented constituents of the flow,

and are easily recognised in the various forms of turbidite. There is however the possibility that turbidity-flow motion generates liquefaction in the substrate it flows over, or settles onto. Such liquefaction would be clearly related to the geometry and stratigraphy of the turbidite, and ought to be easily distiguished as such.

k) Man-made vibration

Machinery and traffic can cause liquefaction in sediment in a critical condition. For example, mud-boils have been observed in soft, saturated sediment resulting from the passage of a motor-vehicle (French 1976, p43). Such occurrences will be very localized.

6.4.4 Concluding statement

Of these different means of producing liquefaction, five appear to be capable of generating liquefaction over wide areas at a single stratigraphic horizon:

a) unloading of sediment by falls in water level,

c) thaw-generated pore-pressures at the permafrost melting,

g) earthquakes,

h) storm-wave loading, and

i) tsunamis.

6.5 OTHER PALAEOSEISMIC DEPOSITS

6.5.1 Peculiar palaeoseismites

Unusual deposits which have been suggested as being of palaeoseismic origin include anomalous white-mud layers in the Dead Sea, Israel (Ben-Menahem 1976), anomalous silt layers in lakes in eastern Canada (Doig 1986), thicker 'seismic varves' showing magnetic anomalies in Sweden (Mörner 1985) and characteristics of pelagic limestone sedimentation (Forti & Postpichl 1984, Seilacher 1984, Cisne 1986). These do not have direct relevance to the thesis and will not be discussed further.

6.5.2 Landslides

Landslides are extremely common, almost ubiquitous accompaniments of large earthquakes. As palaeoseismic indicators they are poorly defined since landslipping occurs under varied conditions, and since even known earthquake-induced landslides are of many forms. Knowledge of local conditions is vital in any assessment of the cause of a landslide; however some general empirical relationships can be established.

Keefer (1984a) has made an analysis of landslips caused by 40 historical, world-wide earthquakes. He differentiates 14 kinds of landslide which have occurred during earthquakes and demonstrates approximate threshold levels of ground-shaking necessary for triggering each type. General threshold levels are:

a) Rock falls, rock slides and disrupted soil slides are initiated by the weakest shaking and susceptible to the high frequency, short-duration shaking characteristics of small earthquakes; common at MM VI.

b) Coherent, deep-seated landslides initiated by stronger, longer duration shaking; common at MM VII.

c) Lateral spreads and flows initiated by still stronger shaking; also common at MM VII.

d) Rock and soil avalanches having the highest thresholds; unspecified.

(Landslides of all types occasionally occur at intensities one or two levels below the levels at which they are common.)

For rock avalanches, Keefer (1984b) showed that susceptible conditions occurred on slopes higher than 150m, steeper than 25 degrees, and almost always on slopes undercut by fluvial or glacial erosion and composed of fractured rock - Fig.6-15. He also attempted correlations of earthquake magnitude to various parameters of landslides, the most applicable of which is the relation to area affected by landslides - Fig.6-16.

6.6 CONCLUSION

In this chapter the basis for a diagnostic seismite in the deformed sediment horizons resulting from earthquake-induced liquefaction has been shown, a model for the performance of a sediment column undergoing earthquake-induced liquefaction has been established, and the various means of producing liquefied deposits have been considered. All these considerations form the basis to a palaeoseismic argument which, however, can only be concluded when a specific example is scrutinized. Such arguments will be developed in chapters 13-16 and then discussed in chapter 18.

```
**********************************
```
CHAPTER SEVEN

The Quaternary Geology of Scotland
```
**********************************
```

7.1 CONTEXT

The Quaternary Period in N.W. Europe is a glacial period punctuated by short interglacial episodes, one of which is the present Holocene.

This synoptic sketch of Quaternary geology provides a context to the proposed palaeoseismic events in Quaternary sediments and fault-rupture events displacing Quaternary markers. A simplified map of the Quaternary geology of Scotland is given in **Fig.7-1.**

7.2 THE DEVENSIAN

Between 14,000 and 13,000 years ago large parts of terrestrial Scotland began to emerge through the retreating Late Devensian ice sheet, which 4000 years before had extended as far south as Wales and Norfolk. At its maximum extent this ice sheet attained a thickness of 1.8km; the volume of eroded material has been estimated at 2000 km^3 with the most intense erosion occurring in the Western Highlands (Boulton et al. 1977). Tills from this glacial episode are usually the first members of Scottish Quaternary stratigraphy. The record prior to this is extremely limited: occasional early Devensian tills (c. 75,000 years BP) have been suggested (Sutherland 1981), a former interglacial at around 35,000 years BP is indicated by peat beneath till in Shetland, and dates from fluvio-glacial deposits beneath till suggest much of Scotland was ice-free at around 27,000 years BP (Sissons 1974a).

Immediately off the coast of western Scotland, tills (probably Late Devensian) lie on bedrock (Boulton et. al. 1981), and further offshore lie on several earlier till and glacio-marine formations (Davies et. al. 1984). A major erosion surface seen throughout the inner continental shelf appears to correlate with the onshore late Devensian erosion. This erosive event is of primary importance to

66

Scotland's landscape and usually marks the onset of onshore Quaternary stratigraphy.

The decay of the Late Devensian ice exposed a mantle of tills onto which wide tracts of outwash sediment were deposited. It is among these deposits that most of the candidates for palaeoseismic layers are found. Tracts of outwash sand and gravel in the Tayside area (Fig. 7-1) can be resolved into two series (Paterson 1974). The older series typically displays ice-contact features (kame-and-kettle topography and esker ridges) and has a hummocky morphology. Lacustrine, esturine and marine-delta facies are locally developed within this series. The younger series constitutes an extensive outwash spread, with a smooth surface occasionally interupted by kettle-holes. It was formed sub-aerially and typically has a more yellow colour than the older series.

7.3 THE LOCH LOMOND READVANCE

A rapid short-lived return to glacial conditions occurred in northern Britain at around 10,800 years BP. The effects of this Loch Lomond Stadial constitute the most visible features of the Scottish landscape. The small ice-cap that developed in the Highlands (Fig.7-1) attained thicknesses of up to 1km. Several isolated valley-glaciers developed in the northern and eastern Highlands and in the Southern Uplands. Decay of this ice (completed by 10,200 years BP) was associated with the development of ice-dammed lakes (Fig.7-1), and localized outwash spreads and river terraces. Scores of landslips in the highlands and islands also appear to be associated with this period of ice decay (Sissons 1983).

7.4 THE FLANDRIAN

The Flandrian is the name given to the warmer climatic stage which commenced at around 10,000 years BP and has continued to the present day (Gray 1983). It is therefore equivalent to the Holocene period. It is characterized by forest and peat-land development. The work of Pennington et al. (1972) and Birks (1977) is summarized below. Juniper and herb growth dominated vegetation immediately following Loch Lomond ice decay, but by 9700 years BP birch-hazel

67

woodland became established throughout most of mainland Scotland.
Invasion by oak and elm at about 8500 years BP resulted in a mixed
deciduous forest with later expansion of pine. This mixed-forest
cover maintained itself until 6000 to 5000 years BP when its gradual
decline was accompanied by the onset of blanket-bog peat. A sudden
demise of pine at c.4000 years BP (due to a combination of climatic
changes and human activity) is often witnessed to by a sub-surface
layer of pine stumps in peat. The growth of peat-land and decline of
natural forest has continued to the present day.

In the lowland areas of the Clyde, Forth and Tay valleys
extensive estuarine (carse) clays were deposited in the Flandrian
marine transgression which culminated at around 6000 years BP (Price
1980).

7.5 ABANDONED SHORELINES

The complex history of relative sea levels in Scotland has been
primarily elucidated by the work of J.B. Sissons. His height-distance
diagram for raised shorelines in S.E. Scotland is shown in
Fig.7-2 and illustrates the general sequence of regressions since
the Devensian. Two transgressions have interrupted this sequence
(Fig. 7-2), one immediately following the Loch Lomond Readvance (at
c. 10,000 years BP) and the Flandrian transgression (c. 6000 years
BP). The shorelines of S.E.Scotland form the most complete record of
relative sea level, however many of these shorelines have also been
recognised along parts of the west and south-west coasts.

The interpretation of these relative sea levels will be
approached in chapters eight (§8.3.3) and seventeen (§17.2). This
section will be limited to the description and correlation of the
shorelines.

7.5.1 Pre- Loch Lomond Readvance shorelines

Regional correlation is difficult for these older shorelines.
They include:-

a) Marine shell beds at heights of upto 140m in the east and south
   of Scotland, probably representing an immediately pre-glacial

shoreline (Sutherland 1981).

b) a submerged wave-cut platform in the Firth of Lorne (at a depth
of 30-40m) and around Orkney and Shetland (at depths of 60-90m),
and possibly of early glacial (early Devensian) age (Flinn 1969,
Hall & Rashid 1977).

c) the 'Main Perth' and associated shorelines in east Scotland, of
Lateglacial age (c.15,000 years BP) (Fig.7-2).

d) Lateglacial raised gravel beaches around the Inner Hebrides,
occurring at heights of up to 40m OD, possibly equivalent to
some of the Perth shorelines (Dawson 1982, Peacock 1983).

7.5.2 The Main Lateglacial Shoreline (Main Rock Platform)

The age and origin of the sharp erosional notch along the coast
of Western Scotland, known as the Main Rock Platform, has puzzled
geologists since first described by Peach et al. (1909). Recent
studies (Sissons 1974b, Gray 1978) have now established a fairly
confident correlation of the platform with the Main Lateglacial
Shoreline of S.E. Scotland (Fig.7-2). Similarities in shoreline
gradients, degrees of erosion and stratigraphic relationships favour
this correlation, the main objection being the implicit short
time-interval available to excavate the Main Rock Platform. This
objection is substantially discredited when the extreme periglacial
climatic conditions prevalent at the time are considered (Sissons
1974a, Dawson 1980). It is thought that a combination of intense
freeze-thaw fracturing and debris-removal by ice allowed the
excavation of the platforms into hard rock in the few hundred years
of the Loch Lomond stadial. The preferential development of the
platform on coasts close to the ice margin and in areas of small
fetch supports this hypothesis. Following this argument, it is
interesting that the lake shorelines of Glen Roy, belonging to the
same climatic episode, also show major notches cut into hard rock.

The terminal date of formation of this shoreline is between
10,500 and 10,300 years BP (i.e. during the Loch Lomond Readvance),
on the basis of radiocarbon dating and stratigraphic evidence
(Sissons 1974a, 1974b).

69

7.5.3 The Main Buried Shoreline

This shoreline has been observed only in the Forth valley (Sissons 1972), where it is buried beneath carse and peat deposits. It has a terminal date of formation of about 9,600 to 9,500 years BP. This beach is one of three associated buried shorelines: the High Buried Beach (c.10,300) and the Low Beach (c. 8800).

7.5.4 The Main Postglacial Shoreline

A confident correlation of shoreline fragments around the Firth of Lorne (Gray 1974b), Islay and Jura (Dawson 1982), the Firth of Forth (Sissons 1972) and the Firth of Tay (Cullingford 1977), and more tentatively in S.W. Scotland (Jardine 1971,1975) and the Inner Hebrides (Peacock 1983), may be made on the basis of regional gradients and stratigraphy (Gray 1974b). This shoreline has an age of abandonment of around 6,500 years BP in the Forth area (Sissons 1974a) but appears to have a younger age in the south-west (c.5000) and an older age in the west (c.6900) (Jardine 1982). This shoreline represents the limit of the Flandrian transgression.

7.5.5 The '3rd' and '5th' Postglacial Shorelines

Up to four shorelines following the Main (i.e. '1st') Postglacial have been observed. The most prominant of these, nominated '3rd' and '5th' in the Firth of Lorne area (Gray 1974b), may be tentatively correlated with two prominant shorelines around the Firth of Forth (Smith 1971, Sissons 1974a). Radiocarbon dates in the Forth area indicate ages of c.4000 and c.2500 years BP (Smith 1971).

7.5.6 Concluding statement

This sequence of shorelines, being regionally correlated and having known dates, forms the basis to calculations of isostatic strain rates in Chapter 17:-

a) The Main Lateglacial Shoreline; 10,500±200 years BP.
b) The Main Buried shoreline; 9,600±100 years BP.
c) The Main Postglacial Shoreline; c.6,500 years BP.

d) The 3rd Postglacial Shoreline; c.4000 years BP.

e) The 5th Postglacial Shoreline; c.2500 years BP.

The pre- Loch Lomond Readvance shorelines (§7.5.1) lack internal correlation and precise dating and are not used in these calculations.

****

CHAPTER EIGHT

Ice-loading models

****

8.1 CONTEXT

Models of the response of the Earth system to ice-mass loading proliferate, in appreciation of the unique opportunity that the glaciation process gives us for understanding the physical nature of the Earth. The recency of concluded glaciations, the geologically short duration of the glacial load and the accessibility of currently glaciated areas have together allowed the formulation of surprisingly well-defined quantitative models. This limited review is primarily aimed at gleaning information of a seismotectonic relevance from some of these models. However, such a review has a broader significance to the thesis in view of the following.

a) The Quaternary of Scotland is overwhelmingly a history of glacial processes.

b) The discontinuity tectonics of earthquake occurrence must be appreciated in the context of continuum tectonics, in which glacial-loading plays a major role in N.W Europe.

c) The timescale of glacial loading, that is 10^3 to 10^4 years (Peltier & Andrews 1976), is precisely the timescale of concern to this thesis (the timescale of rare events on capable faults detected primarily by geological methods).

It must be emphasized that this chapter is not an attempt to review ice-loading models themselves, but an effort to re-view them with a seismotectonic perspective, noting that almost all the authors concern themselves with the rheology of the asthenosphere rather than the lithosphere. The main inferences of this chapter will form a basis to the chapter (17) on the tectonics of glacial loading in Scotland.

8.2 DEFINITION OF SOME TERMS USED IN THIS CHAPTER

8.2.1 **Lithosphere and Asthenosphere:** Since this chapter concerns itself with rheology rather than composition it is appropriate to

72

discuss the shallow earth in terms of 'a relatively strong brittle lithosphere overlying a weaker aesthenosphere which deforms by flow' (Bott 1982, pp 8 & 30). The boundary between the two is poorly defined and gradational, but may be regarded as a transition from dominantly elastic to dominantly plastic behaviour at appropriate tectonic strain rates.

8.2.2 **Seismogenic volume:** is used qualitatively to describe the portion of the lithosphere that is capable of strain by periodic rupture (beyond the elastic limit) on discontinuities. It excludes volumes where strain is accomplished by elastic creep or plastic flow, or volumes where stress is not sufficient to generate rupture.

8.2.3 **Viscoelastic material:** That which behaves both elastically and viscously (Turcotte & Schubert 1982, p.296). Such a material displays an elastic after effect (after removal of a load) which, in the simplest case (a Kelvin body), decays exponentially with a characteristic relaxation time (Scheidegger 1982, p.151).

8.2.4 **Relaxation time:** The time taken for an exponentially decaying function to decrease by $1/e$ in amplitude (Walcott 1980).

8.2.5 **Flexural rigidity:** is a measure of stiffness, or resistance to bending, of an elastic sheet under the action of a bending or flexural couple, and, for a plate of thickness, T, Young's modulus, E, and Poisson's ratio, v, is:

$$\frac{E.T^3}{12.(1-v^2)}$$ (after Love 1906).

8.2.6 **Apparent flexural rigidity:** is the flexural rigidity of an elastic sheet which 'adequately matches' a viscoelastic sheet with a particular viscosity and magnitude of stress (Walcott 1970). The viscoelastic sheet will have an apparent thickness corresponding to the thickness of the same elastic sheet.

8.3 THE REVIEW

The review is conducted by asking three questions of the generic 'Ice-loading-model', namely,

1) How do the rheological properties of the model confine the rheology of a seismogenic volume? (§8.3.1)

2) What does the ice-load response-curve imply about associated seismotectonic activity? (§8.3.2)

3) How can vertical crustal movement be resolved from relative sea-level data? (§8.3.3)

8.3.1 How do the rheological properties of the model confine the rheology of a seismogenic volume ?

Early models of transient loading of the lithosphere (e.g. Haskell 1937) tended to focus on the properties of the less viscous asthenosphere as the primary locus for accommodating a displaced lithosphere, whose nature was poorly defined. Walcott (1970) later argued the importance of the flexural rigidity of the lithosphere as "a parameter which ultimately defines the maximum magnitude and wavelength of those surface loads that can be supported without elastic failure of the lithosphere" (p.3942 of Walcott 1970). His analysis of various loads imposed on continental and oceanic lithosphere led him to suggest that:

a) the apparent flexural rigidity of a viscoelastic lithosphere increases as the relaxation time of the imposed load decreases (the relaxation time being dependant on the magnitude of the of the non-hydrostatic stress as well as on the viscosity distribution of the lithosphere and asthenosphere), and

b) the thickness of the lithosphere involved in elastic deformation decreases as relaxation progresses (i.e. as apparent flexural rigidity decreases and wavelength of flexure increases).

The first of these suggestions implies that the lithosphere can sustain large stress differences for long periods of time, when the relaxation time is large, and yet yield to small stress differences when the relaxation time is small (-**Inference 1**-). The second suggestion postulates an upward migration of the effective base of the lithosphere (i.e. the base of elastic behaviour associated with

74

the corresponding deformation wavelength) as relaxation progresses
(-**Inference 2**-).

Peltier and Andrews (1976) imposed a spherical geometry on
previous plane layer models (notably McConnell 1968 and including
Walcott 1970), and were thus able to remove from them the awkward
necessity of a strongly stratified mantle. Peltier and Andrews'
treatment of a wide spectrum of relaxation times and time-dependent
deformation on a spherical earth led them to suppose that:

    a) since short deformation wavelengths have large amplitudes at the
        ice edges, relaxation times at these locations will also be
        shorter (relaxation time decreases with the square of the
        deformation wavelength), and

    b) the rheology of the lithosphere, as opposed to mantle, governs
        the short deformation-wavelength spectra.

Thus the properties of the lithosphere dominate the strain at the ice
margins (-**Inference 3**-).

Concluding statement: It would seem (from inferences 1,2 &
3) that for short relaxation-time loads the lithosphere behaves
elastically to greater depths, especially at the ice margin where the
strain is more strongly governed by the properties of the
lithosphere. Long deformation wavelengths have longer relaxation
times and deform the lithosphere in a more plastic manner (the
lithosphere having a smaller apparent flexural rigidity and apparent
thickness). The characteristics of the seismogenic volume, during
ice loading and recovery, will be influenced by the rigidity and
maximum depth of elastic behaviour associated with the deformation
wavelengths of the ice load. Therefore, during relaxation, as
deformation wavelengths increase, the associated seismogenic volume
will decrease.

8.3.2 What does the ice-load response-curve imply about associated seismotectonic activity ?

The earlier history of the evolving ice-loading-model generally
assumed a simple exponential relaxation theoretically consistent with
the incompressible, Newtonian viscous fluid with which the mantle was

modelled. Observations fitted this model reasonably well in the Fennoscandian region, but reconsideration was called for on the surprising finding of Crittenden (1967) that the Lake Bonneville region (U.S.A.), despite having a load an order of magnitude smaller than the Fennoscandian ice, had a very similar relaxation time, i.e. of the order of 5000 years. This prompted the study of relaxation times in their association with different deformation wavelengths (c.f. Walcott (1970), §7.3.1 above). A spectrum of relaxation-times varying with time after removal of, and distance from, the load became apparent (and complex!), such that relaxation is now rarely considered as being a single, simple exponential decay. Furthermore, the estimation of relaxation times from real data is prone to large error. Even with precise data, such an estimation assumes the remaining uplift is small. If it is large and unknown, then estimates of relaxation times may be incorrect by an order of magnitude (Walcott 1980). These factors must be borne in mind when making judgements concerning the distribution of uplift rates in deglaciated areas.

Several instances of observed crustal uplift indicate that relaxation does not perform as a simple exponential:

a) The results of Andrews (1970) and Brotchie and Silvester (1969) from the Laurentian ice sheet "indicate that crustal warping is doubly inflected", and Hillaire-Marcel (1980) records several inflections in many areas of Quebec, especially regions peripheral to the ice cap.

b) Hinge lines, dividing gently sloping and steeply sloping portions of depressed crust, have been observed in the profiles of the Lake Agassiz shorelines (N.America), and have been interpreted as the outer limits of significant elastic displacement of the lithosphere (Walcott 1970).

c) Current uplift (apparent in tide gauge data) at Glacier Bay, Alaska (ice loading in a tectonically active area) shows a very pronounced double inflection and strongly peaked strain rate profile - **Fig.8-1** (Hicks & Shofnos 1965).

d) The Mesters Vig area of N.E. Greenland "rose at very high rates (upto 9 cm/year) between 9000 and 5000 years BP, but has been

virtually stationary since" (Crittenden 1967).

e) Mörner (1980) evidences two factors contributing to Fennoscandian uplift curves: "an exponential factor which died out some 2000-3000 years ago", and "a linear factor which seems to have commenced shortly before 7700 BP (continuing to the present)".

There is therefore considerable evidence to suggest that uplift, spatially and temporally close to the applied (removed) load, follows a different relaxation curve to that of later times and more distal areas (-**Inference 4**-). It is reasonable to look for a mechanistic explanation for this dichotomy. Such an mechanism could lie in the asthenospheric (viscous) or lithospheric (elastic) ends of the rheological spectrum.

Meissner and Vetter (1976) have argued the existence of a transition between two creep laws operating at different shear stresses in the mantle. They suggest that the dislocation-glide mechanism transfers to diffusion-creep at shear stresses below one bar and that the transition slows down the formerly faster uplift rate during isostatic uplift. Brennen (1974) came to similar conclusions, also suggesting that the decrease in strain rate with depth in the mantle could explain differences in the relaxation curves of different areas with different scales of loading. It thus seems likely that mantle flow mechanisms have an important influence on observed surface relaxation rates.

However, recalling 'inference 3' (§8.3.1), and realizing the lithosphere cannot be completely passive (even when modelled as purely elastic), the lithosphere must have some influence on strain rates, and perhaps a dominant influence in the early, high strain-rate stages of recovery. Very little is known about lithosphere strain mechanisms in this context, but from the arguments presented above it seems reasonable to suggest that elastic failure of the lithosphere is likely to be a governing strain mechanism in the early stages of recovery, whereas in the later stages recovery is more probably governed by mantle strain mechanisms (-**Inference 5**-).

Finally, a further possible explanation is that the cause of inflection is not mechanistic but phenomenal. Specifically that different portions of the curve relate to different imposed loads or deformations. This has been argued for the Quebec area of the Laurentian ice where three phases of ice loading are regarded as contributing to a composite relaxation curve - **Fig.8-2** - (Hillaire-Marcel 1980), and for the Fennoscandian uplift where the 'linear factor' (see 'e' above, this section) may result from a non-glacial factor, such as regional tectonics or geoid migration (Morner 1980).

Concluding statement: Seismotectonic activity associated with elastic failure of the lithosphere due to recovery of depressed crust is probably strongly weighted towards higher activity temporally and spatially close to the ice load, and may perform in two distinct regimes of strain, somehow associated with the two portions of the commonly observed, doubly-inflected recovery-curve. Vertical movement due to a non-glacial factor may exist as a separate phase added to the glacial, exponential phase, and would correspond to a separate seismotectonic component.

8.3.3 How can vertical crustal movement be resolved from relative sea-level data ?

The study of sea level has become a dense convolution of participating factors, such that a simple resolution of local isostatic uplift from a global eustatic reference is now a discarded search. [Clark (1980) concluded with the words "'Eustatic' sea level cannot be measured anywhere"!] The current trend among workers in this field is to construct local eustatic curves in areas of the scale of 100 km, or so, without attempting to correlate globally (e.g. Clark et. al. 1978, and Newman et. al. 1980). Such a study has been carried out for the U.K. by Flemming (1982).

Nevertheless, an appreciation of the global gamut of factors involved is needed before local tectonic and glacial rebound movements can be discerned. Mörner's (1976) schematic diagram of a sea level model is shown in **Fig.8-3**. The main factors are listed

below, together with their probable scale, and are collated mainly
from Mörner (1976, 1981), who tends to focus on geoidal factors, and
from Farrell and Clark (1976) and Clark et al. (1978), who tend to
focus on mass-gravitation factors.

(The figure in square brackets is an order of magnitude change in
vertical level in metres per 10^4 years.)

Factors influencing sea level after major deglaciation:
[100] 1) The volume of water added to the oceans from melted ice, of
    the order of 100m global sea level rise (Mörner 1981).

[10] 2) The ocean basin volume change due to the change in ocean
    water and ice mass distributions; displacement of ocean
    basin surfaces can achieve 10% of eustatic change (Farrell &
    Clark 1976).

[5] 3) The gravitational attraction of redistributed water masses
    (i.e. the change in the equipotential sea level surface); of
    the order of 5% of eustatic change, but can be larger
    locally (Farrell and Clark 1976).

[100] 4) The absence of the gravitational attraction of the ice mass
    on the oceans; of the same order of 'eustatic rise due to
    ice melting' (i.e. in the vicinity of the ice mass) (Farrell
    and Clark 1976).

Factors influencing land elevation:
[0] 5) Changes in the continent-ocean configuration; very long
    term, on the scale of 10^6 years.

[100] 6) Changes in the geoid configuration; up to the order of 100m
    since glaciation, in some places (Mörner 1976).

[10] 7) Vertical tectonic movement; scales of up to kilometres, but
    having rates generally less than maximum glacial rebound
    rates, e.g. 0.3 mm/year for the uplift of the Himalayas
    (Walcott 1973).

[100] 8) Glacial rebound; 100-200 m for major ice caps.

The strongest influence on sea level comes from factors 1,4,6
and 8. Therefore the scenario after deglaciation at a site close to
the ice load (as with Scotland) would mainly involve: a rise in sea

level due to the melting of ice, offset by a fall in equipotential level due to the absence of the ice-gravitational pull, from which glacial rebound, tectonic and geoid-migration factors would have to be resolved. Even assuming that sea-level history is well known and that the purely glacio-isostatic component can be removed by virtue of its local nature (both approachable assumptions in Scotland), there still remain both a tectonic and a geoidal factor in the residual. The roles of these last two factors are important for a true seismotectonic perception and their relative contributions can only be determined from independant information on tectonics and from global geoidal theory.

Concluding statement: Sea level history must be unravelled for the location of interest (100 km^2), from which local vertical crustal movement may be resolved. A glacio-isostatic component can be determined after which the relative contribution of tectonic movement and geoidal migration must be ascertained from independent geological information.

8.4 CONCLUSIONS

In addition to the specific concluding statements above (§8.3) the following general statements are made.

8.4.1. A pure exponential relaxation of the crust after ice loading is rarely apparent because of a number of complicating factors:

  a) the presence of more than one phase of ice loading.

  b) the involvement of separate, longer term tectonic factors.

  c) the sparsity of knowledge concerning the strain behaviour of the lithosphere and asthenosphere during rebound.

  d) the difficulty in modelling poorly defined data of high complexity (particularly in resolving the 'eustatic reference').

8.4.2. Despite this some seismotectonic inferences are achievable:

  a) the seismogenic volume decreases with progressive relaxation.

  b) the lithosphere behaves elastically to greater depths at the ice

80

margins.

c) seismotectonic activity is strongly weighted towards higher
activity spatially and temporally close to the ice load.

8.4.3. Although regional and global comparisons are
instructive, the seismotectonics of glacial loading can only be
properly understood by intensive, site-specific study.

PART III – SCIENCE

PART III(A)
FAULT ACTIVITY

****
CHAPTER NINE
Lismore
****

9.1 INTRODUCTION

The Isle of Lismore sits within the Great Glen Fault zone like a giant triaxial test cell - the specimen is limestone, its exposed dimensions are 16km long by 2km wide - **Fig.9-1**. It has faithfully recorded the strains of Phanerozoic tectonism in Scotland but has mostly concealed its document from the eyes of a generation of tectonists. It is therefore a most suitable entry into a study of tectonics, neotectonics and seismotectonics in the area. [Lismore was also a foremost entry point for the civilization of Scotland by Saint Moulag in the 6th century A.D. (McNeill & Nicholson 1975).]

Lismore is composed of rocks of the Lismore Limestone Formation which is uppermost in the Ballachullish Group of the Lower Dalradian. A summary of the geology of Lismore is shown in **Fig.9-2.** The limestones have been severely deformed into tight folds during the Caledonian orogenesis. Axial planes of these folds and the dominant foliation have a generally NE-SW trend, along the length of the island (Hickman 1975). The only other rocks outcropping on Lismore are numerous dyke intrusions. These were produced in three volcanic episodes - during the Devonian (late-Caledonian), the Permo-Carboniferous and the Tertiary. On the whole these dykes run across the island in an E-W to NW-SE direction. A large number of fractures also trend across the island. The most prominant of these strike approximately E-W.

This study concerns itself with displacements on fractures, best seen in the outcrop of the dykes. The limestone is treated as the matrix within which the dykes and fractures occur. Resuming the triaxial-cell analogy - this is, therefore, a study of (post-Caledonian) strain in the limestone as detected on fractures and dyke intrusions. The dykes act as both strain markers and indicators of tensional episodes (associated with volcanism). The

83

study comprises field evidence.

9.2 FIELD STUDY PROCEDURE

Attention was drawn to Lismore primarily because of its location within the Great Glen Fault zone. Before this study, no Quaternary faulting had been documented; however Holgate (1969) has described dextrally offset dykes, which he thought to be of Tertiary age, in the NE of the island. Reconnaissance photogeological interpretation of the island (at 1:10,000 scale) indicated the presence of several dykes displaying offset and several fresh-looking fractures. A preliminary visit to the island confirmed the presence of both faulted dykes and 'active-looking' surface fractures. A detailed mapping project was then embarked on.

It was decided to limit the study to the southern end of the island where the most promising features had been identified. The mapped area is about 8km^2. The 'mapping' comprised recording the surface traces of all major fractures, faults and dykes on overlays of air photographs at 1:6250. Significant features along these fractures and dykes were noteed and photographed. Specimens of fracture-fill material were taken for thin section and XRD spectrometric analysis.

In the early stages of the study it had been anticipated that the presence or absence of fault-offsets of Tertiary dykes would indicate a 'background-tectonism', which could then form a basis to a consideration of Quaternary fault movement. This objective was somewhat diffused by the sparsity of Tertiary dykes, the difficulty encountered in actually determining the relative age of individual dykes, and the absence of any unequivocally faulted dykes of Tertiary age. As a result the study developed a broader scope, divulging information on post-Caledonian and post-Permo-Carboniferous as well as Tertiary and Quaternary fault movement.

9.3 PRESENTATION OF THE FIELD STUDY

The map of **Fig.9-3** shows all the dykes and fractures mapped. Each feature is numbered and described in Appendix 1. A more detailed

study of the Miller's Port coastal section is illustrated in the
block diagram of **Fig.9-4.** Each feature from this section is also
described in Appendix 1.

9.3.1 General observations

Fractures: The most prominant fracture traces run
approximately E-W. They mostly run right across the island
cross-cutting the NE-SW structural grain. There are also several
fractures running NE-SW (parallel to strike). These are seen only in
coastal exposures – inland their presence cannot be resolved from the
structural grain, which results in a multiplicity of topographic
linears.

Fracture-infilling material: In their field exposure, most
fracture traces appear as nets of tight, calcite-filled
discontinuities. Each fracture is usually less than 1cm wide, and the
nets of fractures typically form a zone a few tens of centimetres
wide. Strike-parallel fractures tend to be wider (1-2m) and typically
appear as brecciated zones within which individual fractures are
difficult to trace (e.g. Fig.9-5). These two types of fracture are
common; they were not treated with more than a cursory note in the
field study. Significance was, however, placed in two distinctive
kinds of fracture:

a) Fractures containing thick, ochreous, heavily-altered material
   (typically 10-30cm thick) (e.g. locality 69, Fig.9-6). These
   deposits are extremely variable in colour, texture and
   thickness. They are interpreted as hydrothermal deposits (see
   §9.3.2, below).

b) Fractures containing clays and other fine-grained,
   unconsolidated deposits (e.g. locality 54). Such fractures are
   usually 'open' by a few millimetres to a few centimetres. They
   include the fractures which have evidence for recent movement.

Dykes: Exposure of dykes within the area is generally good.
As systematic petrographic and geochemical analysis of these dykes
has not been made it is not possible to be certain about the ages of
individual dykes. However, dyke populations can be resolved by means

of the following criteria:

a) Orientation.

b) Outcrop nature, i.e. sinuous trace or straight trace, even
   thickness or variable thickness, continuous or discontinuous.

c) Alteration fabric.

The resolution of dyke population is discussed in §9.4.1, below.

   Dyke offsets: Several kinds of offset are observed:

a) En echelon offsets: a pinching out and overlapping of the two
   portions of the dyke resulting from the emplacement of the dyke,
   as in **Fig.9–5.** En echelon offsets are usually easily
   resolved from faulted offsets.

b) Emplacement offsets: a rectilinear, stepped offset resulting
   from the emplacment of the dyke. Where exposure is good and
   chilled margins are clear this kind of offset can be readily
   discerned. They are also clear where a marked change in dyke
   thickness occurs at the offset, as with **Fig.9–6.** However, in
   cases where exposure is not good it is often difficult to decide
   whether an offset is a result of faulting or emplacement. In
   such cases, emplacement is assumed unless independent evidence
   (such as a second, identical offset) can be found.

c) Faulted offsets: where field evidence indicates that faulting is
   the cause of offset. For example, at locality 67 – **Fig.9–7–**
   two intersecting dykes and a hydrothermal vein all show similar
   offset (4.5$\pm$0.1m) across a pronounced fracture, which also
   offsets three other dykes by the same amount (localities 64 &
   66). This example displays evidence indicating predominantly
   lateral fault movement since several dykes of differing
   orientation are offset by the same amount.

Table 9–1 (overleaf) lists all the faulted–dyke offsets discovered in
the study.

Table 9-1 <u>List of faulted offsets of dykes on South Lismore</u>

Offset(error) (metres)	Sense	Fault trend	Dyke trend	Probable age of dyke	Locality number
2.1(0.1)	Sinistral	020	060	Caledonain	4 (Miller's Port)
1.8(0.4)	Sinistral	020	057	Caledonian	5 (")
0.5(0.1)	Sinistral	000	052	Caledonian	6 (")
20.0(0.5)	Sinistral	030	050	Caledonian	7 (")
26.0(1.0)	Sinistral	030	085	Caledonian	8 (")
1.9(0.1)	Dextral	154	042	Caledonian	10 (")
1.8(0.1)	Sinistral	018	043	Caledonian	12 (")
2.6(0.1)	Sinistral	175	040	Caledonian	14 (")
0.6(0.1)	Sinistral	030	100	Caledonian	20 (")
40(10)	Sinistral	000	090	Caledonian	26 (")
0.4(0.2)	Sinistral	020	050	Caledonian	27
1.9(0.3)	Sinistral	060	024	Caledonian	47
1.6(0.1)	Dextral	165	100	Permo-Carb.	31
4.5(0.1)	Sinistral	040	100&140	Permo-Carb.	67
50(questionable)	Sinistral	040	150	Permo-Carb.	85

Sum totals: Caledonian - 97.7 metres, sinistral; 1.9 metres, dextral.
Permo-Carb. - 4.5 metres, sinistral; 1.6 metres, dextral.

9.3.2 Hydrothermal alteration fabric and mineralogy

A wide variety of fracture-infilling material and dyke alteration fabric are collectively interpreted as the result of hydrothermal activity. The justification for this interpretation is given below.

Critical evidence is found at an exposure of a vein within an altered dyke at locality 85. **Fig.9-8** shows a field sketch of the exposure. Three kinds of fabric are evident in the 4m-wide dyke at this locality (N.B. the term dolerite is used here in the sense of a field-term - the primary mineralogy has not been established.):

a) Relatively well preserved dolerite, showing jointing and chilled margins.

b) Crumbly, altered, dolerite residue.

c) Onion-skin textured, altered dolerite.

Within the onion-textured portion of the dyke runs a straight, 3-5cm wide vein. Its relationship to the fabric-types suggests that the vein has acted as the source of alteration. The vein displays an internal fabric and mineralogy which suggests a hydrothermal origin:

a) XRD spectrometric analysis indicates the presence of dolomite, siderite, chlorite, and cristobalite veinlets, with lenses of quartz and pyrite.

b) These minerals are all known to occur in hydrothermal veins elsewhere (Deer et al. 1978, Fan 1978, Kristmannsdottir 1978).

c) The vein displays an order of mineralization which appears broadly consistent with a decrease in temperature:

> 1st phase - dolomite, siderite, chlorite & pyrite.
>
> 2nd phase - dolomite, siderite & quartz.
>
> 3rd phase - siderite & cristobalite.

Most of these minerals have a fairly broad range in temperature of formation; however, comparison with hydrothermal zones in Hawaii (in volcanic rocks) would suggest a higher temperature of formation for pyrite and chlorite (290-340°C) than for cristobalite (<325°C) (Fan 1978). Thus the vein could represent the deposits of a decaying hydrothermal system.

This vein mineralogy and the relationship of the vein to the alteration fabric of the dyke are taken to indicate formation of both by hydrothermal activity.

Similar associations of hydrothermal fractures and dyke alteration are observed elsewhere on Lismore - e.g. Locality 89, **Fig.9-9.** They are thought to belong to a suite of hydrothermal deposits occurring throughout the area. The significance of these deposits is discussed in section 9.4.1.

9.3.3 Faulted dykes at Miller's Port

The majority of observations of faulted offsets of dykes on Lismore are observed along a coastal section at Miller's Port (Fig.9-3, Table 9-1). A block-diagram showing the distribution of dykes and faults at Miller's Port is shown in Fig.9-4.

A suite of four dykes outcrops within the area. These four dykes are each between 1 and 2 metres thick, although thinner and thicker portions are seen. Each dyke is near-vertical in orientation, although local flexures in the dykes do result in inclined portions. Dykes A, B and C run approximately parallel to each other in a north-easterly direction. Dyke D has an ESE-WNW trend. Faulted offsets of these dykes are observed on a suite of fractures trending NE-SW. The orientations of these fractures have been measured in the field. These measurements are extrapolated downwards to give the third dimension in Fig.9-4. The fracture planes are either vertical or steeply inclined to the north-west. One minor fracture (fracture 2) inclined to the south-east has been measured.

The vast majority of offsets are of a sinistral sense. One small dextral offset (fracture 10) and two shallow-dipping, thrust, offsets (fracture 13) are also observed. In several cases two or more dykes are observed to be offset by the same amount along one fracture, thus substantiating a fault-derived offset (e.g. fractures 5, 7 and 8). The vertical components to these apparent horizontal offsets are difficult to resolve since the dykes are mostly vertical. However, horizontal (lateral) movement is considered to be the main component since where thrust movement is evident (at fracture 13) it is

89

ancilliary to the apparent lateral offsets.

Fig.9-10 shows a field sketch of offsets of dyke-B on fractures 12 and 13. The offset across fracture 12 is a simple sinsistral offset on a steeply inclined fracture. However, fracture 13 comprises a net of fractures in a complicated arrangement. Two shallow-dipping fracture planes (W and Y) have moved to displace a sliver of rock containing dyke-fragment 'b'. Another fault plane was offset by movement on 'Y' such that fault planes 'X' and 'Z' were once co-incident. This complicated set of fault offsets is interpreted as a group of minor adjustments which occurred during the overall sinistral movement of the Miller's Port Fracture Zone.

The total amount of measured fault displacement within the Miller's Port Fracture Zone (excluding minor thrust movements) is 95.4 metres sinistrally and a single 1.9 metre dextral displacement. The dextral displacement occurs on a NW-SE fracture (154°) whereas the sinistral displacements are all on NE-SW fractures (between 000° and 060°). Thus, the Miller's Port Fracture Zone is interpreted as a zone of mostly sinistral fault displacement trending NE-SW.

The Miller's Port Fracture Zone seen in the coastal section can be traced inland as a zone of topographic linears. Some suggestion of offsets of dykes of a similar order to that seen at the coast can be seen inland (dykes 34 and 36).

9.3.4 Evidence for recent fault movement

Two fractures on Lismore display evidence suggesting recent movement. The term 'recent' is taken to mean post-glacial since most features of the present landscape are thought to post-date the last major glaciation (Devensian).

The Loch Fiart fracture: (That is, between localities 42 and 54, Fig.9-3). Several features along this fracture suggest that it has moved recently:

a) At locality 43, a sharp, clean fracture break is observed to sinistrally offset the limestone morphology and lithology by 0.20±0.05m. That is, scarps in the present rock surface and

90

features of the limestone foliation are both displaced by this amount, suggesting that a fresh, recent break has occurred. The exposure is seen in a stream section.

b) At locality 54, where this fracture meets the shore, it can be observed to pass through an altered dyke. The fracture clearly post-dates the dyke since it is discordant with the alteration and jointing in the dyke. The fracture is open and about 3cm wide. It contains some calcite veining, but alongside the calcite vein a layer (5-10mm thick) of micro-breccia (clasts <2mm in size) and pale green clay is observed. XRD spectroscopic analysis shows the clay to consist of chlorite and calcite. The unlithified nature of the micro-breccia and gouge-clay suggest recent movement of the fracture. No calcite veins are evident.

c) At locality 47, a 0.5m thick dyke is observed to be sinistrally offset in two places, 3m apart, by 0.9 ± 0.1 and 1.0 ± 0.2 metres. The offset was initially noted by the morphology of a turf ridge resulting from the positive relief of the sub-soil dyke outcrop. The offset was then established by shallow excavations. The position of weathered clasts of the dyke in the soil around the fracture offset gave some suggestion that this offset was recent (or partly recent) and not just an ancient offset now weathered. The age of the dyke is unknown, although its trend and field charateristics would suggest a Caledonian age (see §9.4.1, below).

d) At locality 48, a turf ridge running downslope (NW-SE) appeared to display offset at the fracture trace. Shallow excavation showed the ridge to result from a ruined crofter's dyke (a wall made of turf and stone). The stones in the dyke appeared to display an alignment offset by 0.20 ± 0.05m sinistrally (Plate-33). Following this a search was made for other man-made features which might also display an offset across the fracture. Excavations of ruined crofter's dykes at localities 45 and 46 revealed no offsets – the dykes being too ill-defined to resolve offsets of the order of tens of centimetres. Resumed excavations at locality 48 revealed a confused distribution of wall-stones at greater depths within the dyke in which no offset

could be resolved. Walls of this type were frequently rebuilt, often annually (Shaw 1980), such that they are not particularly good linear markers. Offset has only been observed in the uppermost portion of the buried wall and in its pre-excavation surface trace.

Thus historical offset is supported only by inconclusive evidence at locality 48. The history of crofting in the area would suggest that the crofter's dyke at locality 48 dates from the 17th or 18th centuries (Shaw 1980, Crawford pers. comm.).

Miller's Port fractures 5 and 6: Along a 100 metre portion of fracture 6, and on fracture 5 which branches off it, several features indicating recent movement are observed. Their locations are shown in **Fig.9-11.**

Fracture 5 has sinistrally offset two, en echelon halves of dyke C (at 5a & 5c) by a similar amount (1.0+0.3m). Between these two dyke-offsets the limestone morphology (at 5b) displays features offset by a similar amount suggesting that the displacement occurred recently. The fault appears to have freshly exposed a limestone surface to weathering action.

Along fracture 6, five morphological features are found to display a sinistral displacement of the same amount as seen at dyke-C (6c). At one of these features (6a), 2mm of brown clay was observed to display a low-angle slickenside lineation consistent with the morphological offsets observed (Plate-5). The five features are:

6a) A white patch of freshly exposed limestone surface which accurately matches the rock profile on the other side of the fracture in a manner consistent with the clay slickenside lineation and a sinistral displacement of 0.50+0.05m (Plate-4). Foliation surfaces in the vicinity also match across the fracture with a sinistral offset of 0.49+0.02m.

6b) A calcite vein and several foliation surfaces match across the fracture with a sinistral displacement of 0.47+0.02m. The calcite vein is bevelled at the fracture surface but does not display a slickenside lineation.

92

6d) A pale, smooth, relatively unweathered patch on a limestone foliation surface at one side of the fracture matches the slope profile on the other side when a sinistral displacement of 0.55+0.05m is restored (Plate-6).

6e) The pattern of several limestone outcrops and ridges on the raised platform suggests a sinistral displacement of 0.5+0.2m along the fracture.

6f) Where the fracture rises up the raised cliff a darker, less-weathered surface on a limestone foliation plane on one side matches the shape of the soil profile on the other side if a sinistral displacement of 0.5+0.2m is restored (Plates-2&3).

Together these features indicate:

* 0.48+0.03m sinistral offset on fracture 6, and
* 0.8+0.1m sinistral offset on fracture 5.

A dry-stone wall crosses the fracture trace at one point (Fig.9-11). Detailed archaeological excavations of this wall were made in order to discover any displacement of it. None was found. The wall probably dates from the 18th or 19th centuries.

Thus Miller's Port fractures 5 and 6 display evidence for recent, pre-historic movement of about half a metre, sinistrally.

9.4 INTERPRETATION OF FIELD STUDY

9.4.1 Discrimination of relative ages of dykes

Resolution of the relative ages of the dykes on Lismore is difficult without detailed petrographic, geochemical and isotopic-dating techniques (which is beyond the scope of this study). However, much can be discerned using field evidence alone. Three forms of evidence can be utilized:

1) Hand-specimen petrography: Caledonian dykes are usually petrographically distinct from both Tertiary and Permo-Carboniferous dykes (Speight & Mitchell 1979). They are more acidic (comprising felsites, porphyrites, spessartities and minettes) than the

Permo-Carboniferous and Tertiary suites, which comprise a similar petrography (of dolerites, camptonites and monchiquites).

2) **Field appearance:** The Permo-Carboniferous and Tertiary dykes may usually be distinguished by their field appearance (as outlined by Speight & Mitchell 1979):
* Permo-Carboniferous dykes tend to have variable thickness, sinuous borders and frequently exhibit brecciation, mineralization and alteration.
* Tertiary dykes are usually of constant thickness with straight or smoothly-curving borders; are fresh with clear chilled margins and rectilinear joint patterns.

3) **Dyke trend: Fig.9-12A** shows a rose diagram for trends of all the dykes mapped on south Lismore. Three populations are evident:

a) Dykes trending between 130° and 145° (NW-SE).
b) Dykes trending between 090° and 105° (E-W).
c) Dykes trending between 060° and 075° (ENE-WSW).

These dyke-trend populations are thought to correspond to the Permo-Carboniferous (a), the Tertiary (b) and the Caledonian (c) dyke-emplacement episodes for the following reasons:

a) Permo-Carboniferous dyke trends in the whole of Lismore, mapped by Speight and Mitchell (1979) cluster around 120° and envelope dyke population 'a' but not 'b'.
b) The straightest, most continuous and freshest looking dykes occur within trend 'b' (e.g. the dyke at locality 41, Fig.9-3). These are generally distinctive characteristics of dykes of Tertiary age.
c) Dyke population 'c' includes mostly very discontinuous dykes of poor topographic expression. This is consistent with their being Caledonian in age. This trend is also consistent with the trend of Caledonian dykes on the mainland to the east of Lismore (Brown 1983).

Although these dyke-trend populations appear to coincide with

94

the named episodes, some dykes do not fit with this scheme when their field appearance is considered. This is especially so for dykes of the Tertiary and Permo-Carboniferous populations. For example, dyke 40, thought to be Permo-Carboniferous, is parallel to dyke 41, thought to be Tertiary (on the basis of field appearance). Both lie in the 'Tertiary' trend-population. Similarly, some apparently Tertiary dykes (straight and unaltered) lie in the Permo-Carboniferous trend (e.g. the dyke running between localities 50 and 100, Fig.9-3).

Accepting these anomalies, the above field criteria allow some confidence in discerning the relative ages. In general, the dyke-trend populations are assumed unless field appearance indicates otherwise.

Confirmation of the validity of the dyke-trend population argument is found in a consideration of hydrothermal activity. Fig.9-12B shows a rose diagram for the trend of fractures containing hydrothermal deposits (as outlined in §9.3.2). A marked peak in orientation between 130° and 140° is observed. This is co-incident with dyke population 'a'. Studies elsewhere (Speight & Mitchell 1979, Cameron & Stephenson 1985) indicate that this kind of hydrothermal, or deuteric, alteration is common in the Permo-Carboniferous volcanics of Scotland. This substantiates the supposition that dykes of trend 'a' are Permo-Carboniferous in age. Dykes of the Caledonian trend occasionally display discordant hydrothermal alteration (e.g. locality 69, Fig.9-6) indicating that the supposed Permo-Carboniferous hydrothermal activity affected the earlier dyke population.

Fig.9-13 shows the main occurrences of the hydrothermal alteration deposits. They are essentially observed on NW-SE fractures with a spacing of approximately 1km. This regular spacing of the deposits is thought to result from the operation of hydrothermal convection cells during the Permo-Carboniferous volcanic episode.

9.4.2 Age and magnitude of faulted-offsets of dykes

Following on from the interpretation of dyke populations in the previous section, it becomes apparent that the main occurrence of faulted dykes, at Miller's Port, involves dykes of Caledonian age. Almost all the dykes in the Miller's Port section maintain a NE-SW orientation (Fig.9-4, Table 9-1). The only exception is dyke D which has a WNW-ESE trend. The field charateristics of these dykes appear to be consistent with a Caledonian age - they do not show signs of (Permo-Carboniferous type) hydrothermal alteration and they are not straight, fresh and neatly jointed like most Tertiary dykes. Thus it is surmised that the substantial sinistral offsets of dykes at Miller's Port (95.4m) represent post-Caledonian movement.

Two other small offsets of (probably) Caledonian dykes are observed outside the Miller's Port Fracture Zone. These are at localities 27 and 47. Thus, a large majority of the faulted dykes on south Lismore are thought to be of Caledonain age (Table 9-1).

The remaining cases of faulted dykes are a 1.6m dextral offset at locality 31 and a 4.5m sinistral offset along fracture 65. In both these cases dyke-trend and the presence of hydrothermal alteration suggests a Permo-Carboniferous age for the dykes. This is most clearly the case at fracture 65 where a hydrothermal vein is clearly offset with the dykes.

Another, possible, 50m sinistral offset of a Permo-Carboniferous dyke at locality 85 cannot be confirmed by independent evidence. No unequivocally Tertiary dykes have been found to be faulted.

9.4.3 Recent fault movement

Two faults which show signs of displacement of the present land surface and morphology have been identified on south Lismore (§9.3.4). These recent movements comprise:

a) 0.2 metres of sinistral movement on the Loch Fiart fracture (trending between 050° and 080°).

b) 0.5 metres of sinistral movement on Miller's Port fracture-6 and 0.8 metres on the adjoining fracture-5 (both trending between

020° and 030°)

Evidence for movement on the Loch Fiart fracture includes an apparent displacement of a ruined crofter's dyke (wall), probably dating from the 17th to 18th centuries. Independent evidence to substantiate this historical displacement has not been found. Thus the Loch Fiart displacement may have occurred during historic times.

A much larger amount of evidence supports half-a-metre of recent movement at Miller's Port. This latter movement has been shown not to displace an 18th to 19th century dry stone wall. This recent movement comprises reactivation within a Caledonian fault zone.

9.5 SYNTHESIS

9.5.1 Faulting on Lismore

What then is the history of strain recorded on the Isle of Lismore - the triaxial test cell of the Great Glen Fault? The main findings are summarized below and illustrated in Fig.9-13.

1) Substantial sinistral displacement of Caledonian dykes on NE-SW fractures, and most notably on the Miller's Port Fracture Zone where a total of 95 metres of sinistral offset has been measured.

2) Faulting of Permo-Carboniferous dykes and hydrothermal-fracture deposits at two places:

* 4.5m sinistrally on a NE-SW fracture (65), and
* 1.6m dextrally on a N-S fracture (31).

3) No unequivocal faulting of Tertiary dykes.

4) Two fault movements are inferred to be post-glacial:

* 0.2m on the Loch Fiart fracture
(trending between 050° and 080°), and
* 0.5 and 0.8m on two associated fractures
within the Miller's Port Fracture Zone
(Trending between 020° and 030°).

9.5.2 Comparison with previous work on Great Glen faulting

A summary of hypotheses on Great Glen fault movements was given in section 4.4.8, above. With regard to these, this study indicates the following:

a) The substantial sinistral offsets of Caledonian (Lower Devonian) dykes across the Miller's Port Fracture Zone (c.100m) are consistent with the major Devonian sinistral movement along the Great Glen (c.100km), postulated by several workers.

b) No clear evidence has been found to confirm the postulated dextral movements of post- Permo-Carboniferous age (Speight & Mitchell 1979) or Tertiary age (Holgate 1969).

c) Sinistral movement has occurred since the Permo-Carboniferous dyke intrusions on NE-SW faults (c.5m).

d) Recent, post-glacial, sinistral movement appears to have occurred within two approximately north-easterly fault zones (<1m).

****
CHAPTER TEN
The Firth of Lorne
****

This chapter reports levelling surveys made at two localities on the 'Main Rock Platform' raised shoreline found around the coasts of the Firth of Lorne.

10.1 INTRODUCTION

One of the onland, Quaternary fault movements documented before this study (for others refer to §4.4.7) was that reported by Gray (1974) and inferred from levelling of the Main Rock Platform. Gray's study involved accurate levelling of all suitable fragments of the rock platform around the Firth of Lorne. This enabled him to establish the presence of a major shoreline level in the area - the 'Main Rock Platform'. Linear regression and trend-surface analysis indicated a general westward inclination of the shoreline with a gradient of 0.16m per km, falling from 11m above sea level in the east to about 4m in the west. Contours for this surface are shown in **Fig.10-1**. In his analysis of the data, Gray discovered several dislocations of the shoreline level suggesting block movement and faulting. These dislocations involved differential tilting and faulted offsets of up to two metres. In this thesis study was aimed at establishing the validity of these block movements and fault offsets proposed in Gray's study.

Before making field reconnaissance study of the area, Gray's (1974) published data-base was subjected to a small test: If the dislocations are real and the result of tectonic activity (as Gray suggested) do they have any correlation with major faults in the area? **Fig.10-2** shows Gray's data plotted against distance from the Great Glen Fault (the assumption being that this fault was the main locus of activity at the time of dislocation). Plotting Gray's data in this manner indicates that anomalous shoreline heights are more abundant in the vicinity of the Great Glen fault, implying that tectonic movements have indeed affected the shoreline elevations.

99

Reconnaissance field study was then made in order to assess the presence and magnitude of specific dislocations implicated in Gray's study. Following study of air photographs (at 1:25000 scale), several sites were reconnoitered and two were selected as being conducive to intensive levelling survey, having well developed platforms close to suspected fault offsets.

10.2 SURVEY PROCEDURE AND PRESENTATION OF DATA

10.2.1 Description of sites

Shuna - Fig.10-3: The isle of Shuna is in Loch Linnhe at the head of the Firth of Lorne. It is about 1km wide and 2km long. The Main Rock Platform is well developed all the way round the island forming a pronounced notch in Lower Dalradian limestones and slates. Attention was drawn to the island because the levelling measurements of Gray (1974) showed a surprisingly large variation around it - a range of 1.7m (as opposed to the 0.1m which would be expected on account of regional tilt). Study of air photographs indicated a number of fracture lineaments on the island, appearing to cut or modify the trace of the raised sea cliffs. Consequently, seven survey plots were constructed on the island in an attempt to discern any offsets of the platform level across the several fractures present.

Port Donain, Mull - Fig.10-4: Along a section of the east coast of Mull, Gray's data appeared to indicate an offset of 2.3m in the Main Rock Platform level at the point where a post-Mesozoic fault intersects the coast at Port Donain Bay (Fig.10-1). The platform is well developed either side of the bay (Plate-1), cut into Tertiary lavas in the north and Jurassic shales and sandstones in the south. A set of four survey plots was constructed, two on each side of the bay. After preliminary assessment of the results two more survey plots were constructed further south.

10.2.2 Survey procedure

Details of the levelling survey techniques and the data produced are given in Appendix 2. In this section the overall methodology and

approach are discussed.

The aim of the levelling survey at both localities was to resolve any vertically-offset shoreline levels present. There were therefore two stages involved in the survey: firstly, to detect and define 'levels' within the shoreline profile, and secondly, to correlate such levels across suspected loci of offset.

The procedure adopted by Gray (1974) in his study involved probing through the peat cover of the platforms with steel rods in order to locate the break in slope at the back of the platform (i.e. the shoreline) and then measuring this level relative to Ordnance Datum. Such measurements were made every 30-60m along well-developed platform fragments. Measurements from each fragment were combined to produce a mean value to be used in regression analysis.

In the study for this thesis, it was decided to survey the platform profile in a grid of level measurements (termed a 'plot') relative to a permanent local reference (a concrete pillar) - (Plate-1). Each plot typically consisted of four profiles perpendicular to the shoreline with measurements spaced at 3m intervals. The profiles were spaced 10m apart to produce a grid approximately 30 x 30m, varying with the shape of the platform. Each measurement consisted of an elevation of the ground surface and of the rock surface (rockhead) beneath, located by means of a peat bore or soil auger driven downwards until no further penetration was achieved. Material retrieved from the auger or bore allowed some assessment of the nature of the superficial deposits. Profiles from these measurements were then graphically reconstructed in order to detect shoreline levels. The permanent, local, reference points were then levelled-in relative to each other so that relative shoreline levels of each grid could be determined. [Note that measurements were not levelled-in to Ordnance Datum, only to the local reference points, which, being permanent, could, if required, be levelled-in to Datum at a later date. Gray's study indicates the platform to be at around 10m above O.D. at Shuna and around 8m O.D. at Port Donain, Mull.]

Thus the data produced in this levelling survey comprise a series of profiles of the Main Rock Platform shoreline showing surface and rockhead, with fragmentary information regarding the nature of the superficial deposits.

10.2.3 Presentation of the data

Appendix 2 contains maps of the survey plots, tabulated survey data, and graphs of 49 shoreline profiles. Also given are two shoreline-parallel profiles (termed 'traverses') constructed at Port Donain, Mull, in an attempt to more accurately locate the locus of a suspected fault. The following should be noted when considering these profiles:

a) In general the profiles consist of an upslope (back of platform) inflection, a gently dipping 'platform' and seaward 'lip' (see for example, Mull: Plot 2, A2.6). On the landward side of the measured profiles the slope rises rapidly to the raised cliff (typically 10-20m high) and on the seaward side the slope descends rapidly from the 'lip' to the present shoreline (c.10m below).

b) Not all profiles are 'complete' (in terms of the description just given). In some the landward inflection is not apparent (eg. Shuna: Plot5 line4, A2.6), and in others the seaward lip is absent (eg. Shuna: Plot 5: line 3, A2.6). The reason for this is usually topographic irregularity. However, each plot contains at least one profile where all the features are apparent.

c) In some profiles, portions of the rockhead profile are missing due to thick (that is >1m) superficial cover (usually peat) (eg. Mull: Plot 5, A2.6).

d) The zero point for each profile is located on a line approximately parallel to the shoreline and immediately in front of the raised sea cliff. The relationship of this line to the base of the cliff is indicated on the maps of survey grids (A2.4). Some profiles do not start at this zero-point, if local topography dictated otherwise.

This set of profiles provides a valuable portrait of the shape

102

of the Main Rock Platform. Such profiles have not been constructed before. In themselves they may give insight into the method of formation (not the premise of this study) and collectively they allow the resolution of vertical offsets of the platform (considered below).

10.3 INTERPRETATION OF DATA

10.3.1 The formation of the Main Rock Platform

The weight of opinion is now in favour of formation of the Main Rock Platform during the Loch Lomond stadial under conditions of intense freeze-thaw fracturing of rock (see §7.5.2). Consistent with this hypothesis for their formation is the broad similarity of the measured shoreline profiles to that observed in present polar coastal environments. Dawson's (1980) study of shore platform development drew attention to the 'Nab' profile form, idealised by Nansen (1922) and illustrated in **Fig.10-5A**. This profiles involves the development of a coastal 'lip' by enhanced erosion on the landward side of the lip by a freshwater ice-foot. This profile has many similarities to the profiles measured in this thesis - **Fig.10-5B**. However, the Main Rock Platform profiles often have a notch or bench on the landward side of this 'Nab'-type profile. The significance of this bench is not fully understood - it could perhaps represent the high water mark, beyond which ice-foot action developed unhindered by tides. Discussion of shoreline genesis will not be pursued further. It suffices to state that the observed profiles appear consistent with their development under polar climatic conditions, as thought to have occurred during the Loch Lomond stadial. Formation of this shoreline under a short-lived, severe, climatic condition (the Loch Lomond stadial) points to its strong candidacy for a palaeo-level marker, and suitability for the resolution of vertical crustal movements.

10.3.2 A 'first-look' at profile elevations

Shuna: Fig.10-6 shows the profiles of each plot superimposed with each plot displayed at true relative elevation. The profiles have been drawn with a vertical exaggeration of x18 to enable rapid

visual assessment of the position of the platform level. The arrows
show the interpreted elevations of the platform notch in each plot.
This 'first-look' assessment is somewhat premature - other notches at
different elevations (generally lower) could be inferred - however,
it is apparent that substantial variation in the shoreline elevation
is present. It is difficult to conceive of a single Main Rock
Platform level through all seven plots.

Mull: A similar presentation of the Mull plots is shown in
Fig.10-7. Again, substantial variation in elevation of the
platform is apparent. In particular, plots 5 and 1 are substantially
higher than the rest, by over 2 metres. What is interesting here is
that these two higher plots appear to show something of a second
platform notch at the level of the other plots (marked by '?'). More
rigorous analysis is clearly needed.

10.3.3 A statistical approach to resolving offsets

In an attempt to provide a more objective criterion for
assessing platform levels, the height distribution of rock surface
measurements at each plot was treated statistically. A Gaussain
frequency distribution was determined for the data of each plot,
namely,

$$f(X) = \exp[-(X-M)^2/2s^2)]/\text{sqrt}(2.\pi.s^2)$$

where, X= the variable (height), M= the mean of the data, and s=
the standard deviation.

Figs.10-8 to 10-15 show these Gaussian distributions for each
plot (and also the two Mull traverses). Also shown are histograms of
the data (normalized to correspond to the Gaussian curve) and an
'Integer Gaussian' curve (that is, the Gaussian distribution adjusted
to an integer value corresponding to the data histogram).
Presentation of the data in this way allows the following judements
to be made:

a) Determination of the 'sharpness' of the platform level - whether
   the data is peaked (small variance) or is broadly distributed
   (large variance).

b) Assessment of the fit of the real data (histogram) to the
   Gaussian distribution.

c) Detection of levels in the data significantly different from the
   Gaussian distribution (i.e. some significance may be attributed
   to a level where it departs from the integer Gaussain by more
   than one integer).

Plot S:1 is the most peaked distribution. The rest of the Shuna
plots are moderately peaked. (Plot S:3 has a strong peak in the
histogram but the Gaussain distribution is fairly broad.) The Mull
data are mostly moderately peaked, however, M:1 is extremely broadly
distributed. M:1 is interesting in that the measured levels appear to
form two clusters either side of the mean.

In **Fig.10-16** the means and one standard deviation for data
from each plot have been displayed at true relative elevation on
north-south projections of the plot locations. In this way,
statistically significant offsets of platform levels can be
discerned. Only one such offset is apparent at each site:

a) 1.3+0.7m between S:1 and the rest of the plots at Shuna.

b) 0.5+0.4m between plots south of M:1 and north of M:2 at
   Mull.

Although this representation of the data is objective and
reveals some offset in platform level, it does not appear to fully
explain the range in elevation. Recalling the 'first look'
interpretation (§10.3.2), the distribution of means in this analysis
(Fig.10-16) shows a very similar height distribution to the benches
inferred in Figs.10-6&7 (N.B. the sequence for the Shuna plots is
different in the two figures), suggesting that the standard deviation
statistic is masking some real offsets. Furthermore, one should
consider whether geomorphological information could provide a more
definitive assessment of offsets. Thus a fuller consideration of the
platform height variation is appropriate (noting that we are now
trespassing the bounds of statistical confidence).

10.3.4 A judicial approach to resolving offsets

[By 'judicial' I mean the subjective judgements of an inherently prejudiced scientist!]

In Figs.10-17&18 the rock profiles for each plot have been displayed (vertical exageration x18) with the plots placed at true relative distances and elevations. The left-hand axis of each plot corresponds to its relative location. (The Shuna plots have been projected on to a north-south line). Data points have been removed from the profiles in order to improve the visual perception of slope inflections (as opposed to elevation density). At the left-hand axis of each plot the elevations of observed inflections (i.e. a step in the profile) are shown. A 'star' is shown for an inflection level seen on two or more profiles, a 'dot' for one seen on only one. These inflections have then been subjectively correlated to give several levels of undetermined significance. These interpretations are as follows:

Shuna: A lowermost level (L) has been correlated across five of the plots and is inclined gently to the south. Above this occur two other levels (the Middle and Upper, M&U) which appear to be differentially offset from the lower one (L). However plots S:2 and S:3 show all three levels displaced together. Inferred offsets of 1.0m and 0.7m on the 'M' and 'U' levels are shown.

Mull: Three levels are also apparent in these profiles, appearing to be displaced together. The levels in M:5 and M:1 are substantially higher than the rest. An offset is also apparent between M:2 and M:3. It is interesting that questionable (?) levels in the lower half of of M:5 and M:1 align with the lower level drawn through M:6, M:3 & M:4. Offsets of 2.0, 2.7 and 1.0m inferred in this scheme are shown.

It must be acknowledged that this approach to resolving offsets is very subjective. In many cases 'levels' have been inferred from inflections seen on only one profile and comprising only two data points. Furthermore, no previously documented evidence can be found to support the presence of three such levels within the Main Rock

Platform, or similar platforms. However, several points are found to support this scheme:

a) The three levels are apparent at both Mull and Shuna despite their being 25km appart.

b) The spacings of the three levels are similar in all the plots (a little less than one metre).

c) The largest offsets resolved in this scheme are in the same position and sense as the offsets evident in the statistical approach (§10.3.3).

10.3.5 Shoreline parallel traverses at Mull

During the course of the levelling survey at Mull it was decided that traverses between plots M:2 & M:1 and M:5 & M:1 were required in order to more accurately locate main suspected fault; i.e. the 2.7m offset between M:1 and M:2. The locations of the traverses are shown in Fig.10-4 (note that the traverse between M:5 and M:1 also crosses the fault-lineament BB').

The traverse between plots M:5 and M:1 proved disappointing on account of thick superficial deposits (it is shown only in Appendix 2). The traverse between M:2 and M:1 provided valuable information, having a complete rockhead profile. It is shown in **Fig.10-19**, alongside the range of rockhead heights measured at each plot. The profile falls in a series of steps from plot M:1 to a gully, before rising again to plot M:2. **Fig.10-20** shows the same profile without data points, and incorporating the occurrences of sand and gravel detected in auger inspection (the rest of the profile superficial material comprises peat). Sandy deposits were encountered at three places within the traverse – each where a step in the profile occurs. The supposition that these are beach deposits appears to be supported by the fact that the lowermost deposit (3) is on a level with the M:2 platform level. The other deposits occur on the flanks of the M:1 platform level, and appear to coincide with the upper, middle and lower (U,M,L) profile inflections of M:1. Deposit '1' flanks the upper and middle levels and deposit '2' co-incides with the lower level. It is notable that these levels not only

correspond to the beach deposits but also to notches in the traverse profile.

The gully in the profile is thought to correspond to the boundary between Tertiary basalt and Jurassic sediment on the basis of extrapolation of this boundary from its exposure on the shore. The sharp, sandless notch in the profile is thought to correspond to a fault (this is argued on the basis of field evidence in §10.5, below).

Thus the evidence from the traverse between plots M:2 and M:1 appears to support the existence of a faulted offset of the buried shoreline levels and strengthens the interpretation of three shoreline levels within the Main Rock Platform.

10.3.6 Summary of interpreted offsets

Shoreline profile elevations at both sites clearly indicate variations in elevation of 1 to 2 metres. Statistical treatment of the data indicates offsets of the platform level of:

* 1.3+0.7m at Shuna, and
* 0.5+0.4m at Mull.

However more involved consideration of the data suggests that three levels are present at both sites and display multiple offsets of:

* between 0.7 and 1.0m at Shuna, and
* between 1.0 and 2.7m at Mull.

10.4 ASSOCIATED FIELD STUDIES AT SHUNA

All the faults and fractures apparent on air photographs were studied in the field. Lack of exposure hindered this work - most fault traces being covered by peat, soil and beach deposits, and apparent only as topographic features.

Where fracture lineament 'A' (Fig.10-3) meets the southern shore the trace appears to be marked by beach gravels abutting fractured rock. No clearly recent rock fracture was found; however a few

108

centimetres of low angle normal faulting of semi-consolidated beach gravels was seen a few metres away from this trace. These could represent surficial slump failure or differential compaction, but their occurrence close to the fracture trace is at least suggestive of post-glacial fault movement. However, in view of the doubt concerning their origin these surficial displacements cannot be given much significance.

More substantial evidence was, however, obtained at one good exposure in the southern bank of the lochan in the north-west of the island.

10.4.1 Description of the lochan fracture exposure

The locality occurs at the intersection of fracture lineaments 'C' and 'D' (Fig.10-3). It displays several gouge-filled fractures, intersecting one another, within shale country rock also containing a metre-thick igneous intrusion (a felsic dyke - on the basis of hand-specimen examination). A sketch of the exposure is shown in **Fig.10-21.** The clearest fracture runs grossly NW-SE, consistent with it being an expression of the fracture lineament 'D'. Other fractures run NE-SW, parallel to the strike and the fracture lineament 'C'. Also indicated in Fig.10-21 are the results of XRD spectrometric analysis of the fracture-infilling material. Apart from rock fragments, three phases of clayey-gouge are present:

a) A yellow-brown Kaolin and Chlorite phase occurs within most of the exposure of the NW-SE fracture (Plate 30).

b) Where this fracture abuts the igneous intrusion a red, vermiculite clay is developed in the fracture.

c) A black-grey lithic residue, containing only minor clay minerals occurs in many of the strike-parallel fractures (NE-SW).

The significance of these fracture-infilling materials is poorly understood. It is supposed that they represent in-situ (in-fracture) decomposition of adjacent rock as a result of accelerated fluid flow and mechanical break-down along the fracture. This supposition is somewhat supported by the fact the vermiculite, which commonly occurs at the contact between acid intrusives and basic rocks (Deer et al.

109

1978), is only observed adjacent to the felsic dyke (this assumes that the fracture has acted as a locus for chemical reduction of the dyke).

10.4.2 Interpretation of the lochan fracture exposure

The felsic dyke, outcropping within the exposure, is seen to be sinistrally offset by 2.8m along one of the NNE-SSW fractures. The abutments of the dyke against the fracture are heavily fractured and broken and do not appear to have chilled margins. The offset is therefore interpreted as a faulted offset. The dyke is of unknown age. On account of its orientation, location and field appearance it is most likely to belong to the Permo-carboniferous swarm, but could be Caledonian or Tertiary.

The fracture offsetting the dyke appears to pre-date the NW-SE fracture. This later fracture contains the most distinct, least diffuse gouge material (Plate-30). No displacement along this fracture can be readily inferred; however the geometry of the debris-filled cavity between 4.5 and 6.5m (Fig.10-21) suggests a dextral movement of several tens of centimentres. Although these fractures are of unknown age their infilling by unlithified gouge clay suggests geologically young (late Quaternary?) activity, the most recent movement occurring on the NW-SE fracture.

10.5 ASSOCIATED FIELD STUDIES AT PORT DONAIN, MULL.

10.5.1 Field observations

During preliminary investigation it had been supposed that any fault displacement at Port Donain would most likely result from movement of the substantial WNW-ESE fault running across the peninsular (Fig.10-1) and displacing Mesozoic sedimentary rock (Fig.10-4). In the field this fault ('A' in Fig.10-4) has a pronounced topographic expression but is indistinct as a surface trace and is unexposed where it meets Port Donain bay. As the levelling survey progressed it became clear that this fault was not the main locus of shoreline offset. Instead, interest was focussed on the approximately N-S fracture lineament B-B'. Several fractures of

this orientation are evident in the shore, expressed as narrow broken gullys, about 10cm wide (for example C-C'). Several Tertiary dykes with a similar trend are evident, though usually of a more NNW-SSE orientation. Occasionally the fractures run alongside the dykes. None of these showed any clear evidence of recent movement. However the fracture lineament BB' was found to show several features suggesting recent movement:

a) Where it meets the shore it is evident as a several-metre deep, half-metre wide gully running about 10m inshore - more pronounced than any other fracture seen in this coastal section. The gully contains the remnants of a weathered-out dyke and also evidence of abundant veining, shearing and weathered fracture-infilling material.

b) The present shoreline topography is consistently higher on the western side of the gully, by 1-2 metres.

c) On the surface of the Main Rock Platform this lineament is evident in a small scarp, 1-3 metres high, truncating the raised sea cliffs.

d) The lineament then rises up the main raised cliff (north of plot M:1) and runs north as a faint but sharp lineament.

e) In several places, trees form a line along this lineament in the form of isolated occurrences of vegetation not associated with visable surface drainage.

10.5.2 Comparison of field observations with levelling survey data

Is this lineament B-B' a manifestation of a fault which caused offset of the Main Rock Platform? The lineament crosses the survey profiles at four points. The following is observed:

a) The rather poor traverse profile between plots M:5 and M:1 (Appendix 2, A2.6) shows the rock surface descending fairly rapidly to the locus of the lineament.

b) The two profiles of plot M:1 show breaks in slope at their intersection with the extrapolation of the lineament trace (Appendix 2, A2:6).

111

c) The traverse between plots M:2 and M:1 (Fig.10-20) shows a sharp break in slope in the vicinity of the extrapolation of the lineament trace. This break in slope is not associated with beach deposits.

d) In each of these observations the profiles display scarps consistent with fault downthrow to the east.

Thus it is supposed that the north-south lineament B-B' is the trace of the main fault causing offset of the Main Rock Platform, involving downthrow to the east by about 2.7m.

10.6 EVALUATION OF INFERRED FAULT DISPLACEMENTS

10.6.1 Shuna

Levelling survey has established several vertical offsets of the Main Rock Platform level on Shuna, of the order of 1 metre. Study of air photographs and field exposures indicates that NE-SW and NW-SE fractures are the most likely locus of fault movement. Excellent exposure at the lochan fracture locality indicates geologically recent movement of two of these fractures. These features are illustrated in **Fig.10-22.**

The most substantial offsets implicate block movement in the south of the island, with the block containing plot S:1 being lower than adjacent blocks by about 1 metre. Smaller offsets, of the order of decimetres are apparent elsewhere (as indicated in Fig.10-22); however little confidence can be placed in the significance of these. The most recent movement at the lochan fracture locality is on fracture 'D', which is also the locus of the largest and most significant displacement inferred from the levelling study. This association gives considerable confidence to the judgement that the larger offsets of platform level are due to faulting.

10.6.2 Port Donain, Mull

Fig.10-23 summarizes the main information gathered in this study. Levelling survey and field study have together established the role of a northerly fracture (B-B') as the primary locus of fault movement, involving a 2.7m downthrow to the east. Other displacements

112

are also inferred - c.2m between plots M:5 and M:6 and c.1m between
M:2 and M:3. However, no faults have been clearly identified as
responsible for these later displacements. Northerly fracture
lineaments, similar to BB' are observed (e.g. CC') and could be the
locus of these smaller displacements. Again, the association of an
identified fault with the largest platform offset substantiates the
suposition that these offsets result from fault movement.

10.6.3 Age of fault movement

Very little can be said regarding the age of movement except
that they are post- Main Rock Platform (therefore post- Loch Lomond
Readvance). However, the supposition that three levels are present
within the Main Rock Platform would indicate that the faulting
occurred during the time of shoreline formation since at Shuna the
lowest level does not appear to be faulted as much as the two higher
levels.

10.6.4 Concluding statement

Studies at these two localities in the Firth of Lorne were made
in order to determine the validity of differential block movement and
fault offset of the Main Rock Platform raised shoreline apparent in
the levelling survey of Gray (1974). At both sites inferred fault
displacements have been substantiated:

a) Shuna: Gray's study - a height variation of 1.7m
            This study - several offsets of 1.3m and less
b) Port Donain, Mull: Gray's study - an offset of 2.3m
                       This study - an offset of 2.7m and two
                       smaller ones.

At both sites rather more complex movement than a single fault
offset is indicated. Local block movement on groups of fractures is
evident in both cases.

****
CHAPTER ELEVEN
Glen Roy (faulting)
****

11.1 INTRODUCTION

11.1.1 Background and context

Following an intensive levelling programme, Sissons & Cornish (1982) reported fault displacements (of less than 2 metres) of shorelines of the ice-dammed lake which occupied Glen Roy and adjacent valleys in the Central Highlands of Scotland. This lake was developed during Loch Lomond Readvance times. The displacements were observed in the vicinity of a large landslip which had removed the lake shorelines. Field study for this thesis was directed towards elucidating the significance of this reported fault displacement, the results of which are presented in this chapter. Chapter thirteen presents the findings of a study of deformation and slumping in the sediments of the ice-dammed lake, discovered whilst investigating the landslip. These two studies are complementary and, although carried out simultaneously during the summers of 1984 and 1985, are presented separately because of the difference in subject material and in order to avoid unreasoned association of the two phenomena (faulting and soft-sediment deformation). Some overlap of the two chapters is encountered when considering the landslips: the landslips are described in section 13.7.1 whereas all aspects of displacement and faulting (in relation to the landslips) are considered in this chapter.

11.1.2 Summary of the findings of Sissons & Cornish (1982)

The published results of the study of shoreline altitudes made by Sissons and Cornish (1982) are shown in **Fig.11-1.** Their study involved levelling, at 1760 points, of the break in slope of the fossil lake shorelines. Measurements were spaced at 25-30m intervals along the shorelines, and the average closing error for the 4-5km traverses was 0.011m. They found that, in general, the shorelines were close to horizontal, having height ranges of 2.3-2.4m for each

114

of the three main shorelines. However, adjacent to a large area of landslipping (referred to below as the 'Main Roy Landslide') they observed tilting, displacement and anomalously high levels of the shorelines.

In the top part of Fig.11-1 the normally near-horizontal trace of the middle shoreline can be seen to suddenly rise to higher levels and then disappear altogether where the landslide has removed the shorelines. A more detailed display of the anomalous portions of all three shorelines is shown in the lower part of Fig.11-1. In general, the shorelines begin to rise from their normal elevation (at '1') in a series of two or three tilted-step segments, and then rapidly descend into the landslide, eventually disappearing completely.

Sissons & Cornish (1982) interpreted their observations as being the result of reverse faulting along the prominent scarp '1' (Fig.13-27) causing uplift of the shoreline immediately NE of it. The landslide, generated by the fault movement, then removed the shorelines and caused peripheral, downslope drag of the shorelines on the uplifted block. They concluded that the faulting and landsliding must have occurred at the beginning of the Holocene since river terraces formed soon after the deglaciation of the Loch-Lomond-Readvance ice are not affected by the faulting and tilting apparent in the lake shorelines.

11.2 FIELD OBSERVATIONS

Features of interest were identified by stereoscopic study of air photographs at scales of approximately 1:25,000 for most of the Glen Roy and Upper Glen Gloy areas, and 1:10,000 for the area immediately around the Main Roy Landslide. These were then investigated in the field and mapped onto overlays placed on the air photographs. The field study developed to give special attention to features seen along what will be termed the 'main fracture' (M-M'). These features are described with reference to the photo-interpretation shown in **Fig.11-2;** the subsections below correspond to locality numbers used in this figure.

11.2.1 Cleft-and-ridge feature 1

A pronounced scarp, facing upslope, with a gully or cleft on the upslope side runs diagonally up the valley side to the west of the Main Roy Landslide (see Plate-38). This feature was inferred by Sissons & Cornish (1982) to be the fault scarp which produced the shoreline displacements since the upward tilting began at the point at which the extrapolation of this scarp intersected the middle shoreline (Fig.11-1). It is a grossly straight feature, observed over 800m, but has a sinuous surface trace on the 10-metre scale (Fig.13-27). The relationship of its surface trace to topography led Sissons & Cornish (1982) to suppose that the scarp resulted from a fault dipping into the valley side (i.e. north-westwards). This interpretation seems generally valid, but locally the trace suggests a more variable attitude near the surface, occasionally inclined downslope. The scarp faces up the slope implying that the lower half of the hillside was raised relative to the upper half. A faint lineament to the south appears to form a continuation of this feature, below the shorelines.

11.2.2 Cleft-and-ridge feature 2

Similar but less pronounced than feature (1), and roughly parallel to it. This feature approximately marks the highest point on the middle shoreline, after which it begins to descend into the landslide (Fig.11-1).

11.2.3 Headscarp of the landslipped area

A downslope facing scarp up to 5m high immediately above the area of landslipping. It is mostly formed along the foliation plane of the country rocks (Moine), dipping steeply downslope (80° towards 130°. Large blocks of bedrock (up to 10m across) below this scarp have been rotated downslope (by toppling) and are embedded in loose debris and soil.

11.2.4 Main-fracture lineament

A very straight lineament is seen plunging down the mountainside. Where it descends down this south-facing slope it

appears as a simple scarp, up to 2m high and facing west
(Plates-26&27). Occasionally the high (east) side of the scarp shows
bedrock exposure, but mostly the whole scarp is covered by stony
surface rubble. This scarp intersects the shorelines in
approximately the same place as the cleft-and-ridge feature (1), such
that either, or both, mark the point at which the shoreline levels
begin to rise. No clear intersection of the shorelines with this
lineament is seen; the scarp peters out before the shorelines are
encountered. This main-fracture lineament continues south and north
as a series of very straight segments, clearly seen on air
photographs.

11.2.5 Knick points

Two clear knick points are seen in the Upper Glen Gloy stream
profile. These may have a tectonic significance linked to the stream
capture processes further downstream.

11.2.6 Scarp in hillside

A major bedrock scarp, parallel to the regional foliation, is
cut by the main fracture lineament, in a manner suggesting sinistral
offset of several tens of metres.

11.2.7 Features of stream capture

A number of features of the course of the River Gloy in relation
to the main fracture suggest neotectonic activity along it. These
features are discussed with reference to the large-scale map shown in
Fig.11-3 (see also Plate-43).

Most of the main-fracture lineament, in this section, contains a
present-day stream course. However, in one small section the former
course (c2) has been diverted around a topographically raised
block of uncertain origin. The diverted flow joins a substantial,
disused stream course (cl), which at one time may have contained
the bulk of the flow of the present western tributary of the River
Gloy. The stream course then plunges down a waterfall (w5) into
the side of a 10m-deep gorge formed along the fracture. The bulk of
the flow of the present River Gloy comes from the western tributary

117

which plunges over a waterfall (w4) into the side of the same
gorge. It then flows down the gorge. At c3, the stream follows a
very complicated path, being briefly diverted from the fracture line
by a small, topographically raised block. The stream then rejoins the
gorge over another waterfall (w3). After this it continues down
the gorge, over two small waterfalls (w2 & w1) and into the main
Gloy valley to follow a sinuous course down the flat bottom of the
glaciated tough.

East of the 'brief' diversion of the stream at c3, two
curved stream-terrace fragments mark the former course of the river
at an earlier, more active stage (probably an ice-wastage stage). Two
indistinct, broad drainage troughs (c4 & c5) appear to represent
former courses of the western tributary where it used to cross the
fracture, without diversion, gently curving round to join the main
section of the River Gloy. Another indistinct trough (c6) also
appears to mark a former stream course.

11.2.8 Rock and fault morphology

Along much of the fracture trace, downstream from f2 (Fig.11-3),
exposure of a narrow, fresh-looking fracture can be seen within the
gorge. Joints, shear fractures and calcite veins are abundant in the
gorge, but this fresh, usually very straight, fracture is distictive.
In many instances it can be seen to contain a soft, plastic, bluish
clay in fracture cavities a few millimetres thick. At f1 several
phases of gouge-clay are seen in a 20cm wide zone within weathered
rock (Plate-29). The freshest of these, blue-grey in colour consists
of kaolin and chlorite with finely ground rock material of quartz,
mica and feldspar (by XRD analysis). This freshest, blue-grey clay
lies closest to the side of the fracture which appears to have moved
most recently. The morphology of the exposure suggests that this
most recent movement comprised a dextral offset of 30 ± 20cm
(Plate-28). Clay-gouge material from several other locations in the
freshest fracture within the gorge was found to have similar
constituents: kaolin, chlorite and major rock-forming minerals.

At f2 an extremely good exposure of rock fractures in the

118

stream gorge reveals several episodes of fault movement. It is displayed in **Fig.11-4**. The fractures occur in schists and pelites of the Moinian, Eilde Flags formation (Hickman 1975), which being basement rock precludes immediate conclusions as to their neotectonic significance. The exposure depicts a series of sinistral offsets, displacing a distinct black schist layer (BS) and a quartzo-feldspathic vein (QV). The foliation and layering are steeply dipping at this locality (70-80° towards 130°), such that largely horizontal movement is implicated. The apparent sinistral offsets (D-D', C-C' & B-B') are on broken, sinuous fractures, and amount to between 20 and 50cm. They are truncated by a much straighter, fresh-looking fracture (A-A') with an apparent dextral displacement of 0.50±0.03m (measured on four different markers). This dextral displacement also appears to have offset the moulded topography of the stream floor, whereas the earlier sinistral displacements are moulded by fluvial action. Thus the fracture with dextral offset appears very recent. However no clay-gouge was seen within it - it is a very tight fracture at this exposure.

At two other localities dextral offsets of between 15 and 50cm are apparent in the rock type and morphology of the stream floor. In each case it is difficult to be certain that what is seen is a recent morphological offset, but collectively there is a strong suggestion that the freshest fracture moved dextrally by about half a metre during the existence of the present gorge.

Immediately downstream of the lowest waterfall (w1) a 1.5m thick, vertical igneous dyke (d) is truncated against the fracture, on its western side. The continuation of the dyke is seen 38m down stream on the other side of the fault. No other dyke exposures were found in the gorge, despite searching upstream and downstream for hundreds of metres. The abutments of the dyke against the fault were sheared and broken in both cases and did not comprise chilled margins. Thin section and XRD spectrometric analysis of the dyke show it to be a highly altered dolerite or lamprophyre with abundant calcite veins, chlorite and kaolin. Texturally the two halves are very similar, however XRD spectrometry shows the

downstream, eastern half to be more altered, with lower proportions of primary minerals. A suite of eleven samples, from both halves of the dyke, was analysed (by XRD) and it was found that the internal variations within each half of the dyke encompassed the differences between them, and that the least altered portions of both halves were essentially identical in mineral composition and abundance – Fig.11-5. Thus it is concluded that a single, continuous dyke has been sinistrally offset by 38m. The age of the dyke is unknown, but its composition and fabric are most consistent with its being Permo-Carboniferous in age (Bell pers. comm.) and its east-west orientation is consistent with the regional trend of the Permo-Carboniferous dyke swarm to the south.

11.2.9 Glen Gloy landslip

On the northern side of Glen Gloy two tongues of debris appear to descend from a lineament running diagonally up the hillside. They are fairly indistinct and are mostly apparent as a surface scar of former landslipping. The Glen Gloy lake shoreline is weakly developed within the scar. The scar covers the supposed extrapolation of the main fracture lineament seen on the south side of the glen. A continuation of the main fracture lineament is apparent to the north of the landslip scar.

11.2.10 Knick point lineation

Knick points in three streams appear to align with a lineament which appears to join the main fracture lineament.

11.3 SYNTHESIS OF FIELD OBSERVATIONS

11.3.1 The main fracture lineament

The suite of lineaments, comprising the main fracture, shown in Fig.11-2 cannot be confidently extended further north or south on the basis of air photograph analysis. They comprise a segmented fracture trace 7km long. Two main trends are followed by the fracture segments:

a) The segments at localities 4 and 7 trend at between 155° and

165°.

b) Elsewhere a northerly trend is evident (between 000° and 010°).

Splays off this main fracture trend at 020°, by the Main Roy Landslide, and at 140° at locality 10. The fracture trends are all oblique to the regional foliation direction. Grossly, the lineament trends NNW.

11.3.2 Major sinistral displacement

It is notable that restoration of the 38m sinistral offset of the dyke (locality 8) would sensibly realign the drainage pattern (at locality 7) allowing the River Gloy to flow right across the fault and through channel c4 (Fig.11-3). A larger magnitude restoration of the drainage features could be invoked, by matching c1 to c4, and c5 to the present western tributary. However this is not essential to make sense of the drainage - c1 and c5 could have been small feeder tributaries. In view of the known offset of the dyke, it is proposed that c.40m of sinistral offset has occurred since the initiation of the Gloy drainage pattern. It is also proposed that displacements producing this offset resulted in the blocking of the fracture gully, causing local diversions at c2 and c3.

Age of the major sinistral displacement: The offset dyke is most probably Permo-Carboniferous in age. Scottish drainage patterns are almost certainly Tertiary or later (c.f. §4.4.3). However, since the area is known to have been under major Devensian ice caps, it is supposed that small-scale drainage features like these must post-date the last major glaciation. Also the whole of the River Gloy drainage system is developed within a large glaciated trough. Loch Lomond Readvance ice did not reach this locality (Sissons 1979b). Most of the observed features are above the lake shoreline (at 355m), but channels c4 and c5 continue below the shoreline and appear to be blanketed by lake sediment. Thus it seems reasonable to suppose that at least some of the 40m sinistral displacement was accomplished after the Late Devensian glaciation, but before the Loch Lomond Readvance.

11.3.3 The recent dextral displacement

The most recent displacement apparent in the Glen Gloy stream section is a half-metre dextral offset. Offsets are displayed in morphological as well as lithological features and are seen on the freshest looking fracture, also containing gouge-clays.

It is noteworthy that the scarp seen along the fracture lineament at locality 4 would be consistent with a small dextral offset of this order: the east side of the fault, on a steeply inclined, south-facing slope, being raised relative to the west side.

The anomalous shoreline levels measured by Sissons and Cornish (1982) would not be expected to detect lateral offset. However, it is interesting that the raised shoreline segments occur on the far side of splays (localities 1 & 2) which would be expected to be 'pushed up' by dextral movement along the main fracture. It should be noted here that the shoreline level measurements did not actually record a vertical offset, but rather a tilted block elevated at the landslipped end. Continuing this argument, the landslide would be a portion of the hillside thrown up and out (southwards) by the fault rupture movements, and the raised shoreline segments a portion which was thrown up but did not fail into landslipped material.

Thus all the evidence for the most recent movement along the fault can combine to form a coherent picture - fracture offsets, fault scarps and shoreline displacement all resulting from a dextral offset of the order of half a metre along a 7km long segmented surface rupture. It is not possible to be certain about the direction of offset, but it seems to be dominantly horizontal, in view of the offsets in the Gloy gorge and since fault scarps are best developed on steep slopes.

11.4 STUDY OF LANDSAT IMAGERY

11.4.1 Procedure

A study was made of lineaments seen in the Glen Roy area on an extract of a LANDSAT Thematic Mapper image. Details of this study are

122

outlined in Appendix 3. A variety of processing techniques were applied using the GEMS image processing system. Each potentially useful image was photographed on colour slide. These comprised mostly positives and negatives of bands 2,3,4,5&7 and images of principal components and synthetic variables derived from these bands. Line drawings of lineaments seen on each photographed image were constructed, and in order to remove (at least some) spurious lineaments, composites of these individual line drawings were constructed. These composites comprised lineaments occurring on more than one image. Note that some degree of observation bias is necessarily involved in these hand-drawn interpretations.

The purpose of the study was firstly to discover lineament populations to which the main-fracture lineament might belong, and secondly to see if the main-fracture lineament, itself, could be seen, and if so to determine its extent. The main results of this study are presented in Figs.11-6 to 11-12. **Fig.11-6** shows a simplified geological map of the study area, **Fig.11-7** a magnetic anomaly map, and **Fig.11-8** a map of glacial moraines; each presented in order to help decipher the significance of various lineaments.

11.4.2 Evaluation of lineaments

Fig.11-9 shows a composite of lineaments occurring on more than one image of each of five principal components of the five bands 2,3,4,5&7. Three main lineament populations are evident:

a) A set of north-easterly lineaments, parallel to the Great Glen (Loch Lochy). These are almost certainly lineaments arising from the Caledonian basement trend, evident both in the geological map (Fig.11-6) and the magnetic anomaly map (Fig.11-7).

b) A set of NNW lineaments.

c) A set of ENE lineaments (perpendicular to the NNW set).

A rose diagram of these lineaments is shown in **Fig.11-10**, where the three populations stand out very clearly.

The significance of the NNW and ENE populations is not immediately apparent. There are no known faults or geological trends in these directions. An image of the 3rd principal component, with a 16x16 edge enhancement matrix applied, picks out these two populations extremely well - **Fig.11-11**. In this image some curious polygonal-shaped features can be seen. It is suggested that these polygons are glacial features, for the following reasons:

a) Although they are extremely large for ice-polygon features (3-5km across), polygons of this order are known (John 1977).

b) They are developed in an area just behind the frontal moraines of the Loch Lomond Readvance ice-sheet, i.e. beneath former ice cover.

c) They occur on LANDSAT images where the Readvance moraines are most clearly seen.

The fact that the unknown lineament-populations are most evident on the same images on which the 'glacial' features appear, suggests that they could be joint or fracture sets developed during glacial times.

This supposition is supported by the coincidence of the main fracture, with its proposed post-glacial movement, with this lineament population. **Fig.11-12** shows an interpretation of a negated, band-4 image where the mapped M-M' lineament is clearly seen as part of the NNW lineament set. (This image is reproduced in Plate-36.) A possible southward extension of the lineament (M-M') is also apparent. Fig.11-12 also shows up several curved features. These are thought to be related to ice retreat, since the easternmost one corresponds to a mapped moraine (Fig.11-7).

11.4.3 Summary of lineament study

The main fracture, studied in the field, appears to belong to an orthogonal set of lineaments trending NNW and ENE. These trends do not correspond to any known lithological or major structural trends. They are interpreted as being a set of fractures generated during glacial times (by virtue of association with other glacial features).

124

11.5 SEISMICITY

The immediate vicinity of Glen Roy shows no instrumental seismicity. A cluster of microseismic activity is observed several kilometres to the south (Fig.12-6). However, there is some evidence of historical activity in the area. Dollar (1947) reports significant events felt at Roybridge and vicinity in 1924 and 1946. The largest of these occurred on December 25th, 1946, at 17.02 hours. The maximum intensity was Davison-VI (Mercalli-V) and the region enclosed by the Davison-IV (Mercalli III-1/2) was 3500 square miles. A portion of Dollar's report of this event is shown in **Fig.11-13**, revealing quite significant ground shaking. Furthermore, it is interesting to note that an aftershock on the 5th of January, 1947 was heard in west Glen Roy and Glen Spean which (assuming this 'aftershock' occurred on the main-shock fault) suggests that the epicentre could have been on the fault outlined in this study.

Thus, appreciable historical activity has occurred in the vicinity of Glen Roy, but no microseismic activity has been recorded.

11.6 SUMMARY

Field and remote-sensing study of faulting in the Glen Roy area, following the report of landslipping and faulted shorelines by Sissons and Cornish (1982), has revealed the following:

a) A 7km-long, segmented fracture seen on aerial photography and LANDSAT imagery and associated with the shoreline displacement and landslipping.

b) Neotectonic displacements of the fault, including c.40m of lateral, sinistral offset of drainage and lithological features, and a most recent half-metre dextral offset (inferred to be post-glacial).

c) An association of displacement, fault-rupture and landslip observations which collaborate to produce an internally consistent single-event, fault-rupture argument (for the half-metre dextral displacement).

d) LANDSAT lineament study which suggests that the fracture

125

described belongs to a group of NNW / ENE orthogonal lineament sets of 'glacial origin'.

```
************************
      CHAPTER TWELVE
   Kinloch Hourn (faulting)
************************
```

12.1 INTRODUCTION

The most seismically active region in Scotland, during the 15 year (1969-1984) instrumental record, has been the Kintail area of NW Scotland (Fig.5-6). During that period 23 events with magnitudes greater than $3.0M_L$ have been recorded, the largest of which were 4.6 and $4.8M_L$ (Burton & Neilson 1980).

Apart from considering this seismicity (§12.3) air-photograph and field study was made of the area in order to identify the presence of any surface manifestations of fault activity. An extremely prominent surface fracture was identified within the area – the Kinloch Hourn Fault – which also showed some association with epicentral lineations observed in plots of microseismic activity. Study of this fault is outlined in section 12.2. Field study of other faults and related surface features was not pursued, partly because of time contraints, but largely because features as clear as the Kinloch Hourn Fault could not be identified during reconnaissance air photo survey. The Strathconnon Fault, although a major geological fault, is apparent on the surface only as a diffuse ill-defined zone of faulting. The study of LANDSAT imagery in section 12.4, goes some way towards regionallizing the study of surface fault features, by association with the one fracture studied in the field – the Kinloch Hourn Fault.

12.2 FIELD OBSERVATIONS ALONG THE KINLOCH HOURN FAULT

12.2.1 Background and geological setting

The Kinloch Hourn Fault is a major geological fault trending NNW (between 115 and 140°N) and mapped for a distance of almost 30km (BGS 1975). At its north-western end it terminates against the Strathconon Fault (Fig.4-4) and in the south-east it peters out within the Moinian basement within which it lies. The fault has displaced the

127

steeply-dipping Moine rocks by about 1km in a dextral sense –
Fig.12-1. The age of this dextral displacement is difficult to
determine since relationships to younger rocks are not seen. However,
its continuity, consistent offset of Moine, and relationship to the
Strathconon and other major Highland Faults indicate that its main
movement occurred during the early Palaeozoic, i.e. a late-Caledonian
strike-slip fault.

Prominent surface mainifestation of the fault is seen over a
distance of 14km, from its intersection with the Strathconnon Fault
(Grid. 1912 8126) to Loch Quoich (Grid. 2000 8042) (Fig.12.2). It is
this section of the fault which has been studied in detail in the
field. Attempts to trace a surface manifestation of the fault east of
Loch Quoich proved unfruitful. Fieldwork was carried out following
the identification of features of interest on aerial photographs at
1:25,000 and 1:10,000 scales. Field and air-photo interpretation of
the fault is described with reference to the map shown in
Fig.12-2.

12.2.2 General description of the fault

The surface trace of this fault is remarkable for its linearity
and prominence despite passing through strong surface relief
(Plates-7&8). The trace of the fault rises from 90m near the head of
the (sea) Loch Hourn to its highest point at 640m on the flanks of
Sgurr a' Mhaoraich within a distance of 3km. It crosses four separate
drainage basins, plunging across the intervening watersheds without
deviating from its course. These relationships to topography are
easily understood in terms of a vertical fault plane; however, what
is striking about this fault is that throughout its varied
altitudinal range it maintains a sharp surface profile in the
appearance of a 'scored line' running across the topography. This
sharp surface profile is evident in a steep-sided gully (10–20m wide)
or a small scarp (c.5–10m high). In several instances drainage is
deflected across the fault (Plate-7). No geological feature can be
seen crossing the fault without interuption along the 14km of
'prominent surface mainfestation'.

12.2.3 Description of morphological features
(with reference to Fig.12-2)

A to B: At 'A' the Kinloch Hourn Fault is seen to terminate against a short lineament perpendicular to it , which appears to be part of a diffuse zone of discontinuous fractures of the Strathconon Fault. Between 'A' and 'B' the Kinloch Hourn Fault runs obliquely down a hillside where is is marked by large scarps on the upslope side. A small pocket of peat can be seen ponded against the fault.

C to B: A curved linear appearing to splay off the main fault trace. This linear runs through an area of hummocky moraine. The moraine morphology is generally elongated parallel to the fault. Nowhere can the moraine be seen to cross the fault and truncation of moraine by the fault is not seen.

B to D: The fault is evident here in drainage deflected along it and at the base of a large scarp. Relict drainage features are seen to the south-west of the fault, now infilled by blanket-bog peat.

D to E: At 'D' a pocket of river alluvium sits on or close to the fault. Trenches were dug (half-metre deep) in this sediment in order to discover any faulting present. No clear faults were observed, although small normal faults (throws of a few mm) of uncertain origin were seen. Joint lineaments at 'D' and 'E' show little or no displacement across the fault.

E to G: The fault passes through a broad valley covered by blanket-bog peat. The fault line can be traced through these surficial deposits as a faint linear. No exposure of the fault is seen in the banks of the loch at 'F' which sits on the fault line.

G to H: Stream deflection along the fault at 'G' marks the start of a very prominant section of the fault (from G to M) where a narrow, steep-sided gully marks the surface trace of the fault. The fault runs steeply uphill to a crest at 'H'.

H to I: A section of the fault-trace affording the best exposure of fractures within the fault zone. The steep-sided, natural

129

fault-gully (c.10m wide) has been additionally exposed by the North of Scotland Hydro Electricity Board who made excavations when emplacing a line of pylons (between 1982 and 1984). It is within this section (at 'X') that detailed study of the fault was made (section 12.2.4).

I to J: Landslipping and forest cover masks the fault trace for a short section here. A back-scarp to the area of landslip can be seen to the NE. A triangular area of scree and debris has fallen into the fault gully at 'J'.

J to K: A steep-sided gully is seen where the fault rises over a spur; no exposures of fractures were seen.

K to L: The fault gully is not so pronounced, but is marked by a stream running along it. Upslope of the fracture, on the NE side, exposures are seen showing post-glacial slumping of soil and glacial till. Some sharp junctions of till against soil are seen, indicating dislocation during slumping. Up to half a metre of soil is developed above the slumped deposit indicating that, although clearly post-glacial, slumping occurred quite a while before present (i.e at least 100's of years).

L to M: A steep-sided gully rising to the highest point on the fault trace (640m). Several exposures of fractures within the' gully, including a 'most-recent' straight fracture. The fracture zone is only 3m wide here. No fracture-infilling materials were found. At 'L' the fault-trace makes a fairly abrupt lateral step, at a point where a prominant cross-linear is seen. This cross-linear does not correspond to a lithological boundary or a mapped fault. It is interpreted as a major joint. A few fractures, seen to propagate north-eastwards from the step, are also interpreted as joints.

M to P: The fault continues south-eastwards across high ground. The sharp gully ceases to be seen, instead only small scarps and drainage features depict the fault trace. South-west of 'P' traces of the folded foliation in the country rock can be seen.

12.2.4 Study of fracture-infilling materials

At locality 'X' (Fig.12-2) an excellent exposure of rock fractures in the fault gully shows a most recent, sharp, straight fracture within a zone of fractured rock about 5m wide. The most recent fracture can be traced continuously for 50m and at several places is seen to contain two phases of gouge material in fracture cavities up to 50mm wide (Plate 10). The two phases are distinctly coloured, bright orange and blue-grey, and often run alongside each other. At one point the fracture cavity widens to incorporate a wedge of peaty soil up to 0.3m wide (Plates-11&12). This soil wedge contains weathered boulders, apparently having fallen into the cavity with the soil, and several lenses of gouge material passing through it (Plate-9).

Thin section study and XRD spectrometric analysis of the gouge material show the following (c.f. Cover Plate):

   a) XRD spectrometry reveals rocks minerals of quartz and mica, but no clay minerals.
   b) Comparison with XRD spectroscopy of the country rock indicates a similar composition, but the complete absence of plagioclase feldspar in the gouge material, and a tendancy for the mica to develop a more hydrated, mixed composition in the gouge.
   c) In thin section a shear fabric is seen in the gouge, with intense folding and dislocation of the gouge fabric, and the inclusion of rounded quartz grains, up to 5mm across.
   d) Shearing and disruption of the boundary between the two phases of gouge material.
   e) A late, planar, dislocation surface, within the blue-grey phase, which indicates sliding movement within the gouge.

In summary, the gouge consists of a finely-ground, mineral matrix, containing rounded clasts of quartz and deformed by shearing along the fracture. The relationship of the two phases to shear fabric indicates that the blue-grey phase is the later one. [Note that the thin section of the fault gouge, displayed in the cover plate, was made using standard rock thin section techniques since

drying of the sample over several months at room temperature rendered it 'hard as rock'.]

The observed relationships of the gouge phases to the wedge of peaty soil are as follows:

a) The gouge material is best developed and most distinct where both sides of the fracture are rock (not soil).

b) Where the soil wedge is encountered a thin layer of brown, clayey gouge material is developed at one side of the wedge (where soil meets rock). This is the only gouge material found to contain any clay (chlorite). It was not observed beyond the soil wedge, suggesting its development results from alteration of the soil wedge.

c) The two brightly-coloured gouge phases do nevertheless pass into the soil wedge where they occur as discontinuous lenses (Plate-9).

Therefore it is concluded that the gouge materials were developed after the deposition of the soil wedge in the fracture. It is suspected that shear movement along the fracture resulted in the inclusion of the gouge phases in the soil.

Because of this relationship of gouge to the soil wedge a sample from the soil was submitted for radio-carbon dating (Appendix 7). The sample was taken from a portion of the wedge close to the included lenses of gouge material. In order to reduce the possibility of contamination with late carbon from more recent surface processes, 15 to 20cm of the soil wedge was removed before sampling. The exposure, as a whole, was excavated by the Hydro Board less than two years previously (1983/84) (D. Cameron pers. comm.) such that the soil wedge was not exposed for more than 2 years before the hand excavations of this study.

The sample submitted for dating (c. 2kg in weight) was found to contain 1.6% carbon in the <1mm fraction. The date achieved was 2400 ± 50 years BP. There seems no reason to question this date – there was ample carbon for accurate dating and no source of contamination was discerned in field sampling. On the basis of this

date it can be surmised that a major opening of the fracture occurred before 2400 years BP. The cavity created was then infilled by peaty soil from contemporaneous soils around the fracture. Post-2400 years BP activity of the fracture resulted in the intrusion of the gouge phases into the soil wedge and simultaneous and/or later shearing of the gouge material itself. This interpretation is illustrated in Fig.12-3.

12.2.5 Interpretation of stream offsets across the fault

It is readily apparent on air photographs that several stream courses are deflected along the fault before continuing on their south-westerly course across it. At first look the sense of offset of the drainage pattern lacked consistency: the stream crossing at 'B' is deflected sinistrally, but others are deflected in two directions (at 'G' and between 'M' and 'N') or not at all (at 'K'). However, close inspection reveals several former drainage paths which appear to have once aligned with portions of the present drainage. An interpretation of former drainage paths and diversions of present drainage in relation to the fault is shown in **Fig.12-4.** In each instance (1 to 13) restoration of a c.160m sinistral offset allows a systematic reconstruction of the drainage pattern. Former drainage channels (now dry or containing only a trickle of present water flow) are seen on either side of the fault in a manner suggesting capture of flow by fault movement. For example, the broad, peat-filled channel at 'B' (Fig.12-2) is interpreted as the former continuation of the stream '4' (Fig.12-3). Furthermore, there are several instances where the present drainage is seen to enter an 'oversteepened' gully when passing from NE to SW, i.e. the stream becomes more incised on the SW side of the fault.

The measured offsets of reconstructed drainage paths are given in table 12-1. The offsets are found to average at 160m+40m in a sinistral sense. A few features appear to conflict with this interpretation but can be explained as follows:

a) No offset of the stream between '4' and '5' is evident. Where the upper portion of this stream crosses the fault, the stream

runs through peat bog and is incised into the surface by less than a metre, i.e. it is not a long established drainage path. Downstream of this, where it again crosses the fault, it is inferred that the pre-offset drainage ran along the fault, as it does at present, resulting in the apparent lack of offset.

b) Between streams '6' and '7' several streams are seen running straight across the fault. These occur in the area of landslipping and forest cover, such that no reconstruction of drainage is possible.

c) Stream '13' appears to have been offset across two splays of the fault as well as the main fault by about 50m on each, amounting to 150m in total.

Table 12-1 Measurements of inferred stream offsets across the Kinloch Hourn Fault (cf. Fig.12-3)

Stream number	Offset (metres)	Stream number	Offset (metres)
1	200	8	170
2	170	9	160
3	150	10	200
4	150	11	150
5	150	12	140
6	150	13	50+50+50
7	160		
Average = 160±40 metres, in a sinistral sense.			

Thus the drainage pattern suggests a c.160m sinistral offset of the fault and also an unknown amount of downthrow to the NE (resulting in enhanced incision to the SW). If this interpretation is compared to lineaments seen around the fault (Fig.12-2) further credibility is added to this interpretation. The roughly east-west trending lineaments between 'H&I' and 'L&M' and the splays at both ends of the fault can be interpreted as Riedel shears, consistent with sinistral movement along the fault (Fig.12-3). (Note that these lineaments are thought to represent major joints or fractures since they do not correspond to lithological boundaries or mapped faults.) Futhermore, in terms of scarp morphology, most fault scarps face

134

north-eastwards - which is consistent with downthrow to the NE.
However, between 'A' and 'D' south-eastward facing scarps are seen on
the NE side of the fault - presenting an inconsistency in this
interpretation. The topography does not allow these scarps to be
interpreted as the result of lateral sinistral movement. However,
this may be resolved when it is considered that these are very large
scarps in the hillside, such that vertical movement of the required
sense could be masked within the larger scale hillslope morphology.

Age of drainage offset: It is supposed that, although major
Scottish Highland drainage patterns may have a Tertiary origin,
small-scale drainage patterns such as these probably post-date the
last major glaciation. The Loch Lomond Readvance ice probably covered
most of this area, but could not have been thick since the site is at
the western extremity of the ice and since frontal moraines (NE of
the Arnisdale Lochs) are fairly small (2-3m high). Therefore these
drainage features may well pre-date the Loch Lomond Readvance. The
fact that many of the disused drainage channels are infilled by thick
(post-glacial) peat deposits (>1m) suggests that they were abandoned
during, or before, the Loch Lomond Readvance. Thus it is concluded
that the movements producing these drainage offsets occurred sometime
between the last major glaciation and the early Flandrian (i.e.
between c. 13,000 and 6,000 years BP).

12.2.6 Summary of field evidence

At Kinloch Hourn the following is observed:

a) An extremely sharp surface fracture extending for a length of
   14km, trending WNW (between 115 and 140°N), and being a portion
   of a major fault in the Moinian basement, showing 1km of dextral
   displacement.

b) A straight surface trace unmodified by strong topography,
   indicating an essentially vertical fault plane.

c) A sinistral offset of drainage paths crossing the fault,
   amounting to c.160m.

d) An exposure of the fault showing two phases of fault gouge,
   which are sheared by fault movement and 'intruded' into a wedge

135

of soil within the fracture; the soil being dated at
2,400±50 radio-carbon years BP.

12.3 SEISMICITY

12.3.1 Previous work

The historical record of seismicity in the NW Highlands is
extremely poor due to the sparcity of population and the lack of
local records. However, it is clear that the present high level of
activity has been reported before. Davison (1924) documented a spate
of activity between 1888 and 1899 AD which he termed the 'Invergarry
earthquakes'. During that time a large number of events were felt at
Invergarry and neighbouring hamlets (Fig.12-6). Very little
information is available on the location of these events however they
were almost certainly located to the west of Invergarry and probably
within the vicinity of Kintail.

The relatively high level of seismicity in the Kintail area
during the intrumental record (since 1967) was especially evident
during August of 1974 when a swarm of 18 events, having magnitudes of
between 2.6 and 4.6M_L, was recorded by the BGS (Burton & Neilson
1980). Fortuitously, one of these events occurred whilst an array of
60 temporary seismic recorders was in place for the LISPB refraction
experiment (Kaminski et al. 1976). This situation enabled Assumpcao
(1981) to determine a fault-plane solution and accurate hypocentral
locations. Assumpcao's study led him to attribute the earthquake
swarm to fault reactivation, with predominantly sinistral strike-slip
motion - Fig.12-5. Whilst it was not possible to delineate an
epicentral lineation in the swarm (since all the events occurred
within an area smaller than the location uncertainty; 3km wide) a
suggestion of a spatial orientation led Assumpcao to assign the
activity to the NE-SW trending Strathconon fault.

12.3.2 Study of BGS microseismic locations

Detailed association of epicentres, fault-plane solutions and
surface faults (in the manner of Assumpcao's study) is not normally
possible in the NW Highlands due to errors in location - at best

located to +5km and often much poorer (Turbitt 1984, 1985; Marrow
pers. comm.). Despite this it is important to assess the role of
fault reactivation in Scottish seismotectonics. Is the observed
seismicity a manifestation of fault-reactivation or some other
tectonism, such as diffuse strain on joints? This section attempts
to answer that question as far as the existing data on seismicity
allow.

Fig.12-6 shows all the epicentres located by the BGS between
1969 and 1984 in the NW Highlands together with the traces of major
faults. No obvious spatial association of the seismicity with these
faults is evident. Several epicentres do lie on or close to the
faults, but most do not. Two concentrations in the activity are
apparent: one in the vicinity of the southern end of the Strathconon
fault (the Kintail centre) and a second to the east of the southern
end of the Great Glen Fault (the Ben Nevis centre). These
concentrations lie within (and contribute to) the NW-SE belt of
seismicity observed in the overall Scottish and U.K. seismicity
distribution (§5.4 and Fig.5-7). This belt of seismicity is
especially evident in the larger magnitude range. Fig.12-7 shows
the data from the BGS file, 1969 to 1978 (Burton & Neilson 1980) with
all events less than $1.0M_L$, or which were clearly aftershocks of
large events, removed. The plot shows the two concentrations in
Highland seismicity and a third in the Midland Valley to the
south-east of the Ochil fault (the Stirling centre). The three
centres of activity occur roughly where the NE-SW belt intersects
major faults. This is most clearly the case with the Kintail centre.
The other centres are a little 'off-line' (several kilometres to the
south-east) of the Great Glen and Ochil faults, respectively.
Fig.12-8 shows detail of the Kintail and Ben Nevis centres. No
major fault passes through the Ben Nevis centre. It coincides fairly
closely with the mountain massif of the Ben Nevis range. Detailed
study of the Ben Nevis centre has not been made. This study focuses
on the Kintail centre since it shows both a higher level of
seismicity and a clearer association with major faults (including the
Kinloch Hourn fault).

In order to ascertain the extent to which the seismicity of the Kintail centre could be assigned to known faults a study of earthquake-swarm activity was made. **Fig.12-9** shows the total recorded seismicity (1969-1984) in the study area. At this scale close association of the seismicity with mapped faults is not evident. The main concentration in seismicity occurs around the intersection of the Strathconon and Kinloch Hourn faults, but is quite diffuse. Appreciable seismicity also occurs to the north, around the Carron and Loch Maree faults, but again in a fairly diffuse pattern. [In terms of location errors, the expected error of +5km corresponds to about +2mm in these plots, which should be borne in mind when considering lineament-seismicity associations.]

No indication of depth is given in these seismicity plots. The only depth information available is that from the listing of Burton and Neilson (1980) for events between 1969 and 1978. Depths have been estimated for less than half of the events in the Kintail areas during that time. These estimates are mostly less than 11km, with a mode at 10km. Two deeper events at 16 and 22km were also recorded. Errors in these depth estimates are at least +5km (Marrow pers. comm.).

The following swarms of activity in the study area provide useful information:

a) **Fig.12-10:** A swarm of 18 events occurring between the 4/8/74 and 29/8/74. This swarm includes the events studied by Assumpcao (1981), lying very close to the Strathconon fault (Fig.12-6). However the largest event within the swarm occurs well·to the SE of the rest which suggests that a NW-SE fracture may have been the source, rather than the (NE-SW) Strathconon fault (as Assumpcao suggested - §12.3.1).

b) **Fig.12-11:** Temporally diffuse activity occurring between 24/9/74 and 26/6/75 (9 events). Activity following the August-1974 swarm continued in the same location, but also further to the SE. This adds credibility to the supposition of a NW-SE fracture here, with the bulk of the seismicity occurring at one end of the (hypothetical) fracture where it meets the

Strathconon fault. This activity also includes an event on the Kinloch Hourn Fault.

c) **Fig.12-12:** Four events occurring between 21/11/75 and 27/11/75. These include an event close to the intersection of the Kinloch Hourn and Strathconon faults and another close to the Carron fault.

d) **Fig.12-13:** A swarm of 7 events occurring between 26/5/78 and 28/5/78 forming a clear microseismic lineation running SE from Loch Torridon (and also an isolated event in the east of Skye). This lineation does not correspond to any known fault, it cuts across major NE-SW faults, and lies close to a topographical lineament through Loch Torridon.

e) **Fig.12-14:** A swarm of 8 events occurring between 9/9/78 and 10/9/78. The swarm occurs in the vicinity of the intersection of the Strathconon and Kinloch Hourn faults but appears to show a northerly microseismic lineation.

f) **Fig.12-15:** A swarm of 5 events occurring between 9/4/80 and 12/4/80. A NW-SE microseismic lineation is apparent in four of the events, approximately in line with the Cluanie fault.

g) **Fig.12-16:** A swarm of 5 events occurring between 7/2/82 and 8/2/82. Three events in the east of Skye and two close to the Kinloch Hourn fault could indicate a NW-SE microseismic lineation approximately co-incident with the Kinloch Hourn Fault.

This swarm activity indicates that, although major faults are the loci of some individual events, most microseismic lineations have north-westerly or northerly trends and are not associated with major faults. Where these lineations do align with faults they tend to continue beyond the limit of the mapped fault and cross the major NE Caledonian faults. Thus the supposition that the observed seismicity is largely the product of re-activation of major faults is substantially discounted.

If the major faults do not form the primary loci of seismicity, what does? Consideration of LANDSAT imagery in the following section will partly answer this question, but at this point it is interesting

to note several regional lineations apparent in the seismicity
distribution - **Figs.12-17&18.** These are mostly of a northerly
trend, but some NE-trending lineations are seen (not generally
coinciding with the main Caledonian faults). A few NW-trending
lineations are apparent in the Central Highlands. Lines drawn in this
manner through seismicity distributions represent a fairly subjective
exercise! - however, one wonders if such lineations represent major
joints having movement associated with glacial rebound. It has been
pointed out (Papastamatiou pers. comm.) that the more abundant
seismicity of the NW Highlands approximately coincides with the area
of maximum post-glacial uplift - **Fig.12-19.** If post-glacial
rebound did account for a large proportion of the seismicity then
such a set of microseismic lineations corresponding to major sets of
new (glacial) fractures might be expected. This question of the
relation of seismicity to glacial rebound will be developed further
in chapter 17.

12.3.3 Summary of seismicity observations

In the NW Highlands the following are observed:

a) A concentration of activity in the Kintail area, close to the
intersection of the Strathconon and Kinloch Hourn faults, and
one of three centres of activity in Scotland forming a NW-SE
belt.

b) Swarm activity which indicates the presence and 'activity' of
mostly north-westerly but also northerly fractures, only
occasionally coinciding with major faults.

c) Gross lineations in the seismicity distribution having northerly
and north-easterly trends, and generally unrelated to major
faults.

12.4 STUDY OF LANDSAT IMAGERY

12.4.1 Procedure

A study was made of lineaments seen in the Kintail area on an extract of a LANDSAT MSS (multi-spectral-scanner) image. Details of this study are outlined in Appendix 3. The procedure followed was the same as for the study in the Glen Roy area (§11.4.1), however since an MSS image was used, it was decided to study only three bands (4,5&7) and three principal components (as opposed to five on the Thematic Mapper). Also the spatial resolution of MSS imagery is much poorer (80m pixels) than the Thematic Mapper (30m pixels). As a result the images of the Kintail area contain less information (particularly with regard to lineaments) than the Glen Roy images. (Plate-35 shows a band 4,5&7 image of a portion of the Kinloch Hourn Fault).

The purpose of this study was threefold:

a) To identify the Kinloch Hourn Fault and determine its extent as a surface lineament.

b) To ascertain the lineament populations present.

c) To discover any association of the seismicity distribution with the lineaments and lineament populations.

12.4.2 Evaluation of lineaments

Figs. 12-20 to 12-27 show lineaments seen on images of the three principal components (PC's) of the MSS bands - 4,5 and 6. This sequence of lineament 'maps' (approximate scale and not geometrically corrected) is of general interest in contrasting the lineaments picked out in different principal components. However, specific interpretation will focus on a 'composite' (Fig.12-28) of these individual principal component images. Each individual principal component image is discussed below:

a) **PC1 - positive (Fig.12-20):** This image brings out mostly topographical lineaments with a dominantly E-W grain, but also some NE-SW lineaments probably resulting from the main Caledonian structural grain. A small portion of the Kinloch

141

Hourn fault can be seen.

b) **PC2 - positive (Fig.12-21):** Many more NE-SW lineaments (of
   the Caledonian grain) are seen and many of the E-W,
   topographical lineaments are suppressed. The WNW-ESE Kinloch
   Hourn fault is apparent in a more extensive lineament than in
   PC1.

c) **PC3 - positive (Fig.12-22):** A strong NE-SW, Caledonian grain
   is seen, however two NW-SE lineaments appear on this image
   (through Loch Quoich to Loch Duich and through Loch Cluanie).

d) **PC1 - negative (Fig.12-23):** Many more lineaments than can be
   seen on the positive can be seen here, but as with the positive
   PC1 they are mostly of topographic origin and of an easterly
   trend. Two northerly lineaments are seen, one through Loch
   Quoich and one between Lochs Duich and Hourn. The pair of
   lineaments running between Loch Morar and Loch Hourn represent a
   distinctive band of contrasting tone. This feature is of unknown
   origin - it does not correspond to anything mapped by the
   Ordnance or Geological surveys. The Kinloch Hourn lineament is
   clear.

e) **PC2 - negative (Fig.12-24):** This image is similar to the
   positive, but contains many more linears of a predominantly
   easterly trend.

f) **PC3 - negative (Fig.12-25):** Two main lineament populations
   are apparent - an easterly (topographic) trend and a NW-SE
   trend. This latter trend is also seen on the positive, but many
   more lineaments contribute to it on the negative. The Kinloch
   Hourn fault is virtually indiscernible.

g) **Colour composite of PC1 & PC2 - negatives (Fig.12-26&27):**
   Many of the lineaments seen on the individual PC1 and PC2 images
   are 'removed'. What remains is a clear set of NE-SW and NW-SE
   lineaments. A few easterly (topographic) lineaments are evident.
   Fig.12-27 shows an enlargement of the Kinloch Hourn fault area.
   The fault is very clear, although not all the splays seen on the
   air photographs are evident. The trace of the fault does not
   appear to extend any further than indicated on air photographs.
   Traces of the basement foliation are very clear. Several small

easterly lineaments are also seen.

Thus different principal components bring out different lineament populations (negatives displaying more lineaments than the positives):

PC1 - mainly topographic linears of an easterly trend.

PC2 - Caledonian basement trends (NE-SW and WNW-ESE).

PC3 - NE-SW (Caledonian?) trend and a NW-SE trend of
   unknown origin.

A composite composed of lineaments occurring on more than one image of PC's 1,2&3, negative and positive, is shown in Fig.12-28. This process has reduced the number of lineaments considerably and allows the populations to be more easily discerned. The rose diagram of Fig.12-29 depicts the three main populations present and a fourth, less well defined, group:

1) A NE-SW trend corresponding to the Strathconon fault and parallel lineaments, and interpreted as the main Caledonian basement trend.

2) An E-W trend comprising mainly topographic lineaments.

3) A WNW-ESE trend, including the Kinloch Hourn fault, and also interpreted as a Caledonian basement trend.

4) A NW-SE trend, mostly evident in the 3rd principal component, and of unidentified origin.

12.4.3 Comparison of seismicity with lineaments

Microseismic epicentres occurring within the lineament study area have been superimposed on the lineament composite in Fig.12-30: [These epicentres include only those from the published list for 1967-78, Burton & Neilson (1980).] The epicentres are drawn with a 1km diameter circle, which can be assumed a minimum location error - actual errors are variable, undetermined and probably around +5km.

The following correlations are of interest:

a) Many more events lie on or close to lineaments than to mapped faults (Fig.12-9). This may be partly due to the fact there are

143

more lineaments than faults.

b) Events of the August 1974 swarm (c.f. Assumpcao's (1981) study, §12.3.1.) lie on a NW-SE trending lineament (X) with a clear microseismic lineation along it. This adds further weight to the supposition (§12.3.2a&b) that a NW-SE fracture was the source of activity. This lineament will subsequently be referred to as the 'Glenshiel lineament'.

c) Seismicity in the Kintail area is distributed in a ring around a centre at 'Y'. This ring of seismicity approximately coincides with a 'box' of lineaments comprised of the Kinloch Hourn fault, the Strathconon fault and the Glenshiel lineament. A possible fourth side to the box can be seen in the PC1&2-negative image (Fig.12-26) running NE from the head of Loch Hourn.

It was noted in the previous section (§12.3.3b) that swarm activity in the area indicated the presence of NW-SE and N-S trending fractures. The presence of NW-SE fractures is supported by the lineament study; however no northerly lineaments have been found which can be associated with the microseismic lineations. This discrepancy is partly resolved when it is recalled that only one northerly swarm trend was evident (§12.3.2e) and that this was a fairly diffuse lineation (Fig.12-14). Furthermore, in the consideration of regional epicentral lineations (§12.3.2) northerly trends were also proposed - again no corresponding lineaments can be identified. However, it may be that northerly trends in seismicity have a regional significance and are not manifested at a smaller scale. There is some evidence, for instance, that regional northerly lineations are composed of NE-SW lineations on a more local scale (e.g. Fig:12-18, lower-left).

The regional NE-SW epicentral lineations have a corollary with the Caledonian trend and with numerous lineaments of that trend seen on LANDSAT imagery. Their spacing is fairly regular (Fig.12-17) and most do not correspond to known Caledonian faults, such that although aligning with the Caledonian grain, they probably represent a distinct set of fractures.

Concluding statement: Although several anomalies are apparent in the association of seismicity with lineaments the following has been established:

a) Microseismic swarm activity occurs mostly on NW-SE lineations, which occasionally correspond to faults (such as the Kinloch Hourn fault) but mostly do not. Lineaments seen on LANDSAT imagery are, however, found to correspond to these swarm trends, notably the Glenshiel lineament.

b) Regional epicentral lineations in the NW Highlands comprise two sets:

    1. A NE-SW trending set, parallel to the Caledonian basement trend, but not usually corresponding to known faults, and probably representing a distinct set of fractures.

    2. A N-S trending set, not corresponding to any known fault or lineament trend.

12.5 CONCLUSIONS

The geological evidence for post-glacial movement along the Kinloch Hourn fault is substantial. The most recent activity being intrusion and shearing of fracture infilling material since 2400 years BP. The fault is also active in terms of present microseismicity; however, the loci of present (instrumental) seismicity are mostly on other fractures, most notably the Glenshiel lineament (indentified only on LANDSAT imagery). Field inspection of the Glenshiel lineament has not been made; however, late studies located a lineament on air photographs similar but not nearly as prominent as the Kinloch Hourn fault. Further study is warranted.

The lineament study not only identified the Glenshiel lineament and others spatially associated with present seismicity, but showed that the Kinloch Hourn fault is part of a system of fractures appearing to be the source of present seismicity. Specifically, there appears to be a 'box' of fractures forming the Kintail centre of activity in the NW Highlands. Regional study of seismicity patterns suggests that a regional set of N-S and NE-SW lineations is the primary locus of seismicity. Reactivation of ancient faults appears

consequential on the performance of this regional pattern, that is, major faults are occasionally exploited (e.g. the Strathconon fault), but mostly the activity is distinct from them. This regional pattern of seismicity lineations has not been evaluated; however, it has been suggested that they may be related to glacial rebound tectonics.

PART III(B)

PALAEOSEISMICITY

13. Glen Roy (sediments)
14. Arrat's Mill
15. Meikleour
16. Kinloch Hourn (sediments)

****
CHAPTER THIRTEEN
Glen Roy (Sediment)
****

13.1 BACKGROUND AND STUDY PROCEDURE

While investigating the faulted shorelines and landslide in Glen Roy reported by Sissons & Cornish (1982) the author began inspecting the deposits of lake sediment in the vicinity and found them to contain deformation structures. Reconnaissance along newly cut road and track verges in Glen Roy showed deformation to be present in most of the exposed sections of lake sediment. An excavation and logging programme was initiated and carried out during the summers of 1984 and 1985. All accessible exposures of the sediment (road cuts, stream sections, sand and clay pits etc.) were excavated, by hand, to provide 90 sediment sections, each approximately one metre in depth. After preparation of a clean, fresh surface, using sharp cutting tools, each section was photographed and described. Line drawings (from photographs) were made of each section in order to document the deformation structures in detail. These structures were classified and stratigraphic logs were constructed. Particle-size analysis, microscopy and XRD spectrometric analysis were made for two key sections in order to characterize the sediment. This chapter documents these sediment logs which, together with other field observations, comprise the evidence for the occurrence of a palaeoseismic event in the area.

[An attempt was made at dating the lake sediment by radio-carbon analysis. A sample of lake varves from Glen Roy was found to contain insufficient carbon for dating. A sample of wood from laminated silts in Glen Spean was successfully dated but yielded a post-glacial age (Appendix-7: sample-7). Thus a carbon-date for the lake sediment was not achieved.]

13.2 GEOMORPHOLOGY AND LAKE HISTORY

The 'parallel roads' of Glen Roy have been the subject of much geological inquiry since Louis Agasssiz (1842) first advocated former

glaciations in NW Europe and since T.F. Jamieson (1863) elaborated on an ice-dammed-lake hypothesis for the 'roads'. More recently the work of Sissons (1977, 1978, 1979a, 1979b) has elucidated a history of glacial lake development in the area. His studies, which provide a foundation to this work, are documented in this section.

13.2.1 The lake levels

There are three clear 'parallel roads' seen in Glen Roy relating to different shore levels, and several other less obvious levels (Plate-37). They were formed during the Loch Lomond Readvance when an ice mass in the southern Great Glen extended up the adjacent glens of Gloy, Roy and Spean (Fig.7-1). Ice-dammed lakes were created in these glens, and at their greatest extent comprised two arms of water up Glen Roy and Glen Spean covering an area of $73km^2$ and a separate lake in Glen Gloy covering an area of $7km^2$.

Sissons has interpreted the shoreline sequence as a series of lake levels falling with the retreat of the glacier ice. His interpretation is compiled and summarized in **Fig.13-1.** The greatest extent of the ice, evident in prominent end moraines, resulted in the damming of four small lakes. The highest one, in Glen Gloy, had a top water level (TWL) at an elevation of 355m and drained through col 'A' into Glen Roy where a lake with TWL at 350m drained through col 'B'. A third lake was trapped in the Bohennie arm of Glen Roy, having a TWL of 325m, and drained through col 'C' into a lake in Glen Spean with a TWL at 260m. The col for the Spean lake (not shown) was at its eastern limit, beyond the present Loch Laggan. As the ice retreated to its final position before ultimate drainage of the lakes, the level in Glen Roy dropped in stages, as successive cols were made available. It first dropped to the level of the Bohennie arm (at 325m, shoreline not shown) and then to the level of the Spean lake to form one large lake (at 260m). The lake in Glen Gloy maintained one level thoughout, having only one col available for drainage. The final drainage of the lakes was probably in terms of a Jökulhlaup (a catastrophic sub-glacial drainage) as outlined by Sissons (1979a), the inferred paths of which are shown in Fig.13-1. A lake level at an elevation of 113m and several others below have

been documented by Sissons (1979a) who associated them with successive stages in the drainage, after the main Jökulhlaup, and also with the outwash sand deposits.

13.2.2 Shoreline morphology

The shape of the shoreline platforms was interpreted by Sissons (1977) to indicate formation in part by erosion of rock benches and in part by deposition downslope of the shore level. However, a closer look at natural cross-sections of the shorelines (at 'S', Fig.13-1) indicates that the upper two levels in Glen Roy (also being the most visually prominent, Plate-37) are primarily the product of erosion, whereas the 260m shoreline is much more a product of deposition. The inset in Fig.13-1 shows a field-sketch cross-section of the 350m shoreline which displays a cleanly excavated rock bench, over 20m wide, with very little contemporaneous deposition. Glacial talus infilled part of the platform notch soon after its abandonment, with post-glacial hillslope debris infilling and diminishing the severity of the original profile. The 325m shoreline is similar but less well developed. In contrast, cross-sections of the 260m level reveal little rock excavation but abundant beach sediment, consisting of clayey, micaceous silt with boulders (at LPR1, Appendix-4), and extending lakewards to form a shoreline platform ridge.

13.2.3 Morphology of sediment deposits

The sediment which accumulated in the lakes appears in two main forms: as fan deltas and as an overall mantle on the lake floor and sides. Deltas are most common in Glen Roy, occasionally present in Glen Spean, and absent in Glen Gloy. The deltas are flat-topped and lie mostly below the 260m level but usually apex a little above it, their fronts have mostly been cut by subsequent fluvial action (Plates-37&39). The general lake sediment mantle occurs throughout, and is up to 4m thick in the valley floors, but is thin or absent high up steep valley sides.

Localized spreads of outwash sands are developed above or just below the 260m shoreline and have channel or rounded-delta morphologies suggesting fluvial deposition. A series of river

terraces in the valley floors testify to a later period of rapid
wastage of the Loch Lomond Readvance Ice. A sketch illustrating these
morphological types is given in **Fig.13-2.**

13.3 LITHO STRATIGRAPHY

13.3.1 Basal deposits

Basal gravel and boulder deposits invariably underlie the
fine-grained lacustrine sediments. In places, these basal deposits
can be thin (a few boulders on bedrock) but more often they occur as
a boulder or gravel sequence several metres thick. They are the main
constituent of the flat-topped fan deltas (§13.1.3) which typically
consist of a massive, 10-30m thick, boulder bed capped by one or two
metres of fine-grained lake sediment. The boulder deposits are mostly
infilled by finer-grained sediment (sand, silt and laminated clay)
indicative of a lacustrine environment of deposition. These basal
deposits are not easily excavated and have not been studied in
detail; however, they are presumed to be the products of rapid
erosion and deposition in the advancing and active stages of the Loch
Lomond Readvance as reported by Sissons (1977).

13.3.2 Fine-grained lacustrine deposits

These sediments are the main constituent of the 90 sediment
logs. The distribution of these logs is shown in **Fig.13-3.** They
are documented in Appendix 4. Typically they comprise a 1 to 4
metre-thick unit of laminated sand and silt, with minor clay,
overlying the basal boulder deposit. These fine-grained deposits
occur below the 260m level (and below the 355m level in Glen Gloy)
and are not usually observed at higher levels except as interstitial
material to coarser deposits. One major exception to this is found in
Upper Glen Roy (logs GR18-22, Fig.13-3) where up to 2 metres of
fine-grained, laminated deposits are found well above the 260m level.
This is difficult to reconcile with their absence at these levels
elsewhere in Glen Roy, and one is driven to conclude that a perched
lake was dammed at the 350m level in Upper Glen Roy, whilst the level
elsewhere was at 260m. No geomorphological evidence has been found to
confirm this, except that a narrow gorge just west of GR18 (Fig.13-3)

could have contained a small ice mass to form a very effective barrier in the right location. Apart from this anomaly, it is clear from the distribution of sediment and from the beach morphology (§13.1.2) that the fine-grained lacustrine sediment was deposited when the lake was at the 260m level. It is thus presumed that this was a period of stagnant-ice melting whereas the two higher lake levels were formed during an earlier, active stage of the Loch Lomond Readvance.

On the basis of this evidence it seems reasonable to attribute the fine-grained sediment to the later stages of the Loch Lomond Readvance, namely around 10,300 years BP (the Loch Lomond Readvance is usually assigned to the period between 10,800 and 10,300 years BP - Sissons 1983).

A more detailed stratigraphy is best given in relation to the logs RR7,8,9,10,16&18 shown in **Fig.13-4** (ignoring for the moment the deformation structures). The stratigraphy comprises a sequence of laminated silts with occasional sandy layers. (The term 'varve' will be used where a clear, repetitive, fine lamination is apparent in these sequences.) At fine-grained (distal) sites (e.g. RR9 & RR16) the stratigraphy typically consists of clayey, organic varves grading up into silty varves with occasional layers of fine sand, then into sandy varves with thicker and coarser sand layers, and eventually into gravels and coarse sands, the whole of which may be overlain by sub-aerial sands. **Figs.13-5 & 13-6** show particle-size distributions for logs RR9 & RR16. Silt clearly dominates in the RR9 section, with only the red silt-sand layer showing a markedly coarser composition. A much sandier profile is seen in log RR16, although silts still dominate, except in the massive (post-lacustrine) sands. At more proximal, lake margin, sites (RR7 & RR10) a coarsening-up stratigraphy is apparent and consists of silts and sands, followed by sands and gravels, and then gravels. Varves are usually absent and stratigraphy more varied, testifying to a higher energy environment of deposition. At these marginal sites cross-bedding is occasionally seen in the upper sands (e.g. RR10, 0.05m).

The varves of Glen Roy are typically 2-10mm thick, and usually bluish grey in colour. An attempt has been made to count their number in one of the least disturbed sections (RR14, Fig.13-22) where they number about 250. One could therefore suppose at least 250 years of deposition in the lake.

13.3.3 Post-lacustrine deposits

The sands overlying lacustrine deposits are fairly easily distinguished from them by virtue of colour, texture and sedimentary structures. They are usually reddish brown to yellow whereas lacustrine sands are grey or white; they are clean, soft and unconsolidated whereas lacustrine sediments are stiff and overconsolidated; and they show much evidence of fluvial or aeolian deposition, containing cross-beds and climbing ripples. Their particle-size distribution is also distinctive: sample RR16-9 (Fig.13-6) shows a mode at the fine/very-fine sand size with appreciable amounts of coarser sands. They also show a marked difference in the deformation structures they contain. They are not usually deformed, but where deformation is present it consists of reverse faulting and involution structures (these will be discussed in §13.5.3). Finally the morphology of their outcrop is often distinctive - outwash-sand deposits occurring frequently as lobate-fan or moundy deposits. Their occurrence is sporadic, usually as isolated outwash fans.

13.4 DEFORMATION STRATIGRAPHY

The objective in performing this study was to understand the deformation structures seen in the lacustrine sediment and to determine their origin. Deformation was observed over a large area, so that it became important to establish a stratigraphic correlation of the deformed sediment horizons. In most sections, top or bottom of the fine-grained lacustrine sediment could be used as a stratigraphic marker, and in thirteen of them top and bottom were exposed to give a complete lacustrine stratigraphy. Two widely correlated deformation horizons are present. This is demonstrated with reference to six 'key logs' in the central Glen Roy area shown in Fig.13-4 and

described below. (The statigraphy is described with reference to depths, in metres, shown on the logged sections.)

RR7: The basal sand (0.55-0.65m) is undeformed, but slight deformation involving flaming and layer disruption is apparent immediately beneath the gravel (0.55-0.45m). The gravel (0.45-0.25m) is not noticeably deformed, but the sand layer at the top (0.25-0.20m) has been disrupted and rucked into folds. The sand above this is more strongly deformed by pervasive flaming and layer disruption with occasional injection structures. Less disrupted sand (0.00-0.05m) is seen between this and the red sand layer. This is overlain by a strongly deformed slumped-silt unit.
Interpretion: Liquefaction of the surface layer (0.05-0.30m) and at depth, beneath the gravel (0.45-0.55m), occurred during the first event. This was followed by a short period of sedimentation, and then the deposition of the red silt and slumped silt units.

RR8(E): In-situ deformation between 0.7 and 0.5m only. An erosion surface between 0.45 and 0.30m is overlain by a highly disrupted slump deposit. The in-situ sediment and slump deposit are cut by an intrusion of red silt (perhaps a neptunian dyke).
Interpretation: All the described deformations could have occurred in close succession during one event. Erosion and slump deposition may have immediately followed or accompanied the in-situ deformation. However, the red silt injection structure probably results from a second event involving ground cracking and slope failure. This event could correlate with other red silt horizons.

RR9(E): A 'fault-grading' sequence is observed between 2.6 and 1.6m. Closely-spaced faults with small throws (of a few mm) develop upwards into more widely-spaced faults with larger throws (a few cm). At the top of this section liquefaction has occurred causing the formation of clay lenses, load and flame structures and the disruption of layers (1.8-1.65m). Clay and silt varves (1.65-1.55m) remain relatively undeformed (perhaps acting as a seal to liquefaction beneath). Liquefaction (or partial liquefaction) of susceptible layers between 1.55 and 1.0m is manifested in balling of sand (1.5m), ruck folds (1.45 and 1.05m) and layer disruption

154

(1.25-1.15m). This section thus corresponds well with Seilacher's (1969) fault-grading stratigraphy (Fig.6-5): 'segmented zone' between 2.6 and 1.8m, 'rubble zone' between 1.8 and 1.55m (including flame structures and clay lenses) and 'soupy zone' between 1.55 and 1.0m (containing some coherent layers and sand balls in a matrix of homogenized silt). Detail of the rubble zone is shown in Fig.13-7.

Continuing with the stratigraphy, silt varves (1.0-0.7m) remain undeformed, with surface-liquefaction deformation occurring between 0.7 and 0.3m. A clay layer at 0.6m appears to have acted as a fluid seal, enhancing liquefaction below it (0.65-0.6m). Particle-size analysis shows this layer to be significantly finer grained than the most of the profile, and containing appreciable clay (Appendix 6). The surface at the time of the liquefaction event (0.3m) was covered with a grey sand layer containing clay clasts. A period of silt deposition followed, before the deposition of the red sand and slump deposit (0.5-0.0m). The slump is overlain by a poorly laminated, reddish sand.

Interpretation: Deformation of the sediment column, when the surface was at 0.3m, comprised liquefaction of the surface layer (0.3-0.55m) and fault-grading and liquefaction at depth (1.0-2.6m). A period of silt-varve deposition was followed by slumping and then sand deposition in probably fluvial, subaerial conditions.

RR10: Silts and sands between 0.7 and 0.5m have been deformed, in-situ. Silty sediment between 0.5 and 0.4m is undeformed. Deformation below an erosion surface (0.25m) comprises layer-disruption, folding of gravels and the formation of clay lenses. The erosion surface is overlain by a high energy sand deposit displaying climbing ripples and cross-bedding. A small injection structure (0.1-0.0m) rises to. the red silt layer, which shows small micro-faults. Roughly laminated sand with occasional cross-bedding overlies the red sand layer.

Interpretation: A liquefaction event when the surface was at 0.25m caused surface liquefaction (0.40-0.25m) and liquefaction at depth (0.7-0.5m). A period of sand deposition preceeded the red silt

horizon, which was followed by fluvial sand deposition.

RR16: A very disrupted sediment column showing deformation throughout. The deformation stratigraphy is grossly similar to RR9 but more disturbed. A faulted sequence between 2.7 and 1.5m has failed causing fault segments to rotate. A clay diapir is associated with sand injection between 2.6 and 2.3m. Rafts of sediment (1.5-0.5m) have remained intact and are surrounded by deformed sediment containing pillows of silt (e.g. 0.9-0.75m). Surface deformation is severe, involving sand pillows (0.4m), break-up of faulted segments (0.4-0.2m) and slump folding of gravel, sand and clay layers. The top of the deformed sediment is marked by the red silt layer and overlain by massive sands and gravels.
Interpretation: Liquefaction and deformation of a thick sediment column in one event, marked by the red silt layer, and followed by fluvial sands and gravels. A 'fault-grading' sequence is apparent, but partly obliterated by the failure of the sediment column.

RR18: The boulder base to the lacustrine sediment has suffered deformation in terms of flow of the sand layers around boulders (0.7m). Between 0.6 and 0.2m sand pillows and injection structures have formed. Injection into the sediment and mass flow have resulted in the doming of the upper layers (0.2-0.0m) which have been eroded and infilled by a reddish gravel (0.0m). A chaotic layer of varves with boulders follows and is overlain by gravels containing clay clasts.
Interpretation: Liquefaction of the sediment column when the surface was at 0.0m was followed by dumping of the reddish gravel, which was overlain by a slumped varve deposit, superseded by gravel deposition, incorporating varve clasts from the surrounding slumped material.

Synthesis of interpretation: Two deformation events are apparent. The first event involves liquefaction of the sediment column and is followed by a short period of lacustrine sedimentation before the occurrence of the second, 'red silt' event. The red silt is overlain by slumped units in three of the sections and always heralds a new lithostratigraphy, namely coarser, usually fluvial

sediment. In logs RR16 and RR18 the two events are not resolved; top of liquefaction coinciding with the red silt horizon. In the other logs a short period of lacustrine sedimentation occurs between the two events, sediment which is presumably missing from RR16 and RR18. The first event is essentially a liquefaction event, but may involve slumping (e.g. RR8). The second event is usually marked by slump units and involves a facies change.

13.5 CLASSIFICATION AND ZONATION OF DEFORMATION STRUCTURES PRODUCED DURING THE FIRST EVENT

A zonation in the degree of deformation was apparent from the early stages of the excavation programme and with the final total of 90 logged sections this zonation is well demonstrated. Zonation is most apparent in the structures related to the first deformation horizon, but also grossly apparent in the second horizon. The kind of structures which have been associated with earthquake-induced liquefaction elsewhere (e.g. ball-and-pillow and fault-grading) were observed in the central area, showing most intense deformation (i.e. of the 1st event). Elsewhere a wide variety of other structures, not documented as earthquake phenomena, were observed. It then became necessary to quantify this 'apparent' zonation and establish its validity. In attempting to do this a search was made for objective criteria. It was found that 'the density of faulting in sediment' was difficult to quantify, showed little spatial pattern and was strongly influenced by sediment type and situation. 'Thickness of deformed material' proved a slightly more promising criterion but assessment was thwarted by incomplete sections and variety in thickness of the pre-deformation sediment column. Promising results were however obtained by classifying the 'style of deformation'.

13.5.1 Classification of deformation structures

Although details of the style of deformation varied with sediment composition, gross style-groups could be identified in sediment of varying composition and incomplete exposure. The classification arrived at is illustrated in **Fig.13-8,** and is as follows.

Class A: The occurrence of ball-and-pillow (B&P) or fault-grading stratigraphy (FG). These two deformation styles are often found together and both imply that portions of the sediment column have completely liquefied (see Plate-44).

Class B: Confined layer deformation (CLD), surface layer deformation (SLD), incipient fault-grading (IFG) or pillow loading (P). The first two of these criteria are very commonly observed and imply liquefaction or partial liquefaction of portions of the sediment column for considerable lateral distances. However structures implying prolonged liquefied flow of sediment (i.e. Class-A structures) are absent. Incipient fault-grading refers to a segmented fault zone grading up into more plastic deformation, but not displaying the complete 'fault-grading stratigraphy'. 'Pillow-loading' refers to structures where loading into liquefied sediment has occurred but has not progressed to complete detachment and 'balling'. (See Plates-45,46&48).

Class C: Incipient confined-layer-deformation (ICLD) or injection structures (I). Where a layer, at depth, has deformed plastically but for a limited horizontal extent (i.e. not laterally continuous within a 1-2m wide exposure) and has not flowed to produce any clear ball-and-pillow, ruckfold, or pillow-loading structures. Upward injection of sediment from this layer is commonly observed. Injection structures on their own imply some mobility at depth to provide a source for injected material, and are taken to indicate Class-C deformation. (See Plates-47&49).

Class D: Flaming and fissuring only. No clear liquefied zones apparent. Gentle loading and flaming implying some softening and flow of the sediment column. Sediment injection structures are absent, but fissures expelling water (and minor sediment) may be present.

Class N: Undeformed sediment column. Small faults are allowable, implying minor ground settlement (of undetermined origin) only. (See Plate-50).

Class S: Sections comprising slumped material only. Styles
of slumping vary considerably.

It should be stressed that this classification involves limiting
style-types, i.e. Class-B structures can be found in a Class-A
section but not vice versa, etc.. Secondly, it should be noted that
the subjective statement 'incipient', used to describe several
structure-types, has in each case been qualified by an objective
criterion to decide whether the structure is incipient or complete.
Thirdly, although the classification is robust under conditions of
varying sediment type, there are limits on its applicability. On one
hand, sediment columns composed of coarse sand and gravel, fail to
display any of the structures outlined and only show faulting (e.g.
log GR11) and on the other hand, highly compact sediment containing a
lot of clay may be resistant to any form of deformation (e.g. log
BR9). Thus the classification is only applicable to 'normal'
lacustrine sediment, i.e. sediment containing unconsolidated, fine-
to medium-grained sediments. The majority of Glen Roy sediment
profiles are suitable whether being proximal with larger portions of
sand or being distal and composed mostly of finely-laminated silty
varves. Since most columns contain varying sediment type up the
succession there is usually at least some portion which contains
sediment prone to deformation (i.e. crudely, silt). Phrased in
another way, as long as the sediment column contains some silt layers
the appropriate deformation styles would be expected, details of the
styles being dependent on details of composition.

13.5.2 Zonation of deformation structures

The class-types allocated to the sediment logs are listed in
Appendix 4 and displayed in **Fig.13-9.** 67 of the sections were
classifiable. Contours marking the outer limits of styles 'A', 'B'
and 'C' are also shown (style 'D' does not appear to be spatially
resolved from 'C' so no contour has been constructed for it). Each
contour can be seen to encompass styles of a lower order, although
the appropriate style usually dominates. There are only five class-A
sites and the 'limit-of-A' contour includes a large number of class-B
sites. In the A-to-B contour interval 16 out of 26 are class-B (62%)

and in the B-to-C interval 9 out of 13 are C (69%) (slumped sections
are excluded from these estimates).

The main anomaly in the spatial distribution of sediment styles
lies in the occurrence of undeformed sediment (class-N) within the
limit-of-A and limit-of-B contours. Some explanations of these
anomalous sites are forthcoming:

a) The two class-N sites within the limit-of-A contour (BR4 and
   BR5) are sands and gravels which do not contain silty sediment.
b) The two class-N sites within the limit-of-B contour (RR14 and
   RR15) are both deep water sites (water depth = 150m below 260m
   shoreline). A large hydrostatic load is thought to increase
   resistance to deformation.

These two factors, sediment type and water depth, can be called
upon to explain some of the other apparently anomalous sites.
However, since the classification has been applied to sediment of
varying composition, depth and location, some 'noise' in the
distribution would be expected. Despite this the map shows a
consistent style-trend in the form of concentric zonation. This
trend is evident in all the valley traverses, for example the
sequence A,B,C,N is clear in Glen Gloy, and also in the Spean to
Laggan area.

Examples of deformation styles seen in the sediment logs are
shown in **Figs.13-10 to 13-22** and described in their captions.

13.5.3 Freeze-thaw deformation structures

Deformation structures of a completely different kind to those
discussed so far are seen in a few locations. They were not included
in sub-section 13.5.1 on classification as they are clearly not party
to the zoned deformation structures. They have a distinct environment
and style and are attributed to glacial and periglacial processes.

Fig.13-23 shows detail of log RR14, which has been
classified as undeformed (class N) as regards the zoned deformation.
However, on closer inspection, faint varve disruption is seen. The
disruption is intense but does not affect the overall layering. It

tends to occur in discrete layers, 2-4cm thick, is almost ubiquitous at the base of the lacustrine sediment, but becomes less frequent up the column. This deformation is clearly syn-depositional, resulting from processes operating during the accumulation of the varves. Exactly how such structures form beneath a standing body of water is not known - perhaps they are due to periodic melting of permafrost in the sediment beneath the glacial lake. This kind of deformation is fairly common in silt and clay varves but only perceived on close inspection of a cleanly cut surface.

Fig.13-24 shows deformation structures occasionally seen in the outwash sand deposits. These structures are also confined to discrete layers, 5-10cm thick, and include some clear involution structures (e.g. Fig.13-24:layer 3 compared with Fig.6-12). The structures are also accompanied by low-angle reverse faulting which mostly post-dates the deformation horizons. The faults have consistent throws of 1-3cm tending to increase in magnitude downwards. It seems reasonable to attribute these structures to glacial and periglacial action: frost heave, ice melting and involution. The section shown in Fig.13-24 is thus interpreted as comprising 6 involution horizons followed by reverse faulting due to freeze-thaw forces. No ice wedge features have been seen in association with these structures.

These two forms of deformation structure are only occasionally observed, are not ubiquitous over large areas and tend to occur as discrete horizons not affecting the gross layering of the sediment column. They are attributed to glacial processes and readily distinguished from the zoned deformation and slumping already described.

13.6 SEDIMENT SLUMPING DURING THE SECOND EVENT

Fifteen of the sediment logs show a second deformation event following the main zoned deformation event. In all but one of these this second event involves slump deposits. The exception (SB1) shows only minor faulting of questionable origin, and is not considered further. The locations of the rest are shown in Fig.13-25 along

with sites having complete stratigraphies and definitely not showing this second event. It can be seen that sites affected by this second, slump event lie in an area approximately coincident with the limit-of-A contour. Sediment logs which contain slumped material only (Class-S) have also been plotted on Fig.13-25. They occur in the same area as the second-event sites suggesting an association. It is not possible to make a definite correlation of these sites with the second event, since stratigraphic evidence is absent; however, since the second event usually involves slumping,it seems reasonable to suggest a correlation.

An ellipse has been drawn around all the sites containing slumped sediment in order to illustrate the restricted locus of sediment slumping (Fig.13-25). This ellipse is approximately concentric with the contours of deformation styles (Fig.13-9). Several sites show 'anomalous' locations with respect to this ellipse and need some explanation. Three sites with complete stratigraphy and without evidence for the slump event occur within the ellipse. Of these, BR3 comprises only 0.5m of sand and gravel, such that it is unlikely to be sensitive to event discrimination; BR6 (0.8m thick), although comprising finer-grained sediment, is so deformed as to make event discrimination impossible; and GR9 (0.7m thick) contains an unusual stratigraphy of peaty sands and gravels. Slumping at site GR21 occurs well outside the ellipse but in this case the second event comprises only a thin, slightly-deformed layer such that its location does not give rise to a serious anomaly. Sites GS10 and GS11 involve sizable slump deposits and occur well away from the main locus of slumping. However their location close to the 260m-lake ice margin such that this slumping may be due to, or enhanced by, ice-margin processes.

Sediment slumping is by nature a localized phenomenon, such that a clear-cut boundary between areas of slumping and no-slumping is unrealistic. Nevertheless, the ellipse drawn delimits an area within which slumping is frequent and beyond which slumping is increasingly uncommon.

13.7 LANDSLIDES

Seven landslides were identified during the sediment logging exercise, including the one described by Sissons & Cornish (1982). Their locations are shown on Fig.13-25 where it can be seen that they all lie within the sediment-slumping ellipse. The landslides are described below; details of their heights and slopes angles are given in Table 13-1. Only the Main Roy Landslide has been studied in any detail, the others are briefly described from field observation and aerial photography. All appear to be associated with the time of the glacial lakes.

Table 13-1. Glen Roy Landslips

Landslip	Height of top of headscarp or slipped area.	Height of base of slip or steep slope.	Slope angle - average from top to bottom.	Type of Landslip (Terminology of Keefer (1984a))
1. Main Roy	580m	210m	28°	Rock and soil slump.
2. Lodge	520m	320m	31°	Disrupted soil slide.
3. West Roy	360m	200m	14°	Remnants of disrupted soil slides and soil avalanches.
4. East Roy	440m	320m	22°	Rock and soil slump.
5. Corrie	500m	350m	31°	Rock and soil avalanche(?).
6. Bohuntine	370m	280m	27°	Soil slump.
7. Glen Gloy	430m	310m	23°	Disrupted soil slide.

13.7.1 Main Roy Landslide (Plate-38)

This is the largest of the landslides and shows the clearest relationships to the shorelines. It is also related to the offset of the shorelines as measured by Sissons & Cornish (1982). It has been studied in the field and by stereo-photography in order to ascertain its origin. Fig.13-26 shows a photo-interpretation of the landslide area. It is divisible into three main portions:

a) **Main landslip:** This is the main portion of the slipped area, which has 'removed' the upper and middle shorelines, has a clear

head-scarp and contains numerous, slope-parallel, cleft-and-ridge features, indicating surficial, downslope mass movement. In the upper portion of this area large (up to 10m) rotated blocks of bedrock are visible, but lower down only the hummocky surface of soil failure is seen. The lower shoreline is apparent as a faint outline through most of the slipped area, but was also shown by Sissons & Cornish (1982) to be 'dragged down' at the edge of the landslip. Thus the relationship to the shorelines indicates that most of the movement occurred after the upper and middle shorelines but during the development of the lower (260m) shoreline.

b) **Earlier landslip:** An adjacent segment (to the north) of the slipped area which is seen to be cut by all three shorelines and therefore pre-dates them. The surface of this segment is much smoother, but exhibits a few cleft-and-ridge features. A head-scarp is present, but the lack of a clear landslip deposit suggests this area is mostly a scar left from an earlier landslip.

c) **Later landslip:** A small portion at the base of the main landslip has slipped subsequently, and has removed the lower shoreline. The surface here indicates shallow (soil) failure and lacks slump-ridge features. Its location at the point of present under-cutting by the course of the River Roy suggests that this later failure may be the result of (post-glacial) fluvial action.

The three major scarp features related to the Main Roy Landslip (shown in Fig.13-26) are described in chapter 11 (§11.2) where the relationship of the landslip to fault rupture is discussed.

Interpretation: Landslipping has occurred at this location on at least three occasions. The main landslip is most likely to have occurred during the formation of the 260m lake. Landslipping consisted of bedrock rotation and transport, and soil slumping and sliding. The earlier and later landslips occurred before and after all three shorelines and therefore cannot be accurately dated.

13.7.2 Lodge Landslip (Plate 42)

This is the most visually apparent of all the slips. It comprises a massive slump of surficial sediment, incorporating some blocks of bedrock. It has a clear head-scarp with exposed rock and a pronounced toe-ridge which reaches just below the 325m shoreline. The landslip covers the 350m and 325m shorelines and therefore post-dates them.

13.7.3 West Roy Landslip

This is not topographically pronounced, but resembles the remnants of a broad area of chaotic near-surface slips and slumps, being preserved as a 'scar' rather than a slump deposit. All three shorelines have been removed by it. The 350m and 325m shorelines appear to have acted as the major source area.

13.7.4 East Roy Landslip (Plate 40)

This has the form of a hollow in the hillside rather than a landslip deposit. It possesses a fairly clear back scarp including exposure of rock faces. The 350m and 325m shorelines are removed, but the feature does not reach the 260m shoreline. Hummocky ground below the hollow may include the remnants of a slump deposit.

13.7.5 Corrie Landslip

This deep hollow, with a large head-scarp is clearly a glacial corrie, but the base of the corrie contains slumped rough ground, suggesting downslope movement. The 350m shoreline is removed, the 325m shoreline is mostly present, broached only by tongues of slumped sediment. This is thought to be a surficial slip developed within an earlier corrie.

13.7.6 Bohuntine Landslip (Plate 41)

Has the appearance of a slipped fan delta and overlies the 260m shoreline. There is no clear headscarp, but a cavity in the 325m shoreline deposit is clearly the source of slumped material. Only unconsolidated sediment appears to be involved.

13.7.7 Glen Gloy Landslip

A broad 'scar' feature beneath a prominent cleft-and-ridge running diagonally up the hillside. Hummocky ground and a toe-ridge appear to have affected the course of the River Gloy. The 325m Gloy shoreline is developed within the scar area such that it could be a much earlier feature, however the shoreline is less incised into the slipped area than in adjacent slopes such that landsliding during the shoreline formation is more likely.

13.7.8 Interpretation of landslips

All the Glen Roy landslips (1-6) clearly post-date the 350m and 325m shorelines. Three of them displace or overlie the 260m shoreline, but the Main Roy Landslide also has the 260m shoreline faintly developed within the slipped material. The relationship of the other three landslips to the 260m shoreline cannot be determined as they lie above it. The Glen Gloy landslip probably occurred during the 355m lake but could be an earlier feature. Thus all the landslips could be said to have occurred around the time of the 260m lake in Glen Roy and the 355m lake in Glen Gloy.

The landslips show a clear spatial association with the area of sediment slumping. In particular the highest density of landslips (3,4,5&6) coincides with the highest density of sediment slumping sites. Therefore it seems reasonable to suggest contemporaneity of most of the landslips with the slumping seen in the lacustrine sediments. At least two landslips occurred earlier, since shorelines are developed across them.

13.8 INTERPRETATION OF SEDIMENT DEFORMATION AND LANDSLIPPING

13.8.1 Summary of field evidence:

In the Glen Roy area the following are observed:

a) Widespread deformation of fine-grained lacustrine sediment laid down during the existence of the lowest 260m lake in Glen Roy and the 355m lake in Glen Gloy.

b) Two deformation horizons:

1) Involving mostly in-situ sediment deformation, with indicators of liquefied flow and a clear zonation in style of deformation. (Observed in 60 logs)

2) Involving mostly slumping of sediment as plastic-flow and debris deposits composed of lacustrine sediment, occurring in an ellipse-shaped area, which is concentric with the zonation of the first deformation horizon. (Observed in 21 logs)

c) Seven landslips which show a spatial association with deformation and slumping in the lake, and which all probably occurred around the time of the 260m and 355m lakes.

d) A period of lacustrine sedimentation followed the 1st event, after which a red silt/sand horizon usually marks the arrival of a slump deposit of the 2nd event and which heralds a change in stratigraphy with the deposition of fluvial and aeolian sediment. A few sections do not reveal the period of sedimentation between the two events.

e) Localised sediment deformation resembling involution and other freeze-thaw structures occur mainly in the outwash-sand deposits and are readily distinguished from the zoned lake-sediment deformation.

13.8.2 Evaluation of the zonation in deformation structures

Some consideration of the assumptions made and shortcomings encountered in the proposed zonation has been given in section 13.5 Additional features which help establish its validity and origin include:

a) The zonation is observed across three arms of the lakes and is discordant with lake environment (e.g. the highest intensity area occurs in upper Glen Gloy, central (steeped-sided) Glen Roy and the broad area of Glen Spean (Fig. 13-9).

b) The zonation bears no relation to the positions of the ice margins and glacier dams at the time of the lakes (Fig.13-9 cf. Fig.13-1).

c) The class types used in the zonation show little correlation with water depth (Fig.13-27) but are consistent with a zoned

167

spatial distribution (Fig.13-28).

These three points not only conflict with suggestions for a glacial origin for the deformation structures but also enhance the validity of the proposed zonation. [Statistical treatment of the zonation has not been attempted since the number of sites (67) and the point density are rather low for most tests, and since the number of parameters involved makes application of a suitable spatial test very difficult - sediment columns varying in facies, water depth, slope and thickness, within three lake basins of a twisting-ribbon shape covering the concentric zonation with a biased distribution!]

Some further consideration of the third point above is helpful. In **Fig.13-27** class types have been plotted against depth of water in the 260m lake (and in the 355m Glen Gloy lake). This graph shows no clear correlation but is useful in assessing the applicability of the selected class types. Depth of water has already been suggested as a explanation for anomalies in the zoned distribution (§13.5.2). It was argued that two sites within the limit-of-B contour (RR14 & RR15) remained undeformed because of the water depth. This is somewhat supported by the distribution observed in Fig.13-27. Class-B structures, in particular, are concentrated at shallow depths such that the Class-B style may be limited in depth distribution (interestingly, the one exception (GS10) at a depth of 180m occurs near the ice margin, where 'anomalous' slumping also occurs (§13.6)). Most classified sections came from depths of less than 100m and half of the six sites deeper than this (all in lower Glen Spean) are 'mis-classified' class types. Thus the zonation is perhaps most applicable to sediments in water depths less than 100 metres. A final point of note is that the four Class-C sites well above the 260m lake level are all from upper Glen Roy, where it was proposed that a perched lake existed at the time of the 260m lake (§13.3.2).

The graph in **Fig.13-28** was constructed by plotting class types against distance from a median line drawn along the long-axis of the limit-of-A envelope (defined in Fig.13-9). This represents a somewhat circular argument, in that the contours were drawn to fit the class types; however the graph is helpful in demonstrating the

distribution of class types. Class types A & B are very concentrated
at small distances, Class-C has a mode at 8-9km and D and N
structures are fairly evenly distributed. The maximum observed
distance to each class type increases sequentially with class type.

Thus the postulated zonation seems clear and is robust against
suggestions that it might be fortuitous - it shows no relationship to
facies variation, ice margins and water depth. The nature of the
zonation counts against arguments that the deformation might be due
to glacial freeze-thaw action (for which a relationship to facies and
ice-margin would be expected) or due to 'loss of hydrostatic load'
(for which a relationship to water depth would be expected).
Generation by storm activity is inconsistent with the water depths
envisaged at the time of the first deformation event. Accordingly,
generation by earthquake ground-shaking remains the most reasonable
cause of the observed deformation. This supposition is evaluated
below.

13.8.3 Evaluation of deformation event stratigraphy and origin

The two deformation events occurred towards the end of lake
sediment accumulation. The first event was followed by a short
period of sedimentation before the second event which coincided with
the end of lacustrine sedimentation.

Recalling the catastrophic 'Jökulhlaup' - ice-dammed lake
drainage - postulated by Sissons (1979a) for the final drainage of
the 260m lake, an association with the second event seems
unavoidable. Was the sediment slumping a direct result of
catastrophic lake drainage, or was the cause of sediment slumping
also the cause of lake drainage? Conversely, the first event is
clearly not associated with lake drainage - it occurred during
continuing lacustrine sedimentation in the 260m lake. There is a also
a difference in the style of deformation - 1st event, largely
liquefaction, 2nd event, mostly slumping. Despite these differences
it will have been noticed that both events display a zonation
approximately concentric with one another. Do the two events, then,

have a similar or different origin?

It will now be shown that an 'earthquake-generation' model can form a satisfactory explanation for both events, their similarities and their differences.

Structures identified as seismites elsewhere have been observed among the structures of the first event (ball-and-pillow, fault-grading, sand injection). This event also shows a clear zonation in styles and comprises deformation which mostly involves liquefaction and soft-sediment deformation of in-situ sediment profiles. Earthquake-induced liquefaction, therefore, seems a very promising candidate here. As for the second event, the predominance of slumping and absence of in-situ liquefaction could be the result of earthquake ground-shaking after the lake was drained, liquefaction being inhibited by the absence of saturation of the sediment.

Developing this model, some clarity in regard to the landslips becomes evident. Although the seven landslips appear to form one association, the fact that some landslips clearly post-date the 260m shoreline while others have been modified by it suggests that they belong to both events. The Main Roy and Glen Gloy landslips would then correspond to the first event, and the West Roy and Bohuntine landslips to the second. The timing of the other three can only be guessed at since they do not reveal their relationship to the 260m shoreline – it would seem reasonable to allocate them to the second, slump event. The 'later', subsidiary landslip in the Main Roy Landslip could have resulted from the second event also.

The 'red silt/sand' layer is interpreted as the 'drainage event' – a blanketing of oxidized sediment stirred up during turbulence of the lake water during drainage over a period of several days (Sissons 1979a).

This model, then, is adopted as an adequate interpretation of the deformation stratigraphy (alternative means were discounted in §13.8.2). It is summarized below and illustrated in Fig.13-29.

13.8.4 <u>An earthquake-generation model</u>

1st earthquake event: occurring during the later stages of the 260m lake, and causing liquefaction and other soft-sediment deformation over a wide area and in terms of a zonation in style of deformation. Two landslips were probably associated with this event.

Lake drainage: a catastrophic Jökulhlaup, as postulated by Sissons (1979a), and marked in the sediment by a red silt/sand layer.

2nd earthquake event: occurring very soon after the lake drainage and causing sediment slumping over an area slightly smaller than the area of first-event deformation. At least two, possibly five landslips were associated with this event.

13.8.5 <u>Correlation with observations on faulting</u>

Two features of field evidence suggest a correlation of these earthquake events, inferred from the study of sediment deformation, with the fault rupture described in chapter 11:

1) There is a spatial association. Fig.13-29 shows the position of the 7km-long, Glen Roy fault trace (c.f. §11.6). It lies within the northern half of the limit-of-A contour of sediment deformation.

2) There is a temporal association. In section 11.3.3 it was argued that the half-metre dextral displacement resulted in the offset of the shorelines and the failure of the Main Roy Landslide. In this chapter the same landslide is considered to have occurred at the time of sediment deformation in the first event.

Thus it seems reasonable to correlate the half-metre dextral displacement on the Glen Roy fault with the first earthquake event inferred from sediment deformation in the vicinity of the fault. The second event is likely to have been related to the same fault.

****

CHAPTER FOURTEEN

Arrat's Mill

****

14.1 BACKGROUND AND STUDY PROCEDURE

Ball-and-pillow structures were noted by Dr. I.B. Paterson (British Geological Survey) in sands exposed in an excavation now used for waste disposal by the North Angus County Council. The site (NO 3645 7588) lies close to the village of Arrat's Mill and 4km east of Brechin, County Angus (Fig.3-4). A reconnaissance visit during May 1984 confirmed that ball-and-pillow, liquefaction-type structures were present in a portion of the deposit, and a thorough study was made during June and July, 1984. The site was reserved for study until June, 1985, after which the cuttings were covered by landfill. The whole site is due for complete infill and topsoil replacement by around 1990.

At a deeper level within the deposit (c.7m lower), exposed in 1977, Paterson (pers. comm.) has seen another similar ball-and-pillow horizon, up to 2m thick. This horizon was not exposed during this study.

At its greatest extent, the site was around 200m in diameter and 10-15m in depth - **Fig.14-1.** With the help of the site's earth moving vehicle, cuttings were made through the portion of interest, resulting in a 'main face' cutting 80m long and up to 4m deep, and another cutting perpendicular to this, 10m long and 2m deep. The gross nature of the deposit could be seen from these cuttings, but in order to study the sediment in detail, 'logged-sections' (logs) were cut by hand with sharp cutting tools, photographed with colour transparency film and levelled-in with a surveyor's automatic level. Line drawings (produced from 35mm slide) were made for each log, and these together with field notes were used to construct stratigraphic sections. Samples were taken from two logs by inserting tubes (2.5cm in diameter) into layers of interest. Fifteen logs were cut in the main face and five more in a small portion of the site, 100m away

172

from the main face, which showed similar deformation structures. The logs were typically 0.5m wide and up to 3m deep. In addition to these detailed studies, faces throughout the site were inspected and photographed in order to observe the stratigraphy of the whole deposit. Details of the sediment-log survey are given in Appendix 5.

14.2 STRATIGRAPHIC AND GEOMORPHIC SETTING

The Arrat's Mill deposit lies within a group of fluvio-glacial terrace remnants which surround the Montrose basin (Cullingford & Smith 1980). The morphology of the terraces has not been studied in detail. The terrace remnants appear to have variable surface slopes which cannot be easily correlated. However, as a group, the terraces are clearly associated with the group of East Fife shorelines (Cullingford & Smith 1980).

Consideration of the height of the Arrat's Mill terrace (c.19m O.D.) in relation to the raised shorelines of the area (Sissons 1974, Cullingford & Smith 1980) suggests that the terrace is co-genetic with the 'EF-6', East Fife shoreline, dated at 14,750 BP by interpolation with the whole shoreline sequence (Andrews & Dugdale 1970, Sissons 1974). However, in the absence of site-specific, radio-carbon dates, all that can be said with confidence is that the Arrat's Mill deposit is older than the Main Perth shoreline (13,500-13,000 BP) and probably dates at around 15,000 BP, by association with the East Fife shoreline sequence (Paterson, pers. comm.). [The results of radio-carbon dating analysis of samples from this site will be discussed in §14.6: no reliable date was achieved.]

The terrace was probably part of an eastward prograding, marine to fluvial delta. Red, silty clays, probably of marine origin, are seen in the lowest portions of the Arrat's Mill and neighbouring terraces (Paterson, pers. comm.) and these grade up into the fluvio-lacustrine silts, sands and gravels which are seen in the excavations made in this study.

14.3 LITHO STRATIGRAPHY

The strata exposed in the Arrat's Mill excavation comprise a sequence of laminated silts and sands, overlain by gravels. The field sketch of **Fig.14–2** illustrates cross-bedding and channel structures in the West Face which appear to be contemporaneous with a broad, shallow basin in the North Face. This basin sediment is composed of finely-laminated silts and sands with clayey and organic layers, and is devoid of cross-bedding. It is interpreted as a lacustrine deposit. A smaller depression, seen at the east end of the North Face, has developed within the lake basin. This depression contains loose sands and silts, with climbing ripples and occasional cross-bedding and is interpreted as a fluvial deposit. These fluvial sediments grade upwards into more massive sands with thick (tens of cm) cross-bedded units, interpreted as aeolian deposits. These aeolian deposits also overlie the lacustrine sediments, and grade up into the gravel units. The gravels prograde eastwards, and the whole sequence is reasonably interpreted as an eastward migrating delta facies: gravel – aeolian and fluvial sands – lacustrine silts and sands. This stratigraphy is schematically illustrated in **Fig.14–3A.**

The soft-sediment deformation structures are observed in a portion of the lacustrine basin, seen in the North Face – **Fig.14–3B.** It is this portion that has been studied in detail, as illustrated in the stratigraphic sections of **Fig.14–4.** Only the western side of this basin is exposed, so that throughout the exposure the strata dip eastwards at between 2 and 7 degrees. The strata have laminations typically 1-3mm thick, but up to 1 cm thick with occasional sandy laminae up to 3cm thick.

Particle-size analysis of two sediment logs are presented in **Fig.14–5** (log-4) and **Fig.14–6** (log-S). Medium to fine-grained sands are observed at the base of the deposit (log-4). They are loose and poorly consolidated and are interpreted as pre-basin, fluvial deposits. Above these, the finely laminated, lacustrine deposits are composed of very fine sands and silts with clay layers, and are fairly stiff and consolidated. XRD spectrometric analysis of sample

B4 (Fig.14-5) indicates that 'clay' layers are composed of chlorites and micas, and contain no expanding-clay minerals. At the top of the sequence the sediment coarsens up into the fine-grained aeolian sands.

The fluvial deposit, cut into the lacustrine basin, is seen in logs 11, 12 & 13 (Fig.14-4). It has a sticky, organic clay layer close to its base (the Marker Clay Horizon - MCH) and contains loose sandy sediment. The aeolian deposits contain predominantly fine to very fine sands.

Deformation was also observed in another portion of the Arrat's Mill pit, at logs 16-20 (Fig.14-1). Of these logs only 18-20 are illustrated in **Fig.14-7.** This deformation occurs in sediment which appears to be the lateral equivalent of the main face section having a similar stratigraphy: finely laminated sands and silts overlying coarser, looser sands and underlying sands and gravels. However the deposit here is 3-4m below the main face exposure such that it may represent a separate, slightly earlier, lake basin.

14.4 DEFORMATION STRATIGRAPHY

14.4.1 General description

The ball-and-pillow structures are observed within a lens-shaped volume at the western side of the main basin (Fig.14-4) and also in the exposures of logs 18-20 (Fig.14-7).

In the main face the deformation is bounded by three surfaces, illustrated in Fig.14-4 and Fig.14-3B. The top of deformation (T) is a near-horizontal disconformity overlain by undeformed sands and silts. Most of the base of the deformation occurs along a clay horizon (Basal Reference Horizon - BRH) which appears to have acted as a 'fluid seal', since it bounds the deformation and remains unbroken (see Plate-15). Moving eastwards into deeper portions of the basin, the base of deformation (BL) is observed to rise away from this clay seal, migrating across bedding layers, rising to within roughly half a metre of the surface (T). In the western half of the lens the base of the deformation appears as a gentle 'lifting' of

layers above the Basal Reference Horizon (e.g. log-2). Rising upwards, this 'lifting' develops into clear flame structures, which bound large pillows. The largest pillows (up to 1m across) are observed in the lower half of the lens, and these migrate upwards into smaller pillows (e.g. log-4) which have mostly become detached to form pseudo-nodules. Further up, these small pillows become less clear and grade into 'dish structures'. These dish structures become more flattened upwards, until they begin to form fairly continuous layers just below the top of deformation. In the eastern half of the lens, the stratigraphy is similar, but the base is less well defined, occurring at different litho-stratigraphic horizons in each log.

In the other exposure showing deformation (logs 18-20, Fig.14-7) the internal deformation stratigraphy is not so clear. Log-20 shows a very thin deformed horizon (30-50cm thick) with a single layer of pillow structures, and clear relationships to adjacent stratigraphy. The deformed silts and sands overlie poorly laminated, undeformed sands. A clear truncation top to the deformation is overlain by laminated sands and then gravels.

Some specific features of the deformation are now discussed below.

14.4.2 The influence of slope

Where the large basin deposit thins out on its western edge (logs 1 & 2) the flame and pillow structures are observed to tilt downslope - **Fig.14-8A&B** and Plates-20&21. This is particularly so where a local depression creates a steeper slope (Fig.14-8B). There is no evidence here for major mass movement, but these structures are taken to indicate small amounts of downslope movement during dewatering and vertical flow which resulted from loss of shear strength during liquefaction. A similar sense of tilting can be seen in most of the pillows throughout the lens, which are generally rotated by about 10-20°.

14.4.3 Flotation of organics

Small blebs of fine-grained, amorphous material are abundant in

176

the lower portions of the deformed lake sediment, and are commonly seen to rise away from their apparent layer of origin - **Fig.14-9** and Plate-15. They have been termed 'organic' because of their fine-grained, 'greasy' nature, appearing to form a coating to sand and silt grains. They are dull, reddish brown in colour. Their composition is difficult to determine because of their disseminated nature; however, a 1kg, aggregated sample of the 'blebs' contained enough carbon for radiometric dating (see Appendix 7). Whatever their composition, they give the impression of upward migration, appearing to have floated upwards through the sand/silt matrix from clayey layers of origin. The degree of upward migration increases upwards from the base of the lens (a few cm of migration) upwards through the middle of the lens (several tens of cm).

14.4.4 Dish structures

The dish structures seen in the upper portions of the deformation - **Fig.14-10** - bear a strong resemblance to the dish structures described by Lowe & Lopiccolo (1974), who attributed them to gradual dewatering of unconsolidated sediment. At Arrat's Mill, they typically consist of a faint, dirty layer, up to 5mm thick, with oxide staining and local blebs of clay and organic matter (Fig.14-11). Their relationship to organic matter is difficult to appreciate as they are found in massive, structureless silt and sand. However, the fact that they form a continuum with the pillows beneath, which do have laminations parallel to their bases, does suggest they also follow primary laminations. Furthermore, the faint relict of a pillow can be seen in association with the dish structures (Fig.14-11 and Plate-17) suggesting a close genetic relationship.

14.4.5 Syn-deformational faulting

In **Fig.14-11** (and Plate-17) a fault can be seen to displace the faint pillow but not the dish laminae above. The fault is picked out by a line of clay and organic matter in a similar way to the dish structures. This suggests a distinct order of formation: pillowing, under liquefied flow - return of shear strength, with

177

fault-adjustment movements - the formation of dish structures as late dewatering features. All these presumably occurred within a short time-span, as progessive stages in a single process.

In log-18 closely-spaced, normal faults can be seen alongside ball-and-pillow structures (Plate-13). They appear to be syngenetic with the pillows, as the faults both bound incipient pillows and displace some flow features. It seems that a portion of the section (left-hand side) failed by faulting but not complete liquefaction, whereas the rest (right-hand side) completely liquefied to form pillows. The faulted portion is slightly coarser grained (predominantly sand) than the pillowed portion (predominantly silt).

14.4.6 The top of the deformation

The nature of the surface at the top of the deformation and the overlying deposits are the key to understanding the genesis of the deformation. Much of the original top-of-deformation has been eroded away; however, logs 14, 15 and S1 show it preserved.

Fig.14-11 (and Plate-17) shows detail at the top of log-14 and shows dish structures and organic blebs rising to very close to the top of the homogeneous silt. The top-surface is marked by settled or fallen clay clasts, and is followed by a thin unit of conformable, finely laminated, undeformed silt and sand. In log-S1 - **Fig.14-12** - a red silt/clay layer can be seen above the laminated silts on top of which lie loose aeolian sands. Particle-size analysis shows the the aeolian sand to be of markedly different composition to the laminated silts, which which have a similar composition to the deformed unit below. Thus the red silt marks a lithology change (the onset of aeolian sands) and the top of deformation does not. The top of deformation is consequently interpreted as having been a free, sub-aqueous surface, which collected allochthonous clasts of clayey sediment, and which was followed by a short period of continuing lacustrine deposition, before the onset of aeolian deposition.

The top of deformation at log-20 (Fig.14-7 and Plates-18&19) has been eroded away. The thin deformed horizon has a disconformable top surface, in that pillows and flames are truncated by it. Loose,

laminated sands can be seen to unconformably overlie the deformed deposit, and both have been subsequently eroded and overlain by gravels. Thus the original top of deformation has been removed by erosion, and overlain by sands (probably aeolian) and gravels.

14.4.7 Other deformation horizons

Beneath the main deformed lens, on the eastern side of the lens, several layers showing deformation can be seen (logs 5 to 11; Fig.14-4 & Plate-16). These are laterally continuous for several metres and can be correlated between logs. They are usually restricted to a few layers (up to 10cm thick) and do not disturb layering above and below. They most typically display tight, discontinuous folding. Some resemble involution structures (e.g. base of log-7) but at least one such layer (log-6, immediately below the BRH) shows features suggesting a co-genesis with the main deformation: it has much more continuous folding and is sharply confined by clay layers above and below. This suggests liquefaction by virtue of pore-water confinement as a means of generating the deformation. Thus although most of these layers are probably involution features, one or two layers immediately beneath the main deformation (logs 5,6&7) could be the result of a liquefaction processes.

14.5 INTERPRETATION OF SEDIMENT DEFORMATION

14.5.1 Summary of field evidence

a) Liquefaction structures (ball-and-pillow, flaming and dish structures) are observed in a lens-shaped portion at the edge of a lacustrine basin and elsewhere near the top of lacustrine sediment.

b) In the lens the deformation is limited at its base by a clay layer, which appears to have acted as a fluid seal. As this clay layer descends down the slope of the lake basin, the base of deformation leaves it, migrating upwards across layers to close to the surface (at the time of deformation).

c) The sequence of deformation appears to have involved flaming and pillowing of liquefied sediment, accompanied by faulting in some

portions, followed by the regaining of shear strength, settlement, faulting and the formation of dish structures.

d) The top of deformation appears to have been a free, water-sediment interface which collected dislodged clay clasts, and which was overlain by a few layers of silty, lacustrine sediment, before the onset of sub-aerial sands and gravels.

e) Much of the top of deformation has been removed by erosion prior to the deposition of sands and gravels.

14.5.2 Evaluation of the cause of deformation

An acceptable means of generating liquefaction at this site has to satisfy a number of field criteria. The following means of producing liquefaction (outlined in section 6.4) are evaluated below in the light of the field evidence:

a) **Imposed Loads:** There no evidence for this. Sands and gravels overlying the deformed sediment follow a period of either continued lacustrine sedimentation or erosion. Where the top of deformation can be seen it is typically homogenized, contains delicate dish structures and contains organic blebs, indicative of upward migration of porewater – all counting against the imposition of a load or impact.

b) **Slope-induced failure:** This seems unlikely. Although structures tip slightly downslope, the main sense of movement is vertical, with slope being a secondary influence. For failure by this mechanism the sediment would have to be in a critical condition. Since the slopes are not large (up to 7°), there is no reason to believe this – deformation occurred after the lake sediment was well established and the basin had filled up. Furthermore, there are portions of the deformed horizon with very little slope (e.g. log-20).

c) **Ice-thaw pressure:** To involve this kind of mechanism a cap or seal of ice above the deformed lens would be required. There is no evidence for this, and neither are there any associated ice-wedge or cryoturbation features. [Thin deformed layers (§14.4.7) parallel to the sediment layering may well be

180

ice-thaw related but are clearly separate from the main deformed lens.] Furthermore, it is difficult to see how permafrost thaw, from below, should cause liquefaction above the clay layer (BRH).

d) **Loss of hydrostatic load:** This is a very plausible means of generating the observed liquefaction. Had a body of water covering the basin stratigraphy been rapidly removed excess pore pressure could well have been generated as observed. The stratigraphy above the deformation could be compatible with this hypothesis: a partial drop in water would be required, since lacustrine sedimentation continued after the deformation. However a number of items of evidence conflict with this interpretation:

   i) Deposits marking the supposed drop in water level are absent, and marked changes in lithology are not observed.

   ii) The syn-deformational faulting of log-18 would have to be generated by this drop in water level.

   iii) Major topographic features would be required in order to support the idea of an ice-dammed lake in the area. These are not seen and therefore a rapid fall in water-level cannot be easily explained.

Thus, although plausible, this means of producing the deformation has a number of problems when applied to this formation.

e) **Storm loading:** This would be conceivable in the lens under a shallow body of water; however, the deformation would be expected to be most intense at the surface, and would be unlikely to develop to depths of 3m, as observed. No storm deposit is present to support such an argument, rather, calm lacustrine sediment is evident at the top of deformation.

f) **Earthquake loading:** This provides the most adequate explanation for all the field observations and presents the least number of problems. The situation conceived is illustrated in **Fig.14-13.** One has to invoke a small body of water above

the deformed lens in order to allow saturation of the sediment. The basal clay seal (BRH) functions as a confinement to pore water escape, creating a lens prone to liquefaction. The structures observed are quite compatible with earthquake-induced liquefaction - settling of sediment and upward migration of pore-water being the primary modes of movement. The densely-packed faulting of log-18 would also result from ground shaking, in a portion of sediment where liquefaction was not achieved. The clay clasts which lie on the top surface would represent dislodged fragments of surface sediment at the time of ground shaking. Sedimentation in the body of water continued for a short while after the event, soon followed by fluvial and aeolian sedimentation of the prograding delta.

14.5.3 Concluding statement

Soft-sediment deformation, under liquefied conditions, has occurred beneath a free, water-sediment interface. Many conceivable means of generating liquefaction at this site can be discounted in the light of field evidence. An earthquake-induced origin is most compatible with the observations; however, rapid 'loss-of-hydrostatic-load' remains a plausible alternative.

14.6 CARBON-DATING

Three samples of sediment from Arrat's Mill were dated by ^{14}C-analysis. The stratigraphy of these samples and the dates obtained are illustrated in **Fig.14-14.** The results are disappointing. The oldest date (13,440 years) approaches the age which would be expected by virtue of regional study (c.15,000 years - §14.2), but is still apparently too young. Considered together the three dates display a broad range and an inconsistent sequence. It must be concluded that contamination by younger carbon has occurred. The results illustrate the difficulty in radiocarbon dating of sediments of this age and type where shelly or woody material is not present. Each sample and date is discussed in more detail in Appendix-7, samples 4, 5 & 6.

****
CHAPTER FIFTEEN
Meikleour
****

15.1 BACKGROUND AND STUDY PROCEDURE

Alongside the structures seen at Arrat's Mill, Dr. I.B. Paterson (British Geological Survey) had also noted similar soft-sediment deformation in an exposure of the Meikleour Outwash Terrace close to the village of Meikleour, 6km south of Blairgowrie, Perthshire – Fig.15-1. The exposure (NO 3151 7393) is seen where the terrace has been cut by the River Tay, forming a 10-15m bank, and additionally exposed in a 'clay-pit' used for the construction of flood-dykes, during the 1940s ('M' in Fig.15-1). The site was reconnoitered during May 1984 and thoroughly excavated during June and July 1984. The excavation was made with the help of an earth-moving vehicle with hydraulic arm. Scaffolding and ladders were used in order to clean up the face with sharp cutting tools.

The main excavation ('main face') was up to 9m high and 23m wide. Soft-sediment deformation structures were seen throughout this exposure. Extensive photography, sediment sampling and field description of the main face was made, concentrating on a 'vertical section' 8m high and 2m wide, shown in **Fig.15-2 & 15-3**, and a 'horizontal section' 1.5m high and 5m wide, shown in **Fig.15-4** (see also Plates-24&25).

A second smaller excavation, the 'forest pit' (2m deep and 1m wide), was made in the terrace 150m to the south-east of the main cutting ('F' in Fig.15-1). This cutting lacks soft-sediment deformation structures but contains minor faulting. It is illustrated in **Fig.15-5**. These two sites were levelled-in to one another to find their relative heights (Appendix 5).

Paterson (in Armstrong et al. 1985) has also seen similar structures in exposures of the terrace seen in a gas-pipeline excavation, 1.5km to the north ('G' in Fig.15-1). The structures were seen along a 100m long section of the pipeline exposure, where

the excavation was deepest (6-7m). No other exposures of the terrace have been seen.

15.2 STRATIGRAPHIC AND GEOMORPHIC SETTING

The Meikleour Outwash Terrace is a well-defined geomorphic feature. It comprises a smooth-surfaced, outwash spread, whose surface is inclined southwards at around 2.5m/km (Paterson 1974). This smooth surface in interrupted by several large kettleholes, and the whole terrace has been heavily dissected by fluvial action, leaving several isolated outcrops covering over 20km^2. Paterson (1974) interprets the terrace as having been formed initially within wasting ice, but mostly subaerially after the retreat of the late Devensian ice from the area, at about the time of the Main Perth shoreline (13,500-13,000 years BP). [Radio-carbon dating of one sample from this site was made. The date was much younger than expected (2500 years BP) indicating the sample to be heavily contaminated by younger carbon - see Appendix-7, sample 3.]

The Meikleour Terrace overlies an earlier spread of sand and gravel, termed the 'Moundy gravel' (Fig.15-1), which has abundant ice-contact features, a hummocky surface and well-defined, eastward-trending, esker ridges. This lower deposit is much more extensive, and can be associated with similar deposits in the Forfar district, 30km to the east. The nature of the deposit suggests accumulation in association with decaying ice and meltwater flowing from west to east (Paterson 1974)

Thus, the soft-sediment deformation structures are observed in the second of two outwash terrace deposits formed during the decay of the late Devensian Ice across Perthshire (c.f. Fig.7-1). The first terrace was formed in association with the ice, whereas the second was formed subaerially, after the ice had retreated.

15.3 LITHO STRATIGRAPHY

Detailed stratigraphy of the deposit is difficult to elucidate since the sediment is deformed throughout the exposure, and since upper, lower and lateral limits to the deformation are not seen. The

forest-pit excavation helps stratigraphic interpretation since it is not strongly deformed, and reveals a 'top-of-deformation' horizon. However, correlation with the main face is difficult owing to their 150m separation.

15.3.1 Main Face excavation

Key horizons, within the main face excavation, have been labelled 'K-Q' for ease of reference. They are indicated in figs.15-2,3&4.

Particle-size analyses of samples taken from the vertical section of the main face (Fig.15-3) show most of the section to consist of fine to very-fine sand, silt and clay. The section is grossly coarsening-up: the lowest portions of the section are almost devoid of sandy laminae but they become increasingly abundant upwards. The particle-size distributions reveal at least 2 coarsening-upward cycles within this sequence: samples MP12 up to MP8 and MPCB up to MP5. The sparcity of samples in the lower portions of the section together with the severity of deformation probably hides the presence of more coarsening-up sequences within it. Near the top of the exposure, a distinctive, well-laminated sand layer (the 'K layer') contains the coarsest sediment in the profile (sample MP3).

Where bedding can be seen, in the sandier portions, an even lamination is most commonly apparent. Occasionally bedding can be seen in the finer sediment (Fig.15-9) where closely-spaced lamination suggests a lacustrine environment. However, most of the bedding structures in the finer sediment are completely lost. In some pillows cross-bedding can be seen (Fig.15-7) and in the L-horizon sand cross-bedding is common (Fig.15-4). Sandier units can be seen to laterally continuous across the exposure (Fig.15-4). Slight thinning of units southwards (towards the right) is apparent: sands below horizon M are thicker to the north, and the L-horizon sand, although becoming thinner to the north, develops into two sand layers which then thicken northwards (off the left of Fig.15-4); the laminated sand above horizon-L becomes almost twice as thick in exposures (not illustrated) off to the left (north) of Fig.15-4.

This slight southward thinning of the beds and the overall
coarsening-up nature of the sequence suggests a southward-prograding
depositional environment, which is consistent with the regional
southward inclination of the terrace (§15.2). The bedding
structures which can be seen suggest that lacustrine sediment gave
way to fluvial sediment in a number of pulses, i.e. coarsening-upward
cycles.

15.3.2 The Forest Pit

No direct correlation of the forest pit to the main face can be
made; however they are certainly within the same terrace, composed of
very similar sediment and at a similar height within the terrace.
Horizon-T, shown in Fig.15-5 of the forest pit, is 1.13m above
horizon-L, shown in Fig.15-2 of the main face.

The section mostly comprises laminated silts and sands, with
occasional cross-bedded layers. No soft-sediment deformation is
present, but normal faults are seen in the lower half of the
section. The faults terminate upwards at a distinctive, clayey layer
(MF1, Fig.15-5), above which the sediment is completely undeformed.
No change in the stratigraphy is seen at the clayey layer.

More detailed inspection of the fault-terminating, clayey layer
reveals a lower brown, clayey silt (20mm thick) and an upper red silt
(5-10mm thick). The brown, clayey silt is graded, fining upwards. It
contains small plant fragments which are more abundant in the lower
half of the layer. The red silt is uniform and homogeneous. The base
of the brown, clayey silt is a sharp discontinuity, where the offset
of faults is eliminated, or substantially reduced.

Three faults are seen to terminate against the clayey layer
(Fig.15-5). Two of these terminate at the base of the brown, clayey
silt, but one continues, with reduced offset (a few mm) to terminate
at the base of the red silt. The faults have throws increasing
downwards from a few millimetres to several centimetres.

Interpretation of the forest pit stratigraphy: The event
which resulted in normal faulting of the laminated silts and sands

was marked by the deposition of a brown, clayey silt which contains plant fragments and fines upwards. It was followed by a thinner, red-silt layer. Although both layers are post-faulting, minor fault movement on the lower brown, clayey silt is seen, suggesting late settlements after the deposition of this layer. The red silt marks the end of fault movement. The red silt is followed by continuing laminated silt and sand deposition.

15.4 DEFORMATION STRATIGRAPHY

In this section only the soft-sediment deformation of the main face is considered. Faulting in the forest pit has been considered in the previous section. Locations within the main face are given with respect to an indexed grid (shown on Figs.15-2,3&4) with vertical (V) and horizontal (H) gridlines at 1m intervals (e.g. V1.0/H4.5).

15.4.1 Aspects of the vertical variation in deformation

Fig.15-2 illustrates the sequence of ball-and-pillow layers in the section. Continuous layers of pillow structures are clear in the upper portion (e.g. horizon-M and the N and O layers) but in the lower portion the stratigraphy is less clear, and in terms of layers with more-abundant and less-abundant pillows (the P and Q layers). The excavation was extended 3m below the level V2.0, and no lower limit to deformation was seen. With increasing depth sandy pillows became less frequent and the silt increasingly structureless. Because of this, the study has concentrated on the upper portions of the section where structures are more abundant and complete.

Near the top of the section the well-laminated sand layer, 'K', is virtually undeformed and only disrupted by two fissures. The right-hand fissure (Fig.15-2 & Plate-22) displays upturning of the sand lamina suggesting upward injection of material through it. Above this layer more pillow deformation is seen (between V0.2 & V3.0). No upper limit to this deformation was exposed.

Six pillow horizons are clear (a few more vague pillow-layers are seen in the lower portions (not illustrated)). The six main

pillow layers are:

a) **The layer between horizons L and M (the L-to-M layer):** a half-metre thick layer with densely packed pillows in the lower half and a clear structureless zone in the upper half.

b) **The M-horizon layer:** a very pronounced layer comprising at least three sand layers deformed into regularly-spaced pillows which do not appear to have descended much - the whole layer remains intact.

c) **The N layer:** containing some of the largest pillows; similar in form to the L-to-M layer, but not so densely packed in its lower portions and having a structureless zone containing many smaller pillows.

d) **The O layer:** not very distinct; bears some resemblance to the M-horizon layer.

e) **The P layer:** a poorly defined layer of pillows immediately below the O layer.

f) **The Q layer:** a vague layer of rounded and disrupted pillows.

15.4.2 Aspects of the lateral variation in deformation

Discussion here has to be limited to the upper layers only, since only in this portion was substantial lateral exposure made. On the whole the deformed layers are laterally continuous and easily traced across the exposure. Some variations are however apparent (referring to Fig.15-4):

a) the L-to-M layer gets thicker from left to right.
b) the M-horizon layer is symmetrically deformed (evenly-shaped, evenly-spaced pillows) at the left and right, but is asymmetrically deformed in the centre, where pillows appear to be sheared (H2.0 t H3.5).
c) a portion of the M-horizon (H0.0 to H0.7) has remained relatively undeformed.

Some of the reasons for these variations will become apparent when discussing other features below; however, it should be emphasized here that the lateral variations in deformation are small in comparison to the verical variations. This may in part correspond

to the primary lithostratigraphy, but must also have implications for the method of generation of deformation. The deformation is ubiquitous across this exposure (23m) and probably over much larger distances (noting the gas pipeline observations, 1.5km away).

15.4.3 Loading

Loading - the sinking of denser layers into less dense soft substrates - is the primary mechanism involved in most of the structures seen here. Ball-and-pillow structures will be treated separately, below. In this section the distinctive 'loading' of the L-horizon sand layer is discussed.

Between H1.2 and H4.8 the L-horizon sand layer has sunk into the structureless silts below to form load structures. Some of these load structures have become detached and have descended into the silt beneath as pseudo-nodules (e.g. between H3.7 and H4.0).

Between H0.6 and H1.5 a thin layer immediately below the L-horizon has descended by increasing amounts from left to right, portions of it curving to form incipient pillows. At the left (H1.6 to H1.8) the layer has been broken up by normal microfaults to produce a step-like profile.

15.4.4 Loss of shear strength

The structureless silt below the horizon-L sand layer is interpreted as having lost its shear strength to flow as a liquid, allowing the descent of pillows and load structures. Much of the sediment in the column displays this character, and most notably the layers immediately above pillow layers. This relationship to pillow structures, together with the absence of lamination and the evidence of flow in portions immediately adjacent to pillows (Figs.15-6,7,8&9) strongly suggests that these were liquidized portions of the sediment column during liquefaction. Particle-size analysis shows these portions to be significantly finer grained than the pillows (Fig.15-3, samples MP6 & MP9 c.f. MP8 & MP10).

15.4.5 Injection structures

Sub-vertical channels have developed within the K layer (at H2.8/V5.1 and H3.3/V5.1). These injection channels appear to have been fed by horizontal channels through the L-horizon layer (at H2.2/V5.0 and H3.6/V4.9) allowing the flow of material from the structureless silt below. They contain material very similar in composition to the structureless silt layers (Fig.15-3, MP4).

Other sub-vertical channels are apparent where the M-horizon has been curved upwards around the large pillows at H1.7/V4.5 and between smaller pillows at H3.6/V4.4), and in the O layer at H2.5/V3.2.

15.4.6 Mass flow

The injection structures outlined above indicate localized mass flow through channels; however, several other features indicate more substantial mass flow of major portions of the sediment column. At least three features suggest this:

a) the distribution of ball-and-pillow structures suggests a re-distribution of mass within layers, i.e. inversion of whole layers with pillows sinking through structureless silt.

b) horizontal thrust movement (of up to 0.2m) is indicated by the imbrication of the M-horizon (at H3.1/V4.4), and by the shearing of pillows beneath the M-horizon (between H0.0/V4.8 and H0.6/V4.7).

c) features of the variation in thickness of the L-to-M layer suggest thickening and thinning by mass flow (as opposed to being a feature of primary sedimentation):

   i) it is the zone of structureless silt which accounts for most of the variation; the pillow layer is of fairly constant thickness.

   ii) the thrusting and shear of pillows is in the direction of thickening, and is positioned in a manner consistent with the layer thickening.

   iii) injection through the K-layer occurs above the thickest portion of the L-to-M layer, indicating that injection was related to the overall mass flow of the layer.

All these phenomena tend to suggest an inter-related set of mass-flow processes involving:

a) The sinking of pillows and the loading of the L-horizon sand.
b) Lateral thrust movements and thickening of portions of the layers.
c) The injection of liquidized sediment through vertical escape routes.

These processes are most apparent in the L-to-M layer, but probably also occurred in the (not so well preserved) lower layers.

15.4.7 Truncation surfaces

Several surfaces truncating deformation structures are seen in the section. The most prominent is the M-horizon; five others are indicated on Fig.15-2. In general, these surfaces truncate the tops of pillows, as is clearly seen between H4.0 and H4.6 along the M-horizon. Where the trucation surface is less well preserved it may be apparent only as a flat-top to a single pillow structure: many pillows in the L-to-M layer display this (between H4.0 and H5.0). This suggests that pillows formerly aligned beneath a truncation. surface (as with the M-horizon) have fallen away, differentially, to disrupt the truncation surface. Truncation surfaces become less well preserved with increasing depth and in the lowest portions the pillows assume a completely rounded nature, having little evidence of former truncation surfaces (Fig.15-9).

Although, in general, it is the tops of pillows which are truncated, in one location slight truncation of pillow bases is observed. This occurs where the M-horizon appears to have been thrusted (between H3.0 and H3.6).

15.4.8 Pillow morphology

A great variety of form is observed in the ball-and-pillow structures. Their form is discussed with respect to four examples taken from different depths within the section, thus illustrating the variation in form with depth.

191

a) **Fig.15-6, H5.3/V4.3** (Plate-23): A suite of pillowed sand
   layers showing original layering bent round parallel to the
   basal surface, and truncated at the top surface (horizon-M).
   Homogeneous, silty layers below the pillows have probably been
   'winnowed' during flow to provide the clay that coats the base
   of the pillows. (Note that, particle-size analysis of such a
   clay coating from another pillow is shown in Fig.15-3, sample
   MPCB.) Contorted structures seen between the pillows appear to
   be the result of deformation and mass flow involved in the
   accommodation of the pillows during formation. A channel to the
   right of the central pillow has penetrated the horizon-M,
   truncation surface. This channel is lined with clay, and a trail
   of clay blebs below indicates injection from the structureless
   silt beneath. Immediately above the truncation surface (M) a
   thin layer of deformed silt occurs, thought to be the remnant of
   the liquidized material which flowed along the trucation surface
   as the overlying pillows descended.

b) **Fig.15-7, H4.3/V3.5:** Two main pillow units, with deformed
   silts and secondarily deposited clays in between, have
   winnowed-clay deposited at their bases. However, there are two
   additional clay layers, suggesting that two pillows (or pillowed
   layers) have been destroyed and removed by the expulsion of
   material laterally. The remnants of one of the destroyed pillows
   are apparent in the thin, sandy layer above the second clay
   layer from the right. Later development of injection structures
   has disrupted the pillows causing them to begin to break up into
   separate balls. There is an increasing intensity of injection
   from 'X' to 'Y'.

c) **Fig.15-8, H3.4/V3.0:** A tulip-shaped pillow showing some
   bedding features, and completely detached within a
   structureless, silt matrix. The geometry of this pillow is more
   complex than pillows 'a' and 'b'. The basal clay deposit here
   mantles most of the pillow and has been removed, broken or
   folded at the base. A truncation surface is evident at the top,
   but has been broken by dewatering and injection of pillow
   material at 'X', and by channelling of liquidized matrix at

'Y'.

d) **Fig.15-9, H3.0/V0.9:** A tulip-shaped pillow with a
   tightly-folded internal structure, which appears to exhibit
   remnants of a truncation surface now curved around to form the
   top and right-hand side of the pillow. Vertical channel
   development, involving substantial mass transport of liquidized
   matrix, encapsulates the pillow. A disrupted clayey raft
   displaying original layering is seen to the left of the pillow.
   The raft has suffered injection (for example at 'X') and
   peripheral erosion by channel flow (at 'Y').

The tulip shape of the pillows 'c' and 'd' results from the
development of a 'pinched stem' feature in the lower side. It is
thought to result from the rapid movement of liquidized matrix,
laterally and upwards, creating a lower pressure zone at the base.
That the tulip shape is a later stage of pillow development is
apparent from the fact that the winnowed clay deposit, surrounding
the pillow, is drawn out with the stem, as seen in pillow 'd'.

15.4.9 Resistance to deformation

It is clear that sandier (coarser grained) portions of the
sediment column have resisted the deformation the most. The best
preserved layer, the K-layer, contains the coarsest sediment and also
has the most poorly sorted (well distributed) particle-size
distribution (Fig.15-3). The sands within the M-horizon layer have a
similar size-distribution, but are more peaked in the fine sand
fraction (i.e. better sorted). Although this layer has been pillowed
the layering is still recognisable, and some portions of the layer
have suffered very little deformation (H0.0 to H0.5). The L-horizon
layer, which is the only other layer to have remained intact, is
substantially finer-grained, peaking in the very-fine sand fraction
(Fig.15-3, MP5). It contains much less silt than the structureless
silts beneath. The loading it has developed would appear to result
from its intermediate grain-size between the coarser, undeformed
K-layer above and the finer, structureless silts beneath.

In contrast to these layers, portions of the sediment which have

been strongly deformed contain substantial amounts of silt. Pillows within the deformed sediment are slightly coarser grained (e.g. MP10, Fig.15-3).

Thus there is a strong correspondance of the degree of deformation and grain size. However, this correspondence is partially 'over-printed' by the variation in degree of deformation with depth – coarse sediment is found within pillows near the base, whereas the fairly fine-grained, L-horizon layer is still largely intact at the top of the section.

15.5 INTERPRETATION OF SEDIMENT DEFORMATION

Interpretation of the deformation at this site is severely hampered by ignorance of the nature of the limits of the deformation. Consideration of the cause of deformation must, therefore, rest largely on the internal features of the deformed sediment. The forest pit section does, however, provide some clues concerning the limits of deformation.

15.5.1 The correlation of the forest pit site

It can be inferred that the faulting and red-silt event at the forest-pit site correlates with the soft-sediments deformation at the main-face site. There is no certainty regarding this correlation, since no lithological correlation is apparent: the correlation rests entirely on the association of deformation features. The following can be stated in favour of correlating the deformation at the two sites:

a) Deformation at the two sites occurs in similar sediment of the Meikleour Outwash Terrace, at a similar height (horizon-T is 1.13m above horizon-L).

b) Soft-sediment deformation is known to be widespread in the terrace (i.e. gas-pipe-line exposure 1.5km north of the main face) such that syn-sedimentary faulting (at the forest-pit site) is likely to be co-genetic with the other sediment deformation.

c) On purely mechanistic grounds, syn-sedimentary faulting is a

likely accompaniment of soft-sediment deformation which involved substantial mass flow (i.e. layer thinning/thickening and injection).

These inferences are as much as can be stated. All that can be said with certainty is that syn-sedimentary faulting at the forest-pit site occurred during the red-silt event, and may be correlated to the (or one of the) soft-sediment deformation event(s) at the main-face site. The faulting/red-silt event occurred during continuing, 'normal', sediment deposition within the Meikleour Terrace.

15.5.2 Interpretation of the main-face deformation

Summarizing the field evidence, the following are observed:

a) Several layers of ball-and-pillow structures, separated by layers of structureless silt.

b) The degree of deformation increasing downwards, with pillows displaying increasing maturity of deformation with depth.

c) Evidence for mass flow within deformed layers in terms of layer thickening and thinning, thrust movements and injection phenomena.

d) The injection of substrate through pillow horizons during pillow formation.

e) Evidence for the flow of sediment under liquidized conditions, silty portions of the sediment being the primary locus of flow.

The possibility that the observed deformation is a product of many phases of deformation cannot be ruled out; however there is much to indicate that all that is seen is the result of a single 'event' (of unknown duration):

a) There is a similarity in the style of deformation thoughout the column.

b) There is progression in the style of deformation, with structures lower down appearing to be mature, or developed forms of those higher up.

c) There is inter-connection of deformed layers by injection

195

structures.

d) There is no complete hiatus in deformation within the sequence:
even the prominent M-horizon is disrupted at some points
(H1.9/V4.4).

These features are collectively taken to suggest a single
deformation event which is inferred to have involved the following
sequence of processes, illustrated in **Fig.15-10:**

1) Reduction in shear strength of siltier (finer-grained) layers.

2) Loading and sinking of sandier layers into silt to form pillows,
and resulting in the inversion of stratigraphic units (pillows
sinking to the bottom).

3) Lateral flow and inter-layer injection of sediment resulting in
changes in thickness of layers, local thrust movements and
shearing of pillow layers.

4) Prolonged flow and deformation of sediment at depth, with
completely detached pillows subjected to further deformation.

5) The resumption of shear strength in the sediment column,
allowing the 'freezing' of the structures as is now seen.

15.5.3 Conceivable means of producing the sediment deformation

The exposure at Meikleour displays well-preserved deformation
structures but lacks evidence for the stratigraphic relationships of
the deformed horizon to adjacent undeformed units. This makes
discussion of the means of deformation difficult. Liquefaction of
some kind is implicated, both by the type of structure and by clear
evidence for flow of much of the sediment column. Thus the discussion
can focus on the possible means of producing liquefaction in this
horizon.

Some means can be very quickly dismissed: the lateral extent of
the deposit counts against local impacts of surface loads, the lack
of directional structures and slopes counts against slope failure,
and the large thickness of deformation negates storm loading.
However, the following appear to be acceptable candidates:

a) Loss of hydrostatic load.

b) Freeze-thaw pressure.

c) Earthquake ground-shaking.

a) Loss of hydrostatic load

The main factor determining the onset of liquefaction under these conditions is the rate of pore pressure dissipation (section 6.4.1). It would therefore be expected that layers trapped between fluid seals (low permeability layers) would be most prone to liquefaction. This is not what is observed in the Meikleour profile - it is the finer, silty layers which have deformed most, leaving the 'sealed' pillow layers better preserved. The Meikleour profile also necessitates fairly prolonged deformation, which under loss-of-hydrostatic-load conditions could only be achieved if the overall permeability of the sediment column was low. With regard to which, the sandy, K-layer would seem to provide a very suitable, high-permeability layer capable of fairly rapid dissipation of excess pore pressures.

Furthermore, the type of sediment - interbedded fluvial and lacustrine - and the form of the Meikleour Terrace - a broad, flat outwash spread - both count against the presence of the large body of water necessary for this process. Loss of hydrostatic load, therefore, seems an unlikely means.

b) Freeze-thaw pressure

No ice-wedge, heave or involution structures have been seen in the Meikleour sections, which counts against the action of freeze-thaw processes in the deformation. However, the scenario envisaged by Vandenberghe & Van Den Broek (1982) (§6.4.1c), involving the final melting of a deep permafrost layer could be applicable here.

Had the Meikleour terrace been laid down on a permafrost substrate, which later thawed through the terrace, the observed deformation might have been produced. This means could account for the severity of deformation at depth, with the thaw-produced

liquefaction front rising through the sediment column, having reduced effect with decreasing depth. It should be noted that the presence of kettleholes in the Meikleour Terrace, 4-6km north of this site (Paterson 1974), is supporting evidence for the melting of ice within the terrace.

However, under these conditions the finer (silty) layers are required to act as fluid seals, and the coarser (sandy) layers would be expected to develop liquefaction (§6.4.4). This is not observed. It is the silty portions that are the primary loci of liquefaction. Also, they have flowed and have been injected in a manner which counts against their role as confinements to pore-water migration.

Furthermore, even a very rapid amelioration of climate would take several years to melt the permafrost layer, such that there ought to be at least a few repetitions of permafrost melting in successive springs. The Meikleour Terrace deformation should, then, show some evidence of more than one phase of deformation, if produced by this mechanism - it does not appear to. Also, the presence of kettleholes several kilometres to the north, and not at this site, in fact counts against this means since we would expect the liquefaction structures to be accompanied by kettleholes if permafrost thaw was the mechanism involved.

c) Earthquake ground-shaking

The substantial volume of deformed sediment at this site - to depths in excess of 9m, and over a large area - gains credibility in the context of earthquake ground-shaking. Modelling studies (§6.2.3) have shown that, under earthquake loading, cohesionless sediment columns can liquefy to depths of tens of metres, being especially prone to liquefaction at depth. Experimental study has shown fine-grained sediments (silts and very fine sands) to be the most prone to loss of shear strength - precisely what is observed at Meikleour. Furthermore, the evidence for injection of silt from deeper, liquefied layers upwards (presumably to the surface) is highly consistent with earthquake-induced liquefaction (it is the most commonly observed phenomenon -§6.1).

Earthquake-induced liquefaction thus appears to be the most promising candidate for the cause of deformation at Meikleour. It is postulated to have involved the following (c.f. Fig.15-10):

1) Cyclic-loading generating liquefaction in the most prone layers, that is silty layers, and especially silty layers at depth (several metres).

2) The sinking of sandier layers into liquefied zones, as pillow structures.

3) Mass re-distribution driven by gravitational instabilities, and allowed by the loss of shear strength, and causing internal erosion and the formation of truncation surfaces, local thrust movements, layer thickening and thinning, and the expulsion of liquefied sediment, upwards.

4) Continued deformation with mass flow movements disrupting earlier structures at depth, and as new, higher layers are liquefied by pore-water migration.

5) The resumption of shear strength, as escape of pore water brings liquefaction to an end, occurring first near the surface and only later at depth, where pore-water escape routes are longer.

This earthquake-induced-liquefaction model for the deformation thus gives reasonable explanation for the complex stratigraphy observed. Additionally, if the forest-pit stratigraphy is correlated with the deformation at the main face (§15.5.1), this earthquake model becomes more favourable. A surface-faulting event, marked by an anomalous silt layer, would then be interpreted as the settling out of turbid water, after earthquake disruption, involving soft-sediment faulting at the surface and liquefaction at depth.

15.5.3 Concluding statement

The thick sequence of ball-and-pillow soft-sediment deformation at Meikleour is interpreted as the result of a single liquefaction event. Lack of evidence regarding relationships to undeformed sediment makes interpretation of the cause of deformation difficult. Earthquake ground-shaking is the most reasonable cause, however loss-of-hydrostatic-load and permafrost-melting cannot be ruled out.

15.6 A COMPARISON WITH BALL-AND-PILLOW STRUCTURES IN THE LOWER DEVONIAN

Cursory study has been made of two localities showing ball-and-pillow structures, within the Lower Devonian, Old Red Sandstone of the Tayside Region. This brief study, although off the main coarse of this thesis, serves to improve the interpretation of the Quaternary ball-and-pillow horizons by placing them in the context of their occurrence throughout the geological column.

15.6.1 Lower Devonian ball-and-pillow sites

Ball-and-pillow horizons are 'very common in the lacustrine facies intercalations within the Lower Devonian of the Tayside area' (Paterson pers. comm.). Two localities (intimated to the author by Dr. Paterson) revealed ball-and-pillow horizons sufficiently well exposed for comparative analysis. They are found within the Arbuthnott Group of the Lower Devonian, at a quarry near Aberlermo, County Angus (NO 3526 7551) and at a natural exposure near Fowlis, Perthshire (NO 3323 7333) (the locations are shown in Fig.3-4). Sketches of the stratigraphy around the ball-and-pillow horizons at each site are shown in **Fig.15-11.** Analysis of thin sections from these sites are given in Appendix 6.

At Aberlermo, the ball-and-pillow horizon is up to 2m thick, thinning out laterally in a channel form, and exposed over a distance of 10 metres. The pillows are 0.2 to 1.0m wide and up to 0.2m thick. Lamination curved around with the pillow is often seen. A planar top-surface of deformation is seen in parts of the exposure, where broken-up clasts of fine-grained sediment sit chaotically within a structureless sand. Overlying the deformed horizon lie fining-up sand units. Thin sections were made of samples taken from the centre of a pillow, the matrix around the pillows, and from the sediment immediately below the top of deformation. The sediment consists predominantly of fine to very fine sand grains in the pillows and silt-sized grains in the matrix.

At Fowlis, a much less distinct ball-and-pillow horizon, only 0.5m thick is observed within a sequence of planar and cross-bedded

sandstone. The pillows are only 0.1-0.2m wide and roughly half as thick. The deformed horizon is followed by a 5-10cm thick cross-bedded unit and then by planar laminated sediment. Thin sections were made of samples taken from cross-bedded units below the deformed horizon, from a pillow structure and from the planar beds above the deformed horizon. Again, the sediment was found to consist predominantly of very fine sand and silt grain sizes.

15.6.2 Interpretation of the Lower Devonian ball-and-pillow horizons

At the two sites outlined, the ball-and-pillow soft-sediment deformation occurs in laminated sediment, with thin cross-bedded units, and with fine-sand to silt sized grains. The environments of deposition have not been studied in detail, but the channel form of the Aberlermo horizon, the thinly bedded fabric and regional study of the Arbuthnott Group (Armstrong and Patterson 1970, Mykura 1983) collectively suggest a lacustrine environment.

In both cases, no surface load appears to have been responsible, but rather the deformation occurs beneath a free, sedimenting surface, with little change in the composition after deformation. No storm deposit is apparent, no directional structures indicate slope failure, and ice-thaw is extrememly unlikely in a sub-tropical, terrestrial environment (Mykura 1983). Thus from this sketchy field study, earthquake generation seems the most reasonable cause of the deformation observed here. A supposition which is consistent with the high level of tectonic and volcanic activity in Lower Devonian times; the Arbuthnott sandstones and conglomerates are intercalated with lavas and pyroclastic deposits (Mykura 1983).

15.6.3 Comparison of grain size in the Meikleour and Arrat's Mill sites with the Devonian ball-and-pillow horizons

Thin section study of the Lower Devonian ball-and-pillow horizons shows them to contain very similar sediment to that of the Quaternary ball-and-pillow horizons at Arrat's Mill and Meikleour (Appendix 6). Pillows contain fine to very-fine sand and the structureless matrix contains predominantly silt. In the thin section

study a rough measure of roundness of grains was made by counting the number of 'elongate' grains (i.e. those with long dimensions more than twice the short dimension, as seen in thin section). The Devonian samples contained substantially more elongate grains (16-26%) than the Meikleour (9-21%) and Arrat's Mill (6-10%) sediments. No correlation of grain shape with deformation style or degree is apparent. The differences presumably reflect the different depositional environments and ages of the sediments.

Thus despite the difference in climatic environment (glacial cf. arid) the ball-and-pillow horizons have a very similar composition (fine sand to silt), fabric (well laminated with occasional cross-bedding) and depositional environment (fluvio-lacustrine).

****
CHAPTER SIXTEEN
Kinloch Hourn (sediments)
****

16.1 BACKGROUND AND STUDY PROCEDURE

During field investigations along the Kinloch Hourn Fault, the author discovered soft-sediment deformation features in two small pockets of sediment at the base of upland valleys in the Kinloch Hourn region. The locations of these outcrops of sediment are shown in Fig.12-2. They are: a 9 hectare outcrop to the east of the Upper Arnisdale lochs (NG 1901 8097) and a 12 hectare outcrop south of Loch Coire Shubh (pronounced 'corrie hoo') on the Hourn River (NG 1960 8054). The two sites are 7.5km apart and each about 1km south-west of the Kinloch Hourn Fault. In both cases, exposure of the sediment was seen in the banks of streams during low water of the dry summer of 1984. These natural stream cuts were excavated by hand, using sharp cutting tools, to construct sections for logging. Sections were surveyed into a local reference, photographed and described. Line drawings from colour slide were used to construct stratigraphic sections. Twelve sections were cut at Arnisdale across a 174m profile and three at Coire Shubh across a 34m profile.

A search was made for similar sediments throughout the area (using a hand-auger), but these were the only two exposures found. Elsewhere, only peat and river deposits were observed.

16.2 STRATIGRAPHIC AND GEOMORPHIC SETTING

The two sites are very similar: a thin blanket of sediment in the hollows of upper portions of glaciated valleys (Plate-32). Small lochs cover the lower portions of these hollows, leaving sediment exposed in the higher, peripheral, portions. The stratigraphy grossly comprises: gravel - sand - sandy peat - peat - soil and vegetation. The sediments are flat-lying, mostly less than 2 degrees. Exposures are less than 2m deep.

At the Arnisdale site the sediment overlies and onlaps a

'moraine' ridge (Fig.16-1). This ridge is composed of rounded boulders in a dirty sand matrix; it is topographically very fresh and marks the limit of rough, hummocky ground to the east (up valley) and smooth sediment surface to the west. The freshness of this feature, and its location — a high valley in the NW Highlands — suggests a Loch Lomond Readvance date (cf. Fig.7-1). Such a date is compatible with the overlying stratigraphy. At both sites, sandier sediment, at the base of the stratigraphy, grades up into recent peat beneath the vegetation of the current soil surface. At Arnisdale, a layer of pine stumps in the peat, helps establish the age of the sediment, correlating with a widespread demise of pine throughout Scotland roughly 4000 years BP (c.f. §7.4). Thus it is clear that the sediments at these sites represent a post- Loch Lomond Readvance, that is a Flandrian, sequence.

16.3 ARNISDALE

16.3.1 Litho stratigraphy

The locations of the fifteen logs cut at this site are shown in Fig.16-1. They are illustrated in Fig.16-2. A fairly consistent stratigraphy is apparent, seen best in log-5: basal gravel — greenish, massive sands — moderately-laminated, yellow sands — peat. The laminated sands tend to grade up into the peat, that is they become 'peatier' upwards, but the onset of peat is usually marked by a clean, yellow sand (LS), which can be correlated from logs 1 to 8. Wood fragments are abundant in logs 3 to 7, which is also the portion where the layer of pine stumps is seen (indicated only in log-4). The layer of pine stumps is usually 30-50cm above the onset-of-peat horizon, and typically has 1m of peat overlying it.

It can be seen from Fig.16-2 that the sediment occurs in three depressions. One (logs 1 and 2) north of the moraine ridge, a second (logs 3 to 8) between the moraine and a sand bar (seen in log 8A), and the third (logs 9 to 12) beyond the sand bar. The third depression continues downslope towards the present lake and is thus the main depression in the valley. It should also be noticed that the facies of peat changes along the profile: being dark brown to black

in the north (logs 1-7) and grading southwards into brown, sandy, vaguely-laminated, alluvial peats (logs 8-12). This is interpreted as reflecting an increasing energy of fluvial action, southwards; the dark (blanket-bog) peat collecting in higher, restricted depressions away from fluvial activity. The nature of the sands below the peat supports this interpretation: lenticular bedding and sand bars seen in the south and evenly laminated sands in the north.

16.3.2 Deformation stratigraphy

Deformation of the sediment is observed around the peat-sand boundary in each log. A top-of-deformation surface (T), within the peat is clear in most of the logs. It is marked by an abrupt cessation in deformation (e.g. logs 6 & 7, Plate-34) and by a slight colour change in the peat: paler below, due to the presence of mixed-in sand, with darker, purer peats above. The undeformed peat above appears conformable to its surface. The base of the deformation (B) is not so clear, usually being a gradual disappearance of signs of deformation downwards through the sand.

The structures observed within the deformed horizon include:
* pillow-loading of sandy layers (logs 5,11&12)
* flaming, loading and contortion of the sand/peat boundary (log 6)
* ruck-folding of the sand horizon (LS) (logs 1 to 5)
* upward injection of sand into peat (log 7, Plate-34)
* fissuring of sand layers (log 9).

The deformed horizon is mostly around 0.5m thick, and never more than 0.7m. Each of the three depressions has a separate deformation lens; the central depression (logs 3 to 8) tending to divide into 3 further lenses. The only log not showing deformation (log 8A) is where the peat/sand boundary is highest - above the sand bar separating the second and third depressions. Deformation is more severe to the north of the sand bar than to the south of it.

16.3.3 Interpretation of sediment deformation

Summarizing what is clear from the field evidence:

a) Deformation occurred during the early stages of peat

accumulation.

b) The deformation horizon is separated into three discrete lenses located in three syn-sedimentary depressions.

c) The top of deformation is a palaeosurface which was followed by conformable peat accumulation; nowhere is this surface inclined at greater than 1 degree.

d) Structures observed include a variety of soft-sediment deformation structures implying, at least partial liquefaction.

e) There is no reason to believe that more than one event produced the deformation: the top surface of deformation is clearly correlated across the section at one horizon and no other deformation-tops are seen.

Accepting that the deformation is the result of liquefaction, some resolution of the cause of deformation is possible:

a) There is no evidence for a load imposed on the surface at the time of the deformation.

b) There is no reason to believe that the mechanics of 'peat resting on sand' caused deformation at the peat/sand boundary, since sand is both injected up into peat (log 7) and loaded down into peat (logs 11 & 12).

c) There is no evidence for removal of a water load at the time of deformation. The depressions must have been saturated, and may have contained small pools of water, but no substantial lake can have existed above these sediments at the time of deformation since:

  * peats are accumulating,
  * sands below indicate a predominantly fluvial environment.

d) There is no storm deposit at the top of deformation.

It is therefore argued that, in the absence of credible alternatives, earthquake ground-shaking is the most likely cause of deformation at the site, being compatible with all the features observed:

a) The deformation horizon contains structures similar to those produced by earthquake-induced-liquefaction elsewhere (cf.

206

§6.1) - notably pillow and injection structures.

b) The horizon is widely correlated throughout the site, at a single horizon, and in different sediment facies.

c) The deformation occurred in depressions containing, probably, saturated sediment.

d) The site is close to an identified earthquake source - the Kinloch Hourn Fault (see Chapter 12).

16.4 COIRE SHUBH

16.4.1 Litho stratigraphy

At this site much less can be seen of the overall stratigraphy and much has to be inferred. The base of the peat, or of alluvial peat is not seen, and much of the lower parts of the basin is covered by thick (greater than 1m) blanket-bog peat. At the portion logged, a stream cutting in higher ground reveals alluvial, sandy peats, showing lamination and deformation structures. It is illustrated in Fig.16-3 and in Plate-31.

The uppermost bed is a clean, moderately-laminated, yellow sand, immediately underlying the present-day grass turf. Beneath this lies vaguely-laminated, sandy peat showing some fluvial features - lenticular bedding, troughs and rises. The sand in log 3 is probably a small channel deposit. The top of the peat in log 2 comprises what approaches a dark blanket-bog peat with only faint layering; the rest of the peats are sandy and more clearly layered.

Interpretation of this deposit in terms of regional stratigraphy is difficult. It is clearly post-glacial (i.e. Flandrian) in composition and by comparison with the Arnisdale stratigraphy. All that is evident at the site is a recent period of sand deposition following a period of mostly alluvial peat accumulation.

16.4.2 Deformation stratigraphy

A deformation horizon is observed within the alluvial peats. Only the top of the deformation (T) is seen. It comprises a fairly distinct surface, often having a slightly reddish colour and a higher abundance of small wood fragments (c.2-3mm in diameter). Larger wood

207

fragments are also abundant at or below it. In logs 1 and 2 it marks an abrupt cessation of deformation with undeformed peats above. It is fairly flat-lying, inclined at 1.6 degrees or less.

The deformation structures observed include:

* pillowing of sand layers (base of log-2, Plate-31)
* flaming, loading and contortion of the peat/sandy-peat boundary in log-2 (Plate-31)
* ruck-folding of sandy layers (logs 1,2&3)
* sinuous, vertical 'fluidization'(?) structures within peat (log-3).

It seems clear that the deformation belongs to one event, occurring within a similar horizon within the three logs. It might be suspected that the sand pillow at the base of log-2 represents a separate event, apparently having a separate truncation surface above it, and being below a fairly intact black, peat layer. However, comparison with the deformed sand lens of log-3, suggests that the pillow in log-2 is a similar channel-sand-lens which has 'balled up' to a greater degree, creating an apparent (not continuous) truncation surface above it.

16.4.3 Interpretation of sediment deformation

Summarizing the field evidence:

a) Deformation occurred during the accumulation of alluvial peat, and a little after the onset of purer peat (at log-2).
b) The top of deformation is a flat-lying palaeosurface.
c) Structures observed imply soft-sediment deformation under, at least partially, liquefied conditions.
d) The deformation is reasonably attributed to one event.

Most of the arguments developed in interpreting the Arnisdale sediment deformation apply here, since the stratigraphy and stratigraphic position of the deformation are similar. Some major differences in the stratigrpahy of the two sites are apparent: sediment at Coire Shubh has an absence of basal sands and has laminated sand as its most recent member. However, a correlation is

also clear: comparison of log-2 at Coire Shubh with log-6 at Arnisdale shows the deformation top at a very similar horizon - soon after the onset of peat and at a concentration of large woody fragments. The differences in composition at the two sites, must therefore represent different environments - the sands of Arnisdale being synchronous with sandy, alluvial peat at Coire Shubh. Thus on the basis of gross stratigraphy and deformation stratigraphy the deformation horizon at the two sites is correlated.

Deformation by earthquake-induced-liquefaction, as with the Arnisdale site, is argued along similar grounds.

16.5 DATE OF THE DEFORMATION EVENT

Dating, by radio-carbon analysis, has been done for a sample of sediment taken from the mixed peat/sand layer immediately beneath the top of deformation (at log-7, Arnisdale) (see Appendix 7). The date achieved is 3490 ± 50 radiocarbon years. **Fig.16-4** illustrates the position of the dated sample in relation to various stratigraphic horizons which can be regionally correlated. The date achieved confirms a Flandrian age for the sediment, but appears too young in relation to dates suggested by regional correlation of the 'onset of blanket-bog peat' and the 'demise of pine' as argued by Pennington et al. (1972) and Birks (1977). It is unwise to place too much emphasis on these regional dates for a site outwith their study, especially when regional variations were noted in their studies. The onset of blanket-bog peat is later in the NW Highlands than in Central and Southern Scotland (Birks 1977) and younger 'demise of pine' horizons are known (Pennington et al., 1972). However, the dates shown in Fig.16-4 are in accordance with dates suggested for the NW Highlands and seem reasonable, such that one is brought to suspect that the radio-carbon date is too young. It lies only one metre below the present-day surface such that it could have been contaminated by younger carbon. This discordance cannot be resolved without further dating the site. With the present information one can be confident of a date between the onset of peat (c.6000) and the radiocarbon date (3500).

16.6 INTERPRETATION OF KINLOCH HOURN SEDIMENT - SYNTHESIS

Single deformation horizons are observed at the two sites at similar stratigraphic positions. They are observed throughout the sections at both sites (174m at Arnisdale and 34m at Coire Shubh). Deformation by earthquake-induced-liquefaction is the only reasonable explanation for the observed deformation stratigraphy. Credence is added to this interpretation by the sites' proximity to the Kinloch Hourn Fault and their correlation across 7.5km. The date of the deformation event by radiocarbon dating is 3490+50 years, although this value appears too young in comparison with regional correlations. The event certainly occurred after the c.6000 years BP onset of blanket-bog peat.

PART IV

HYPOTHESIS

17. The Tectonics of Glacial Rebound
18. Glacio-lacustrine Liquefaction
19. Earthquake Magnitude Estimates
20. Seismotectonic Implications

This portion of the thesis assimilates the review of previous science (Part II) and the science propagated in this thesis (Part III) to produce a set of hypotheses. In order to emphasize this change in thought-mode - the construction of ideas - I will use the personal pronoun. [You may counter my review and science with information or data beyond which I have presented or you may incorporate it into your own science and hypothesis; however, you must counter or accept my hypothesis with argument - and argument is personal.]

In chapter 17 I present some thoughts on post-glacial tectonics, in general, and in chapter 20 this is extended into consideration of seismotectonics during the post-glacial stage in Scotland. Chapter 18 presents my assessment of the proposed palaeoseismic deposits in their particular context of the glacio-lacustrine environment and chapter 19 attempts some judgement on the size of the implicated earthquake events. These are then also assimilated into chapter 20 which is essentially a synthesized statement on the results of this research.

```
*********************************
```
CHAPTER SEVENTEEN

The Tectonics of Glacial Rebound
```
*********************************
```

17.1 THE CONCEPT

In chapter 4 a background to Scottish tectonics was presented. An increasingly stable post-Mesozoic tectonism was evidenced and gentle uplift was suspected as continuing to the present (§4.4.9). However, both the resolution of this on-going tectonism and the discernment of the level of associated seismic energy release (§5.4) was found to be impaired by the effects of glacio-isostatic crustal movement (Ch.8). Thus an understanding of glacio-isostatic seismotectonics is a prerequisite to an understanding of present-day seismotectonics in Scotland.

In this chapter I present a database on what is known about post-glacial uplift in Scotland and then propose a simple model with which to discern the regional strain that might be expected to result from the removal of an ice load. I will then interpret the field evidence I have presented in the light of this and present conclusions on the contribution which glacial-recovery tectonics plays in seismotectonic activity.

17.2 A DATABASE ON POST-GLACIAL UPLIFT IN SCOTLAND

17.2.1 Presentation of the database

In chapter 7 the evidence for several post-glacial, abandoned shorelines was reviewed. It was found that, despite some uncertainty, five shorelines of known age could be regionally correlated. These are:

a) The Main Lateglacial shoreline; $10,500 \pm 200$ years BP.

b) The Main Buried shoreline; $9,600 \pm 100$ years BP.

c) The Main Postglacial shoreline; c.6,500 years BP.

d) The 3rd Postglacial shoreline; c.4000 years BP.

e) The 5th Postglacial shoreline; c.2500 years BP.

Table 17-1. DATA USED IN COMPILING MAPS OF ABANDONED SHORELINES IN SCOTLAND. (Figs.17-1 to 17-4)

AGE OF SHORELINE (years BP) (Date of cessation - from pollen or radio-carbon dating)	LOCAL NAME OF SHORELINE (Location)	REGIONAL IDENTITY OF SHORELINE ('*'- if correlation inferred)	SOURCE
10,500 to 10,300	Buried Gravel Layer (Forth Estury)	Main Lateglacial	SISSONS 1974b
Loch Lomond Advance Stadial (c. 10,500)	Main Rock Platform (MRP) (Firth of Lorne)	Main Lateglacial	GRAY 1974a
"	MRP (Argyll)	Main Lateglacial	GRAY 1978
"	MRP (Islay & Jura)	Main Lateglacial	DAWSON 1980
(N.B. Loch Lomond Advance ice margin constructed from - SISSONS 1974a & 1979)			
9,600 to 9,500	Main Buried Shoreline (Upper Forth valley)	Main Buried	SISSONS 1972
c.6,500 (cessation) 6,900-6,600 (culmination) (These dates represent a regional synthesis of all available information - SISSONS 1974, SISSONS & BROOKS 1971)	Main Postglacial (MPG) (Earn-Tay valley)	Main Postglacial	CULLINGFORD 1977
	MPG (Upper Forth valley)	Main Postglacial	SISSONS 1972, 1974a
	Descriptive (Aberlady bay)	Main Postglacial *	SMITH 1971
	Descriptive (Wigtown/Troon)	Main Postglacial *	JARDINE 1971
	MPG (Islay/Jura)	Main Postglacial	DAWSON 1982
	MPG (Firth of Lorne)	Main Postglacial	GRAY 1974b
	Descriptive (Skye)	Main Postglacial *	PEACOCK 1983
c.4000 (interpolated)	PS3 (Firth of Lorne)	3rd Postglacial *	GRAY 1974b
"	PG3 (Firth of Forth)	3rd Postglacial *	SISSONS 1974a
(2505±100 at Aberlady)	Descriptive (Aberlady Bay)	5th Postglacial *	SMITH 1971
c.2500 (interpolated)	PS5 (Firth of Lorne)	5th Postglacial *	GRAY 1974b
"	PG4 (Firth of Forth)	5th Postglacial *	SISSONS 1974a

213

In Figs.17-1 to 17-4 I have shown all the available data on the present elevation of these shorelines, and have constructed contours of equal elevation for each (i.e. shoreline isobases). The sources of data used in the construction of these maps is shown in Table.17-1. Figs.17-5 to 17-7 show maps of rates of uplift inferred from these shoreline levels. I have assembled relevant curves for 'eustatic' sea-level (Fig.17-8A and Table.17-2) in order to discern a 'true' rate of uplift. It should be noted that pure eustatic sea level is almost impossible to discern (§8.3.3) and that what is presented here is 'to the best of our knowledge'. Then I have considered the rates of uplift at two selected sites in greater detail, graphs of which are shown in Figs.17-8B and 17-9A&B.

Table 17-2 SOURCE INFORMATION FOR SEA-LEVEL CURVES

'Eustatic' curves (Fig.17-8A):

Curve	Database	Source
1	U.K. with 0.73m regional subsidence correction	Flemming 1982
2	U.K. without 0.73m subsidence correction	Flemming 1982
3	Worldwide average continental shelf data	Shephard 1963
4	South Scandinavian data	Morner 1976

Relative sea level curves - Scotland (Fig.17-8B):

Curve	Description
A	Extrapolated contour values (from Figs.17-1 to 17-5) for Loch Gilphead.
B	The curve from Peacock et al. (1977) for Loch Gilphead (errors indicated).
C	Data from Jardine (1975) for the Solway / East Kirkcudbrightshire area: bars - Wigtown Bay circles - E. Kirkcudbright (errors in age indicated).
D	Curve 'C' adjusted by Jardine (1975) to give 'mean sea level' (as opposed to the high water beach level measured in the field).
E	Extrapolated contour values (from Figs.17-1 to 17-5) for E. Kirkcudbright.

17.2.2 Discussion of shoreline-isobase maps
Figs.17-1 to 17-4

Each map shows contours for the height of the shoreline above present sea level (Ordnance Datum - O.D.). The figure in brackets on each contour is an adjusted value allowing for sea level at the time of shoreline formation (the value for sea level is taken from Flemming's (1982) curve '2' - Fig.17-8A). On each map the data used in constructing the shoreline isobases are shown by either,

a) single values, or

b) lines with end-point values, representing a survey of shoreline elevations (in each case the line is a regression line calculated by the author concerned - Table.17-1).

Note, that in two cases (Fig.17-1 and 17-2) these regression lines are interrupted by dislocations. These dislocations are:

Fig.17-1 Offsets of 0.9 and 0.2m in the level of the Main Rock Platform in the Firth of Lorne, measured by Gray (1974a).

Fig.17-2 Offsets of 1.0 and 1.5m in the level of the Main Buried shoreline of the Upper Forth valley, measured by Sissons (1972).

In each of these cases the isobase-contours have been drawn with the offsets restored (e.g. in Fig.17-2 the '9m' contour goes through the '11.5m' value for the Main Buried shoreline, allowing for 2.5m of offset).

Where possible I have drawn the contours to conform to a regular ellipse, similar to the isobase-maps drawn by previous workers (e.g. Gray 1978, Jardine 1982). However, with two of the maps the data forced a distortion of the ellipses. Specifically, the Main Postglacial and 3rd Postglacial shorelines display distension of the ellipses over Mull. This distension is not apparent in the earlier or later shorelines. Three possible explanations for this distortion of the contours come to mind:

1) They are artefacts of mis-correlation of shoreline levels between different regions.

215

2) They are artefacts of the mis-match of different regression analyses.

3) They are real and result from a variation in crustal uplift.

With regard to 'explanation-1' - I maintain an element of doubt on the correlation of the 3rd and 5th Postglacial shorelines because several, indistinct shoreline levels of a similar age and altitude are difficult to correlate. However, correlation of the Main Postglacial shoreline is much clearer and is supported by others (e.g. Gray 1974b, Dawson 1982, Jardine 1982), and it is with this shoreline that the distortion is most apparent. Therefore I discount this explanation.

With regard to 'explanation-2' - Regression analysis may result in biased averages, especially at the end of a regression line, but again with the Main Postglacial shoreline the evidence counts against this as the cause of distortion. Measurements on Jura (Dawson 1982) do not occur above 11m and measurements on Mull (Gray 1974b) do not occur below 11m when considerable overlap would be expected with the construction of regular isobase ellipses (Fig.17-3).

Thus, with the Main Postglacial shoreline, at least, I consider the distortion to be real (i.e. explanation-3). Following on from this - if the distortion is real, its location, intriguingly, suggests enhanced strain in the region of the Great Glen fault. That is, since the time of formation of the Main Postglacial shoreline, the region to the NW of the Great Glen fault, around Mull, has experienced anomalous additional uplift (this conclusion is taken as supposition-1).

A second major observation regarding these isobase maps is the south-eastward migration of the centre of uplift. The centre-point of the isobase contours drifts from 'A' (at the time of the Main Lateglacial shoreline) to 'D' (5th Postglacial) - a distance of 70km (Fig.17-4). Although some of this drift might be due to error in contouring (e.g. the difference between 'C' and 'D'), the general sense of migration is unavoidably consequential on the given shoreline data. Thus the centre of uplift has migrated about 70km

216

south-eastwards in the interval between 10,500 and 2500 years BP
(suppostion-2).

17.2.3 Discussion of maps of uplift rate
Figs.17-5 to 17-7.

I have manually subtracted the isobase contours of successive
shorelines to produce maps of equal uplift during each intervening
stage. [I have not constructed a map for the 10,500 to 9,600 years BP
interval because of lack of eustatic sea-level data and poor
information on the Main Buried shoreline (no data in the west).] Each
contour shows the total amount of uplift occurring between the
shoreline levels assuming a correction for sea level according to
Flemming's (1982) curve '2' (Fig.17-8A). The figure in brackets on
each contour is the rate of uplift in metres per millennium (or
mm/yr).

The map for 9600 to 6500 years BP (Fig.17-5) shows contours
increasing inwards. This is anomalous and is the result of steeper
gradients in the Main postglacial shoreline (contrary to what one
would expect). The gradient of uplift contours is reversed if the
displacements of the Main Buried Shoreline are not restored (as
indicated by the small italic numerals on the contours in Fig.17-5).
Without more data on other shoreline levels of this age little more
can be said and this anomaly remains difficult to explain.

The maps for 6500-4000 and 4000-2500 years BP (Figs.17-6&7) have
contours derived from much more complete shoreline isobases, and
display several features of note:

a) The distortion of contour ellipses over Mull (as with
   supposition-1, above).
b) A south-eastward migration of the centre of contours (as with
   supposition-2, above).
c) Undulation of uplift-rate profile in the SE of Scotland.

Of these, the first two have been discussed already (§17.2.2),
however point 'c' warrants further discussion. This undulation
results from the south-eastward migration of the contours. Note that,

217

not only is the centre of uplift migrating to the south-east, but also the contours are decaying outwards (i.e. the radial gradient decreases with time). This has the consequence that the area in front of the migrating centre (the SE) experiences highly variable uplift rates. It is then of note that the faulting of the Main Buried shoreline reported by Sissons (1972) occurs precisely in this area. Thus it seems that anomalous uplift rates in the east-central area of Scotland may have given rise to anomalous strains resulting in fault displacement (**supposition-3**).

17.2.4 <u>Discussion of uplift-rate graphs for two sites -</u> <u>Lochgilphead and Kirkcudbright</u>

These two sites were chosen because they were the location of detailed studies of relative sea level by other workers - Lochgilphead (Peacock et al. 1977) and Kirkcudbright (Jardine 1975). Note that Lochgilphead is fairly close to the centre of uplift and Kirkcudbright somewhat away from it (Fig.17-4). At each site relative sea-level curves derived from field data have been added to selected eustatic sea-level curves to provide graphs of uplift rate.

Eustatic curves (Fig.17-8A): Curves '1' and '2' are the result of Flemming's (1982) 'multiple regression analysis of eustatic sea level change in the United Kingdom in the past 9000 years'. Curve '1' was adjusted by Flemming to allow for 0.73m/millennium of regional subsidence, whereas curve '2' is his unadjusted curve. The correction for regional subsidence was identified by adjusting the isobases derived from the regression analysis to fit a known point of zero uplift in the SE of England. Since this adjustment does not seem valid for the north of the U.K., where if anything tectonic uplift is suspected, I have used Flemming's unadjusted curves in my calculations. Curve '3' is an example of a curve derived from a worldwide database and is given for comparison only. Curve '4' is Mörner's (1976) curve derived from Scandinavian data - its evident detail depicts many minor fluctuations which may well have occurred in the U.K. but which are not evident in Flemming's regression.

Relative sea-level curves - Lochgilphead and Kirkcudbright
(Fig.17-8B). Some features of these are of particular interest:

a) At Lochgilphead a rapid fall in relative sea level is apparent
   just before 12,000 years BP. This fall then levelled off, rising
   slightly to a peak at 6-7000 years BP before falling to its
   present level. This progression is commonly observed in Scottish
   shoreline data and is interpreted as being due to initial, rapid
   isostatic-rebound followed by a major transgression, culminating
   in the Flandrian transgression at c.6000 years BP (Jardine 1982,
   among others).

b) In the south-west of Scotland, Jardine's (1975) work allows a
   comparison of his uplift curves with those derived in my study.
   My curve 'E' (from a regional analysis) is a little higher at
   older ages than Jardine's (site-specific) curve 'C' ,but in
   general there is good agreement. Curve 'D' was adjusted by
   Jardine to represent mean sea level (his adjustment was derived
   from present-day tide data). This correction has not been
   applied in my study, and must be borne in mind as a source of
   systematic error since the shoreline levels represent high
   water levels.

Uplift-rate curves (Fig.17-9): In the Kirkcudbright area the
addition of Jardine's curve 'D' to Flemming's curve '2' provides a
credible uplift-rate curve - meeting the present time at present
sea-level and implying a present uplift rate close to that implicated
in Flemming's study (i.e. c.2.5m/millennium). However, the curves
derived for Lochgilphead all appear to meet the present time at
several.metres above present sea level. This could, in part, result
from the high-water/mean sea level correction; however, the present
tidal range at Lochgilphead is low (c.2m, Admiralty 1941). Therefore
one is driven to conclude either that a sudden change in uplift rate
occurred c.2000 years ago or that an additional component of uplift
has been operating. Rapid changes in uplift rate by means of local
faulting (<2000 years ago) seems unlikely -there is no known evidence
for such faulting. However, an uplift of about 1m per millennium
would make sense of the data (as indicated by curve 'T', Fig.17-9B).

219

Thus, I feel there is some basis for supposing that the west of Scotland is subject to a component of long-term uplift in addition to the post-glacial rebound (**suppostion-4**). This may be of tectonic origin or may represent a long-period glacio-isostatic component.

Table.17-3 DATA FOR MODELLING THE DEFORMATION OF A SPHERICAL SEGMENT

	Input parameters				Parameters derived from geometrical model						Membrane stresses (bars)	
	d(km)	P(km)	h(km)	O(deg.)	r'(km)	Δr(km)	Δl(m)	A(km²)	ΔA(m²)	ΔA/A(×10⁻⁹)	maximum	minimum
A.	0.01	160	0.5	0.72	6531	171	0.22	19981	2.72	0.136	1.83	0.92
	0.01	225	1.0	1.01	6393	33	0.12	39961	1.06	0.027	0.70	0.35
	0.01	319	2.0	1.44	6393	33	0.34	79922	2.16	0.027	1.40	0.70
	0.01	504	5.0	2.27	6365	5	0.23	199805	0.92	0.005	0.53	0.26
	0.01	1008	20.0	4.55	6364	4	1.19	799221	2.36	0.003	1.70	0.85
	0.015	160	0.5	0.72	6598	238	0.30	19981	3.74	0.187	2.55	1.28
	0.015	225	1.0	1.01	6425	65	0.24	39961	2.10	0.053	1.38	0.69
	0.015	319	2.0	1.44	6409	49	0.51	79922	3.20	0.040	2.08	1.04
	0.015	504	5.0	2.27	6372	12	0.50	199805	1.97	0.010	1.27	0.64
	0.015	1008	20.0	4.55	6365	5	1.72	799221	3.40	0.004	2.13	1.07
	0.03	160	0.5	0.72	6809	449	0.54	19981	6.70	0.336	4.80	2.40
	0.03	225	1.0	1.01	6524	164	0.58	39961	5.18	0.130	3.50	1.75
	0.03	319	2.0	1.44	6458	98	1.01	79922	6.30	0.079	4.17	2.09
	0.03	504	5.0	2.27	6391	31	1.29	199805	5.10	0.026	3.29	1.65
	0.03	1008	20.0	4.55	6370	10	3.30	799221	6.54	0.008	4.25	2.13
	0.05	160	0.5	0.72	7111	751	0.84	19981	10.53	0.527	8.03	4.02
	0.05	225	1.0	1.01	6661	301	1.04	39961	9.21	0.230	6.37	3.19
	0.05	319	2.0	1.44	6524	164	1.66	79922	10.39	0.130	6.98	3.49
	0.05	504	5.0	2.27	6417	57	2.35	199805	9.25	0.046	6.05	3.03
	0.05	1008	20.0	4.55	6376	16	5.41	799221	10.70	0.013	6.81	3.41
B.	0.20	225	1.0	1.01	7911	1551	4.15	39961	36.55	0.915	32.81	16.41
	0.20	319	2.0	1.44	7068	708	6.36	79922	39.50	0.494	30.11	15.06
	0.20	504	5.0	2.27	6617	257	10.07	199805	39.60	0.198	27.29	13.65
	0.20	713	10.0	3.21	6489	129	14.76	399611	40.95	0.102	27.43	13.72
	0.20	1008	20.0	4.55	6424	64	21.18	799221	41.54	0.052	27.23	13.62
C.	0.83	504	5.0	2.27	7616	1256	39.97	199805	150.28	0.762	133.39	66.70
	0.83	713	10.0	3.21	6934	574	59.45	399611	159.72	0.400	122.06	61.03
	0.83	1008	20.0	4.55	6635	275	86.09	799221	163.35	0.204	117.00	58.50

Reference radius for all calculations = 6360km (i.e. at latitude 56 degrees). The geometry is illustrated in Fig.17-11; stress calculations are after Turcotte (1974).

17.3 A MODEL FOR POST-GLACIAL CRUSTAL STRAIN

Given a portion of the crust undergoing rapid post-glacial rebound, we may ask – 'What are the resulting strains and stresses that crust is subjected to?' A general consideration of the seismotectonic implications of glacial rebound was given in chapter 8 (§8.3.2). Here, I present a specific model of the lateral strains and stesses associated with the known vertical strain of rebound. This model will then be considered in the context of other work on post-glacial crustal stress and strain.

17.3.1 The model

I have modelled the surface of a portion of the crust undergoing glacial loading and rebound as a segment of a sphere subject to changes in curvature. A solution to this geometrical problem is given in Fig.17-10 (the proof was developed with the help of Mr.I.Stewart, Dept. of Mathematics, Heriot-Watt University). According to this geometry the change in length of an arc subject to a change in curvature can be found, since:

$$\theta' = 2.\sin^{-1}(P/2r') \quad \text{and,} \quad r' = \left[P^2 + \left(\frac{4(h-d)^2 - P^2}{8(h-d)} \right)^2 \right]^{\frac{1}{2}}$$

where, θ' is the angle subtended by the deformed arc

    P is the common cord length of the deformed arc and the reference arc

    r' is the radius of curvature of the deformed arc

    h is the width of the reference arc

    d is the displacement of the centre of the deformed arc from the reference arc.

The change in surface area (ΔA) of a spherical segment of equivalent dimensions – as illustrated in Fig.17-11 – can then be found since:

the area of a sphere cut by parallel planes, h apart $= 2\pi r h$

(We utilize the condition where one of the planes is a tangent to the

sphere.)

Thus the geometry of the rebound of the crustal surface relative to a reference sphere can be modelled. The model assumes the following:

a) The shape of the crustal surface at different stages of deformation is a spherical segment.

b) A reference sphere, corresponding to the present crustal surface, with a radius of 6360km (i.e. the radius of the earth a a latitude of 56 degrees).

c) Zero strain at the perimeter of the spherical segment.

17.3.2 Discussion of modelling results

Table 17-3 shows the parameters derived for this model from input data appropriate to Scottish and Fennoscandian rebound. Three data-sets are considered:

A) Data considered appropriate for Scottish post-Loch-Lomond-Readvance rebound.

B) Data considered appropriate for the total post-Devensian uplift in the U.K.

C) Data from Morner's (1981) study of post-glacial uplift in Fennoscandia - **Fig.17-12A.**

The most poorly defined input parameter is the size of the spherical segment (defined by P). It is difficult to decide on the geographical limits of rebound deformation. Thus for each input value 'd' (maximum vertical displacement), a range of values for P are considered.

It is clear that the linear strains (Δl) are small - of the order of 1m for dataset-A, 10m for dataset-B and up to 80m for dataset-C. Area strains (ΔA) are correspondingly small. These strains are considered insignificant in terms of crustal tectonics (metres of strain over 100's of km - i.e strains of 10^{-5}). One should not, therefore, expect any faulting to result directly from lateral rebound-strain (**supposition-5**).

What is significant, however, is the stress developed by this deformation. Turcotte (1974) has considered stresses due to bending of the earth's crust when modelled as a thin spherical shell - 'membrane tectonics'. **Fig.17-12B** shows his modelled stresses in the continent of Africa as a result of its drift northwards towards the equator (involving an increase in radius of curvature). It is significant that the changes in curvature associated with glacial loading are of the order, or greater than, *those associated with changes in latitude*. Turcotte showed that the greatest (tangential) stress occurs at the edge of the spherical segment and is given by:

$$\sigma_{max} = \frac{E \cdot \Delta r \; \theta^2}{4r}$$

and that the minimum stress occurs at the centre and is given by:

$$\sigma_{min} = \frac{E \cdot \Delta r \; \theta^2}{8r}$$

where, E=Young's modulus (taken as 1.72×10^{12} dynes/cm^2 (Turcotte 1974)).

This assumes no loading at the edge of the thin shell (see Turcotte (1974) for a full account of assumptions). Note that the stress is a function of the change in curvature (Δr) and the size of the shell (θ). The last two columns in Table 17-3 show stresses, thus calculated, for the glacial rebound model data. Since in these cases θ is small the stress is heavily dependent on 'Δr'. Stresses of 1-100 bar are implicated. Note that these figures ought to be regarded as rule-of-thumb(!) since they do not constitute systematic analysis of stress in the whole spherical segment - they indicate a probable range of stress in terms of the model.

With the decrease in radius of curvature operative during glacial rebound the inner portions of the spherical segment will be under tension and the peripheral areas will be subject to compression. It is thus inferred that near the centres of glacial rebound lateral tensile stresses of the order of 1-100bar are developed (**supposition-6**). In the case of post-glacial Scotland these stresses are 1-4bar (Table 17-3, A).

It is worth briefly comparing this with other stresses relevant
to glacial loading tectonics:

1. **Hydrostatic ice-load:** 1-3km of ice = 0.9-2.7bar.

2. **Horizontal shear stresses** due to the basal shear of an ice
   mass: up to 1bar - calculated for the edge of the Greenland
   ice-cap (Robin 1981).

3. **Topographic stresses:** of the order of 1kbar for major
   mountain chains (Turcotte & Oxburgh 1976).

4. **Erosion and thermal stresses:** a few hundred bars for major
   erosion and uplift (Turcotte & Oxburgh 1976).

5. **Stress drops during earthquakes:** typically in the range of
   10-100bar for moderate to large events (Kanamori 1978).

Thus the stresses inferred from the modelling of post-glacial
rebound are considered significant. In the short-lived post-glacial
episode (10^4 years) one should consider these stresses alongside
other major tectonic stresses (topographic, plate-tectonic, thermal
etc.).

17.4 CONSIDERATION OF OBSERVED POST-GLACIAL FAULTING IN SCOTLAND

Fig.17-13 shows the occurrences of post-glacial faulting
discovered during this study, and also the displacement in the upper
Forth valley reported by Sissons (1972). I should emphasize that this
map of post-glacial faulting is derived from a geographically biased
sample - my field investigation was concentrated on the western
Highlands. Despite this several patterns are evident:

a) West coast faulting occurs close to the centre of post-glacial
   uplift - contour 'A' is for the 10m/millennium uplift rate for
   6500-4000 years BP (from Fig.17-6). It is particularly notable
   that the distortion of this contour over Mull (cf.
   supposition-1, §17.2.2) coincides with several occurrences of
   post-glacial faulting (3,4&5 Fig.17-13).

b) The post- 9600-year-BP faulting in the upper Forth reported by
   Sissons's (1972) occurs in the area of anomalous, variable
   uplift rates - contour 'B', Fig.17-13 (as noted above
   supposition-3, §17.2.3).

224

c) The faults involved in post-glacial dislocation are mostly of northerly trend, an exception being the WNW Kinloch Hourn fault. Note that they do not display any radial or concentric pattern corresponding to the uplift contours.

d) Where discernible these faults mostly display sinistral strike-slip movement, the exceptions being:

    1) The most recent dextral movement on the Glen Roy fault (2) otherwise displaying sinistral movement.

    2) Offsets measured in shoreline levels (3,4&6) do not allow the resolution of lateral movement. However, the nature of these vertical offsets on Mull and Shuna (Figs.10-17&18) does not appear consistent with simple normal or reverse faulting; rather the evident multiple-block tilting is, quite conceivably, the result of significant amounts of lateral fault movement.

It is worth noting the consistency of these observations with some of the inferences made in the review chapters. In chapter 8 it was argued that 'seismotectonic activity is strongly weighted towards higher activity spatially and temporally close to the ice load' (§8.4.2). The field evidence in Scotland supports this. Secondly, in chapter 4 knowledge of the state of stress in the British crust was reviewed (§4.5.4). The database was shown to be poor, but a NW-NNW direction of maximum principal horizontal compressive stress was suspected. The orientation of post-glacial faults in Scotland, which show a mostly northerly trend, appears broadly consistent with this. I hesitate to suggest that the dominant northerly trend of these faults indicates a more northerly maximum stress direction in northern Britain. (One must await the results of the first reliable stress measurement in this area!)

17.5 WHAT CONTRIBUTION - GLACIAL-REBOUND TECTONICS?

In view of the suppositions presented in this chapter and the evidence presented in the thesis I wish to suggest the following:

1) Post-glacial rebound stress conditions have played a major role in permitting post-glacial faulting in western central Scotland.

2) These fault displacements nevertheless represent release of regional, tectonic, crustal stress - specifically, sinistral movement on north to north-westerly faults.

3) This is achieved by the tension associated with post-glacial rebound causing reduction in the normal stress across faults, thus allowing the release of pre-existing, tectonic stress.

****
CHAPTER EIGHTEEN
Glacio-lacustrine Liquefaction
****

18.1 THE CONCEPT

In this chapter I will attempt to assess the likelihood of earthquake-induced liquefaction in glacio-lacustrine deposits and contrast this to the likelihood of other means by which liquefaction in such deposits might be generated. The review chapter on palaeoseismic deposits included discussion of the different means of achieving liquefaction (§6.4). This is presumed upon, and discussion in this chapter will concentrate on the 'means capable of generating liquefaction over wide areas at a single stratigraphic horizon' (listed in §6.4.4). Having assessed the likelihood of earthquake-induced liquefaction in this type of deposit, I will then assess the palaeoseismic cases proposed in chapters 13-16. Finally, I will draw some conclusions on what can be said about the diagnosis of palaeoseismic deposits, in general, as a result of this thesis (on the special case of glacio-lacustrine palaeoseismites).

18.2 THE LIKELIHOOD OF EARTHQUAKE-INDUCED LIQUEFACTION IN GLACIO-LACUSTRINE DEPOSITS

Earthquake-induced liquefaction in glacio-lacustrine sediments is likely on two accounts:

1) Post-glacial rebound tectonics involves enhanced seismic activity.

2) Post-glacial sedimentary environments involve large amounts of the sediment-type especially prone to earthquake-induced liquefaction, that is, lacustrine sediments.

With regard to the first point, some circularity of argument is involved since deposits interpreted as palaeoseismites have in the first place been used to argue higher levels of ground shaking during post-glacial times (§5.3). However, the evidence from fault-movement alone provides strong, independent evidence that the post-glacial

stage involves enhanced seismotectonic activity (§5.2). Furthermore, a conceptual and theoretical justification for supposing that post-glacial seismotectonics are significant and additive to background seismotectonics has been outlined (§8.3.2 & Ch.17). Thus the very fact of higher levels of seismic activity during post-glacial times makes earthquake-induced liquefaction during that time more likely. This aspect is likely to be especially pronounced in areas, such as Scotland, which exhibit an otherwise low level of seismicity.

With regard to the second point, the susceptibility of fine-grained, clastic sediments (especially lacustrine) to earthquake-induced liquefaction was demonstrated in chapter 6. I have not specifically demonstrated the high abundance of such deposits in the post-glacial environment; however, this is explicit and testified to by many workers (e.g. Embleton & King 1975). The abundance of surface water and of artificially-ponded, onland basins (ice-dammed, moraine-dammed and regional crustal depressions) gives rise to a super-abundance of lakes during, and subsequent to, times of ice wastage. The high energy and erosion rates of the glacial environment also ensures a high clastic input into these lakes such that fine-grained, clastic lacustrine sediment is almost ubiquitous within this period.

Thus the deglaciation process not only heralds an enhanced seismotectonic stage but also presents an ideal recipient for earthquake-induced liquefaction. [Note that I have excluded glacio-lacustrine deposits of the advancing stages of a glaciation from this discussion, since this category does not include any of the deposits documented in this thesis and since such deposits (e.g. the remnants of englacial lakes) are often disrupted by glacial activity to render them useless for any palaeoseismic diagnosis.]

This high likelihood of earthquake-induced liquefaction now needs to be contrasted to the likelihood of other causes of liquefaction in the post-glacial environment. There is no doubt regarding the abundance and severity of glacially associated soft-sediment deformation - freeze-thaw convolutions, ice-push

deformations ice-collapse and drop-stone features, and the effects
of rapidly changing hydrostatic loads. However, only two such
processes appear capable of producing liquefaction over wide areas at
a single stratigraphic horizon. They are:

a) Unloading of sediment by falls in water level
b) thaw-generated pore-pressure increase at permafrost melting.

(cf. §6.4.4)

These two processes pose as alternatives to earthquakes as the
cause of liquefaction deformation in late-/post- glacial times. They
have been proposed as the cause of such deformations in Finland
(Vesajoki 1982) and the Netherlands (Vandenberghe & Van Den Broek
1982). Both are undoubtedly pertinent to the environment in question,
both are capable of generating liquefaction, and both are
conceptually able to produce this deformation over wide areas at a
single stratigraphic horizon (§6.4.1a&c). There are some differences
in the details of the deformation processes involved in each when
compared to earthquake-induced liquefaction (e.g. grain-size and
deformation stratigraphy). These were outlined in chapter 6 and are
important to any specific diagnosis of a deformation horizon.
However, here I wish to contrast these processes only in terms of the
likelihood and context of their occurrence during post-glacial
times.

Earthquakes would be expected to be to be frequent, although
irregular, thoughout a span of time during the 'post-glacial rebound
seismotectonic phase'. Consequently, earthquake-induced liquefaction
should be non-unique within a sediment column of this period - it
should occur from time to time during ongoing sedimentation. In
contrast, 'liquefaction by loss of hydrostatic load' would be
expected to change the sedimentary environment (ie. appear as a
stratigraphic as well as a deformation event) and occur only in
specially suited conditions (a body of water prone to large drops in
water level). Also in contrast, 'thaw-generated pore-pressures at
permafrost melting' would be expected to occur at a special stage in
postglacial sedimentary environments - the permafrost melting. Even
if an annual thaw is invoked, such annual deformations should occur

229

during a span of time preceeding the final permafrost melt. Thus these two processes should be stratigraphically constrained and environmentally unique.

Therefore, earthquake-induced liquefaction should be resolvable in terms of regional stratigraphy and abundance as well as the site-specific deformation stratigraphy. By this argument, I consider earthquake-induced liquefaction to be expected and resolvable in post-glacial lacustrine sediments.

18.3 PALAEOSEISMIC DIAGNOSIS AT THE FOUR STUDY SITES

Each of the four deformed-sediment deposits submitted as candidates for palaeoseismic diagnosis were given preliminary treatment as to the possible causes of deformation (in chapters 13-16). These preliminary diagnoses, derived from the constraints of the field evidence, are summarized below.

> **Glen Roy:** A concentrically-zoned pattern, in the deformation observed in the ice-dammed lake sediments, is thought to result from at least two earthquake events. An unzoned lake-drainage event is also evident. Alternative causes of deformation were all discounted on account of the nature of the zonation (§13.8).

> **Arrat's Mill:** A single deformed horizon in a lacustrine basin appears to be most consistent with an earthquake-induced origin. Liquefaction by 'loss of hydrostatic load' is a plausible alternative, although no positive evidence was found to support it (§14.5).

> **Meikleour:** Three possible causes for the deformation of a thick complex of soft-sediment deformation structures in laminated silts, at this site, appear possible. No positive evidence can be found to substantiate two of these - 'loss of hydrostatic load' and 'freeze-thaw pressure', whereas a number of features of the internal deformation fabric appear consistent with deformation by earthquake ground shaking. A single earthquake-induced liquefaction event can account for the whole

complex of deformation.

Kinloch Hourn: Soft-sediment deformation in post-glacial sands and peats, correlated between two sites 7.5km apart and each within 2km of a fault shown to be active, is interpreted as being due to earthquake ground shaking. No alternative means of deformation appear reasonable.

In each of these four cases earthquake ground shaking and resulting liquefaction appears to be consistent with the field evidence. In two of these cases (Arrat's Mill and Meikleour) alternative means of deformation could not be discounted. These alternative means were those proposed by other workers for similar deformations observed in glacial and post-glacial silts elsewhere (Vesajoki 1982 - Finland, Vandehberghe & Van Den Broek 1982 - Netherlands). Despite this ambiguity as to the cause of deformation at these two sites, no positive evidence can be found to substantiate the alternatives. Since an earthquake origin was shown to be generally likely in this type of sediment (§18.2), I consider an earthquake-induced origin for the deformation at these two sites to be more probable. In order to believe the alternative means of deformation the following positive criteria would need to be demonstrated:

Loss of hydrostatic load: A substantial basin and a facility for drainage must be at least conceivable at the site and a change in sedimentation should be evident immediately following the drainage event.

Freeze-thaw pressure: Other known freeze-thaw structures (such as ice-wedges) ought to be associated with the deformation and evidence for a regional thaw-event around the time of deformation should be demonstrated.

No such features have been observed at either site.

In the two other cases (Glen Roy and Kinloch Hourn) more regionally extensive study of the deformed deposits has allowed

231

confident assertion of an earthquake origin. The zonation and stratigraphy at Glen Roy and the regional correlation at Kinloch Hourn appear uniquely consistent with earthquake-induced liquefaction. At both sites capable faults have been identified as sources of seismic activity, and at both sites there is evidence for these sources being active at the time of sediment deformation. These two cases demonstrate many of the criteria necessary for confident palaeoseismic diagnosis. Additional evidence is found at Glen Roy, where a concentric zonation in the deformation is observed - which does not appear consistent with any other cause of deformation.

Recalling the discussion on the likelihood of earthquake-induced liquefaction in glacio-lacustrine sediments (§18.2) - Do the proposed Scottish palaeoseismites satisfy the supposition that they should be non-unique within lacustrine sediments of the post-glacial sediment column? Yes. Assuming all the deposits are earthquake-induced and remembering the fragmentary nature of the onland, Quaternary record in Scotland (Ch.7), the following can be stated.

a) The deformed horizons come from deposits of a wide span of age - 15-13,000 for Arrat's Mill and Meikleour, c.10,000 for Glen Roy and c.3500 for Kinloch Hourn (years BP.).

b) The deformed horizons occur in a variety of sedimentary environments - ice-dammed lake deposits, pro-glacial outwash sands and post-glacial sand and peat deposits.

c) At two of the sites, more than one such horizon has been observed within an uninterrupted sedimentary sequence - Glen Roy and Arrat's Mill (where a second horizon was observed but not studied - §14.1).

Thus I consider the palaeoseismic diagnosis to be credible.

18.4 TOWARDS CONFIDENT PALAEOSEISMIC DIAGNOSIS

Throughout this thesis I have drawn attention to several elements which contribute to a palaeoseismic diagnosis. Attention was focused on palaeoseismites in glacio-lacustrine sediments, as this issue dominates the consideration of susceptible deposits in the

Scottish Quaternary. However, I wish to synthesize these observations into a general consideration of palaeoseismic diagnosis. Accordingly, I have ammended and amalgamated the seven criteria, proposed by Sims (1975), for diagnosing the occurrence of earthquakes in geologically young sediment (§6.1.2), to give five such criteria.

Five criteria for the diagnosis of a palaeoseismite:

a) The presence of potentially liquefiable sediments, i.e. fine sand and silt in a saturated condition (most commonly lacustrine sediment).

b) The presence of deformed structures similar to those which have been demonstrated as produced by earthquake ground shaking (in the field or simulated in the laboratory). These include:

  * ball-and-pillow style deformation

  * fault-grading stratigraphy (occurring on slopes)

  * injection and sand volcano structures.

c) The structures all relate to deformation at a single chrono-stratigraphic horizon which can be correlated over a large area within the sedimentary basin (in some cases a concentric zonation may be evident).

d) Other causes of liquefaction can be discounted in terms of the field evidence (e.g. loss of hydrostatic load, freeze-thaw events (in glacial areas), atmospheric and hydrological storm wave loading).

e) The deformed horizon is in the proximity of faults active at the time of deformation and capable of producing ground-shaking at the site at a level equivalent to intensity MM VI or greater.

Further work is needed in order to confidently apply these criteria. In particular,

1) Laboratory studies are needed to quantify the criteria 'a' and 'b'. Work already done in this respect has been reviewed in chapter 6. Further work is especially required in natural-scale simulation of earthquake-induced soft-sediment deformation structures.

2) Laboratory and case-study analysis of alternative means of producing liquefaction over wide areas (criteria 'd') is also

needed. Most of these alternatives have not been subjected to the depth of analysis that earthquake-induced liquefaction has.

3) A data-base on palaeoseismites needs to be assembled in association with seismotectonic studies so that judgements with regard to criteria 'c' and 'e' can be facilitated. Work is also needed in order to quantify the ground-shaking intensities necessary to produce the structure-types identified in observed zoned palaeoseismic deposits.

[Note that 'Recommendations for further research' are discussed more fully in chapter 22.]

****
CHAPTER NINETEEN
Earthquake Magnitude Estimates
****

Given the palaeoseismic evidence presented in this thesis - what
are the likely sizes of these pre-historic earthquakes? A number of
empirical formulae exist in the literature for relating earthquake
magnitude to fault-length, fault-displacement and surface deformation
effects. In each case the database involves a large amount of scatter
- any one parameter-value corresponds to a range of at least one
magnitude, e.g. **Fig.19-1A&B**. Regression-line relationships
derived from these data sets are instructive as rule-of-thumb but are
generally inappropriate for estimating earthquake magnitudes from
field data. Thus where possible I have selected relationships which
were specifically designed to estimate (unknown) magnitudes from
pre-instrumental field data (Table.19-1).

Bullen & Bolt's (1985) formula is derived from data assembled by
Bonilla (and other workers), but incorporates errors of regression in
the analysis to give a realistic estimate of the probable range in
magnitude. Ambraseys and Melville's (1982) relationship was
specifically devised for magnitude estimation from field data (fault
length and displacement) for Persian and European earthquakes. Such
a formula is not available for relating magnitude to displacement
alone so I have used Bonilla's (1970) relationship, of Fig.19-1A,
where the fault length is unknown. Kuribayashi & Tatsuoka's (1975)
plot of maximum distance to observed liquefaction against magnitude
(c.f. §6.1.1, Fig.6-2) was derived for estimating liquefaction
occurrence from a given magnitude. I have, nevertheless, used this to
estimate likely magnitudes appropriate to observed liquefaction
distribution in palaeoseismic deposits. Finally, I have used Keefer's
(1984a) plot of area affected by landslipping against magnitude (c.f.
§6.5.2, Fig.6-16) to give an indication of the magnitude at Glen
Roy.

Table 19-1. RELATIONSHIPS USED IN ESTIMATING MAGNITUDES OF PALAEOSEISMIC EVENTS

Author	Relationship	(units)	Database
Bonilla (1970)	$Log\ D = 0.57M_L - 3.39$	(feet)	Best fit for all types of fault (cf. Fig.19-1A).
Bullen & Bolt (1985)	$M_S = (6.10\pm0.25) + (0.70\pm0.13)\ Log\ L$	(km)	23 world, strike-slip ruptures (with errors of regression)
Ambraseys & Melville (1982)	$M_S = 1.1 + 0.4\ Log\ (L^{1.58}\ D^2)$	(cm)	Specifically designed to estimate magnitude from L and D.
Kuribayashi & Tatsuoka (1975)	$Log\ R = 0.87M_L - 4.5$	(km)	Regression line for 44 Japanese earthquake-liquefaction events.
Keefer (1984a)	Plot of area affected by landslides against magnitude		(see Fig.6-16.)

where: L = length of surface rupture
D = maximum relative displacement
R = distance to furthest liquefaction from earthquake epicentre.

236

Table 19-2. MAGNITUDE ESTIMATES FOR PALAEOSEISMIC EVENTS

Event	Location	Date (x10³ years BP)	Field data	Relationship used	Magnitude
A.	Glen Roy	10.3±0.3	7km fault length	Bullen & Bolt (1985)	6.7±0.4 ⎫
			0.5m displacement (dextral)	Ambraseys & Melville (1982)	6.2 ⎬ 6?
			15km to furthest liquefaction	Kuribayashi & Tatsuoka (1975)	6.3 ⎪
			80km² landslip area	Keefer (1984a)	5.0-6.2 ⎭
B.	Firth of Lorne	*after 10.3	Several vertical displacements of 1 to 3m	Bonilla (1970)	6.4-6.9
C.	Upper Forth (Sissons 1972)	9.6-6.5	Two vertical displacements of 1.0 and 1.5m	Bonilla (1970)	6.4-6.6
D.	Kinloch Hourn	¶13-10?	14km fault length	Bullen & Bolt (1985)	6.9±0.4
E.	Kinloch Hourn	3.5-2.4	Liquefaction observed 2km from fault	Kuribayashi & Tatsuoka (1975)	>5.5
F.	Lismore	§since 2?	0.5m displacement (sinistral) of morphological features	Bonilla (1970)	6.1
G.	Lismore	since 0.3?	0.2m displacement (sinistral) of crofter's wall	Bonilla (1970)	5.7

* - Faulting of the Main Rock Platform is considered to have occurred 'soon' after the formation of the shoreline.

¶ - The date of the rupture(s) which caused the prominent Kinloch Hourn Fault linear is unknown, but inferred as being soon after ice-retreat.

§ - The offset morphological features on Lismore are considered as 'recent' - the last one or two thousand years.

237

Thus, this selection of empirical relationships (Table.19-1) has been chosen as appropriate for the estimation of palaeoseismic magnitudes. [Note that magnitude is in many ways an inappropriate parameter for palaeosiesmic studies - a surface intensity value would be more reasonable - however, since a well-defined alternative parameter is not available and since 'magnitude' is widely understood, this scale is used. Since large errors are involved in these estimates ($\pm$ half a magnitude) qualification of the different magnitude scales (M_S, M_L) is pedantic, although the listed formulae do specify the scale.]

Table.19-2 shows a complete list of palaeoseismic field data for Scotland along with magnitude estimates and the relationships used [Sissons' (1972) measurements of displacements of the Main Buried shoreline in the Upper Forth have been included]. For the Glen Roy event several estimates are possible since the field data are more complete. These agree closely, allowing a confident estimate of a magnitude 6¼ event. Note however, that the landslip estimate is based on an area of landslips which were attributed to two events at Glen Roy (§13.7 & §13.8.4). Both these events would have been in the range indicated, they cannot otherwise be resolved. The estimates for other events are all from disparate data (most commonly fault displacement only) and less confidence can be placed in them.

In Fig.19-2 these estimates are plotted against time, incorporating an assumed arror of $\pm$ half a magnitude and a range in event-age inferred from the available information. This graph represents a plot of large palaeseismic events in Scotland and constitutes a summary of the results of this research. Greatest confidence can be placed in events 'A' and 'E' where dates are well-constrained by stratigraphy and radio-carbon dating and where both faulting and ground-shaking effects can be assigned to the same event. In general it can be inferred that in early post-glacial times (13-6,000 years BP) several events of magnitude 6 to 7 occurred and that in more recent times (4000 years BP to the present) several events of magnitude 5 to 6 have occurred.

****
CHAPTER TWENTY
Seismotectonic Implications
****

The study of this thesis comprises the essential elements of seismotectonic mapping. However, a coherent seismotectonic analysis is not possible at this stage since the data produced are geographically limited. Nevertheless several implications can be drawn.

20.1 MAXIMUM EARTHQUAKE SIZE AND RECURRENCE

In this thesis I have demonstrated the occurrence of earthquakes larger than any previously reported in the U.K.. Some of these, less well substantiated, indicate magnitudes as high as M=7. Well substantiated field evidence has demonstrated a magnitude $6\frac{1}{4}$ event at Glen Roy, 10,300 years ago, and a 5.5-6.0 event 3500 years ago at Kinloch Hourn. Establishing the probable recurrence of such events is difficult on two accounts:

a) Some of the larger events were probably triggered by anomalous, post-glacial rebound stress, and would not be expected to occur under present stress conditions.

b) The evidence is geographically and temporally fragmentary.

However, accepting these shortcomings, I would like to suggest the following with regard to the recurrence of large events in Scotland.

a) Magnitude 7 events are unlikely to recur, but could conceivably occur today under favourable stress conditions. Conservative hazard assessments should therefore consider a magnitude 7 event to have a 1 in 10,000 year probability of recurrence in Scotland.

b) Magnitude 6 events are infrequent but likely and should be considered to have a 1 in 2-3000 year probability of recurrence.

239

These suggestions appear consistent with other observations on earthquake recurrence in the U.K., although they tend to push the large magnitude threshold a little higher.

1) Western Europe instrumental seismicity up to $M_L=6.0$ (Ahorner 1975).

2) U.K. instrumental seismicity up to $M_L=5.4$ (Turbitt et al. 1985).

3) U.K. historical seismicity up to $M_L=5.5$ (Ambraseys & Jackson 1985).

Thus geological study has complemented the historical and instrumental record to indicate an upper magnitude threshold of greater than $M_L=6.0$. This threshold does not appear to have been reached during the historical record (c.700 years in England and c.300 years in Scotland).

20.2 SEISMOTECTONIC ZONATION

In the absence of more regional study, only one conclusion with regard to zonation seems reasonable. Since most of the evidence in this thesis pertains to western-central Scotland, and since this is the area of maximum post-glacial uplift, this area should be considered as a seismotectonic zone having seismicity levels as outlined above (§20.1). In regional studies western-central Scotland should, therefore, be considered as a source area with this seismicity level. For convenience this seismotectonic zone can be delimited by the central (maximum) contour of present crustal uplift derived by Flemming (1982). The zone, so defined, contains all the palaeoseismic events outlined in chapter 19 and also the bulk of Scottish instrumental seismicity greater than $M_L=2$ (c.f. Figs.5-5 to 5-7). This seismotectonic zone is illustrated in Fig.20-1 where approximate seismicity recurrence levels are indicated. Note that a seismotectonic zone so defined falls within the rheological province (NW of the Highland Boundary Fault) proposed in chapter 4 (§4.2.4), comprising metamorphic rock and behaving elastically to great depths within the crust.

20.3 SEISMIC HAZARD

I hope that the results of this thesis will be of use to members of the engineering community involved in seismic hazard design in Scotland and onland and offshore U.K.. No information on ground acceleration and intensity levels has been given but the evidence outlined should give some basis for a 'scaling-up' of design accelerations for hazardous engineering facilities, especially where probabilities of less than 10^{-3} are of concern.

In addition to these implications for seismic vibration design, I would like to draw attention to two areas of seismic hazard which have been previously underestimated or ignored, but which are evident in these geological studies.

1) Surface displacements of up to 0.1m **can** occur in the U.K. and ought to be considered in hazardous engineering which involves foundation in rock, especially in the western-central Scotland seismotectonic zone proposed in the previous section.

2) The risk of liquefaction has been demonstrated (c.f. Kinloch Hourn deposits, c.3500 years ago). Liquefaction can be expected in susceptible deposits (silts) at higher U.K. seismicity levels (>M=5, >0.1g acceleration – Kuribayashi & Tatsuoka 1975). Such deposits are known to occur in coastal and offshore U.K. waters.

Although many U.K. seismic design engineers are aware of these hazards, I hope that these geological studies have **realized** the risk to design perception. They are demonstrable hazards.

****
CHAPTER TWENTY-ONE
Conclusions
****

21.1 SIGNIFICANCE OF THIS STUDY

This thesis documents the results of a search for seismotectonic information in Scotland – an area having a low level of instrumental seismicity and one where previous evidence for recent earth movements was extremely sparce. The results have been rewarding and the success of the study demonstrates the validity of such studies in areas of low seismicity. This should give confidence to the commencement of similar studies elsewhere and also to the extension of the work in Scotland, leading eventually to the construction of a regional seismotectonic scheme.

The work has been mostly based on field study, the rewards of which can largely be attributed to three facets of approach:

a) **A multi-disciplinary approach.** This is most obviously illustrated by the parallel study of fault activity with the study of the effects of surface ground-shaking in unconsolidated sediment. It is also evident in the variety of techniques involved. These included the study of:

* remotely-sensed imagery
* micro-earthquake locations
* historical catalogues of earthquakes
* stratigraphy
* geomorphology
* geodetic information (levelling survey)
* deformation fabric in sediments
* particle-size and geochemical analysis.

b) **A geological approach.** Careful consideration of the stratigraphic and environmental context of suspected palaeoseismites has allowed useful seismotectonic information to be retrieved where it otherwise might not have been (best illustrated by the study at Glen Roy). The value of a

242

'geological' approach is also illustrated by the informative
comparison of the Quaternary field-studies to more ancient
geological examples. In particular the study of faulting on
Lismore helped place recent movement in a longer-term tectonic
context, and the study of liquefaction horizons in late-glacial
sediments was improved by comparison to similar horizons in the
Devonian.

c) **A global approach.** Comparison with observations from
seismically-active areas has been a key element in this study.
The more obvious effects of seismic activity in active areas
can be observed in a low-seismicity area like Scotland if
they are diligently searched for. In particular the resolution
of palaeoseismic horizons in Scottish sediments relied heavily
on an understanding of earthquake-induced-liquefaction derived
from more active areas.

It is hoped that the success of this broad-based approach to
field study will set a precedent for similar studies elsewhere. The
most significant findings of the study are listed below.

21.2 SUMMARY OF FIELD-DATA

1. Lismore: Two post-glacial fault movements of 0.2m and
c.0.5m (sinistrally) were inferred within ancient fracture zones. The
movements were inferred by matching morphological and lithological
features across the fractures. The fractures trend roughly
north-eastwards. The precise dates of movement are unknown; at least
one of the movements could have occurred during historical times.
Much evidence for ancient faulting on Lismore was also found,
involving measured displacements of c.100m of sinistral offset of
Caledonain dykes and c.5m mostly sinistral offset of
Permo-Carboniferous dykes; all on north to north-easterly fractures.

2. Firth of Lorne: Intensive levelling survey at two
localities on the 'Main Rock Platform' raised shoreline has indicated
several vertical offsets of up to 2.7m. Associated surface fractures
have been identified. The shoreline has a Loch Lomond Readvance age
(c.10,300 years BP).

3. Glen Roy: A large body of field data has been assembled
relating to at least two earthquake events which occurred during the
retreating stages of the Loch Lomond Readvance at Glen Roy. The most
significant event is recorded by soft-sediment deformation observed
in ice-dammed lake sediment. The deformation displays a concentric
zonation around a 7km-long surface fracture. Half a metre of dextral
movement along this north to NNE-trending fracture is inferred from
the matching of morphological and lithological features across it.
The offset and surface rupture are considered to be associated with
the same earthquake event which caused the soft-sediment deformation.
An event of magnitude $6\frac{1}{4}$ is estimated from the field data.

4. Kinloch Hourn: A prominent surface fracture, 14km long
and trending WNW, displays multiple evidence for late- and
post-glacial movements:
* drainage paths are offset across the fault by c.160m sinistrally
  (the drainage is thought to post-date the Devensian ice),
* soft-sediment deformation in post-glacial sediment, close to the
  fault, indicates an earthquake ground-shaking event in the area
  which occurred c.3500 years BP.
* fracture-infilling material within the fault indicate shearing
  and unquantified fault-movement to have occurred since 2400
  years BP.
* the fault occurs in an area which is presently seismically
  active (instrumental events upto M=4).

5. Arrat's Mill and Meikleour: At these two sites
soft-sediment deformation in late-glacial outwash sands and silts is
interpreted as the result of earthquake-induced liquefaction. The
deposits display extremely well preserved deformation structures
which allow much to be inferred about the deformation processes
involved. Alternative means of deformation could not be completely
discounted, but in each case the field relations and deformation
stratigraphy appeared most consistent with an earthquake origin.
Ground-shaking levels are unspecified; no related faults have been
identified.

21.3 <u>SUMMARY OF THE MAIN CONCLUSIONS DRAWN IN THE THESIS</u>

1. Post-glacial tectonics: Post-glacial rebound stress is considered to have played a significant role in triggering large earthquakes and fault ruptures in the millennia immediately following deglaciation. Nevertheless, the observed fault displacements appear to represent the release of regional tectonic stress. This is manifested mainly in sinistral movement on north to north-easterly faults.

2. Glacio-lacustrine liquefaction: Although some ambiguity remains regarding the cause of deformation in the post-glacial sediment sequences which have been interpreted as palaeoseismites, in each case earthquake-induced liquefaction appears to be most consistent with the field evidence. When the context of their occurrence is considered, in relation to tectonics and the susceptibility of the sediment to liquefaction, the earthquake-induced hypothesis finds added credibility.

3. Palaeoseismic diagnosis: Rigorous diagnosis of pre-historic earthquakes is possible with intensive field-study. This is best illustrated at Glen Roy where disparate pieces of field evidence have been assembled into a detailed portrait of the effects of a fairly shallow, magnitude 6½ earthquake event, having surface fault rupture.

4. Seismotectonics: A seismotectonic zone in the west of Scotland has been proposed in which probable levels of earthquake recurrence have been suggested on the basis of field evidence:
   * Magnitude-7: 1 in 10,000 years,
   * Magnitude-6: 1 in 2-3,000 years.
Surface fault displacements of up to 0.1m, on fractures favourably orientated with respect to the present-day stress field, should be considered as a seismotectonic hazard within this zone.

****

CHAPTER TWENTY-TWO

Recommendations for Further Research

****

22.1 GENERAL RECOMMENDATIONS

The need for elucidation of the following general areas of research became evident during this study:

a) Modelling of glacial-rebound stress in relation to other stresses in the Upper Crust.

b) Analysis of fault gouge material with respect to its significance in discovering fault activity, especially of ancient, reactiviated faults.

c) The use of (other than radio-carbon) dating techniques in palaeoseismic studies.

d) Associated study of means, other than earthquakes, of producing liquefaction-type soft-sediment deformation, so as to allow confident diagnosis of palaeoseismites.

In addition to these, two specific avenues of research appear ripe for development as a direct result of the study, as follows.

22.2 ESTABLISHING CONFIDENT PALAEOSEISMIC DIAGNOSIS

Evidence for soft-sediment deformation resulting from earthquake ground shaking should be sought and established in seismically active areas of varying sedimentological environment. In this way palaeoseismic studies could be established as a reliable method of evaluating earthquake recurrence.

Secondly, the zonation observed at Glen Roy, although in an unusual environment (ice-dammed lake deposits), ought to be quantified, preferably in association with other zoned palaeoseismites (as yet undiscovered). In their study of Japanese liquefaction, Kuribayashi & Tatsuoka (1975) noted that liquefaction phenomena were observed at JMA (Japanese Meteorological Agency) intensities of greater than 5 - equivalent to maximum ground accelerations of 80-250gals. That is to say, that liquefaction

246

phenomena occur at maximum accelerations of more than 0.1-0.2g. At any one site numerous factors affect the onset of liquefaction; however, in terms of zoned liquefaction deformation, it should be possible to assign acceleration levels to the different zones. To illustrate this a preliminary assessment of likely accelerations appropriate to the Glen Roy zoned deformation is helpful.

Ground accelerations at Glen Roy:

Attenuation relationships appropriate to the near-field are difficult to establish; however, Joyner & Boore (in Bullen & Bolt 1985) have designed the following relationship to be valid for the near-field (and seemingly appropriate for the Glen Roy situation).

Maximum horizontal acceleration 'y' is given by

$$\text{Log } y = -1.02 + 0.249M - 0.5\text{Log}(R^2 + 7.3^2) - 0.00255\sqrt{R^2 + 7.3^2}$$

where 'y' is in fractions of 'g' and 5.0<M<7.7.

Taking M=6.25 and R=15,6&2km (i.e. approximate radii of the Glen Roy palaeo-intensity contours), the following (horizontal) accelerations are obtained:

R=15	y=0.23
R= 6	y=0.35
R= 2	y=0.44

Which is to say that, at Glen Roy, liquefaction (zone C) occurred at accelerations greater than about 0.2g, that zone B style deformation occurred at accelerations greater than about 0.3g, and that ball-and-pillow and fault-grading style deformation (zone A) occurred at accelerations greater than about 0.4g. These estimates make no account for vertical accelerations, which in this 'near-field' situation are likely to be large. Nevertheless, these figures appear consistent with the observations of Kuribayashi & Tatsuoka (1975), above.

Such, 'guesses' need to be replaced by detailed deterministic study, which should include:

a) The establishment of a database on case studies of zoned palaeoseismic deposits, including those associated with known events.

b) Simulation of the deformation structures by shaker-table studies on natural-scale models.

c) Theoretical consideration of soft-sediment deformation under realistic conditions of earthquake ground-shaking.

22.3 THE SEISMOTECTONICS OF SCOTLAND AND OFFSHORE

This study has made a start in exposing seismotectonic evidence in Scotland and has demonstrated the validity of such study in an area of low seismicity. The work needs to be extended both geographically and in depth of analysis before any regional seismotectonic analysis is possible. In particular,

a) The seismicity/lineament associations suggested in this study need to be studied in detail - the role of post-glacial-rebound 'mega-joints' in current seismicity release might be established.

b) Other active faults and palaeoseismic deposits need to be sought and studied in order to increase the database, onland. Promising areas include:

* Faulting in the NW of Scotland, including the Loch Maree fault.

* Faulting in the Inner Hebrides, including Kerrera and Mull.

* Palaeoseismic deposits in other late-glacial and post-glacial deposits, especially in Inverness-shire and coastal areas of eastern Scotland.

c) Studies on offshore Quaternary faulting, especially in the area around the Hebrides and the the North Sea grabens.

d) Research on historical accounts of Scottish seismicity.

KEY WORD INDEX

[A list of key references of terms defined or explained in the text.]

LIST OF REFERENCES

ADAMS, J. (1980), Contemporary uplift and erosion of the Southern Alps, New Zealand. Geol. Soc. Am. Bull., part 2, v.91, 1-114.

ADAMS, J. (1982), Deformed lake sediments record prehistoric earthquakes during the deglaciation of the Canadian Shield. EOS, 63(18), P.436.

ADMIRALTY (1941), Admiralty Manual of Tides, by A.T. Doodson and H.D. Warburg. Hydrographic department, Admiralty, HMSO, London.

AGASSIZ, L. (1840), On the evidence of the former existence of glaciers in Scotland, Ireland and England, Proc. Geol. Soc. Lond., 3, 327-332.

AHORNER, L. (1975), Present-day stress field and seismotectonic block movements along major fault zones in central Europe. Tectonophysics 29, 233-249.

ALLEN, J.R.L. (1982), Sedimentary Structures Vol. II: Their charater and physical basis. Elseiver. - (Chapters 8 & 9 on liquidization and soft sediment deformation structures.)

AMBRASEYS, N.N. (1983), Evaluation of seismic risk, in " Seismicity and Seismic Risk in the Offshore North Sea area" (Eds) A.R. Ritsema and A. Gurpinar, NATO Series C, 365-376.

AMBRASEYS, N.N. & JACKSON, J.A. (1985), Long-term seismicity in Britain. In "Earthquake Engineering in Britain", Thomas Telford Ltd., London.

AMBRASEYS, N.N. & MELVILLE, C.P. (1982), A History of Persian Earthquakes. Cambridge University Press, 219p.

ANDERTON, R. (1985), Sedimentation and tectonics in the Scottish Dalradian. Scott. J. Geol., 21(4), 407-436.

ANDERTON, R., BRIDGES, P.H., LEEDER, M.R. & SELLWOOD, B.W. (1979), A Dynamic Stratigraphy of the British Isles. Allen and Unwin, London.

ANDREWS, J.T. (1970), Present and postglacial rates of uplift for glaciated northern and eastern North America derived from postglacial uplift curves, Can. J. Earth Sci., 7, 703-715.

ANDREWS, J.T. & DUGDALE, R.E. (1970), Age appreciation of glacio-isostatic strandlines based on their gradients. Bull. Geol. Soc. Am., 81, 3769-71.

ANKETELL, J.M., CEGLA, J & DZULYNSKI, S. (1970), On deformational structures in sysmems with reversed density gradients. Rosz. Polsk. Tow. Geol., 40(1), 3-30.

ARMSTRONG, M., PATERSON, I.B. & BROWNE, M.A.E. (1985), Geology of the Perth and Dundee district. BGS Memoir.

ASSUMPCAO, M. (1981), The NW Scotland earthquake swarm of 1974. Geophys. J. R. astr. Soc., 67, 577-586.

AUDEN, J.B. (1954), Drainage and fracture patterns in north-west Scotland. Geol. Mag., 91(5), 327-51.

BAILEY, E.B. et al. (1924), Tertiary and post-Tertiary geology of Mull, Loch Aline and Oban. Memoir of the Geological Survey, Scotland.

BAMFORD, D. (1979), Seismic constraints on the deep geology of the Caledonides of northern Britain. in, "The Caledonides of the British Isles - reviewed", eds, A.L. Harris, C.H. Holland, & B.E. Leake, Scottish Academic.

BARTON, P., MATTHEWS, D., HALL, J. & WARNER, M. (1984), Moho beneath the North Sea compared on wide angle seismic records. Nature, 308, 55-56.

BASHAM, P.W., FORSYTH, D.A. & WETMILLER, R.J. (1977), The seismicity of northern Canada. Can. J. Earth Sciences 14, 1646-1667.

BATH, M. (1978), Energy and tectonics of Fennoscandian earthquakes. Tectonophysics 50, T9-T17.

BAUMANN H. (1981), Regional stress field and rifting in Western Europe. Tectonophysics 73, 105-111.

BEN-MENAHEM, A. (1976), Dating of historical earthquakes by mud profiles of lake-bottom sediments. Nature 262, July 15, 200-202.

BEVAN T.G. & HANCOCK P.L. (1986), A late Cenozoic regional mesofracture system in southern England and northern France. J. Geol. Soc. Lond., 143, 355-362.

BINNS, P.E., McQUILLIN, R., FANNIN, N.G.T., KENOLTY, N. & ARDUS, D.A. (1975), Structure and stratigraphy of sedimentary basins in the sea of the Hebrides and the Minches. in "Petroleum and the Continental Shelf of NW Europe", ed, A.W. Woodland, Applied Science Publishers Ltd.

BIRKS, H.J.B. (1977), The Flandrian forest history of Scotland: a preliminary synthesis. in "British Quaternary Studies: recent advances" ed. F.W. Shotton, Clarendon press, Oxford.

BONILLA, M.G. (1970), Surface faulting and related effects. in "Earthquake Engineering", ed R.L. Weigel, Prentice-Hall, U.S.A., ch 3, pp. 47-74.

BONILLA, M.G. & BUCHANAN, J.M. (1970), Interim report on worldwide historic surface faulting. U.S.G.S. Open file report, Dec. 1970, Washington D.C.

BOOTH, E.D. & ROBERTS, C.J.B. (1985), Response to extreme earthquakes of an offshore gravity platform in the North Sea. in "Earthquake Engineering in Britain", Thomas Telford, London.

BOSTROM, R.C. (1984), Crustal extension under ice loads. Modern Geology, 8, 249-59.

BOTT, M.H.P. (1982). The Interior of the Earth: its structure, constitution and evolution. 2nd edition. Edward Arnold.

BOULTON, G.S., JONES, A.S., CLAYTON, K.M. & KENNING, M.J. (1977), A British ice sheet model and patterns of glacial erosion and deposition in Britain. in "British Quaternary Studies: Recent Advances", ed. F.W. Shotton, Clarendon press, Oxford.

BOULTON, G.S., CHROSTON, P.N. & JARVIS, J. (1981), A marine seismic study of late Quaternary sedimentation and inferred glacier fluctuations along western Inverness-shire, Scotland. Boreas, 10, 39-51.

BRENNEN, C. (1974), Isostatic recovery and the strain rate dependant viscosity of the earth's mantle. J. Geophys. Res., 79(26), 3993-4001.

BREWER, J.A., MATTHEWS, D.H., WARNER, M.R., HALL, J., & SMYTHE, D.K. (1983), BIRPS deep seismic reflection studies of the British Caledonides. Nature, 305, 206-210.

BROTCHIE, J. F. & SILVESTER, R. (1969), On crustal flexure. J. Geophys. Res., 74, 5240-5252.

BROWN, P.E. (1983), "Caledonian and earlier magmatism", in Geology of Scotland, Ed. G.Y. Craig, Scottish Academic Press, Edinburgh.

BULLEN, K.E. & BOLT, B.A. (1985), An Introduction to the Theory of Seismology. 4th Edn., Cambridge Univ. Press.

BURTON, P. & NEILSON, G. (1980), Annual catelogue of British earthquakes recorded on LOWNET (1967-1978). Inst. Geol. Sci. Seismologial Bull. No.7.

CACCHIONE, D.A. & DRAKE D.E. (1982), Measurements of storm-generated bottom stresses on the continental shelf. J. Geoph. Res., 87, C3, 1952-1960.

CAMERON, I.B. & STEPHENSON, D. (1985), "The Midland Valley of Scotland (3rd Edn)", British Regional Geology, HMSO 1985.

CAPUTO, M. (1977), A mechanical model for the statistics of earthquakes, magnitude, moment and fault distribution. Bull. Seism. Soc. Am. 67, 849-861.

CASAGRANDE, A. (1970), On liquefaction phenomena: report of a lecture. Geotechnique, 21(3), 197-202.

CASTRO, G. (1975), Liquefaction and cyclic mobility of saturated sands. J. Geotech. Eng. Div. ASCE, 101(GT6), 551-569.

CAVANAUGH, M.A. (1985), Scientific creationism and rationality. Nature v.315, 185-189.

CHAMBERLIN, T.C. (1879), The method of multiple working hypothesis. Journal of Geology, 5, 837-848.

CHESTER, J.A. & LAWSON, D. (1983), The geology of the Moray Firth. Rep. Inst. Geol. Sci., 83/5.

CHESTER, J.A., SMYTHE, D.K. & BISHOP, P. (1983), The geology of the Minches, Inner Sound and Sound of Raasay. Rep. Inst. Geol. Sci., 83/6.

CHINNERY, M.A, & NORTH, R.G. (1975), Frequency of very large earthquakes. Science 190, 1197-1198.

CISNE, J.L. (1986), Earthquakes recorded stratigraphically on carbonate platforms. Nature 323, 320-322.

CLARK, J.A. (1980), A numerical model of worldwide sea level changes on a viscoelastic earth, in Earth Rheology, Isostasy and Eustasy, ed. Morner 1980.

CLARK, R.A. & STUART, G.W. (1981), Upper mantle structure of the British Isles from Rayleigh-wave dispersion. Geoph. J. R. astr. Soc., 67,59-75.

CLARK, J.A., FARELL, W.E. & PELTIER W.R. (1978), Global changes of postglacial sea level: a numerical calculation, Quat. Res., 9, 265-287.

CRAIG, R.F. (1983), "Soil Mechanics", 3rd Edn., Van Nostrand Reinhold, U.K..

CRITTENDEN, M.D.Jr. (1967), Viscosity and finite strength of the mantle as determined from water and ice loads, Geoph. J. R. astr. Soc.,14,261-279.

CULLINGFORD, R.A. (1977), Lateglacial raised shorelines and deglaciation in the Earn-Tay area. in "Studies in the Scottish Lateglacial Environment", ed. J.M. Gray & J.J. Lowe, Pergamon.

CULLINGFORD, R.A. & SMITH, D.E. (1980), Late Devensian raised shorelines in Angus and Kincardineshire, Scotland. Boreas, 9, 21-38.

DAVENPORT, C.A. (1983), North Sea seismotectonics and the role of geology in offshore seismic risk assessment. in "Seismicity and Seismic Risk in the Offshore North Sea Area", eds. A.R. Ritsema and A. Gurpinar, D.Reidel, Dordrecht.

DAVENPORT, C.A. & RINGROSE, P.S. (1985), Fault activity and palaeoseismicity during Quaternary time in Scotland - preliminary studies, in "Earthquake Engineering in Britain", Thomas Telford Ltd. London.

DAVENPORT, C.A. & RINGROSE P.S. (1987), Deformation of Scottish Quaternary sediment sequences by strong earthquake motions, Special publ. of the J. Geol. Soc. Lond. - 'Deformation of sediments and sedimentary rocks' (in press).

DAVENPORT, C.A. & RINGROSE P.S. (1987b), Earthquake hazard assessment in central Scotland, unpublished report to Detla Pi Associates.

DAVIES, H.C., DOBSON, M.R. & WHITTINGTON, R.J. (1984), A revised seismic stratigraphy for Quaternary deposits on the inner continental shelf west of Scotland between 55[30'N and 57[30'N. Boreas 13, 49-66.

DAVIS, R.O. & BERRILL, J.B. (1982), Energy dissipation and seismic liquefaction in sands. Earthquake Eng. Struct. Dynamics, 10, 59-68.

DAVIS, R.O. & BERRILL, J.B. (1983), Comparison of liquefaction theory with field observations. Geotechnique, 33, 455-460.

DAVISON, C. (1924), "A History of British Earthquakes", Cambridge Univ. Press.

DAWSON, A.G. (1980), Shore erosion by frost: An example from the Scottish Lateglacial. in "Studies in the Lateglacial of North-west Europe", eds. J.J. Lowe, J.M. Gray & J.E. Robinson, Pergamon.

DAWSON, A.G. (1982), Lateglacial sea-level changes and ice-limits is Islay, Jura and Scarba, Scottish Inner Hebrides. Scott. J. Geol. 18(4), 253-265.

DEER, W.A., HOWIE, R.A. & ZUSSMAN, J. (1977), "An Introduction to the Rock-forming Minerals. Longman, London.

DIKMEN, S.U. & GHABOUSSI, J. (1984), Effective stress analysis of seismic response and liquefaction: theory. J. Geotech. Eng., 110(5), 628-644.

DOIG, R. (1986), A method for determining the frequency of large magnitude earthquakes using lake sediments. Can. J. Earth Sci., 23, 930-937.

DOLLAR, A.J.T. (1947), The Inverness-shire earthquake of December 25th, 1946. Nature 1947, May 10th, 648-9.

DOLLAR, A.T.J. (1950), Catelogue of Scottish Earthquakes, 1916-1949. Trans. Geol. Soc. Glasgow 21, 283-361.

EHLERS, J. & GRUBE, F. (1983), Meltwater deposits in north-west Germany, in "Glacial Deposits in NW Europe", Ed. J. Ehlers, A.A. Balkema / Rotterdam.

EMBLETON, C. & KING, C.A.M. (Eds) (1975), "Glacial Geomorphology", Edward Arnold.

EMELEUS, C.H. (1983), Tertiary Igneous Activity, in "Geology of Scotland", ed, G.Y. Craig, Scottish Academic, Edinburgh.

EVANS, D., CHESTER, J.A., DEEGAN, C.E. & FANNIN N.G.T. (1982), The offshore geology of Scotland in relation to the I.G.S. shallow drilling programme, 1970-1978. Rep. Inst. Geol. Sci., 81/12.

FAN, P-F. (1978), Clays and clay minerals of hydrothermal origin in Hawaii. in, Developments in Sedimentology, V27, eds. M.M. Mortland and V.C. Farmer, Elsevier. (Proc. VI International Clay conference 1978).

FARRELL, W.E. & CLARK, J.A. (1976), On postglacial sea level. Geophys. J. R. astr. Soc., 46, 647-667.

FIELD, M.E., GARDNER, J.V. JENNINGS, A.E. & EDWARDS, B.D. (1982), Earthquake-induced sediment failures on a 0.25[slope, Klamath River delta, California. Geology, 10, 542-546.

FINN, W.D. L., BRANSBY, P.L. & PICKERING, J. (1970), Effect of strain history on liquefaction of sand. J. Soil Mech. Found. ASCE, 96(SM6), 1917-1933.

FINN, W.D.L., YOUNG, R.N. & LEE K.W. (1978), Liquefaction of thawed layers in frozen soils. J. Geotech. Eng. Div. ASCE, 104(GT10), 1243-1255.

FLEMMING, N. C. (1982), Multiple regression analysis of earth movements and eustatic sea-level change in the United Kingdom in the past 9000 years, Proc. Geol. Assoc., 93(1), 113-125.

FLINN, D. (1973), The topography of the sea floor around Orkney and Shetland and the northern North Sea. J. Geol. Soc. Lond., 129, 39-59.

FORTI, P. & POSTPISCHL, D. (1984), Seismotectonic and palaeoseimic analysis using karst sediments. Marine Geol., 55, 145-161.

FRENCH, H.M. (1976), The Periglacial Environment, Longman, London.

GARSON, M.S. & PLANT, J. (1972), Possible dextral movements on the Great Glen and Minch Faults in Scotland. Nature, 240, 31-35.

GEORGE, T.N. (1966), Geomorphic evolution in Hebridean Scotland. Scott. J. Geol., 2(1), 1-34.

GEORGE, T.N. (1974), Prologue to a geomorphology of Britain. In "Progress in Geomorphology: papers in honour of D.L. Linton", eds. E.H. Brown and R.S. Waters, British Geomorphological Research Group.

GHABOUSSI, J. & DIKMEN, S.U. (1984), Effective stress analysis of seismic response and liquefaction: case studies. J. Geotech. Eng., 110(5), 645-658.

GILL, W.D. & KUENEN, P.H. (1957), Sand volcanoes on slumps in the Carboniferous of County Clare, Ireland. Q. J. geol. Soc. Lond., 113, 441-460.

GRAY, J.M. (1974a), The main rock platform of the Firth of Lorn, western Scotland. Trans. Inst. Br. Geogr., 61, 81-98.

GRAY, J.M. (1974b), Lateglacial and postglacial shorelines in western Scotland. Boreas, 3, 129-138.

GRAY, J.M. (1978), Low-level shore platforms in the south-west Scottish Highlands: altitude, age and correlation. Trans. Inst. Br. Geogr., 3, 151-164.

GRAY, M. (1983), Update - The Quaternary Ice Age. Dept. Geography, Queen Mary College, University of London, Special publ. 5.

HALL, A.M. (1985), Cenozoic weathering covers in Buchan, Scotland and their significance. Nature, 315, 392-295.

HALL, D.H. & DAGLEY, P. (1970), Regional magnetic anomalies: An analysis of the smoothed Aeromagnetic map of Great Britain and Northern Ireland. Rep. Inst. Geol. Sci. 70/10.

HALL, J. & RASHID, B.M. (1977), A possible submerged wave-cut platform in the Firth of Lorne. Scott. J. Geol., 13(4), 285-288.

HARRIS, A.L. (1983), The Growth and Structure of Scotland. In "Geology of Scotland", ed. G.Y. Craig, Scottish Academic, Edinburgh.

HASKELL, N.A. (1937), The viscosity of the aesthenosphere. Amer. J. Sci., 33, 22-28.

HASZELDINE, R.S. (1984), Carboniferous North Atlantic palaeogeography: stratigraphic evidence for rifting, not megashear or subduction. Geol. Mag. 121(5), 443-63.

HEMPTON, M.R. & DEWEY, J.F. (1983), Earthquake-induced deformational structures in young lacustrine sediments, East Anatolian Fault, southeast Turkey. Tectonophysics, 98, T7-14.

HICKMAN, A.H. (1975), The stratigraphy of late Precambrian metasediments between Glen Roy and Lismore. Scott. J. Geol., 11(2), 117-142.

HICKS S.D. & SHOFNOS W. (1965). The determination of land emergence from sea level observations in southeast Alaska, J. Geophys. Res., 70, 3315-3319.

HILLAIRE-MARCEL, C. (1980). Multiple component postglacial emergence, Eastern Hudson Bay, Canada. in, Earth Rheology, Isostasy and Eustasy, ed. Morner, 1980.

HIPKIN, R.G. & HUSSAIN, A. (1983), Regional gravity anomalies: 1 Northern Britain. Rep. Inst. Geol. Sci., 82/10.

HOLGATE, N. (1969), Palaeozoic and Tertiary transcurrent movements on the Great Glen Fault. Scott. J. Geol., 5, 97-139.

HUSEBYE, E.S., BUNGUM, H., FYEN, J. & GJOYSTDAL H. (1978), Earthquake activity in Fennoscandia between 1947 and 1975 and intraplate tectonics. Norsk. Geol. Tids. 58, 51-68.

HUTTON, James (1788), "Theory of the Earth", Vol.1, Trans. Roy. Soc. Edin.

ILLIES J.H., BAUMANN H. & HOFFERS B. (1981), Stress patterns and strain release in the Alpine foreland. Tectonophysics 71, 157-172.

ISHIHARA, K. & TOWHATA, I. (1982), Dynamic response analysis of level ground based on the effective stress method. In "Soil Mechanics - Transient and Cyclic Loads" eds. G.N. Pande & O.C. Zienkiewicz, John Wiley, Chichester.

JAMIESON, T.F. (1863), On the Parallel Roads of Glen Roy, and their place in the history of the glacial period. Q. J. Geol. Soc. Lond., 29, 235.

JARDINE, W.G. (1971), Form and age of Late Quaternary shorelines and coastal deposits of south-west Scotland: Critical data. Quaternaria, 14, 103-114.

JARDINE, W.G. (1975), Chronology of Holocene marine transgression and regression in south-western Scotland. Boreas, 4, 173-196.

JARDINE, W.G. (1982), Sea-level changes in Scotland during the last 18,000 years. Proc. Geol. Ass., 93(1), 25-41.

JOHN, B.S. (1977), "The Ice Age, Past and Present", William Collins Sons and Co. Ltd., London. (p103).

JOHNSON, M.R.W. & FROST, R.T.C. (1977), Fault and lineament patterns in the Southern Highlands of Scotland. Geol. en. Mijnbouw, 56(4), 287-94.

KAMINSKI, W., BAMFORD, D., FABER, S., JACOB, B., NUNN, K. & PRODEHL, C. (1976), A Lithospheric seismic profile in Britain: II. Preliminary report on the recording of a local earthquake. J. Geoph. 42, 103-110.

KANAMORI, H. (1978), Quantification of earthquakes. Nature 271, 411-414.

KASTENS, K.A. & CITA, M.B. (1981), Tsunami-induced sediment transport in the abyssal Mediterranean Sea. Geol. Soc. Am. Bull. 92, 845-857.

KEEFER, D.K. (1984a), Landslides caused by earthquakes. Geol. Soc. Am. Bull., 95, 406-421.

KEEFER, D.K. (1984b), Rock avalanches caused by earthquakes: source characteristics. Science, 223, 1288-1289.

KENNEDY, W.Q. (1946), The Great Glen Fault. Quat. J. Geol. Soc. Lond., 102, 41-72.

KERR, R.A. (1985), Unexpected young fault found in Oklahoma. Science 227, 1187-1188.

KLEIN, R.J. & BROWN, E.T. (1983), The state of stress in British rocks. Rep. Dept. Environ. DOE/RW/83.060.

KNILL, J.L. (1972), Engineering geology of the Cruachan underground power station. Engng. Geol., 6, 289-312.

KRISTMANNSDOTTIR, H. (1978), Alteration of basaltic rocks by hydrothermal activity at 100-300 degrees Centigrade. in, Developments in Sedimentology, V27, eds. M.M. Mortland and V.C. Farmer, Elsevier. (Proc. VI International Clay conference 1978).

KUENEN, P.H. (1948), Slumping in the Carboniferous rocks of Pembrokeshire. Q. J. geol. Soc. Lond. 118, 65-101.

KUENEN, P.H. (1958), Experiments in geology. Trans. Geol. Soc. Glasgow, 23, 1-28.

KUHN, T.S. (1962), The Structure of Scientific Revolutions", Univ. Chicago Press.

KUJANSUU, R. (1964), Recent faults in Finnish Lapland. Geologi, V.16, p30.

KURIBAYASHI, E. & TATSUOKA, F. (1975), Brief review of liquefaction during earthquakes in Japan. Japan Soils & Found., 15 (4), 82-92.

LAGERBACK, R. (1979), Neotectonic structures in northern Sweden. Geol. For. Stockholm Fourhand., V.100(3), 263-269.

LAMBERT, A. & VANICEK, P. (1979), Contemporary crustal movements in Canada. Can. J. Earth Sci. 16, 647-668.

LEEDER, M. (1987), Sediment deposition, deformation and the analysis of faulting in sedimentary basins. in, "Deformation in sediments and sedimentary rocks", Special publ. of the J. Geol. Soc. Lond. (in press).

LOVE, A.E.H. (1906), A Treatise on the Mathematical Theory of elasticity, 2nd ed., Cambridge University Press, London.

LOWE, D.R. (1975), Water escape structures in coarse-grained sediments.

Sedimentology, 22, 157-204.

LOWE, D.R. (1976), Subaqueous liquefied and fluidized sediment flows and their deposits. Sedimentology, 23, 285-308.

LUNDQVIST, J. & LAGERBACK R. (1976), The Parve fault: A late-glacial fault in the Precambrian of Sweedish Lapland. Geol. Foren. Forhand. 98, 45-51.

MAIN, I.G. & BURTON P.W. (1984), Physical links between crustal deformation, seismic moment and seismic hazard for regions of varying seismicity. Geophys. J. R. astr. Soc. 79, 467-488.

MARROW, P.C. & ROBERTS, G. (1984), Source mechanisms of aftershocks of the 1979 "Carlisle" earthquake. Brit. Geol. Surv., Global Seismology Unit Report No. 217.

McCONNELL, R.K. (1968). Viscosity of the mantle from relaxation time spectra of isostatic adjustment, J. Geophys. Res., 73(22), 7089.

McGEARY, S. & WARNER, M.R. (1985), Seismic profiling of the continental lithosphere. Nature 317, 795-6.

McNEILL & NICHOLSON (Eds.) (1975), Historical Atlas of Scotland, c.400-1600 AD, University of St. Andrews publication.

McQUILLIN, R. & BINNS, P.E., (1973), Geological structure in the Sea of the Hebrides. Nature, 241, 2-4.

MEISSNER, R. O. and VETTER, U. R. (1976), Isostatic and dynamic processes and their relation to viscosity. Tectonophysics, 35, 137-148.

MITCHELL, G.F. (1977), Raised beaches and sea-levels. in "British Quaternary Studies", ed, F.W. Shotton, Clarendon press, Oxford.

MORNER, N. -A. (1976). Eustasy and geoid changes, J. Geol., 84(2), 123-151.

MORNER, N-A. (1978), Faulting, fracturing, and seismicity as functions of glacio-isostasy in Fennoscandia. Geology 6(1), 41-45.

MORNER, N.-A. (1980), The Fennoscandian uplift: geological data and their geodynamical implication. in, Earth Rheology, Isostasy and Eustasy, ed. Morner N.A. 1980.

MORNER, N. -A. (1981), Eustasy, paleoglaciation and palaoclimatology, Geol. Rundschau, 70(2), 691-702.

MORNER, N-A. (1985), Palaeoseismicity and geodynamics in Sweeden. Tectonophysics 117, 139-153.

MORRIS, D.V. (1983), A note on earthquake-induced liquefaction. Geotechnique, 33, 451-460.

MUIR WOOD, R. (1983), What happens to the Rhine Graben "sub-plate boundary" where it meets the North Sea. In "Seismicity and Seismic risk in the Offshore North Sea Area", eds. A.R. Ritsema and A. Gurpinar, D.Reidel, Dordecht, Holland.

MUIR WOOD, R. (1985), The seismotectonics of North-West Europe. In "Earthquake Engineering in Britain", Thomas Telford Ltd., London.

MULILIS, J.P., SEED, CHAN, MITCHELL & ARULANANDAN (1977), Effects of sample preparation on sand liquefaction. J. Geotech. Eng. Div. ASCE, 103(GT2), 91-108.

MUSSON, R.M.W., NEILSON, G. & BURTON, P. (1985), A comparison of two historical earthquakes in North Wales. In "Earthquake Engineering in Britain", Thomas Telford Ltd., London.

MUSSON, R.M.W., NEILSON, G. & BURTON P.W. (1986), The 1852 November 9 Irish Sea earthquake. Geophys. J. R. astro. Soc. 19, 270.

MUTTI, E., LUCCHI, F.R., SEGURET, M. & ZANZUCCHI, G. (1984), Seismoturbidites: a new group of resedimented deposits. Marine Geology, 55, 103-116.

MYKURA, W. (1983), "Old Red Sandstone", in Geology of Scotland, Ed. G.Y. Craig, Scottish Academic Press, Edinburgh.

NANSEN, F. (1922), The strandflat and isostasy. Videnskapselkapets Skrifter, 1. Math.-Naturw. Kl. (Kristiana), 11.

NEWMAN, W.S., MARCUS, L.F., PARDI, R.R., PACCIONE, J.A. and TOMECEK,S.M. (1980), Eustasy and deformation of the geoid: 1000-6000 radiocarbon years bp. In (Morner, N.A., ed) "Earth Rheology, Isostasy, and Eustasy", John Wiley and Sons, Chichester. pp. 555-67.

OBERMEIER, S.F. et al. (1985), Geologic evidence for recurrent moderate to large earthquakes near Charleston, South Carolina. Science 227, 408-410.

OLSEN, H.W., CLUKEY, E.C. & NELSON C.H. (1982), Geotechnical characteristics of bottom sediment in the northeastern Bering Sea. Geol. en Mijnbouw, 61, 91-103.

PATERSON, I.B. (1974), The supposed Perth Readvance in the Perth district. Scott. J. Geol., 10(1), 53-66.

PEACH, B.N. et al. (1909) 'The geology of the seaboard of Mid-Argyll', Mem. geol. Surv. Gt. Br.

PEACOCK, J.D. (1969), Coastal features on the Isle of Rhum. Scott. J. Geol. 5(3), 301-302.

PEACOCK, J.D. (1983), Quaternary geology of the Inner Hebrides. Proc. Roy. Soc. Edinburgh, 83B, 83-89.

PEACOCK, J.D., GRAHAM, D.K. ROBINSON, J.E. & WILKINSON, I. (1977), Evolution and chronology of lateglacial marine environments at Lochgilphead, Scotland. in "Studies in the Scottish Lateglacial Environment, (eds.) J.M. Gray and J.J. Lowe, Pergamon, Oxford.

PEDDY, C.P. (1984), Displacement of the Moho by the Outer Isles thrust shown by siesmic modelling. Nature, 312, 628-630.

PEDERSON, G.K. (1985), Thin, fine-grained storm layers in a muddy shelf sequence: an example from the Lower Jurassic in Stenlille 1 well, Denmark. J. Geol. Soc. Lond., 142, 357-374.

PELTIER, W.R. & ANDREWS, J.T. (1976), Glacio-isostatic adjustment - I. The forward problem. Geophys. J. R. astr. Soc., 46, 605-646.

PENNINGTON, W., HAWORTH, E.Y., BONNY, A.P. & LISHMAN, J.P. (1972), Lake sediments in northern Scotland. Phil. Trans. R. Soc. Lond., 264B, 191-294.

POPPER, (Sir) K.R. (1963), "Conjectures and Refutations: the growth of scientific knowledge." Routledge & Kegan Paul.

PRICE, R.J. (1980), Geomorphological implications of environmental changes during the last 30,000 years in Central Scotland. Z. Geomorph. N. F., 36, 74-83.

RANALLI, C. & CHANDLER, T.E. (1975), The stress field in the upper crust as determined from in situ measurements. Geol. Rundschau, 64, 653-674.

RINGROSE, P.S. & DAVENPORT, C.A. (1986), Earthquake faulting in Scotland during the late Quaternary. Paper given at the U.K. Geophysical Assembly, University of Glasgow, April 1986; abstract in Geoph. Journal 19, p266.

ROBIN, G de Q. (1981), Polar ice sheets: developments since Wegener. Geol. Rundshau 70 (2), 648-663.

RUSSELL, M.J. & SMYTHE, D.K. (1983), Origin of the Oslo graben in relation to the Hercynian-Alleghenian orogeny and Lithospheric rifting in the north Atlantic. Tectonophysics, 94, 457-72.

SBAR, M.L. & SYKES, L.R. (1973), Contemporary compressive stress and seismicity in eastern North America: an example of intra-plate tectonics. Bull. Geol. Soc. America, 84, 1861-1882.

SCHEIDEGGER, A.E. (1982), Principles of Geodynamics. 3rd completely revised edition, Springer-Verlag, Berlin.

SEEBER, L. (1986), The mystery of intraplate earthquakes: United States and Eastern China. In "Lamont-Doherty Geological Observatory of Columbia University / 1983-1986", ed R. Jellinek, Lamont-Doherty, Palisades, New York.

SEED, H.B. (1968), Landslides during earthquakes due to liquefaction. J.Soil Mech. & Found. Div ASCE, 94, SM5, p.1053.

SEED, H.B. & IDRISS, I.M. (1971), Simplified proceedure for evaluating soil liquefaction potential. J. Soil Mech. Found. Div. ASCE, 97, SM9, 1249-1273.

SEED, H.B. & IDRISS, I.M. (1982), On the importance of dissipation effects in evaluating pore pressure changes due to cyclic loading. In "Soil Mechanics - Transient and Cyclic loads", eds. G.N. Pande and O.C. Zienciewicz, John Wiley.

SEILACHER, A. (1969), Fault-graded beds interpreted as seismites. Sedimentology, 13, 155-159.

SEILACHER, A. (1984), Sedimentary structures tentatively attributed to seismic events. Marine Geology, 55, 1-12.

SELLEY, R.C., SHEARMAN, D.J., SUTTON, J. & WATSON J. (1963), Some underwater disturbances in the Torridonian of Skye and Raasay. Geol. Mag., 100, 224-243.

SHAW, F.J. (1980), "The northern and western islands of Scotland", John Donald Publications.

SHEN, C.K., VRYMOED, J.L. & UYENO, C.K. (1977), The effect of fines on the liquefaction of sands. Proc. 9th Int. Conf. on Soil Mechanics and Foundation Engineering, Vol.2, 381-385, Tokyo 1977.

SHEPARD, F.P. (1963), Thirty-five thousand years of sea level. in T. Clements (ed), "Essays in marine geology in honour of K.O. Emery", Los Angeles, Univ. Southern Calif. Press, p1-10.

SHOTTON, F.W. (1965), Normal faulting in British Pleistocene deposits. Quart. J. Geol. Soc. Lond., 121, 419-34.

SIBSON, R.H. (1983), Continental fault structure and the shallow earthquake source. J. Geol. Soc. Lond. 140(5), 741-767.

SIEH, K.E. (1978), Prehistoric large earthquakes produced by slip on the San Andreas fault at Pallett Creek, California. J. Geoph. Res., 83-B8, 3907-3939.

SIMS, J.D. (1975), Determining earthquake recurrence intervals from deformational structures in young lacustrine sediments. Tectonophysics, 29, 141-152.

SIMS, J.D. (1982), Earthquake-induced deformation in sediment as a palaeoseismic indicator. EOS, 63(18), 435-436.

SISSONS. J.B. (1972), Dislocation and non-uniform uplift of raised shorelines in the western part of the Forth valley. Trans. Inst. Br. Geogr., 55, 145-159.

SISSONS, J.B. (1974a), The Quaternary of Scotland: a review. Scott. J. Geol., 10(4), 311-337.

SISSONS, J.B. (1974b), Late-glacial marine erosion in Scotland. Boreas, 3, 41-48.

SISSONS, J.B. (1977), "The Parallel Roads of Glen Roy", Nature Conservancy Council Booklet.

SISSONS, J.B. (1978), The later lakes and associated fluvial terraces of Glen Roy, Glen Spean and vicinity. Trans. Inst. Br. Geogr., 3, 12-29.

SISSONS, J.B. (1979a), Catastrophic lake drainage in Glen Spean and the Great Glen, Scotland. J. Geol. Soc. Lond., 136, 215-224.

SISSONS, J.B. (1979b), The limit of the Loch Lomond Advance in Glen Roy and

vicinity. Scott. J. Geol., 15(1), 31-42.

SISSONS, J.B. (1982), The so-called 'interglacial' rock shoreline of western Scotland. Trans. Inst. Br. Geogr., 7(3), 309-315.

SISSONS, J.B. (1983), chapter 14 : 'Quaternary', in "Geology of Scotland", ed. G.Y. Craig, Scottish Academic Press, Edinburgh.

SISSONS, J.B. & BROOKS, C.L. (1971), Dating of early postglacial land and sea-level changes in the western Forth valley. Nature phys. sci. 234, 124-7.

SISSONS, J.B. & CORNISH, R. (1982), Rapid localized glacio-isostatic uplift at Glen Roy, Scotland. Nature, 297, 213-215.

SMITH, S.M. (1971), Palaeo-ecology of postglacial beaches in East Lothian. Scott. J. Geol., 8(1), 31-49.

SPEIGHT, J.M. & MITCHELL, J.G. (1979), The Permo-Carboniferous dyke-swarm of northern Argyll and its bearing on dextral displacement on the Great Glen Fault. J. geol. soc. Lond., 136, 3-11.

STUART, G.W. (1978), The upper mantle structure of the North Sea region from Rayleigh-wave dispersion. Geoph. J. R. astr. soc., 52, 367-382.

SUTHERLAND, D.G. (1981), The high-level marine shell beds of Scotland and the build-up of the last Scottish ice-sheet. Boreas, 10, 247-254.

SYKES, L.R. (1978), Intraplate seismicity, reactivization of pre-existing zones of weakness, alkaline magmatism, and other tectonisms postdating continental fragmentation. Rev. Geophys. Space Phys. 16, 621-688.

TER WEE, M.W. (1983), The Saalian glaciation in the northern Netherlands, in "Glacial Deposits in NW Europe", Ed. J. Ehlers, A.A. Balkema / Rotterdam.

THRELFALL, W.F. (1981), Structural framework of the Central and Northern North Sea. in, "Petroleum Geology of the Continental Shelf of NW Europe", eds, L.V. Illing and G.D. Hobson, Institute of Petroleum, London, Heyden & Son.

TURBITT, T. (ed) (1984), Catalogue of British Earthquakes recorded by the BGS Seismograph Network 1979, 1980, 1981. Brit. Geol. Surv. Global Seis. Unit Report No. 210.

TURBITT, T. (ed) (1985), Catalogue of British Earthquakes recorded by the BGS Seismograph Network 1982, 1983, 1984. Brit. Geol. Surv. Global Seis. Unit Report No. 260.

TURBITT, T. et al. (1985), The North Wales earthquake of 19 July 1984. J. Geol. Soc. Lond., 142, 567-571.

TURCOTTE, D.L. (1974), Membrane Tectonics. Geoph. J. Roy. Astr. Soc., 36, 33-42.

TURCOTTE, D.L. & OXBURGH, E.R. (1976), Stress accumulation in the lithosphere. Tectonophysics, 35, 183-199.

TURCOTTE, D.L., & SCHUBERT, G. (1982), Geodynamics: application of continuum physics to geological problems. John Wiley & Sons.

VANDENBERGHE, J. & VAN DEN BROEK, P. (1982), Weichselian convolution phenomena and processes in fine sediments. Boreas, 11, 299-315.

VAN DYKE, H. (1923), "The story of the other wise man." Harper bros. publ., London, (p28, 1947 edn.).

VESAJOKI, H. (1982), Deformation of soft sandy sediments during deglaciation and subsequent emergence of land areas; examples from northern Karelia, Finland. Boreas, 11, 11-28.

VITA-FINZI, C. (1986), "Recent Earth Movements: an introduction to neotectonics." Academic Press, London.

WALCOTT, R.I. (1970), Flexural rigidity, thickness, and viscosity of the

lithosphere. J. Geoph. Res., 75(20), 3941-3954.

WALCOTT, R.I. (1973), Slow vertical movements in continental interiors. Report on the third GEOP research conference on vertical crustal motions and their causes. EOS. Trans. Am. Geoph. Union., 54, 1257-1260.

WALCOTT, R.I. (1980), Rheological models and observational data on glacio-isostatic rebound, in Earth Rheology, Isostasy and Eustasy, ed. Morner 1980.

WANOGHO, S.O. (1985), The forensic analysis of soils with particular reference to particle size distribution analyisis. Ph.D. thesis, Univ. Strathclyde, Glasgow.

WATTS, A.B. (1971), Geophysical investigations on the continental shelf and slope north of Scotland. Scott. J. Geol., 7, 189.

WEAVER, J.D. (1976), Seismically-induced load structures in the basal Coal Measures, South Wales. Geol. Mag. 113(6), 535-543.

WINCHESTER, J.A. (1973), Pattern of regional meatmorphism suggests a sinistral displacement of 160km along the Great Glen Fault. Nature, 246, 81-84.

YOUD, T.L. (1977), Discussion of " Brief reveiw of liquefaction during earthquakes in Japan" by Kuribayashi & Tatsuoka. Soils found., 17(1), 82-85.

ZEIGLER, P.A. (1982), Faulting and graben formation in western and central Europe. Phil. Trans. R. Soc. Lond., A305, 113-143.

ZIENKIEWICZ, O.C. & BETTES, P. (1982), Soils and other saturated media under transient, dynamic conditions; general formulation and the validity of various simplifying assumptions. In "Soil Mechanics - Transient and Cyclic Loads" eds. G.N. Pande & O.C. Zeinkiewicz, John Wiley, Chichester.

MULL & LISMORE

Plate-1. The raised shoreline of the Main Rock Platform at Port Donain, Mull (background) with the surveying instrument and tripod (foreground) positioned above the permanent reference marker (small concrete pillar) as used for the levelling survey (Chapter 10).

Plates 2-6. Evidence for recent movement on fracture 6, Miller's Port, Lismore.

Plate-2. Limestone foliation surface showing dark staining (right-hand side) interpreted as the result of recent exposure of a previously sub-soil surface to sub-aerial weathering. Note the abundance of lichen on the whiter surface (top left) in contrast to the darker surface and the greater etching of micro-fractures on the whiter side than on the darker side (where they are deeper but finer). Hammer head – 20cm long. (Locality 6f in §9.3.4 and Fig.9-11)

Plate-3. The position of the dark patch (of Plate 2) in relation to the adjacent soil profile. The dark patch (above and to the right of the hammer) would be covered by the soil profile if a lateral, sinistral displacement of 0.5±0.2m was restored along the foliation plane.

Plate-4. The white patch seen on this limestone fracture surface appears to match the adjacent rock profile on the other (near) side of the fracture. The two points marked by 'v' are thought to have been coincident before a sinistral displacement of 0.50±0.05m occurred. Foliation surfaces match across this fracture with a similar amount of sinistral offset – 0.49±0.02m. (Locality 6a in §9.3.4, Fig.9-11)

Plate-5. Slickenside lineation seen on the surface of a clay layer within the fracture of Plate 4 (the white circle in plate 4 marks the position of the coin in Plate 5). The lineation (white arrow) dips slightly down to the left in a manner consistent with the direction of movement inferred by matching the two points 'v' in Plate 4.

Plate-6. A pale, smooth, relatively unweathered patch on a limestone foliation surface (delineated by black triangles) appears to match the adjacent soil/turf profile when a lateral, sinistral displacement of 0.55±0.05m is restored. (Locality 6d in §9.3.4 and Fig.9-11)
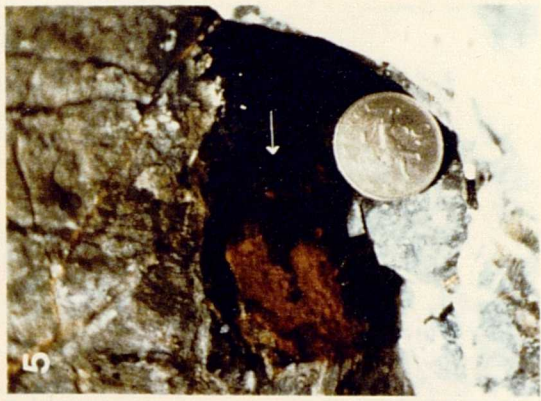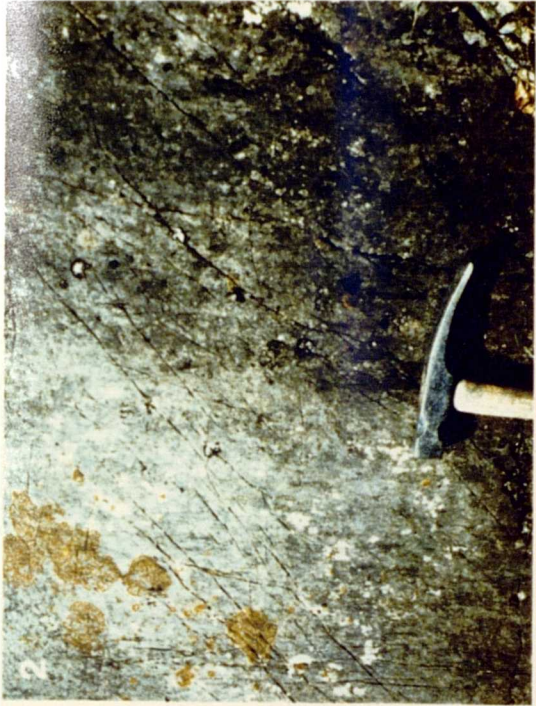
THE KINLOCH HOURN FAULT

Plate-7. A black and white air-photograph stereographic pair illustrating a portion of the Kinloch Hourn fault (between 'H' and 'N' in Fig.12-2, section 12.2.3). Note the prominence of the surface-fault feature and the several instances where drainage is deflected along the fault. North is to the left of the photo; the scale is approximately 1:25000. (Reproduced with permission of the Ordnance Survey of Great Britain - OS/64/167 V.31/8/64, frames 17&18).

THE KINLOCH HOURN FAULT

Plate-8. View along the Kinloch Hourn Fault (looking east from point 'H' in Fig.12-1) displaying its persistence as a surface feature despite passing through strong topography.

Plate-9. The bluish-grey fault gouge seen within the peaty soil wedge in the Kinloch Hourn fracture zone. Faint, disseminated traces of the orange gouge phase are also visible. Sample tube is 2.5cm in diameter. (See §12.2.4 for discussion).

Plate-10. The two phases of fault gouge are here seen alongside one another within a rock fracture close to the peat wedge. The thin section of this sample is displayed on the cover plate. Sample tube is 2.5cm in diameter.

Plate-11. The wedge of peaty soil before detailed excavation. 'C' marks the clay-filled fracture trace. (Yellow rule = 1m)

Plate-12. The wedge of peaty soil after excavation. The positions of the samples shown in Plates 9 & 10 are indicated. (The distance between 9 & 10 is approximately 5m.)

Plate-13. Low sun-angle photograph of the sediment section of Log-18, Arrat's Mill, showing closely spaced normal faults (centre left) which have been rotated clockwise. This soft-sediment faulting grades upwards and laterally (to the right) into a zone of ball-and-pillow deformation and other structures indicating liquefied flow. Measuring-staff graticules in centimetres. (For discussion see §14.4.5 and Fig.14-5).

Plate-14. The upper half of Arrat's Mill sediment section, Log-4, displaying pillow structures and layer contortions indicating liquefied flow of the sediment. Sample tubes are seen in place; the hole at the base corresponds to sample-B6 in Plate 15. (cf. Fig.14-6)

Plate-15. The lower half of the sediment section of Log-4 showing the base of deformation at the basal reference horizon (BRH , above which sediment layers become turned up to form pillows. Note the dark specks of organic matter which appear to rise from dark (organic) layers. These are taken to indicate upward migration of water during deformation. Red and yellow bars on rule are decimetres. (cf. Fig.14-6)

Plate-16. One of the layers at Arrat's Mill, below the main lens of deformation, which show deformation structures of uncertain origin. These layers are laterally continuous for several metres and are usually bound, above and beneath, by clayey layers (as can be seen here). The structures comprise tight, discontinuous, soft-sediment folds. Black graticules on scale = centimetres. (For discussion see §14.4.7 and Fig.14-4)

Plate-17. Detail of the top of deformation seen in Log-14, Arrat's Mill. Faint pillow and dish structures can be seen and also a soft sediment fault (F) along which dark blebs of organic matter have been deposited. The top surface of deformation (T) is marked by fallen clay clasts (dark brown) and overlain by conformable, laminated silts and sands. Pencil is approximately 10cm long. (cf. Fig.14.11)
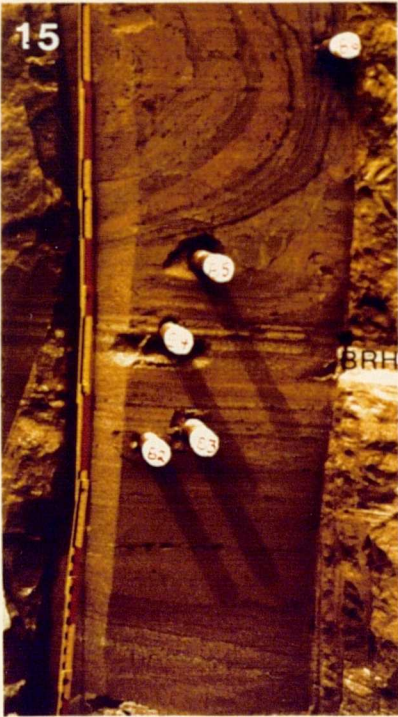
13

14

16

15

17

Plate-18. Log 20 of the Arrat's Mill sediment sections. The soft-sediment deformation layer can be seen overlying undeformed sands, and is itself overlain by undeformed sands and gravels. Metric measuring staff. (See also Fig.14-5 and §14.4.6)

Plate-19. Detail of a portion of the Log-20 section (centre-right in Plate-18) showing the relationships at the top of deformation. The liquefied unit has been eroded to form an undulating surface, later filled in by loose (probably aeolian) sands. Subsequently the the fine-grained sediment was unconformably overlain by a thick gravel unit.

Plates-20&21. Sediment sections between Logs 1&2, Arrat's Mill, which display tilting of flame and pillow structures towards the local depression seen in the right of Plate-21. Towards the left (Plate-20) where the base of the deposit is near-horizontal the amount of tilting is much less. (See also §14.4.2 and Fig.14-8)
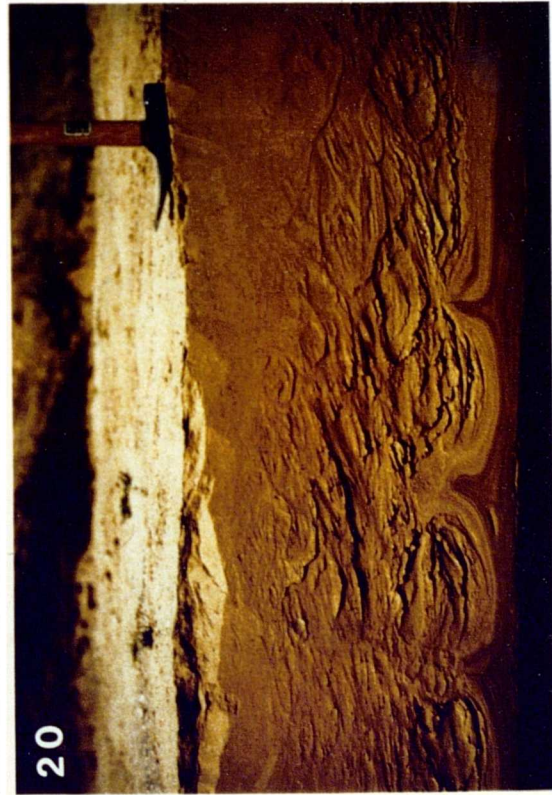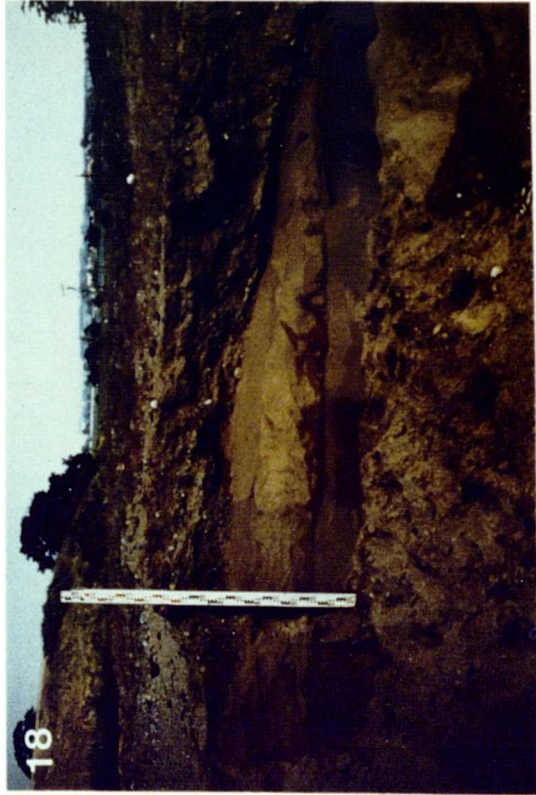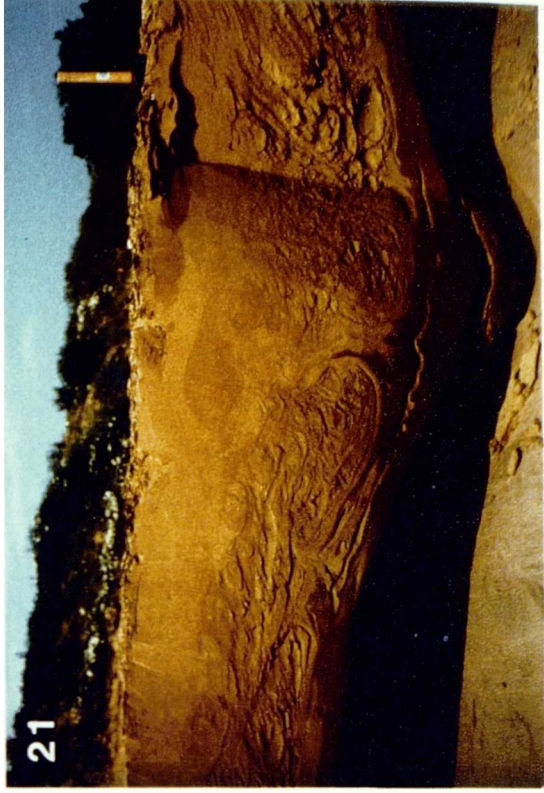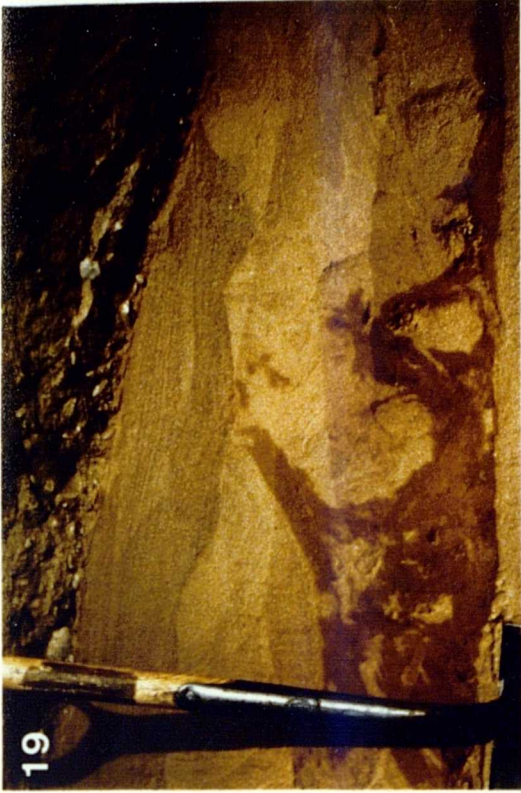
MEIKLEOUR

Plate-22. Detail of the L-horizon (sand) displaying loading into silts beneath. Above the L-horizon an injection structure (also seen in the top right of Plate 25) displays upward turning of sand layers in a form resembling a volcano. (c.f. §15.4.1)

Plate-23. Detail of the M-horizon layer (seen in Plate 24) showing the regularly-spaced pillows characteristic of this layer. Note the grey-clay coating on the base and sides of the pillows and the sharp truncation surface (M), which is broken by a small injection structure to the right of the central pillow. (See also §15.4.8 and Fig.15-6)

Plate-24. Right-hand end of the horizontal section at Meikleour (displayed in Fig.15-4) showing the 'L' and 'M' horizons and various pillow structures. Scale is the same as in Plate-25.

Plate-25. Central portion of the horizontal section at Meikleour (displayed in Fig.15-4) showing the 'L' and 'M' horizons and the intervening pillow distribution. Scale: tape-measure graticules in decimetres.

24

23 M

22 L

25 L

M

GLEN ROY AND SHUNA

Plates 26&27. Views looking south along the main fracture lineament (at locality 4, Fig.11-2 and §11.2.4). The south side of Glen Roy is seen in the distance. Plate-26 was taken in winter and from higher up the mountain side than Plate-27, taken in summer. Both display the westward-facing scarp (up to 2m high) of the lineament interpreted as the surface-fault rupture of the Glen Roy earthquake. The high (east) side of the scarp commonly displays an abundance of fractured rock and stoney rubble (Plate 27).

Plate-28. View towards the north of an exposure of the Glen Roy fault rupture at 'f1' in Glen Gloy (section 11.2.8 and Fig.11-3). The fracture line is indicated by the hammer shaft. The morphology suggests a most recent dextral displacement of 30+20cm with the right-hand side of the fracture (on which the hammer rests) having moved towards the viewer. Hammer head is 20cm long.

Plate-29. Detail of fault gouge material seen at 'f1' in Glen Gloy (position of Plate-29 is marked by a white box in Plate-28). The freshest-looking, soft, plastic, bluish gouge can be seen by the hammer head (25mm across) and lies closest to the side of the fracture which appears to have moved most recently.

Plate-30. The freshest-looking fracture at the Lochan exposure on Shuna, is seen here to contain a soft, yellow-brown fault gouge (composed of Kaolin and Chlorite). The country rock is shale. The photograph is of the section between 7 and 8 metres as displayed on Fig.10-21. (See also §10.4.1)
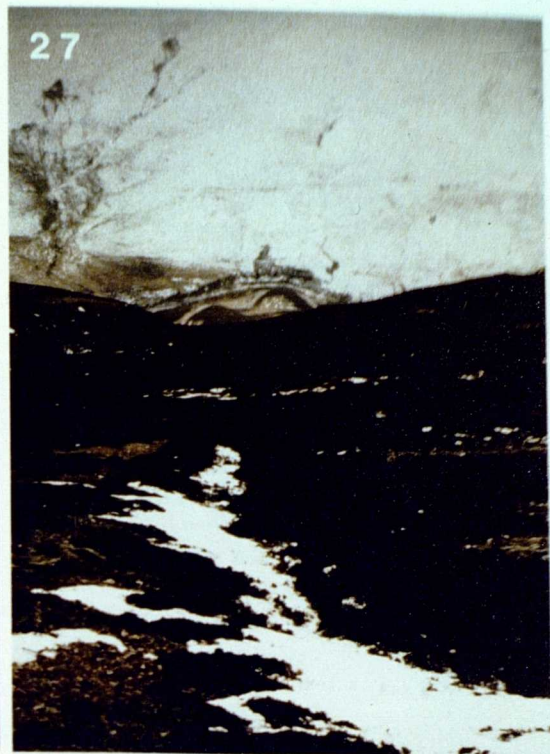
KINLOCH HOURN AND LISMORE

Plate-31. Sediment section Log-2, at Coire Shubh, near the Kinloch Hourn Fault. The section shows a sequence of sandy peats (yellow and grey), peat (dark brown) and sands (white). Deformation involving flaming (centre) and pillowing of sand (bottom right) is observed in the lower half. The top of the deformation (T) occurs within the peat, above which slightly darker, undisturbed peat is seen. The deformation is interpreted as being the result of earthquake ground-shaking (see §16.4 and Fig.16-3). The section shown is 1m deep.

Plate-32. View west towards the Upper Arnisdale Lochs, Kinloch Hourn, showing the type of high valley depression in which post-glacial sediment has been deposited and in which soft-sediment deformation is observed. The two white arrows show the moraine thought to be a Loch Lomond Readvance terminal moraine. The Arnisdale sediment sections (Fig.16-1&2) were cut in the far bank of the river in the foreground.

Plate-33. Excavation of a crofter's 'turf dyke' (field-boundary wall) on Lismore. The excavation seen here was made after observing an apparent offset in the grass ridge above the ruined wall. Soil and grass was removed and stones (larger than knuckle-size) were left in place to reveal the trace of the wall appearing to have an offset of 0.20+0.05m sinistrally (seen in the centre of the photo). Hammer head 0.2m long. (Locality 48, §9.3.4d)

Plate-34. Sediment section Log-7 at Arnisdale, Kinloch Hourn. Sands overlain by peats show deformation beneath the 'top of deformation' surface at 'T'. Note the injection of sand up into the peat to produce a mixed zone. Note also the similarity of this deformation stratigraphy with that seen at Coire Shubh (Plate 31) 7km away. Both are interpreted as the result of earthquake ground-shaking (section 16.3, Fig.16-2). A sample of peat taken from immediately below horizon 'T' at this section was dated at 3490±50 radiocarbon years BP (Appendix 7). Scale: metric staff.

Plate-35. LANDSAT MSS image of the Kinloch Hourn Fault running ESE from the blue arrow (pointing north). The field of view is approximately 15km. The two white areas are Loch Hourn (left) and Loch Quoich (right). The grain of the (Moine) metamorphic basement rocks (trending NNE) can be seen in the centre-right of the image. The image is a negative of bands 4,5&7 (image 1/37 in Appendix 3).
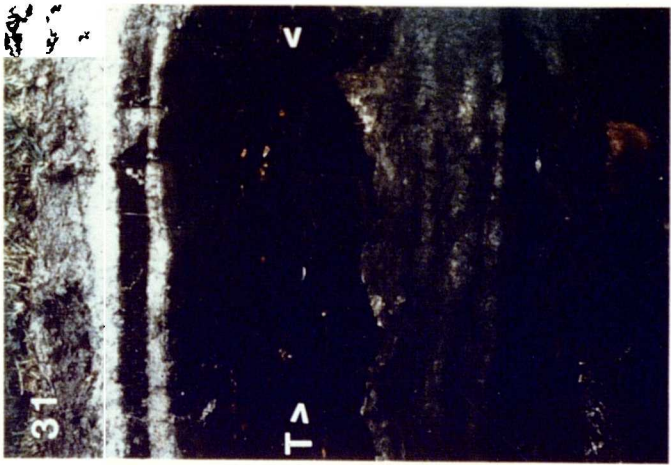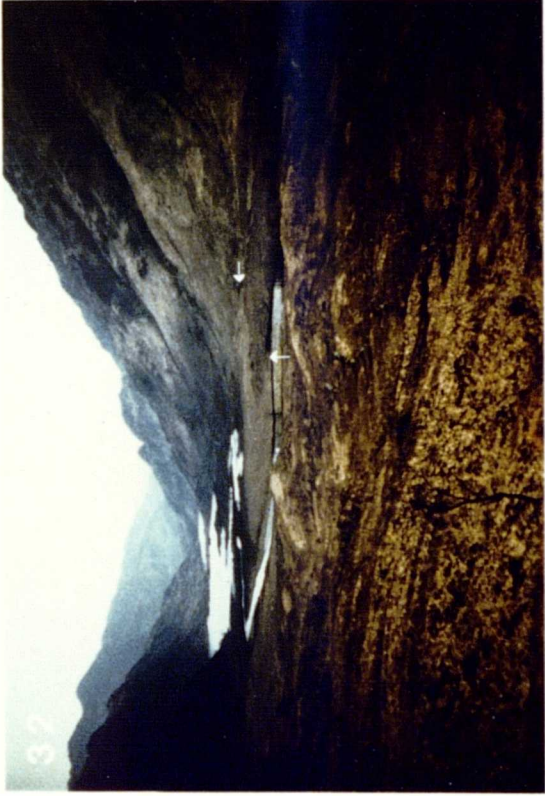
GLEN ROY

Plate-36. LANDSAT Thematic Mapper image of Glen Spean (across the bottom of the image), Glen Roy (centre) and Glen Gloy (left of centre). The white area on the left is Loch Lochy which lies along the Great Glen Fault. This negative image of band-4 displays the 'Main Fracture Lineament' thought to be the Glen Roy Fault rupture (dark line seen running between the two white arrows). There is a suggestion on this image that the fault trace continues further south of the southern white arrow. North is towards the top. Field of view is approximately 20km. (See Fig.11-12; image 5/10 in Appendix 3).

Plate-37. Low sun-angle view of the parallel 'roads' of Glen Roy (looking northwards onto the east side of the glen). The upper (u), middle (m) and lower (l) shorelines are prominent, however several other shoreline levels can be picked out – at least two between the upper and middle shorelines and one between the middle and lower ones. A fan delta can be seen in the foreground beneath the lower shoreline.

Plate-38. View of the Main Roy Landslip (outlined by black triangles). The lake shorelines can be seen either side of the landslip but are absent within the slipped area, except for a faint trace of the lower shoreline. 'l' indicates the 'cleft-and-ridge' feature running diagonally up the mountain side and thought to be a fault-rupture feature. (See §11.2.1 and Fig.13.26)

Plate-39. View looking east from the Main Roy Landslip area down onto a dissected fan delta in Glen Roy. Note that the apex of this delta (and the one seen in Plate-37) is just above the level of the lower shoreline. (See also Fig.13-26)

GLEN ROY

Plate-40. East Roy Landslip, Glen Roy (viewed from the south). The headscarp is marked by white dots; the three main shoreline levels are indicated. The landslip has removed the upper two shorelines. (c.f. §13.7.4)

Plate-41. Bohuntine Landslip, Glen Roy (viewed from the east). Note its appearance as a coherent slipped mass overlying the line of the lower shoreline. (c.f. §13.7.6)

Plate-42. Lodge Landslip, Glen Roy (viewed from the south). A surficial mass has slipped several tens of metres to cover the upper and middle shorelines. (c.f. §13.7.2)

Plate-43. View northwards down the Upper Glen Gloy stream section (described in section 11.2.7 and illustrated in Fig.11-3). 'cl', 'c2' and 'c3' mark abandoned river courses; 'r' marks the present main flow of the River Gloy before it is deflected down the gorge of the 'main fracture lineament' (marked by the line of trees).

41

43

c3

c2

r

c1

40

42

GLEN ROY SEDIMENT SECTIONS

Plate-44. Section GS5 (CLASS-A), Glen Spean, showing a complete lacustrine sequence displaying a 'fault-grading-stratigraphy': faulted silts and sands (with fault-throws increasing upwards) breaking up at higher levels into liquefied sediment containing pillows of sand (P). The deformed sediment was later eroded and infilled by channel 'C'. Loose fluvial/aeolian sands and gravels are seen at the top. Scale: white label = 15cm long. (cf. Fig.13-10)

Plate-45. Section GS10 (CLASS-B), Glen Spean, displaying incipient pillow and loading structures in a subsurface layer. Note the yellow sand layers and the grey gravel layers loading and 'balling-up' into the grey-green silts beneath. The sediment surface at the time of deformation was probably at the top of the yellow sand layers. Note also the thin red silt layer 'R'. Scale: white label = 15cm long. (cf. Fig.13-13).

Plate-46. Section GR14 (CLASS-B), Glen Roy, showing tight, soft-sediment folds in a confined layer within a silt-varve sequence. Note also the chaotic injection structure above the black triangle. Scale: white label = 15cm long. (c.f. Fig.13-12)

45

46

44
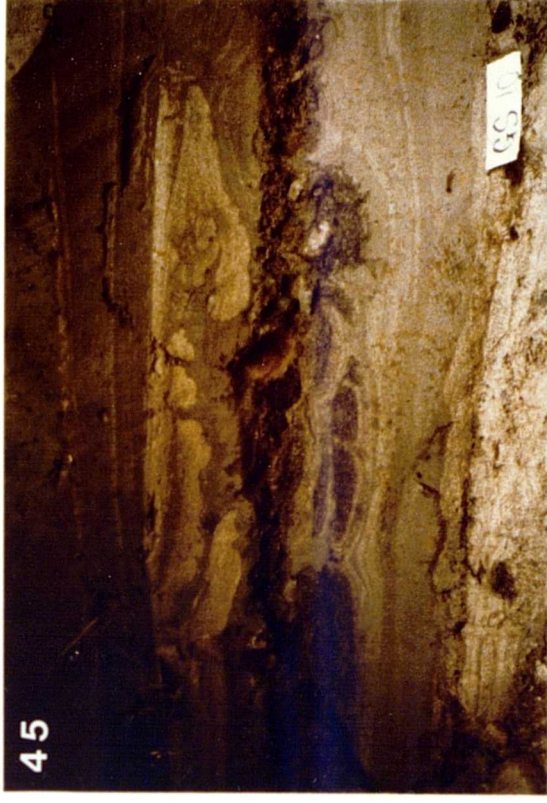
P-PILLOW STRUCTURES

C-BASE OF CHANNEL CUT INTO DEFORMED SEDIMENTS

FAULTED LACUSTRINE SEDIMENTS

B-BASE OF LACUSTRINE DEPOSITS

GLEN ROY SEDIMENT SECTIONS

Plate-47. Section GS12 (CLASS-C), Glen Spean, displaying soft-sediment deformation beneath a gravel/sand bar and injection of silts upwards through it. Because this confined layer deformation does not continue across the exposure, only occurring beneath the gravel, it is termed 'incipient' and allocated to Class-C. Scale: white label = 15cm long. (cf. Fig.13-18)

Plate-48. Section GR9 (CLASS-B), Glen Roy, displaying flaming and loading of sand and peaty layers. Note the detachment and 'balling-up' of pockets of yellow sand. Scale: white label = 15cm long. (cf. Fig.13-16)

Plate-49. Section GR22 (CLASS-C), Glen Roy, displaying incipient confined layer deformation (c) from which sediment has been injected upwards (black arrows). Scale: white label = 15cm long. (cf. Fig.13-17).

Plate-50. Section RR14 (CLASS-N), Glen Roy, showing undeformed lacustrine varves overlain by fluvial/aeolian sands. Scale: white label = 15cm long. (cf. Fig.13-22)

48

RR ○14

50

GS12

47

49